High Altitude Observatory
National Center for Atmospheric Research, Boulder, CO

TIEGCM V1.94 Model Description

June 1, 2011

Author: HAO
e-mail: maute@ucar.edu

This is the documentation of TIEGCM1.94. The HAO team is constantly working on the documentation to 1. fill in the gaps, 2. correct errors, 3. update to newer versions.
Every help is very much appreciated. If you have comments or corrections please send them to maute@ucar.edu.
Thank you very much.

Contents

List of Figures

V

List of Tables

Chapter 1

Introduction

The High Altitude Observatory at the National Center for Atmospheric Research has developed a series of numeric simulation models of the Earth's upper atmosphere, including the upper Stratosphere, Mesosphere, and Thermosphere. The Thermospheric General Circulation Models (TGCM's) are three-dimensional, time-dependent models of the Earth's neutral upper atmosphere. The models use a finite differencing technique to obtain a self-consistent solution for the coupled, nonlinear equations of hydrodynamics, thermodynamics, continuity of the neutral gas and for the coupling between the dynamics and the composition.

Models in the series include a self-consistent aeronomic scheme for the coupled Thermosphere/Ionosphere system, the Thermosphere Ionosphere Electrodynamic General Circulation Model (TIEGCM), and an extension of the lower boundary from 97 to 30 km, including the physical and chemical processes appropriate for the Mesosphere and upper Stratosphere, the Thermosphere Ionosphere Mesosphere Electrodynamic General Circulation Model (TIME-GCM). A global mean, or column model, has also been developed in parallel with the TGCM's. The global mean model is used as a time-dependent, one-dimensional platform from which new chemical, dynamic and numeric schemes are developed and tested before being introduced into the 3-d GCM's.

This documentation presents the governing equations, physical parameterizations and numerical algorithms used in the NCAR Thermosphere Ionosphere Electrodynamics GCM (TIE-GCM) version 1.94. The model descrip-

tion provides help on the major model component, numerics and coding implementation.

Conventions	
command	bold
template filenames	italics
flags	medium bold
directories, files	slanted
`source code`	typewrite
keywords	emphasize

Chapter 2

Input

2.1   Solar Input

Solar input, ionization rates, dissociation rates, and heating rates, are calculated in the module `qrj.F`, which contains the `subroutines qrj`, `init_sflux`, `init_qrj`, `ssflux, and alloc_q`. The acronym "qrj" is historically based on a convolution of Q (heating rate) and RJ (O_2 dissociation rate).

2.1.1   Solar Irradiance

The solar irradiance proxy model

The thermosphere absorbs solar radiation in the soft X-ray ultraviolet (XUV, 0.05 nm – 30 nm), extreme ultraviolet (EUV, 30 nm – 120 nm), and far ultraviolet (FUV, 120 nm – 200 nm) wavelength ranges, primarily by O, O_2, and N_2 through photon ionization and dissociation. The ionization threshold of O, O_2, and N_2 are 91.3 nm, 102.6 nm, and 79.8 nm, respectively. The dissociation threshold of N_2 is 98.6 nm. The spectrum longward of 102.6 nm is mainly absorbed by O_2 dissociation, especially in the Schumann-Runge continuum from 132–175 nm.

The TIE-GCM uses the EUVAC solar proxy model as the default solar input [18] in the spectral range from 5–105 nm. This model is an empirical representation of solar irradiance and its variability. It includes two parts, a reference spectrum at solar minimum and a wavelength-dependent solar variability. The variability is usually parameterized by solar indices that are historically available. The most widely used solar index is the $F_{10.7}$ index. Solar flux at a given solar activity level is obtained from $F_{10.7}$ and its 81 day average $< F_{10.7} >$ as follows:

The EUVAC model [18] is used between 5 nm and 105 nm.

$$f(\lambda) = f_{ref}(\lambda)[1 + A(\lambda)(P - 80)] \tag{2.1}$$

where f_{ref} is the reference spectrum, A is the solar variability factor, and $P = (F_{10.7} + < F_{10.7} >)/2$. It is apparent that the solar spectrum is equivalent to the solar minimum reference spectrum when P = 80. For solar minimum conditions when P is less than 80, the proxy model imposes the limit that solar irradiance is no less than 80% of the solar minimum reference spectrum in any given wavelength band.

EUVAC is based on the F74113 reference spectrum, with the EUV fluxes

between 15 nm and 25 nm doubled and the EUV flux below 15 nm increased by a factor of 3; the solar variability scale factors are based on the AE-E and calibration rocket measurements. The F74113 spectrum was measured on April 23, 1974 by a rocket flight [11],[12] at low solar activity. EUVAC has been compared with more recent measurements by the SEE instrument on the TIMED satellite [31] and found to be in reasonable agreement, although SEE fluxes at low solar activity are slightly higher in the XUV wavelengths. For the spectral region shortward of 5 nm, GOES X-ray measurements in its two channels, 0.05–0.4 nm and 0.1–0.8 nm, are used to establish the reference irradiance and the solar variability factor for the first two bins. The third bin, i.e., from 0.8–1.8 nm, is based on some early X-ray/XUV measurements as described in Solomon and Qian [28]. The Hinteregger model [13] is used for the wavelength range from 1.8–5 nm, based on the SC21REFW reference spectrum and variability factors, but with the fluxes in this wavelength range increased by a factor of 3. The SC21REFW reference spectrum is based on the AE-E EUV measurements [14].

The Woods and Rottman model [32] is used from 105 nm to 175 nm. The Woods and Rottman model is based on UARS (Upper Atmosphere Research Satellite) SOLSTICE (SOLar STellar Irradiance Comparison Experiment) measurements from 119–200 nm and a 1994 rocket measurement. This model uses a two-parameter fit based on $F_{10.7}$ and $< F_{10.7} >$, but the implementation in the TIE-GCM simplifies this using the P and A factors as described above for the EUVAC model, which results in differences from the original formulation generally less than 1%.

Solar input is segmented into optimized low-resolution bands as described by Solomon and Qian [28]. This paper includes a detailed description of the band structure, the ionization and photoionization scheme, and tables of solar flux, cross sections, and branching ratios. These tables are coded directly into the module . The reference spectrum and solar variability factors for the solar proxy model are given here in table 2.1. All values are specified at 1 AU; the fluxes are multiplied by the factor $sfeps$ to account for the Earth's orbital eccentricity effect on Sun-Earth distance, which is calculated in `advance.F`.

Use of solar irradiance measurements

Although solar proxy models have been widely used in aeronomy studies, solar irradiance can deviate significantly from empirical parameterizations, on time scales ranging from solar flares, to the solar 27-day rotation, to the 11-year solar cycle. Therefore, the TIE-GCM has an option to use measured solar irradiance spectra directly. The TIMED/SEE instrument has measured solar spectral irradiance from 0.1–195 nm from 2002 to present [31]. It covers nearly from the solar maximum to the solar minimum of solar cycle 23. It uses two types of instruments: the XUV Photometer System (XPS) and the EUV Grating Spectrograph (EGS). The XPS measures solar irradiance from 0.1–34 nm with a resolution of 5–10 nm. The EGS measures irradiance from 27–195 nm with 0.4 nm spectral resolution. TIMED/SEE data are available from February 2002 through March 2011. More information is available at the TIMED/SEE web site: http://lasp.colorado.edu/see. These data are pre-processed from 1-nm resolution to the binning scheme in table 2.1, and provided in a netCDF data file for input to the TIE-GCM. If the namelist input parameter **SEE_NCFILE** is set to specify this file, these data will be used for solar irradiance input instead of the EUVAC proxy model, interpolated to current model time. Any environment variables imbedded in the file path will be expanded by the model input module.

Ionization Rates

Direct solar ionization rates The solar flux in each spectral interval at each level of the atmosphere is calculated by applying the Beer-Lambert law:

$$I(\lambda, z) = I(\lambda, \infty)exp[\tau(\lambda, z)] \tag{2.2}$$

where the optical depth τ as a function of altitude z is:

$$\tau(\lambda, z) = \sum_j \sigma_j(\lambda)N_j(z) \cdot Ch \tag{2.3}$$

N_j and σ_j are the column density and total absorption cross section for each species, and Ch is the Chapman grazing incidence integral correction factor, calculated by `subroutine chapman`. The process–specific rate for each species j and process k is then:

$$R_{j,k}(z) = \sum_\lambda I(\lambda, z)\sigma_j(\lambda)\beta_{j,k}(\lambda) \tag{2.4}$$

where $\beta_{i,j}$ is a branching ratio, e.g., for ionization, dissociative ionization, or dissociation. Tables containing these parameters are available in Solomon and Qian [28], at http://download.hao.ucar.edu/pub/stans/euv, and in `module qrj.F`.

Photoelectron ionization rates The photon ionization process generates energetic electrons called photoelectrons or secondary electrons. Photoelectrons generated by shorter EUV wavelengths have sufficient energy to ionize, dissociate, and excite neutral species. The photoelectron flux and its impact on ionization, dissociation, and excitation can be calculated using models that are based on radiative transfer methods [e.g. [15] [27]]. However, such detailed calculations are not practical for a global general circulation model. The method of Solomon and Qian [28] is used to estimate the additional proportion of photoelectron ionization to direct photoionization that occurs in each wavelength band, which are also tabulated as specified above.

Dissociation Rates

- *EUV and XUV*: Dissociation rates of N_2 and O_2 are obtained from each wavelength band in the EUV and XUV using the tabulated process-specific branching ratios and photoelectron enhancement factors described above. They are then integrated over wavelength to calculate the production of atoms (and, in the case of dissociative ionization, atomic ions) at each altitude level.

- *Lyman-alpha*: Ionization of nitric oxide by the solar H Lyman-alpha emission at 121.6 nm is calculated using the parameter **beta9**, which is specified as a pseudo rate coefficient in chemrates as the product of the Lyman-alpha solar flux and the NO cross section:

$$beta9 = 2.91 \times 10^{11} \cdot (1 + 0.2(F_{10.7} - 65)/100) \cdot 2 \times 10^{-18} \qquad (2.5)$$

- *Schumann-Runge continuum*: Solar flux in the spectral range from 132–175 primarily dissociates O_2 in the thermosphere, resulting in production of one ground state $O(^3P)$ atom and one excited $O(^1D)$ atom. Solar flux in 5 nm bands as a function of altitude is calculated from Beer's law, then multiplied by the O_2 dissociation cross section for each band, and integrated across wavelength, to obtain the dissociation rate.

- *Schumann-Runge bands (SRB)*: For O_2 dissociation and heating in the SR bands (197–200 nm), which results in two ground state $O(^3P)$ atoms, a simple approximation is employed for the optically thin region above 97 km:

$$p3f = \text{(erg/s in SRB)(solar activity factor)(Sun-Earth distance factor)}$$
$$p3f = (9.03 \times 10^{-19})(1 + 0.11(F_{10.7} - 65.))(\text{sfeps})$$
$$rj = p3f/do2 \tag{2.6}$$

  with do2 is the dissociation energy of O_2 in ergs $= 8.2 \times 10^{-12}$.

Heating Rates

- *Neutral heating rates*
  EUV: Direct solar heating of the neutral gas, primarily from photo-electron impact and from the kinetic energy of dissociation products, is approximated as 5% of the total photon energy absorbed at each altitude level. This is a small fraction of the heating that is ultimately attributable to ionization and dissociation caused by solar EUV, but these other pathways are calculated as chemical heating, electron heating, and ion heating.
  FUV: The heating rate is calculated by subtracting the sum of the O_2 bond energy and the excitation energy of the $O(^1D)$ state (do22=1.1407 erg) from the photon energy, and assuming that the remainder goes into the energy of the products, and ultimately neutral heating. Quenching of $O(^1D)$ resulting in kinetic and vibrational excitation of N_2 and O_2 is also assumed to result in neutral heating; this is calculated in `module qrj` (rather than in the chemistry module) for historical reasons.
  SRB: 33% of the dissociation rate is assumed to result in neutral heating (approximately the difference between the O_2 bond energy and the photon energy in the center of the SRB region).

- *Electron and Ion Heating Rates*
  Electron and ion temperatures are calculated in `subroutine settei`, see chapter 6.3.

λ_{min}	λ_{min}	Reference Spectrum(f_{ref}) Variability	Factor(A)
0.05	0.40	5.010e+01	6.240e-01
0.40	0.80	1.000e+04	3.710e-01
0.80	1.80	2.000e+06	2.000e-01
1.80	3.20	2.850e+07	6.247e-02
3.20	7.00	5.326e+08	1.343e-02
7.00	15.50	1.270e+09	9.182e-03
15.50	22.40	5.612e+09	1.433e-02
22.40	29.00	4.342e+09	2.575e-02
29.00	32.00	8.380e+09	7.059e-03
32.00	54.00	2.861e+09	1.458e-02
54.00	65.00	4.830e+09	5.857e-03
65.00	79.80	1.459e+09	5.719e-03
65.00	79.80	1.142e+09	3.680e-03
79.80	91.30	2.364e+09	5.310e-03
79.80	91.30	3.655e+09	5.261e-03
79.80	91.30	8.448e+08	5.437e-03
91.30	97.50	3.818e+08	4.915e-03
91.30	97.50	1.028e+09	4.955e-03
91.30	97.50	7.156e+08	4.422e-03
97.50	98.70	4.482e+09	3.950e-03
98.70	102.70	4.419e+09	5.021e-03
102.70	105.00	4.235e+09	4.825e-03
105.00	110.00	3.298e+09	3.007e-03
110.00	115.00	3.200e+09	2.099e-03
115.00	120.00	8.399e+09	2.541e-03
121.57	121.57	3.940e+11	4.230e-03
120.00	125.00	1.509e+10	3.739e-03
125.00	130.00	7.790e+09	2.610e-03
130.00	135.00	2.659e+10	2.877e-03
135.00	140.00	1.387e+10	2.632e-03
140.00	145.00	1.824e+10	1.873e-03
145.00	150.00	2.802e+10	1.202e-03
150.00	155.00	5.080e+10	1.531e-03
155.00	160.00	7.260e+10	1.125e-03
160.00	165.00	1.055e+11	1.043e-03
165.00	170.00	1.998e+11	6.089e-04
170.00	175.00	3.397e+11	5.937e-04

Table 2.1: Reference spectrum and solar solar variability factors for the solar proxy model used in the TIE-GCM.

2.2   Magnetospheric Input

The documentation group for the magnetospheric inputs to the TIEGCM model consists of Barbara Emery, Wenbin Wang and Yue Deng, with help from others as needed.

2.2.1   Parameters to define the magnetospheric inputs

Magnetospheric inputs are the high latitude ion convection model (Heelis or Weimer 2005) and the aurora, which are described in the following sections. The aurora depends on the Hemisphere Power (`HP`), where the auroral radius can depend on the Cross Polar Cap Potential (`CPCP`) of both hemispheres. The Heelis ion convection [9] depends on the `CPCP` and the IMF By. The input parameters for the Weimer 2005 model [30] are solar wind density N_{sw} and speed V_{sw}, and the IMF By and Bz.

The potential model is specified in the input file as:

1. POTENTIAL_MODEL = 'NONE'

2. POTENTIAL_MODEL = 'HEELIS'

3. POTENTIAL_MODEL = 'WEIMER05'

where 'NONE' means the high-latitude ion drift velocity and electric potential is zero. The aurora is specified in the input file as:

1. AURORA = 0

2. AURORA = 1

where 0 means no aurora and '1' means calculate and use a model aurora ([23]).

The magnetospheric input parameters for the convection and auroral models can be defined in two ways in the namelist input file:

1. Directly specify them in the namelist file as single-valued parameters under the names of: POWER, CTPOTEN, BYIMF, BZIMF, SWVEL, and SWDEN. Multiple-valued parameters can be specified under the

names of: POWER_TIME, CTPOTEN_TIME, BYIMF_TIME, BZ-IMF_TIME, SWVEL_TIME, and SWDEN_TIME, where four values are given for each time as: ut_daynumber, ut_hour, ut_minute, value.

2. Specify and use the "*gpi.F*" file (GPI_NCFILE) for the Heelis ion convection model or the "*imf.F*" (IMF_NCFILE) for the 2005 Weimer ion convection model in the namelist file, but not both. It is best to comment out the single- or multiple-valued parameters listed above when using this option because the default is to use the listed input namelist values. The code will stop if CTPOTEN is given and 'WEIMER05' is requested.

The GPI_NCFILE provides 3-h Kp, daily 10.7 cm solar flux data, and 81-day 10.7 cm solar flux data centered on the given day. The "*gpi.F*" code calculates `HP` and `CPCP` from the Kp index. For this case, in the namelist file, comment out the F107, F107A, POWER, and CTPOTEN lines, and select POTENTIAL_MODEL = 'HEELIS' and the GPI_NCFILE (a netcdf file). The formulas are [34]

$$\begin{aligned}
&\text{if} \quad Kp \leq 7 \\
&hp = 16.82 \cdot e^{(0.32kp)} - 4.86 \\
&\text{if} \quad Kp > 7 \\
&hp = 153.13 + \frac{kp - 7}{9 - 7}(300 - 153.13)
\end{aligned} \tag{2.7}$$

$$cpcp = 15 + 15kp + 0.8kp^2 \tag{2.8}$$

The IMF_NCFILE also provides Kp and 10.7 cm solar flux data, but additionally provides hourly interplanetary magnetic field (IMF) data and solar wind speed (Vsw) and density (Dsw). The satellite IMF and plasma data are time-shifted to the bow shock nose of the Earth's magnetosphere as described in the NASA Geophysical Data Center web site for OMNI data at http://omniweb.gsfc.nasa.gov/ow.html. All data time-shifted to the bow shock that lie between 0000 and 0100 UT are used in the hourly average centerd at 0030 UT. The "*imf.F*" code interpolates the data to the model time. No lag is done between the bow shock and the polar cap for hourly data, although polar ground magentometer stations respond between 9 and 25 minutes later (Weimer, 2009 private communication). When we go to higher resolution IMF and plasma data, then we will add a lag time between

the bow shock and the high-latitude ion convection. If the hourly By, Bz, V_{sw}, or N_{sw} are missing in the IMF_NCFILE and also absent (commented out) in the namelist, then the code will stop because there is no provision for filling in IMF or plasma gaps. Since N_{sw} has little effect on the Weimer 2005 `CPCP` as described later, it can be set in the namelist (SWDEN = 4) to avoid the code stopping during periods when N_{sw} is missing. If POWER is absent from the namelist, `HP` is calculated from Emery et al. (2008) [5] from IMF Bz (in nT) and the solar wind velocity (Vsw in km/s). For this case in the namelist file, comment out the F107, F107A, POWER, CTPOTEN, BXIMF, BYIMF, BZIMF, SWVEL, and SWDEN lines, and select POTEN-TIAL_MODEL = 'WEIMER05' and the IMF_NCFILE (a netcdf file). The formulas are [5]

$$
\begin{aligned}
\text{if} \quad & Bz < 0 \\
hp = & (6.0 + 3.3 \cdot abs(Bz) + (0.06 + 0.003 \cdot abs(Bz)) \\
& \cdot (min(Vsw, 700) - 300)) \cdot fac \\
\text{if} \quad & Bz \geq 0 \\
hp = & 5.0 + 0.05 \cdot (min(Vsw, 700) - 300) \cdot fac
\end{aligned} \tag{2.9}
$$

where fac = 2.0, so the NOAA/DMSP estimated `HP` is doubled to be closer to the GUVI estimated `HP`. Zhang and Paxton (2008) [34] show in their Figure 2. that the GUVI energy flux and the DMSP-F14 energy flux are similar along the cut of the DMSP satellite, but they show in their Figure 11, that the GUVI estimated `HP` is larger than either the DMSP-F15 estimated `HP` or the NOAA estimated `HP`. Their Figure 8a with GUVI `HP` as a function of Kp is approximately double the intercalibrated NOAA/DMSP `HP` versus Kp in Figure 9 of Emery et al. (2008) [5]. Thus, the factor of 2.0 increase of the NOAA/DMSP `HP` agrees with the GUVI `HP` within 10% for Kp 0 to 7 and is approximatley 25% lower than GUVI HP for Kp 8 and 9. In addition, TIEGCM modeling studies have shown that the auroral energy flux needs to be increased in order to fit the observed nitric oxide [NO] observations (private communication S. Solomon and L. Qian). Finally, `HP` is not allowed to be less than 5.0 GW when calculated from IMF Bz and Vsw. The order of calls is:

1. Read namelist and open any netcdf input files in module `init.F`

2. Advance time-step in module `advance.F` and interpolate input parameters with possible calls to getgpi in module `gpi.F` or to getimf in module

`imf.F`. If the potential model is WEIMER (01 or 05), and POWER is not provided by the namelist, then call hp_from_bz_swvel in module `util.F`.

3. Call aurora_cons in module `aurora.F` from module `advance.F`

4. Call convection model from module `advance.F` (and override auroral constants found in aurora_cons if the Weimer 2005 model is used)

5. Call module `dynamics.F` from module `advance.F`, which in turn calls aurora in module `aurora.F`.

It is possible to insert different ion convection or auroral patterns into the TIEGCM, such as AMIE derived patterns, but this requires interpolation to the TIEGCM magnetic and auroral circle grids, and is not currently supported in the public version TIEGCM1.92.

2.2.2 The Heelis convection pattern

The input to `module heelis` is summarized in table 2.2. The output of module `heelis.F` is summarized in table 2.3.

*Note: the following material is from [33], and copyright to the University of Michigan. Some of the material has been modified based on the updated TIEGCM.

The auroral ion convection pattern in the TIEGCM is parameterized using the Heelis model [9], which is modified to account for IMF By effects on the shape of the convection pattern. In general, only two parameters are needed to define the auroral ion convection pattern: the cross-tail potential Φ in kilovolts and the interplanetary magnetic field B_y component (in nanotesla), where a local variable `byloc` is set to the IMF B_y in the range $-11.0 \leq byloc \leq 7.0$ in the northern hemisphere, and in the range $-7.0 \leq byloc \leq 11.$ in the southern hemisphere. [NOTE: This By range is only correct for NH in aurora_cons, and not for SH!] In versions earlier than version 1.9, the IMF By dependancy was removed. Other parameters are set up based on these two parameters that define the convection pattern.

The first parameter defined is the radii θ_0 of the convection flow reversal circle where the potential peaks

$$\theta_0 = -3.80^0 + 8.48^0 \Phi^{0.1875} \tag{2.10}$$

Where Φ is the cross polar cap potential (CPCP in kV). The center of the circle is located away from the geomagnetic poles by `offc` along the magnetic noon-midnight line and `dskofc` in the dawn-dusk direction

$$\texttt{offc} = 1.1^0$$
$$\texttt{dskofc} = -0.08^0 - \pm 0.15^0 \texttt{byloc} \tag{2.11}$$

where $+/-$ applies for southern/northern hemisphere, respectively. The TIEGCM grid is then transformed into grid points in the new ion convection coordinate system defined by `offc` and `dskofc` relative to the geomagnetic poles. In this coordinate the auroral electric potential is generally expressed as

$$\Psi = G(\theta)F(\phi, \theta) \tag{2.12}$$

where G and F represent the strongest latitude and local time dependencies, respectively, θ and ϕ correspond to the corrected magnetic colatitude and magnetic local time.

Latitude variations of the potential are represented in the TIEGCM by two functions, one describing the variation when colatitude is smaller than θ_0, the other one describing the variation when colatitude greater than θ_0 . The latitude gradient of the potential, and therefore the meridional electric field, is discontinuous at θ_0 in the TIEGCM implementation of the Heelis model. The TIEGCM neglects a few degrees of turnover region around the ion convection reversal because of the five-by-five degree grid spacing used in the TIEGCM. However, this neglect introduces sharp changes in ion velocity and neutral wind near the convection reversal which are an obvious discrepancy between the calculated and observed convection patterns. In the TIEGCM

$$\Psi(\phi, \theta) = \left(\frac{\sin\theta}{\sin\theta_0}\right)^{r_1} F(\phi, \theta) \quad \text{for} \quad \theta > \theta_0$$
$$\Psi(\phi, \theta) = F_3(\phi, \theta)\left(\frac{\theta}{\theta_0}\right)^3 + F_2(\phi, \theta)\left(\frac{\theta}{\theta_0}\right)^2 + F_1(\phi, \theta))\left(\frac{\theta}{\theta_0}\right) + \texttt{pcen} \quad \text{for} \quad \theta \leq \theta_0 \tag{2.13}$$

where $r_1 = -2.6$, $F(\phi, \theta)$, $F_1(\phi, \theta)$, $F_2(\phi, \theta)$ and $F_3(\phi, \theta)$ are functions accounting for the local time dependencies of the convection pattern. They are chosen such that $\Psi(\phi, \theta)$ is continuous at θ_0, `pcen` is the potential at the center of the convection reversal circle due to the B_y effect

$$\texttt{pcen} = (-0.168 \pm 0.027 B_y)\Phi \tag{2.14}$$

Positive B_y increases the evening cell and negative B_y enlarges the morning cell in the northern hemisphere. The opposite behavior occurs in the southern hemisphere.

The cross tail potential is split between the evening and morning potentials `psie` and `psim`. The evening cell is usually larger than the morning cell based on both satellite and ground measurements, so the normal split used in the TIEGCM is

$$\texttt{psim} = 0.44\Phi \quad \texttt{psie} = -0.56\Phi \tag{2.15}$$

The local magnetic time dependencies are described by 6 angles. The longitude 0° (12 MLT) in the TIEGCM ion convection coordinate system is defined at noon. The longitude is positive when rotating clockwise. `phid` and `phin` are local time angles determining the daytime entrance and nighttime exit of the ion convection pattern (zero potential line) across the polar cap. Their position are also affected by the magnitude and orientation of IMF B_y

$$\texttt{phid} = (9.39 \pm 0.21 \texttt{byloc} - 12.)15^o/hr \texttt{phin} = (23.5 \pm 0.15 \texttt{byloc} - 12.)15^o/hr \tag{2.16}$$

where $\pm$ applies for the southern/northern hemispheres, respectively. The first expression in each formula is in MLT, where 12 hours is then subtracted because zero is noon MLT. The MLT value is converted first to degrees and then to radians in the code.

The regions over which the flow paths are not parallel to the convection reversal circle are specified by local hour limits on either side of the zero potential line. The dayside convergence region is called the throat region whereas the region on the nightside is the Harang discontinuity. The angular limits of these two convergence zones at θ_0 are given by positive and negative departures from `phid` and `phin`, respectively, which are denoted by `phidp`, `phidm`, `phinp` and `phinm`. Figure 2.1 is illustration of an example of the Heelis model output marked with various parameters.

It should be noticed that the Heelis model is suitable only for IMF B_z negative (southward) conditions. As discussed in Chapter 2.2.1, when B_z is positive (northward), the ion convection patterns can have a configuration quite different from the two-cell pattern simulated by the Heelis model. Up until now, the latest TIEGCM and TIME-GCM still use this simple model for the parameterization of the convection pattern.
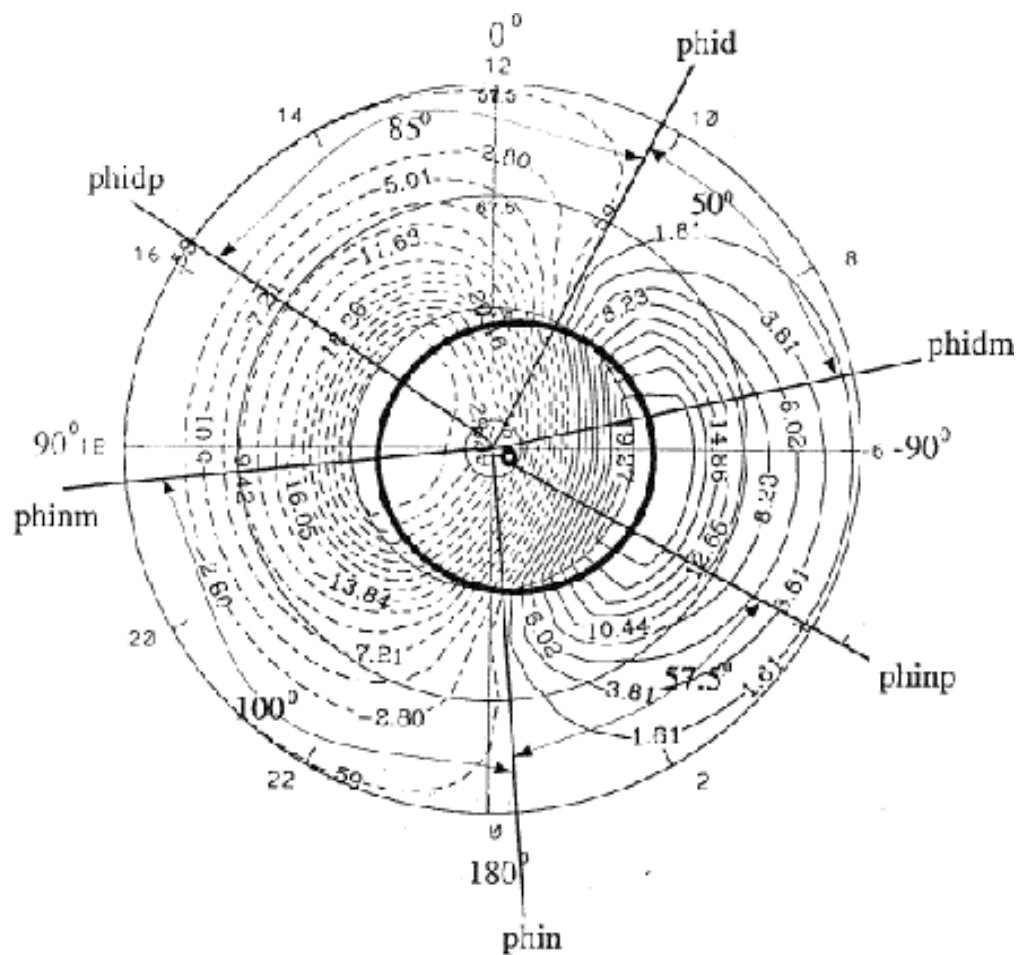
Figure 2.1: The ion convection pattern (northern hemisphere) for cross-tail potential of 60 KV and the IMF By = 7 nT. Many of the specification parameters are illustrated.

2.2.3 The Weimer convection pattern

The input to module `weimer` is summarized in table 2.4. The output of module `weimer.F` is summarized in table 2.5. The input parameters for the 2005 Weimer model [30] are solar wind density (N_{sw}) and speed (V_{sw}), and the IMF B_y and B_z, where the sign of the IMF B_y is changed for the potential pattern in the southern hemisphere. The figure (2.2) shows Weimer 2005 Northern Hemisphere electric potentials with $B_y = 0$ for $V_{sw} = 400$ km/s where B_z decreases from +20 to -30 nT and for Bz=-5 nT where Vsw increases from 250 to 1500 km/s. The ion convection pattern and the `CPCP` are very sensitive to IMF B_z, IMF B_y, and V_{sw}, but `CPCP` is relatively insensitive to N_{sw}. For example, `CPCP` changes from 158 kV to 155 kV for V_{sw}=450 km, $By = 0$ nT, and $Bz = -15$ nT while N_{sw} increases from $1cm^{-3}$ and $16cm^{-3}$ (Maute, 2008 private communication). Thus, because there are numerous drop-outs of the hourly plasma density Nsw, we recommend setting the namelist SWDEN = 4 as a constant which is always used. Alternatively, the filled 15 minute averaged IMF files can be used where values from time -20 to -5 minutes is used for time=0. Sometimes the filled values are not reasonable, especially for large gaps in the IMF (e.g. during the Halloween storm, 03301.6-03304.3, Oct 28-31, 2003).

 The output parameters are the Weimer convection circle location variables of `theta0` (= half of bndyfitr from the `subroutine setboundary`), `offc` (= 4.2^o), and `dskofc` (= 0.0^o), which are set in the Weimer 2005 model, and the convection entrance and exit in MLT-12 hours converted to radians, `phid` and `phin` which were calculated from the Weimer potential patterns. The auroral circle location variables of `rrad`, `offa` (= 4.2^o), and `dskofa` (= `diffrac` or approximatley -2.5^o) are similar to the parameterizations calculated in `aurora.F`, which are discussed in the next section.

The figure (2.2) shows bndyfitr as a dashed black circle where the potential goes to zero. This is below 50 geomagnetic latitude for large V_{sw} (>700 km/s). Half of this is the radius of convection `theta0`, shown as a red dashed circle. The offsets, `offc` and `dskofc` are shown as the center of this red circle as a red dot on the 0 MLT line. The magenta dot is the center of the dashed magenta circle, determined mostly from the minimum and maximum potentials shown as black dots for MLTs around dusk and dawn. As shown in figure (2.2), the convection radius `theta0` is about 20 degrees for V_{sw}=700 km/s and about 30 degrees for V_{sw}=1500 km/s. This compares
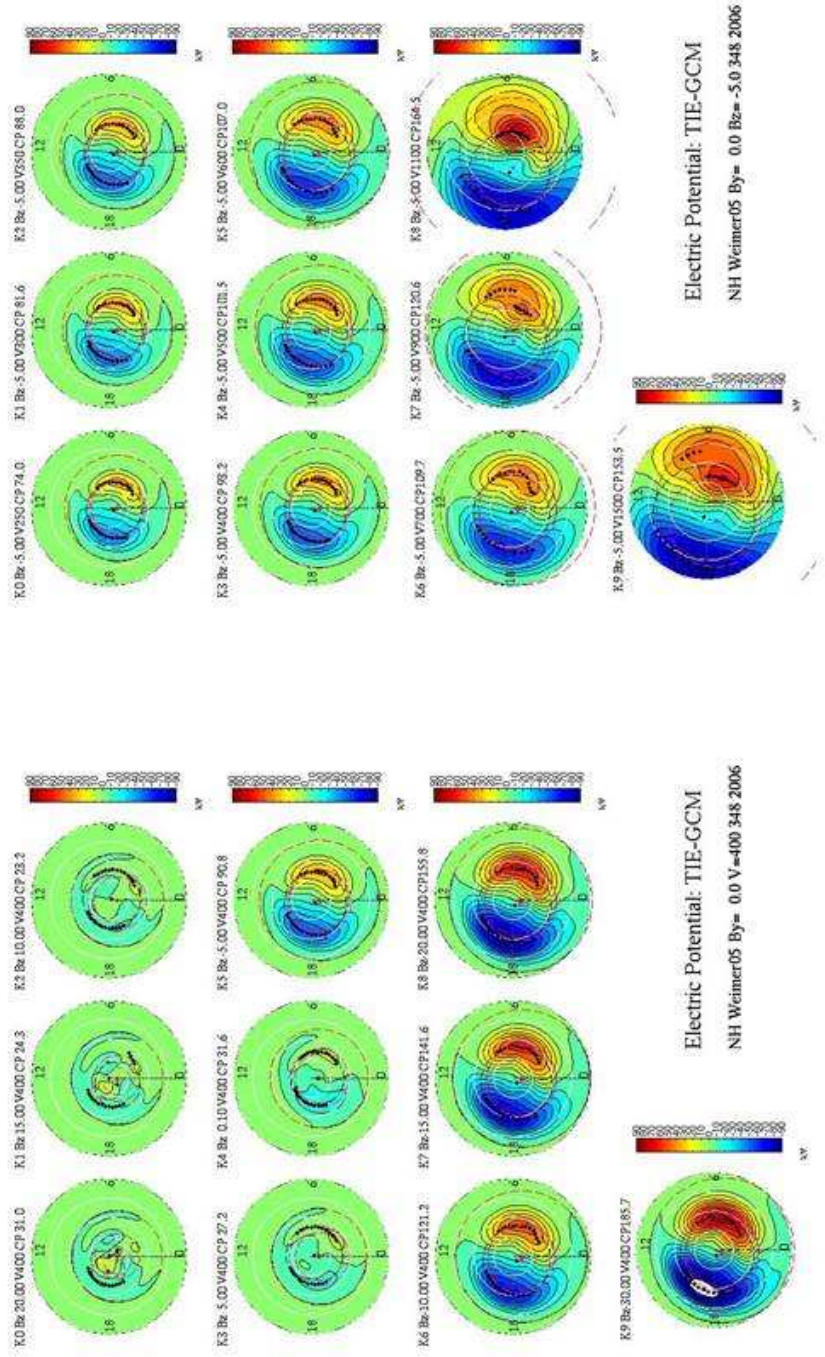
Figure 2.2: Northern hemisphere electric potential [kV] from TIEGCM using Weimer 2005 empirical model with $B_y = 0$ nT.

to an increase in the convection radius for the Heelis model from 11 degrees at Kp=0 to 19 degrees for Kp=9. There were a very small number of high velocity cases used in the construction of the Weimer 2001 and 2005 models. Thus the electric potential patterns for large solar wind velocities V_{sw} (>900 km/s, but especially 1100 km/s in this figure and for other values of Bz and By) can be unrealistic. The data used in the construction of the models also had very few cases with IMF magnitudes greater than 15 nT. Through the use of a saturation curve, the 2005 model appears to be realistic (i.e., lower potential drops consistent with observations of saturation) at high IMF magnitudes (> 20 nT), although results may not be as accurate as at lower IMF levels.

2.2.4 High latitude auroral pattern

The input to module `aurora.F` is summarized in table 2.6. The output of module `aurora.F` is summarized in table 2.7. Ion ionization rates and electron heating rate by auroral precipitation are added to the total ionization rates (variables `qo2p, qop, qn2p and qnp`) and electron heating rate (variable `qteaur`) (solar part is calculated in) within the `auroral.F` module itself (subroutine `xxxx`), so they are not the outputs of the module.

The precipitation in the `auroral.F` module includes electron precipitation, soft electron precipitation, cusp precipitation, polar rain (drizzle), and ion precipitation. The contribution of each precipitation to ion production and electron heating is added to the total ionization and heating rates.

The auroral parameterizations described in the following sections are for version 1.9 and later when IMF By effects were restored. **Note: the following material is from [33], and copyright to the University of Michigan. Some of the material has been modified based on the updated TIEGCM.**

Electron precipitation

The characteristics of the auroral oval used in the TIEGCM are shown in Figure 2.3. The oval is circular and is offset toward the magnetic nighttime by `offa`, which is assumed to be 1.0^o with the Heelis convection (`offc = 1.1^o`) and 4.2^o with the Weimer 2005 convection (`offc = 4.2^o`). The aurora is shifted towards the dawn with respect to the convection reversal circle, and is larger in radius than the convection circle (e.g. Heelis et al., 1980

[10]). The dawn-dusk offset of the Heelis convection (`dskofc`) is related to the direction and strength of the IMF B_y component and is given by equation (2.11), and so is -0.08 degrees (negative towards dawn) for $B_y = 0$. However, the dawn-dusk offset of the aurora that goes with the Heelis convection is zero (`dskofa` $= 0.0^o$). There is no IMF B_y dependance in the Weimer 2005 convection center location, so `dskofc` $= 0.0^o$ and similarly `dskofa` $= 0.0^o$ also for the location of the aurora. Thus in both convection cases, the ion convection center and the center of the auroral oval is away from the magnetic poles.

The auroral radius (Ra) is set by the larger of:

$$Ra(CPCP) = -0.43 + 9.69(CPCP^{0.1875}) \qquad (2.17)$$

or

$$Ra(HP) = 14.20 + 0.96 P_l \qquad (2.18)$$

where $P_l = 2.09 \ ln(HP)$ is the hemisphere power level, and HP is the hemispheric power in [GW], so

$$Ra = max(Ra(CPCP), Ra(HP)). \qquad (2.19)$$

Recall from Equation (2.10), that the Heelis radius of convection (theta0) is similar to $Ra(CPCP)$ above, where $CPCP^{0.1875}$ is also used. [CONSIDER adding a plot of θ_0 and $Ra(CPCP)$ and $Ra(HP)$ for Kp formalizations of HP and CPCP.] For the Weimer 2005 convection model, the Weimer $CPCP$ averaged from both hemispheres is used to find the parameterized $\theta_0(param)$ from Eq.(2.10) , even though the real $\theta_0 = bndyfitr/2$. $Ra(param)$ is the larger of $Ra(CPCP)$ from Eq. (2.17) or $Ra(HP)$ from Eq. (2.18). The difference between the larger auroral radius and convection radius, or $diffrac$ in $wei05loc$, is approximately 2.5 degrees, but varies. [CONSIDER another plot based on plot above of the difference between $Ra(param)$ and $\theta_0(param)$.] This parameterized difference in the radii is then used to find the auroral radius used with the Weimer 2005 ion convection radius where

$$Ra(with \ Weimer \ 2005) = \theta_0(= bndfitr/2.) + diffrac \qquad (2.20)$$

The TIEGCM defines the auroral oval in a new auroral coordinate system with poles in the center of the auroral oval. The width of the auroral zone is assumed to be a Gaussian distribution having a half-width of the form

$$h = h_0(1 - r_h \cos \lambda) \qquad (2.21)$$

where $h_0 = 0.5(h_1 + h_2)$, $r_h = \frac{(h_1 - h_2)}{(h_1 + h_2)}$. λ is the angle clockwise from the entrance of the auroral convection throat, which is away from the magnetic local noon by an angle of χ_h. h_1 (daytime) and h_2 (nighttime) are the half-widths of the auroral zone at $\lambda = 0^o$ and $\lambda = 180^o$, respectively, and given by

$$h_1 = min(2.35, 0.83 + 0.33P_l)$$
$$h_2 = 2.5 + 0.025 \cdot max(HP, 55) + 0.01 \cdot min(0, HP - 55)$$

The angle χ_h (variable `rroth` in the code, the clockwise rotation from noon of dayside h_1 Gaussian) is defined as

$$\chi_h = 15^o(0.81 - 0.06P_l) \tag{2.22}$$

Thus for $P_l = 1$, the thinnest auroral width (h_1) is at 12 MLT - 0.75 MLT, or at 1115 MLT, while the maximum auroral width (h_2) is 12 hours later at 2315 MLT.
E_1 and E_2 are the energy flux of the precipitating particles (ergs cm-2 s-1) in the noon sector and midnight sector, respectively, and given by

$$E_1 = max(0.5, -2.15 + 0.62P_l)$$
$$E_2 = 1. + 0.11HP$$

Usually $E_2 > E_1$ so the maximum energy flux is on the nightside and the least is on the dayside.
There is also an angle χ_e (variable `rrote` in the code, the clockwise rotation from noon of peak dayside energy), it is defined as

$$\chi_e = 15^o(0.17 - 0.04P_l) \tag{2.23}$$

Thus for $P_l = 1$, the minimum (usually) dayside auroral flux (E_1) is at 12 MLT - 0.13 MLT, or at 1152 MLT, while the maximum (usually) nightside auroral flux (E_2) is 12 hours later at 2352 MLT.
  The auroral particle precipitation number flux is then assumed to be a product of functions describing the λ (longitude) variations and a latitudinal Gaussian distribution [23]

$$F = E_0[1 - r_e \cos(\alpha - \chi_e)]exp[-(\frac{\phi - \phi_0}{h})^2]/(2\alpha_m 1.602 \cdot 10^{-9}) \tag{2.24}$$
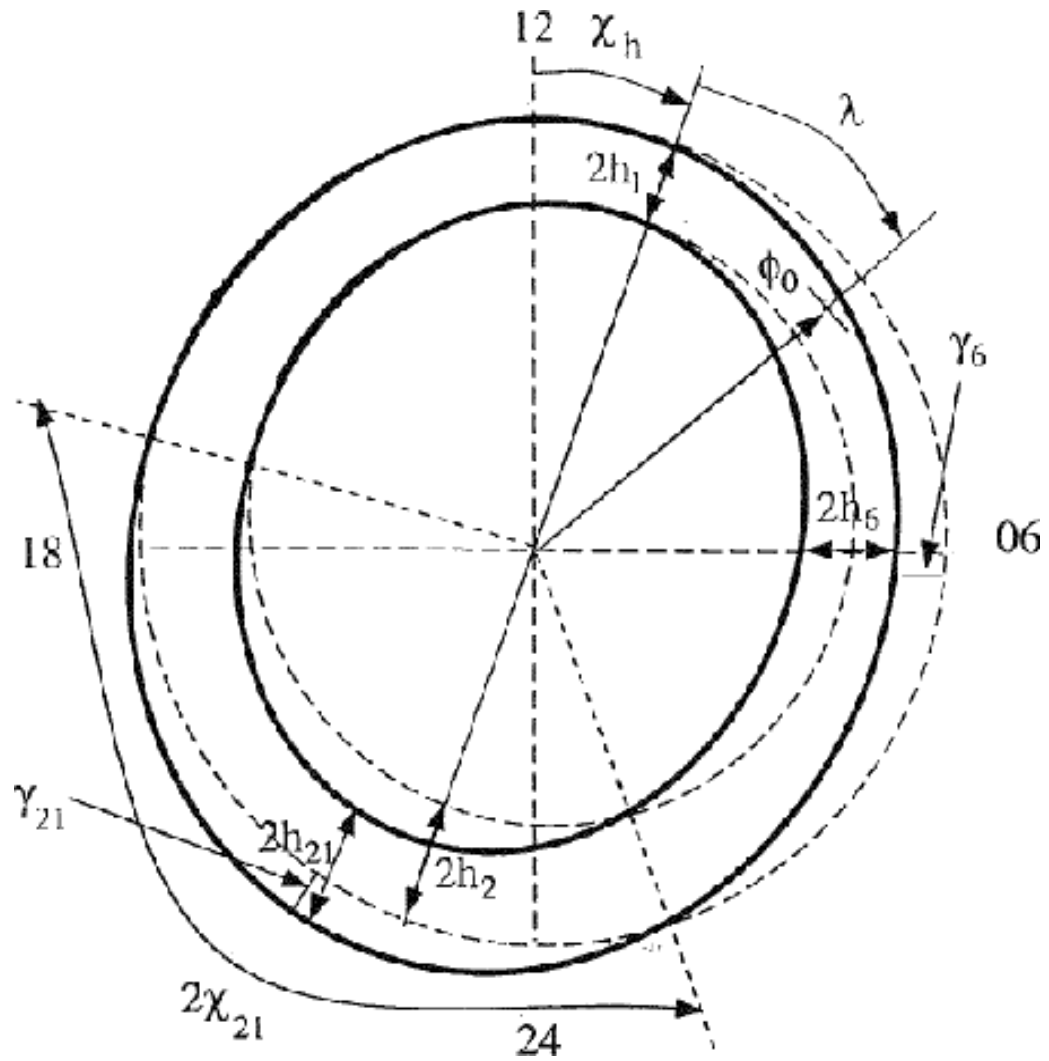
Figure 2.3: Illustration of the parameterization of the auroral oval in the TIGCM - SHOULD REPLACE WITH Roble and Ridley (1987) alfa1,2 fig.

where α is the longitude, ϕ is the colatitude in the newly defined auroral coordinate system, ϕ_0 (named `arad` in the code) is the radii of the auroral oval expressed as

$$\phi_0 = max(-0.43 + 9.69C_p^0.1875, 14.20 + 0.96P_l) \tag{2.25}$$

where C_p is the cross tail potential in unit of kV and α_m is the characteristic Maxwellian energy of the precipitating particles in keV and $2\alpha_m$ is the mean Maxwellian energy. For the Heelis convection, C_p is the same in both hemispheres, but for the 2005 Weimer convection, C_p is the average of `CPCP` from both hemispheres. The angle χ_e (variable rrote in the code) is defined in 2.23 such that

$$\begin{aligned} E_0[1 - r_e \cos(\alpha - \chi_e)] &= E_1 \quad \text{when } \alpha - \chi_e = 0^o \\ E_0[1 - r_e \cos(\alpha - \chi_e)] &= E_2 \quad \text{when } \alpha - \chi_e = 180^o \end{aligned} \tag{2.26}$$

where $E_0 = 0.5(E_1 + E_2)$ and $r_e = (E_1 - E_2)/(E_1 + E_2)$.

The characteristic energy α_m is defined using the statistical patterns measured by satellite (e.g. Hardy et al., 1985). As defined in Roble and Ridley (1987) [23], there is a dayside α_1 and a nightside α_2 that are fixed to the dayside E_1 and nightside E_2 energy fluxes rotated by the angle χ_e. Since version 1.8, the characteristic Maxwellian electron energies have been nearly constant at:

$$\begin{aligned} \alpha_1 &= 1.5keV \\ \alpha_2 &= 2.0keV \end{aligned} \tag{2.27}$$

where

$$\alpha_0 = 0.5(\alpha_1 + \alpha_2)$$
$$r_a = (\alpha_1 - \alpha_2)/(\alpha_1 + \alpha_2)$$
$$F = E_0[1 - r_e \cos(\alpha - \chi_e)]exp[-(\frac{\phi - \phi_0}{h})^2]/\alpha_m = \alpha_0 \cdot [1 - r_a \cos(\alpha - \chi_e)] \tag{2.28}$$

Thus the characteristic energy of electron precipitation over the entire auroral oval is not changing with geomagnetic storm intensities (i.e. Kp), although Zhang and Paxton (2008) [34] show in their Figure 8b that $2\alpha_m$ increases from 1 keV to 3 keV between Kp 0 and 9 from GUVI FUV images.

Soft electron precipitation

Soft electron precipitation is defined the same as the auroral oval in Section 2.2.4. At present, it is turned off in the TIEGCM by setting the soft electrons to be zero (characteristic energy is set to be 75 eV).

Cusp Electron precipitation

The polar cusp region is also subject to intense soft particle precipitation with an average energy around 100 eV. (The characteristic energy (not mean energy!) of the cusp precipitation used in TIEGCM is 100 eV.) Most of the energy of the precipitating electrons is deposited in the F-region, causing localized enhanced electron density and temperature, or a so called hot spot (Fontheim et al., 1987; Heikkila and Winningham, 1971). The longitude extent of the polar cusp is about 30 to 40 degrees (2-4 MLT hours) around magnetic local noon. The polar cusp is more constrained in the latitudinal direction with an average width about 2-3 degrees (e.g. Lockwood and Davis, 1995; Newell and Meng, 1992), and is located between 75° and 80° magnetic latitudes. The location and size of the polar cusp may change dramatically under various IMF conditions.

In the TIEGCM cusp precipitation is parameterized by assuming Gaussian distribution in both latitude and longitude. The location of the cusp is assumed to be at the daytime convection reversal throat which is determined by the strength and direction of the IMF By and Bz components. The Gaussian half width in the longitude direction is 20° and the half width in the latitude direction is 5°. Thus the TIEGCM, because of the limitations of its grid size, overestimates the latitude extent by about 5 times as compared to the observed average latitude width of 2° to 3° discussed above. One consequence of this parameterization is the overestimation of the sizes of enhanced plasma density and temperature regions produced by the cusp soft precipitation and, in turn, the overestimation of the coupling effect between neutrals and ions, and the amount of plasma transported from the dayside ionosphere into the nighttime polar cap.

The typical energy flux of cusp electron precipitation is about $0.32erg/cm^2/s$ varying with geomagnetic and IMF conditions (Hardy et al., 1985; Candidi and Meng, 1984; Heikkila and Winningham, 1971). In the TIEGCM, the

energy flux of the cusp precipitation is given by

$$
\begin{aligned}
E_c &= 3.12 \times 10^8 (2.4 \times 10^{-1} + 6.7 \times 10^{-3} H_p) \quad eV/cm^2/s \\
&= -.5(2.4 \times 10^{-1} + 6.7 \times 10^{-3} H_p) \quad erg/cm^2/s
\end{aligned}
\tag{2.29}
$$

(in TIEGCM 1.9 E_c is defined as $(2.4 \times 10^{-1} + 6.7 \times 10^{-3} H_p)/5$ do not know why) Thus, the energy flux is $0.14 erg/cm^2/s$ when $H_p = 5.0 GW$ during magnetic quiet times, and $0.63 erg/cm^2/s$ when is 150.0 GW during a storm.

Polar rain (drizzle)

Spatially homogeneous precipitation of soft particles in the polar cap, the so called polar rain, is also included in the TIEGCM. The polar rain particles come from the solar corona and get into the upper atmosphere through the magnetosheath (Fairfield and Scudder, 1985). The energy fluxes of polar rain commonly vary from 10^{-3} to $10^{-2} erg/cm^2/s$ (Sotirelis et al., 1997; Hardy et al., 1986; Riehl and Hardy, 1986; Gussenhoven et al., 1984; Winningham and Heikkila, 1974), although sometimes very strong polar rain may occur with energy fluxes up to about $10 erg/cm^2/s$ (Newell and Meng, 1990, Meng and Kroehl, 1977). The occurrence frequency of polar rain events for the IMF Bz southward is about twice that for IMF Bz northward conditions (Gussenhoven et al., 1984). Polar rain has strong hemispherical asymmetry, with the Earth's north (south) hemisphere favored for away (towards) IMF Bx directions (Hardy et al., 1986; Gussenhoven et al., 1984). The energy flux of polar rain also has a dawn-dusk gradient controlled by IMF B_y conditions. Polar rain is stronger during magnetic storms than during magnetically quiet times (Winningham and Heikkila, 1974).

The energy spectrum of polar rain can be described by a single or by two Maxwellian distributions. The lower energy component of polar rain has a very narrow energy distribution centered at 80 eV with a standard deviation of 13 eV. The energy spectrum of the high energy component has a outstanding peak centered at 525 eV but extending over a wide range from 100 eV to several thousand eV. The mean energy of the high energy component of the polar rain is about 1250 eV with a standard deviation of 750 eV (Hardy et al., 1986; Riehl and Hardy, 1986).

In the TIEGCM, polar rain is parameterized by a single Maxwellian distribution with a characteristic (not mean energy) energy of 500 eV. This simple approach may underestimate the contributions of the low energy component

of polar rain to the ionization rate of the upper atmosphere, while overesti-
mating the contributions of the high energy component. The peak altitude
of the ionization rate is thus moved to lower heights affecting the calculation
of the F-region electron density in the winter hemisphere polar cap greatly.
The energy flux and its variations with the geomagnetic activity is described
in the TIEGCM by

$$
\begin{aligned}
E_p &= 3.12 \times 10^8(0.012 + 0.006H_p) \quad eV/cm^2/s \\
&= 0.5(0.012 + 0.006H_p) \quad erg/cm^2/s
\end{aligned}
\tag{2.30}
$$

Ion precipitation

Solar proton precipitation inside the polar cap is included in TIEGCM. The
characteristic energy was assumed to be 10 keV. The energy flux is cur-
rently set to be 1.E-20, so practically zero. There is also a logical variable
`add_sproton`, which has a default value of `false`. You have to change this
to `true` and specify the energy flux `e_sp` if want to include this precipitation
in the model calculation.

Ion ionization and electron heating rates

It is assumed that particle precipitations has a Maxwellian energy distribu-
tion. The total energy flux is given by (Roble and Rees, 1977; [23])

$$
F_E = 2\alpha F_P
\tag{2.31}
$$

where F_P is the total number flux of the precipitating particles, α is char-
acteristic energy of the energy distribution and 2α is the mean energy. The
ionization rate produced by collisions between precipitating particles and
neutral particles is then calculated using an analytic relationship derived by
Lazarev (1967). Contributions from both primary and secondary electrons to
the production of ionospheric plasma are included. The detailed description
of this calculation is given by [23].
The number fluxes of auroral electron precipitation, soft electron precipita-
tion and polar drizzle are calculated in the auroral coordinate system based
on 2.31. The coordinate transfer for each geographic grid points, and the
final characteristic energies number fluxes (variable `alfa`, `alfa2`, `drizl`,
`flux1`, `flux2`) and auroral heating (`qteaur`: used in `subroutine`) at each
grid points are calculated in `subroutine` .

Number flux for the cusp precipitation is obtained in `subroutine` .

The detail of how to obtain ionization rates need to written in detail later. (`subroutines aurora_ions, aion and bion`). Formulas need to be added here too.

physical field	variable	unit	pressure level	timestep
Radii of convection flow reversal circle	θ_0 theta0	radians		t_n
Offset between the center of the convection circle and the geomagnetic pole along the geomagnetic noon and midnight line	offc	radians		t_n
Offset between the center of the convection circle and the geomagnetic pole along the geomagnetic dawn-dusk line	dskofc	radians		t_n
Potential at the center of the convection circle	pcen			t_n
Potential of the evening cell	psie			
Potential of the morning cell	psim			
Daytime entrance of convection in MLT-12 converted to radians	phid	radians		
Daytime exit of convection in MLT-12 converted to radians	phin	radians		
Negative departure from phid	phidm			
Positive departure from phid	phidp			
Positive departure from phin	phinp			
Negative departure from phin	phinm			
	rr1			
Sun's longitude in dipole coordinale (MAGFIELD.F)	sunlons			
Critical colatitudes (CONS.F)	crit			

Table 2.2: Input fields to `module heelis`. All these variables but `sunlons` and `crit` are specified in module `AURORA.F`

physical field	variable	unit	pressure level	timestep
Fractional presence of dynamo field	`Pfrac` (used in)			t_n
Heelis potential in geomagnetic coordinates	`phihm` (used in `dynamo.F`)			t_n

Table 2.3: Output fields of module `heelis.F`

physical field	variable	unit	pressure level	timestep
UT year, daynumber, hour				t_n
Sun's longitude in dipole coordinale (`MAGFIELD.F`)	`sunlons`			
Solar wind density		cm^3		t_n
Solar wind speed		km/s		t_n
IMF B_y, B_z		nT		t_n

Table 2.4: Input fields to module `weimer`.

physical field	variable	unit	pressure level	timestep
Radii of convection flow reversal circle	θ_0 `theta0`	radians		t_n
Offset between the center of the convection circle and the geomagnetic pole along the geomagnetic noon and midnight line	`offc`	radians		t_n
Offset between the center of the convection circle and the geomagnetic pole along the geomagnetic dawn-dusk line	`dskofc`	radians		t_n
Daytime entrance of convection in MLT-12 converted to radians	`phid`	radians		
Daytime exit of convection in MLT-12 converted to radians	`phin`	radians		
Radii of peak energy flux in the auroral circle	`rrad`	radians		t_n
Offset between the center of the auroral circle and the geomagnetic pole along the geomagnetic noon and midnight line	`offa`	radians		t_n
Offset between the center of the auroral circle and the geomagnetic pole along the geomagnetic dawn-dusk line	`dskofa`	radians		t_n
Fractional presence of dynamo field	`Pfrac` (used in)			t_n
Heelis potential in geomagnetic coordinates	`phihm` (used in `dynamo.F`)			t_n

Table 2.5: Output fields of module `weimer.F`.

physical field	variable	unit	pressure level	timestep
Cross polar cap potential	`ctpoten`			t_n
Hemisphere power	`power`			t_n
IMF By	`byimf`			
Sun's longitude in dipole coordinale (`magfield.F`)	`sunlons`			

Table 2.6: Input fields to module `aurora`.

physical field	variable	unit	pressure level	timestep
Radii of the convection flow reversal circle	θ_0 (theta0) (used in heelis.F)	radians		t_n
Offset between the center of the convection circle and the geomagnetic pole along the geomagnetic noon and midnight line	offc (used in heelis.F)	radians		t_n
Offset between the center of the convection circle and the geomagnetic pole along the geomagnetic dawn-dusk line	dskofc (used in heelis.F)	radians		t_n
Potential at the center of the convection circle	pcen (used in heelis.F)			t_n
Potential of the evening cell	psie (used in heelis.F)			
Potential of the morning cell	psim (used in heelis.F)			
Daytime entrance of convection in MLT-12 converted to radians	phid	radians		
Daytime exit of convection in MLT-12 converted to radians	phin	radians		
Negative departure from phid	phidm (used in heelis.F)			
Positive departure from phid	phidp (used in heelis.F)			
Positive departure from phin	phinp (used in heelis.F)			
Negative departure from phin	phinm (used in heelis.F)			

Table 2.7: Output fields of module aurora.F.

2.3   Lower Boundary

At the lower boundary of TI(M)EGCM the background thermosphere has to be specified. In addition tidal perturbations can be optionally added in. Note that not all TIMEGCM option for the lower boundary are describe here.

The lower boundary conditions in TIEGCM are specified at pressure level -7. Note that TIEGCM uses two different height grids. One is called the interface grid, which starts at the pressure level -7, the other one is called the midpoint level grid, which starts at -6.75 (height resolution 2 grid points per scale height), or -6.875 (height resolution 4 grid points per scale height). Except for the geopotential height, the vertical dimensionless velocity and the electron density, all fields are output on the midlevel grid.

In TIEGCM at the lower boundary (pressure level =-7, approximately at 97 km) we specify a constant background field for the geopotenial height of 96.37229 km, for the neutral temperature of 181.0 K, and the neutral zonal and meridional winds are set to zero. The background does not vary with day of the year.

Note that for TIMEGCM the lower boundary is at pressure level -17, approximately at 32 km. However concerning the interface and midpoint pressure levels TIMEGCM and TIEGCM are the same. The background field in TIMEGCM for the geopotential height are from an analytical fit to a model called zatmos , the neutral temperature is specified by the same model zatmos. Both fields vary with latitude and day of the year. The background neutral zonal and meridional winds at the lower boundary are calculated by assuming geostrophic balance. The calculation is done in `subroutine tuvbnd` . At the equator when the Coriolis force is zero, and geostrophic balance is not valid to assume, additional tunable Rayleigh friction is introduced (see `subroutine tuvbnd`). The background can also be specified by using daily averaged data from ECMWF for specific time periods.

In TIEGCM as well as TIMEGCM tidal perturbations caused by solar radiation can be added to the background. For classical tidal theory we refer to Chapman and Lindzen [1]. In TIEGCM only migrating tidal components which propagate westward with the apparent motion of the sun should be specified at either 2.5-degree/4 grid points per scale height or 5-degree/ 2

grid points per scale height resolution until nonmigrating tidal propagation is validated in the high resolution version of the TIEGCM. These components are thermally driven by the periodic absorption of solar radiation throughout the atmosphere, primarily the absorption of UV radiation by stratospheric ozone and of IR by water and water vapor in the troposphere. In TIMEGCM we recommend using migrating and non-migrating tides only with the double resolution version of TIMEGCM (version TIMEGCM1.3 and higher). The single resolution version of TIMEGCM is too coarse to capture the propagation of the tides in the right way. Non-migrating tides which can be include in TIMEGCM are global-scale waves, however they do not follow the apparent motion of the sun. They can either not propagate horizontally, move eastward or westward.

Both models provide two ways of specifying the migrating tidal perturbations:

- Hough Modes

- Global Scale Wave Model (GSWM)

However, we recommend using only the Global Scale Wave Model option to include tidal perturbations, and using Hough Modes only for numerical experiments done by experienced users. Both options will be explained in the following.

2.3.1   Migrating tides specified by Hough Modes

Using Hough modes is one way to decompose the tidal perturbations with respect to longitude and latitude for the different wave components. Hough functions are described in e.g. Chapman and Lindzen [1], Flattery [6]. A single tidal mode has a horizontal structure which can be described by a single Hough function. The atmospheric tides which migrate westward with the apparent motion of the Sun are called migrating tides. In TI(M)EGCM only a limited number of upward propagating migrating tidal modes are defined. The modes with a diurnal period have a wavenumber s=1, and a Hough Mode with (s,n)=(1,1) can be specified. For the semidiurnal modes with a wavenumber s=2 the following Hough modes can be specified: (2,2), (2,3), (2,3), (2,4), (2,5).
To specify the Hough modes the amplitude and phase of the corresponding

mode has to be given in the namelist read input for the semidiurnal tides `TIDE`, and the diurnal tides `TIDE2` by setting the amplitude and phase of the component. The order of the semidiurnal Hough mode specification is from n=2 (2,2) to n=5 (2,5). The amplitude has to be in [cm] and the phase of the Hough mode components

$$slt = -bhour + 12 \qquad (2.32)$$

with the solar local time *slt*, and *bhour* the phase of the tidal component in the TI(M)EGCM input. A 24 hrs/12 hrs shift may be applied to the diurnal / semidiurnal components since *bhour* should be

$$
\begin{aligned}
(-12 < bhour < 12) & \quad \text{for the diurnal} \\
(-6 < bhour < 6) & \quad \text{for the semidiurnal}
\end{aligned}
\qquad (2.33)
$$

2.3.2 Migrating and non-migrating tides specified by GSWM

The Global Scale Wave Model (GSWM) [7],[8] is a numerical model of planetary waves and solar tides in the Earth's atmosphere from 0 - 125 km developed at HAO (High Altitude Observatory), NCAR (National Center for Atmospheric Research) by M. Hagan. GSWM solves for non-migrating or migrating waves with 2-dimensional, linearized, steady-state assumptions and a realistic zonal mean atmosphere. The forcing is due to thermospheric absorption of solar extreme ultraviolet (EUV) radiation, absorption of solar radiation in the Schumann-Runge (S-R) bands and continuum in the mesopause region, strato-mesospheric absorption of solar ultraviolet (UV) radiation, tropospheric absorption of solar infrared (IR) radiation, and tropospheric latent heating associated with deep convective activity (DCA). GSWM also includes dissipation due to ion drag, thermal conductivity, molecular and eddy diffusivity, and gravity wave drag. Both migrating (sun-synchronous) and non-migrating (longitude-dependent) tidal components are included (s=-6 to 6) for both the diurnal and semidiurnal harmonics.

In TI(M)EGCM the use of GSWM at the lower boundary has to be specified by the namelist read parameters

- migrating diurnal tides (s=-6 to 6) `GSWM_MI_DI_NCFILE`

- migrating semidiurnal tides (s=-6 to 6) `GSWM_MI_SDI_NCFILE`

- ONLY TIMEGCM: non-migrating diurnal tides (s=-6 to 6)
  `GSWM_NM_DI_NCFILE`

- ONLY TIMEGCM: non-migrating semidiurnal tides (s=-6 to 6)
  `GSWM_NM_SDI_NCFILE`

and the location of the corresponding GSWM file. Note that compared to the Hough mode approach the perturbations at each grid point will be provided, already including the 13 wavenumbers (s=-6 to s=6).

2.3.3   Specifics about the Lower Boundary of TIMEGCM

This chapter applies to TIMEGCM version 1.41 and higher. The basic change with respect to the lower boundary compared to older versions is that we separate the background from the perturbations of the geopotential height Z, the neutral temperature Tn, and the neutral wind components Un and Vn. The lower boundary in TIME-GCM is at pressure level -17, approximately at 32 km.

Background fields

In the model we set the background in `subroutine lbc`. There are three options available, and all have in common that these are daily values, so no tidal perturbations are included.

- ECMWF (only 2.5 deg): sets Z, Tn, Un, Vn

- NCEP (only 5 deg): sets Z, Tn + calculation of Un, Vn

- model zatmos (2.5 and 5 deg): sets Z, Tn + calculation of Un, Vn

zatmos is an analytical model which sets the geopotential height and the neutral temperature. For both background cases using NCEP and the model zatmos the neutral winds are not specified, and have to be calculated. In TIME-GCM this is done in `subroutine uvbgrd`, and for the first two time steps in `subroutine uvbnd`. The calculation of the neutral winds at the lower boundary is using the background fields of Z. It's considering horizontal advection, the pressure gradient force, and horizontal diffusion on the left hand side, and the right hand side consists of the Coriolis force, Rayleigh friction and momentum force. It should be added that there is some tuning

friction close to the equator which is set to zero. The time derivative of the neutral winds are discretized and split on the left and right hand side. We are not using the vertical advection term anymore. This term had a neglectable influence on the winds at the lower boundary, and it wouldn't have justified the effort to separate the term into a background and perturbations. The `subroutine uvbnd` calculates the winds fields for the background and the perturbations while `subroutine uvbgrd` calculates it only for the background. Except for the first two time steps, when the splitting into background and perturbations of Z, Un, Vn from the two previous time step is not know, `subroutine uvbgrd` is called to determine the background winds.

Perturbations fields

The perturbations of tides and waves are set in `subroutine lbc`, after the background is specified. The options are:

- Hough Modes (2.5 and 5 deg): sets Z, Tn, Un, Vn

- GSWM: sets Z, Tn, Un, Vn

    – migrating (2.5 and 5 deg)
    – nonmigrating (only 5 deg)

- planetary waves etc. (2.5 and 5 deg): sets Z, Tn + calculation of Un, Vn

The planetary wave etc. option is not tested in the model, and the source code is just kept. Also since only the geopotential and neutral temperature from these waves are set the winds have to be calculated like it is done for the background. Therefore only for this perturbation option the perturbations are added to the background field, and then the background + planetary wave neutral winds are determined in `subroutine uvbgrd`. The nonmigrating tides from GSWM should only be used with the 2.5 degree grid resolution since otherwise the tidal propagation is not right.

Chapter 3

Neutral Dynamics

The TIE-GCM solves the primitive equations in pressure coordinate, and the detailed information on the equations and the numerics employed can be found in [3]. In this Chapter, we will first give a brief summary of the model dynamics, and then discuss the main components in solving dynamic equations. The solution of the thermodynamics will be discussed in the next Chpater.

The zonal and meridional winds are solved from the momentum equations in the zonal and meridional direction, respectively. The tendencies (acceleration) of the horizontal winds come from horizontal and vertical momentum transport, horizontal gradient of geopotential, eddy and molecular viscosity, Coriolis force, and ion drag (Section 3.3). The vertical wind is determined from the continuity equation by integrating the divergence of the horizontal winds vertically (Section 3.2). The geopotential is calculated from the hydrostatic equation by integrating temperature vertically (Section 3.1).

The equations are solved using 4th order finite difference method. The vertical grid is staggered with horizontal winds, neutral, ion, and electron temperature, and mass mixing ratios defined on the so-called midpoints, and vertical wind and geopotential defined on the interfaces. Leapfrog scheme is used for time integration of momentum transport, geopontential gradient, Coriolis force, and ion drag, and implicit scheme is used for eddy and molecular viscosity in the vertical direction. To achieve better numerical stability, Shapiro filter (reference?) is applied in meridional and zonal directions.

physical field	variable	unit	pressure level	timestep
neutral temperature	T_n	K	midpoints	t_n
mass mixing ration of O	Ψ_O	–	midpoints	t_n
mass mixing ration of O_2	Ψ_{O_2}	–	midpoints	t_n
neutral meridional velocity	v_n	cm/s	midpoints	t_n

Table 3.1: Input fields to `subroutine addiag`

physical field	variable	unit	pressure level	timestep
$\cos\lambda\cdot$ neutral meridional velocity	$\cos\lambda v_n$	cm/s	midpoints	t_n
mean molecular mass	$\overline{m}$	$g/mole$	interfaces	$t_n + \Delta t$
conversion factor mmr to $\#/cm^3$	$N\overline{m}$ `xnmbar`	$\#/cm^3 g/mole$	midpoints	$t_n + \Delta t$??
conversion factor mmr to $\#/cm^3$	$N\overline{m}$ `xnmbari`	$\#/cm^3 g/mole$	interfaces	$t_n + \Delta t$??
conversion factor mmr to $\#/cm^3$	$N\overline{m}$ `xnmbarm`	$\#/cm^3 g/mole$	midpoints	$t_n + \Delta t$??

Table 3.2: Output fields of `subroutine addiag`

3.1 Calculation of geopotential height

The input to `subroutine addiag` is summarized in table 3.1. The output of `subroutine addiag` is summarized in table 3.2. The module data of `subroutine addiag` is summarized in table 3.3. First the term $\cos\lambda v_n$ is calculated on the midpoint pressure level and stored in the variable `vc`. The mean molecular mass is determined by

$$\overline{m} = \left[\frac{\Psi_{O_2}}{m_{O_2}} + \frac{\Psi_O}{m_O} + \frac{\Psi_{N_2}}{m_{N_2}} \right]^{-1} \tag{3.1}$$

with the mass mixing ratio of N_2 determined by $\Psi_{N_2} = 1 - \Psi_O - \Psi_{O_2}$. Before the mean molecular weight is returned from the subroutine it is transferred

physical field	variable	unit	pressure level	timestep
cosinus	$\cos\lambda$	$-$	-	$-$
height step	Δz	$-$	-	$-$
dzgrav	g/R^*		interfaces	t_n
timestep size	Δt	s	-	$-$
expz	$e^{-z-\frac{1}{2}\Delta z}$	$-$	midpoints	$-$
expzmid	$e^{-\frac{1}{2}\Delta z}$	$-$	-	$-$
expzmid_inv	$e^{\frac{1}{2}\Delta z}$	$-$	-	$-$
Boltzman constant	k_B	$1.38\cdot10^{16}$	-	t_n
freqsemidi	$\frac{4\Pi}{24\cdot60\cdot60}$	rad/s	-	$-$
ci		$(0,1)$	interfaces	t_n

Table 3.3: Module data of `subroutine addiag`

to the interface pressure level by averaging.

$$\overline{m}(z) = \frac{1}{2}\left(\overline{m}(z+\frac{1}{2}\Delta z) + \overline{m}(z-\frac{1}{2}\Delta z)\right) \tag{3.2}$$

with the lower boundary value extrapolated

$$\overline{m}(z_{bot}) = 1.5\overline{m}(z_{bot}+\frac{1}{2}\Delta z) - 0.5\overline{m}(z_{bot}+\frac{3}{2}\Delta z) \tag{3.3}$$

The conversion factor from mass mixing ratio to number density is first evaluated at the midpoint level

$$n\overline{m}(z+\frac{1}{2}\Delta z) = p_0 e^{-z-\frac{1}{2}\Delta z}\frac{\overline{m}(z+\frac{1}{2}\Delta z)}{k_B T_n(z+\frac{1}{2}\Delta z)} \tag{3.4}$$

which is stored in the variable `xnmbarm`. I'm not sure why this is done, but again is the conversion factor from mass mixing ratio to number density calculated and stored in `xnmbar`. The only difference to the above factor is that now the mean molecular mass is already on the interface pressure level and converted back to the midpoint pressure level. Afterward the mean molecular mass on the interface pressure level is determined

$$n\overline{m}(z) = p_0 e^{\frac{1}{2}\Delta z}e^{-z-\frac{1}{2}\Delta z}\frac{\overline{m}(z)}{k_B T_n(z)} \tag{3.5}$$

with $T_n(z_{top}) = T_n(z_{top} - \frac{1}{2}\Delta z)$, and the value $e^{-\frac{1}{2}\Delta z}e^{-z_{top}+\frac{1}{2}\Delta z}$ at the upper boundary.

The geopotential height is calculated by using the hydrostatic equation

$$\frac{\partial Z}{\partial z} = \frac{R^* T_n}{\overline{m}g} = H \tag{3.6}$$

with $\Delta Z = H\Delta z$. First the term $H\Delta z$ is set which is stored in the variable `w1`

$$w1(z + \frac{1}{2}\Delta z) = \frac{\Delta z R^*}{g}\frac{T_n(z + \frac{1}{2}\Delta z)}{\overline{m}(z + \frac{1}{2}\Delta z)} \tag{3.7}$$

The lower boundary values of the geopotential height are set from the Hough modes or GSWM with possible contribution from the semidiurnal migrating tide Z_{SD}, the migrating diurnal tide Z_D, the annual tide Z_A, and the non-migrating semidiurnal and diurnal tides Z_{nSD} and Z_{nD}, respectively.

$$Z(z_{bot}) = Z_{SD} + Z_D + Z_A + Z_{nSD} + Z_{nD} \tag{3.8}$$

All the tidal contributions are defined at the lower boundary pressure level $z = -7$. The geopotential height is evaluated then by

$$Z(z + \Delta z) = w1(z + \frac{1}{2}\Delta z) + Z(z) \tag{3.9}$$

with $w1 = \frac{\Delta z R^*}{g}\frac{T_n}{\overline{m}}$ (see eq. (3.7))

physical field	variable	unit	pressure level	timestep
neutral zonal velocity	u_n	cm/s	midpoints	t_n
neutral meridional velocity	$\cos \lambda v_n$	cm/s	midpoints	t_n

Table 3.4: Input fields to `subroutine swdot`

physical field	variable	unit	pressure level	timestep
'dimensionless' vertical velocity	W	$1/s$	interfaces	$t_n + \Delta t$

Table 3.5: Output fields of `subroutine swdot`

3.2   Calculation vertical velocity W

The input to `subroutine swdot` is summarized in table 3.4. The output of `subroutine swdot` is summarized in table 3.5. The vertical velocity is calculated by solving the continuity equation of the thermospheric neutral gas. The continuity equation takes the following form

$$\frac{1}{R \cos \lambda} \frac{\partial}{\partial \lambda}(v_n \cos \lambda) + \frac{1}{R \cos \lambda} \frac{\partial u_n}{\partial \phi} + e^z \frac{\partial}{\partial Z}(e^{-z}W) = 0 \qquad (3.10)$$

with the 'dimensionless' vertical velocity is $W = \frac{dZ}{dt}$. The 'real' vertical velocity w relative to a pressure level (note that for the vertical velocity relative to the ground you have to add the vertical movement of the pressure level) is obtained by integrating the continuity equation over Z to get W, and then multiply W by the scale height H.

The horizontal divergence $\nabla_H \cdot \mathbf{v}_n$ is calculated in `subroutine divrg`.

$$
\begin{aligned}
\nabla_H \cdot \mathbf{v}_n = & \frac{1}{R_E \cos \lambda} [\frac{2}{3\Delta\phi} \left[u_n(\phi + \Delta\phi, \lambda) u_n(\phi - \Delta\phi, \lambda) \right] - \\
& \frac{1}{12\Delta\phi} \left[u_n(\phi + 2\Delta\phi, \lambda) u_n(\phi - 2\Delta\phi, \lambda) \right] \\
& \frac{2}{3\Delta\phi} \left[\cos(\lambda + \Delta\lambda) v_n(\phi, \lambda + \Delta\lambda) \cos(\lambda - \Delta\lambda) v_n(\phi, \lambda - \Delta\lambda) \right] - \\
& \frac{1}{12\Delta\lambda} \left[v_n(\phi, \lambda + 2\Delta\lambda) v_n(\phi, \lambda - 2\Delta\lambda) \right]]
\end{aligned}
\tag{3.11}
$$

The integration is done by an integration from the top to the bottom of the model, with the condition at the upper boundary being

$$
\frac{\partial w}{\partial z} = 0 \tag{3.12}
$$

and in descritized form

$$
W(z_{top}) = \nabla_H \cdot \mathbf{v}_n (z_{top} - \frac{1}{2}\Delta z) \tag{3.13}
$$

and then do the integration

$$
W(z - \Delta z) = e^{-\frac{1}{2}z} \left[e^{-\frac{1}{2}z} W(z - 2\Delta z) + \Delta z \nabla_H \cdot \mathbf{v}_n (z + \frac{1}{2}\Delta z) \right] \tag{3.14}
$$

The vertical velocity W is then filtered in longitude to remove the high wave numbers. The filter is in `subroutine filter_w` and is part of the file `swdot.F`.

3.3 Momentum equation

The input to `subroutine duv` is summarized in table 3.6. The output of `subroutine duv` is summarized in table 3.7. The zonal and meridional momentum equation is solved to get the neutral horizontal velocities u_n and v_n. For the vertical velocity the continuity 3.10 equation is solved. In the code the `subroutine addiag` solves for the dimensionless vertical velocity w.

The momentuum equation in the zonal direction can be written as

$$\frac{\partial u_n}{\partial t} = \frac{ge^z}{p_0}\frac{\partial}{\partial Z}\left[\frac{\mu \partial u_n}{H \partial Z}\right] + f^{cor}v_n + \lambda_{xx}(v_{ExB,x} - u_n) + \lambda_{xy}(v_{ExB,y} - v_n) -$$

$$\mathbf{v}_n \cdot \nabla u_n + \frac{u_n v_n}{R_E}\tan\lambda - \frac{1}{R_E cos\lambda}\frac{\partial \Phi}{\partial \phi} - W\frac{\partial u_n}{\partial Z} - hd_u \tag{3.15}$$

with λ_{xx} and λ_{xy} the ion drag coefficients. The meridional momentum equation is defined as

$$\frac{\partial v_n}{\partial t} = \frac{ge^z}{p_0}\frac{\partial}{\partial Z}\left[\frac{\mu \partial v_n}{H \partial Z}\right] - f^{cor}v_n + \lambda_{yy}(v_{ExB,x} - u_n) + \lambda_{yx}(v_{ExB,y} - u_n) -$$

$$\mathbf{v}_n \cdot \nabla v_n + \frac{u_n u_n}{R_E}\tan\lambda - \frac{1}{R_E}\frac{\partial \Phi}{\partial \lambda} - W\frac{\partial v_n}{\partial Z} - hd_v \tag{3.16}$$

Horizontal diffusion hd_u and hd_v is also included in the momentum equations (needs documentation look at hdiff3; not consistent in equations) The time rate of change in the horizontal velocity on the left hand (1. term) side is equal to the forcing terms on the right hand side. The forcing terms are the following in this order: the vertical viscosity (2. term), the Coriolis force (3. term), the ion-drag force (4.+5. term), the nonlinear horizontal advection (6. term) and momentum force (7. term), the pressure gradient force (8. term),the vertical advection (9. term) and horizontal diffusion (10.term). Using a Leapfrog scheme leads to

$$\frac{u_n^{t+\Delta t} - u_n^{t-\Delta t}}{2\Delta t} = \frac{ge^z}{p_0}\frac{d}{dz}\left[\frac{\mu d u_n^{t+\Delta t}}{H dz}\right] + fv_n^{t+\Delta t} + \lambda_{xx}(v_{ExB,x}^t - u_n^{t+\Delta t}) +$$

$$\lambda_{xy}(v_{ExB,y}^t - v_n^{t+\Delta t}) - \mathbf{v}_n^t \cdot \nabla u_n^t + \tag{3.17}$$

$$\frac{u_n^{t+\Delta t}v_n^t}{R_E}\tan\lambda - \frac{1}{R_E cos\lambda}\frac{d\Phi^{t+\Delta t*}}{d\phi} - W^{t+\Delta t}\frac{du_n^{t+\Delta t}}{dZ}$$

and

$$\frac{v_n^{t+\Delta t} - v_n^{t-\Delta t}}{2\Delta t} = \frac{ge^z}{p_0}\frac{d}{dZ}\left[\frac{\mu dv_n^{t+\Delta t}}{HdZ}\right] - fu_n^{t+\Delta t} + \lambda_{yy}(v_{ExB,y}^t - v_n^{t+\Delta t})+$$
$$\lambda_{yx}(v_{ExB,x}^t - u_n^{t+\Delta t}) - \mathbf{v}_n^t \cdot \nabla v_n^t - \quad\quad (3.18)$$
$$\frac{u_n^{t+\Delta t}u_n^t}{R_E}\tan\lambda - \frac{1}{R_E}\frac{d\Phi^{t+\Delta t*}}{d\lambda} - W^{t+\Delta t}\frac{dv_n^{t+\Delta t}}{dZ}$$

The terms of the discretized equation are added to the matrices $\mathbf{Q}$ at the height level k, $\mathbf{P}$ at $k-1$, and $\mathbf{R}$ at $k+1$. The first line in the matrices is the zonal equation and the second line the meridional one. In the following text we will describe the contribution to the matrices for each term. The right hand side goes into **rhs**. Note that in the code the two equations are divided by e^z

The time derivatives $\frac{u_n^{t+\Delta t}-u_n^{t-\Delta t}}{2\Delta t}$ i.e. $\frac{v_n^{t+\Delta t}-v_n^{t-\Delta t}}{2\Delta t}$ lead to

$$\mathbf{Q}^1 = e^{-z}\begin{pmatrix} \frac{1}{2\Delta t} & 0 \\ 0 & \frac{1}{2\Delta t} \end{pmatrix} \quad\quad (3.19)$$

in units of $1/s$, and the right hand side

$$\mathbf{RHS}^1 = e^{-z}\begin{pmatrix} \frac{u_n^{t-\Delta t,smooth}}{2\Delta t} + hd_u \\ \frac{v_n^{t-\Delta t,smooth}}{2\Delta t} + hd_v \end{pmatrix} \quad\quad (3.20)$$

in units of cm/s^2 with hd_u and hd_v the horizontal diffusion terms calculated in `subroutine hdiff3` . The velocities $u_n^{t-\Delta t}$ and $v_n^{t-\Delta t}$ at the previous timestep $t-\Delta t$ are smoothed with the Shapiro method. First in meridional direction and then a zonal smoothing is applied.

$$f_{merid}^{smooth} = f(\phi,\lambda) - c_{shapiro}\{f(\phi,\lambda+2\Delta\lambda) + f(\phi,\lambda-2\Delta\lambda)-$$
$$4\left[f(\phi,\lambda+\Delta\lambda) + f(\phi,\lambda-\Delta\lambda)\right] + 6f(\phi,\lambda)\} \quad\quad (3.21)$$
$$f_{zonal}^{smooth} = f_{merid}^{smooth} - c_{shapiro}\{f_{merid}^{smooth}(\phi+2\Delta\phi,\lambda) + f_{merid}^{smooth}(\phi-2\Delta\phi,\lambda)-$$
$$4\left[f_{merid}^{smooth}(\phi+\Delta\phi,\lambda) + f_{merid}^{smooth}(\phi-\Delta\phi,\lambda)\right] + 6f_{merid}^{smooth}(\phi,\lambda)\}$$
$$(3.22)$$

The Shapiro constant is set to $c_{shapiro} = 0.03$. The smoothing is done in the `subroutine smooth`.

The vertical viscosity term includes the eddy μ_{ed} and molecular μ_{mol} viscosity.

$$\frac{ge^z}{p_0}\frac{d}{dz}\left[\frac{\mu du_n^{t+\Delta t}}{HdZ}\right] = e^z\frac{g^2(\mu_{ed}+\mu_{mol})\overline{m}}{p_0 k_B T_n^{int}\Delta z^2} \tag{3.23}$$

with $\frac{1}{H} = \frac{g\overline{m}}{k_B T_n}$. The term is calculated at the interface level. We substitute in the following in $[1/s]$

$$\frac{f_{vis}}{\Delta z^2} = \frac{g^2\mu\overline{m}}{p_0 k_B T_n^{int}\Delta z^2} \tag{3.24}$$

The second derivative is discretized by

$$\begin{aligned}
\frac{\partial}{\partial z}\left(f_{vis}\frac{\partial u_n^{t+\Delta t}}{\partial z}\right)(z+\frac{1}{2}\Delta z) &= \frac{\left[f_{vis}^{int}\frac{\partial u_n^{t+\Delta t}}{\partial z}\right](z+\Delta z) - \left[f_{vis}^{int}\frac{\partial u_n^{t+\Delta t}}{\partial z}\right](z)}{\Delta z} = \\
&= \frac{1}{\Delta z}(f_{vis}(z+\Delta z)\frac{u_n(z+\frac{3}{2}\Delta z)-u_n(z+\frac{1}{2}\Delta z)}{\Delta z} \\
&- f_{vis}(z)\frac{u_n(z+\frac{1}{2}\Delta z)-u_n(z-\frac{1}{2}\Delta z)}{\Delta z}) = \\
&= \frac{1}{\Delta z^2}(f_{vis}(z)u_n(z+\frac{3}{2}\Delta z) \\
&- (f_{vis}(z+\Delta z)+f_{vis}(z))u_n(z+\frac{1}{2}\Delta z) + f_{vis}(z)u_n(z-\frac{1}{2}\Delta z))
\end{aligned} \tag{3.25}$$

Note that f_{vis} is at the interface level with z denoting the index k, and the neutral velocity on the midpoints with $z+\frac{1}{2}\Delta z$ being the k level. The same applies to the derivative of the meridional velocity. The terms from the above equation are added to the matrices $\mathbf{Q}$ for the height level k, $\mathbf{R}$ for the values at the level $k+1$, and $\mathbf{P}$ for the $k-1$ height level

$$\mathbf{Q}^2 = \mathbf{Q}^1 + \begin{pmatrix} \frac{1}{\Delta z^2}(f_{vis}(z+\Delta z)+f_{vis}(z)) & 0 \\ 0 & \frac{1}{\Delta z^2}(f_{vis}(z+\Delta z)+f_{vis}(z)) \end{pmatrix} \tag{3.26}$$

$$\mathbf{P}^2 = \begin{pmatrix} -\frac{1}{\Delta z^2}f_{vis}(z) & 0 \\ 0 & -\frac{1}{\Delta z^2}f_{vis}(z) \end{pmatrix} \tag{3.27}$$

$$\mathbf{R}^2 = \begin{pmatrix} -\frac{1}{\Delta z^2} f_{vis}(z + \Delta z) & 0 \\ 0 & -\frac{1}{\Delta z^2} f_{vis}(z + \Delta z) \end{pmatrix} \tag{3.28}$$

The third terms in the momentuum equations $f^{cor} v_n^{t+\Delta t}$ and $-f^{cor} u_n^{t+\Delta t}$ are the Coriolis forcing with the Coriolis parameter $f^{cor} = 2\Omega \sin \lambda$. The terms are added to the matrix $\mathbf{G}$ in units of $[1/s]$

$$\mathbf{Q}^3 = \mathbf{Q}^2 + e^{-z} \begin{pmatrix} 0 & -f^{cor} \\ f^{cor} & 0 \end{pmatrix} \tag{3.29}$$

The fourth and fifth term in the momentuum equation $\lambda_{xx}(v_{ExB,x} - u_n^{t+\Delta t}) + \lambda_{xy}(v_{ExB,y} - v_n^{t+\Delta t})$ and $\lambda_{yy}(v_{ExB,x} - u_n^{t+\Delta t}) + \lambda_{yx}(v_{ExB,y} - u_n^{t+\Delta t})$ are the ion drag terms. The terms with the electrodynamic drift velocity are added to the right hand side.

$$\mathbf{RHS}^2 = \mathbf{RHS}^1 + e^{-z} \begin{pmatrix} \lambda_{xx}^{t,mid} v_{ExB,x}^{t,mid} + \lambda_{xy}^{t,mid} v_{ExB,y}^{t,mid} \\ \lambda_{yy}^{t,mid} v_{ExB,y}^{t,mid} - \lambda_{yx}^{t,mid} v_{ExB,x}^{t,mid} \end{pmatrix} \tag{3.30}$$

The values $\lambda_{**}^{t,mid}$ and $v_{ExB,*}^{t,mid}$ are the ion drag coefficient and the electrodynamic drift velocity at the time step t and at the midpoints. Therefore in the code the values from the interface height level k and $k+1$ are averaged to get the midpoints values. Both the ion drag coefficients and the electrodynamic drift velocity are on the interface levels.
The terms with the neutral velocity are added to the left hand side in units of $[1/s]$.

$$\mathbf{Q}^3 = \mathbf{Q}^2 + e^{-z} \begin{pmatrix} \lambda_{xx}^{t,mid} & \lambda_{xy}^{t,mid} \\ -\lambda_{yx}^{t,mid} & \lambda_{yy}^{t,mid} \end{pmatrix} \tag{3.31}$$

The horizontal advection terms in zonal direction $-\mathbf{v}_n^t \cdot \nabla u_n^t$ and meridional direction $-\mathbf{v}_n^t \cdot \nabla v_n^t$ are added to the right hand side in units of $[cm/s^2]$.

$$\mathbf{RHS}^3 = \mathbf{RHS}^2 + e^{-z} \begin{pmatrix} -\mathbf{v}_n^t \cdot \nabla u_n^t \\ -\mathbf{v}_n^t \cdot \nabla v_n^t \end{pmatrix} = \mathbf{RHS}^2 + e^{-z} \begin{pmatrix} -u_n^t \frac{\partial u_n^t}{\partial \phi} - v_n^t \frac{\partial u_n^t}{\partial \lambda} \\ -u_n^t \frac{\partial v_n^t}{\partial \phi} - v_n^t \frac{\partial v_n^t}{\partial \lambda} \end{pmatrix} \tag{3.32}$$

The advection term is calculated in the `subroutine advec` by taking the fourth order stencil for the derivative. The average velocity is denoted by $u_n^{avg} = \frac{1}{2}(u_n(\phi + \Delta\phi, \lambda) + u_n(\phi - \Delta\phi, \lambda))$ and $u_n^{2avg} = \frac{1}{2}(u_n(\phi + 2\Delta\phi, \lambda) +$

$u_n(\phi - 2\Delta\phi, \lambda))$. The same is done for the meridional velocity v_n which leads to $v_n^{avg} = \frac{1}{2}(v_n(\phi, \lambda + \Delta\lambda) + v_n(\phi, \lambda - \Delta\lambda))$ and $v_n^{2avg} = \frac{1}{2}(v_n(\phi, \lambda + 2\Delta\lambda) + v_n(\phi, \lambda - 2\Delta\lambda))$. The discrete advection of the zonal velocity for the point (ϕ, λ) is

$$u_n \frac{\partial u_n}{\partial \phi}(\phi, \lambda) = \frac{1}{R_E cos\lambda}(\frac{2}{3\Delta\phi}u_n^{avg}(\phi, \lambda)\left[u_n(\phi + \Delta\phi, \lambda) - u_n(\phi - \Delta\phi, \lambda)\right] -$$
$$\frac{1}{12\Delta\phi}u_n^{2avg}(\phi, \lambda)\left[u_n(\phi + 2\Delta\phi, \lambda) - u_n(\phi - 2\Delta\phi, \lambda)\right]) \quad (3.33)$$

and

$$v_n \frac{\partial u_n}{\partial \lambda}(\phi, \lambda) = \frac{1}{R_E}(\frac{2}{3\Delta\lambda}v_n^{avg}(\phi, \lambda)\left[u_n(\phi, \lambda + \Delta\lambda) - u_n(\phi, \lambda - \Delta\lambda)\right] -$$
$$\frac{1}{12\Delta\lambda}v_n^{2avg}(\phi, \lambda)\left[u_n(\phi, \lambda + 2\Delta\lambda) - u_n(\phi, \lambda - 2\Delta\lambda)\right]) \quad (3.34)$$

$$u_n \frac{\partial v_n}{\partial \phi}(\phi, \lambda) = \frac{1}{R_E cos\lambda}(\frac{2}{3\Delta\phi}u_n^{avg}(\phi, \lambda)\left[v_n(\phi + \Delta\phi, \lambda) - v_n(\phi - \Delta\phi, \lambda)\right] -$$
$$\frac{1}{12\Delta\phi}u_n^{2avg}(\phi, \lambda)\left[v_n(\phi + 2\Delta\phi, \lambda) - v_n(\phi - 2\Delta\phi, \lambda)\right]) \quad (3.35)$$

and

$$v_n \frac{\partial v_n}{\partial \lambda}(\phi, \lambda) = \frac{1}{R_E}(\frac{2}{3\Delta\lambda}v_n^{avg}(\phi, \lambda)\left[v_n(\phi, \lambda + \Delta\lambda) - v_n(\phi, \lambda - \Delta\lambda)\right] -$$
$$\frac{1}{12\Delta\lambda}v_n^{2avg}(\phi, \lambda)\left[v_n(\phi, \lambda + 2\Delta\lambda) - v_n(\phi, \lambda - 2\Delta\lambda)\right]) \quad (3.36)$$

The advection term is calculated at midpoints and is in units of $[cm/s^2]$. The 8. term is due to the horizontal momentum in the zonal direction $\frac{u_n^{t+\Delta t}v_n^t}{R_E}\tan\lambda$ and the meridional one $\frac{u_n^{t+\Delta t}u_n^t}{R_E}\tan\lambda$. These terms are added to the left hand side $\mathbf{G}$ matrix in $[1/s]$.

$$\mathbf{Q}^4 = \mathbf{Q}^3 + e^{-z}\begin{pmatrix} 0 & -\frac{v_n^t}{R_E}\tan\lambda \\ \frac{u_n^t}{R_E}\tan\lambda & 0 \end{pmatrix} \quad (3.37)$$

in the code it's $+\frac{u_n^t}{R_E}\tan\lambda$ due to northward/meridional direction.

The pressure gradient term in the zonal and meridional directions is $-\frac{1}{R_E \cos\lambda}\frac{d\Phi^{t+\Delta t*}}{d\phi}$

and $-\frac{1}{R_E}\frac{d\Phi^{t+\Delta t*}}{d\lambda}$ (9. term) which is added to the right hand side matrix **RHS** in units of $[cm/s^2]$

$$\mathbf{RHS}^3 = \mathbf{RHS}^2 + e^{-z}\left(\begin{matrix} -\frac{1}{R_E\cos\lambda}\frac{d\Phi^{t+\Delta t*}}{d\phi} \\ -\frac{1}{R_E}\frac{d\Phi^{t+\Delta t}}{d\lambda} \end{matrix}\right) \tag{3.38}$$

The geopotential is calculated in `subroutine glp`. The input to `subroutine glp` is summarized in table 3.8. The output of `subroutine glp` is summarized in table 3.7. The parameters are summarized in table 3.10. Firstly, an average temperature $\overline{T}_n$ is calculated by using

$$\overline{T}_n = T_n^t + wgt * \left[-2T_n^t + T_n^{t-\Delta t} + T_n^{t+\Delta t}\right] \tag{3.39}$$

The mean molecular weight is determined at the midpoints by

$$\overline{m}(k+\frac{1}{2}) = 0.5 * (\overline{m}(k)\overline{m}(k+1)) = \overline{m}^{mid}(k) \tag{3.40}$$

The geopotenial is defined by the hydrostatic equation

$$\frac{\partial\Phi}{\partial z} = \frac{R^*\overline{T}_n}{\overline{m}} \tag{3.41}$$

which is integrated from the bottom of the model to the top.

$$z^*(k) = z^{t+\Delta t*}(k) = \int_{k_{bot}}^{k(z)} \frac{R^*\overline{T}_n}{g\overline{m}^{mid}}\Delta Z \tag{3.42}$$

in units of $[cm]$ with $\Phi = Zg$, the gas constant R^* in $[erg/K/mol]$, and the mean mass $\overline{m}$ in $[g/mole]$. The geopotential height uses already an mix of neutral temperature, which includes $T_n^{t+\Delta t}$ and there it's neither z^t not $z^{t+\Delta t}$. ??? check units???. Note that $z^* = z^{t+\Delta t*}$ is at the interfaces, since the value which is integrated is on the midlevels.

The derivatives are determined in `subroutine dldp` by taking the fourth order derivative. In the zonal direction the previous calculated geopotential height $z^{t+\Delta t*}$ is used while in the latitudinal direction the updated geopoten-

tial height $z^{t+\Delta t}$ is applied.

$$
\frac{dz^*}{d\phi}(\phi, \lambda, z) = \frac{2}{3\Delta\phi}[z^*(\phi + \Delta\phi, \lambda, z) - z^*(\phi - \Delta\phi, \lambda, z)] -
$$
$$
\frac{1}{12\Delta\phi}[z^*(\phi + 2\Delta\phi, \lambda, z) - z^*(\phi - 2\Delta\phi, \lambda, z)] \qquad (3.43)
$$
$$
\frac{dz^*}{d\lambda}(\phi, \lambda, z) = \frac{2}{3\Delta\lambda}[z^*(\phi, \lambda + \Delta\lambda, z) - z^*(\phi, \lambda - \Delta\lambda, z)] -
$$
$$
\frac{1}{12\Delta\phi}[z^*(\phi, \lambda + 2\Delta\lambda, z) - z^*(\phi, \lambda - 2\Delta\lambda, z)] \qquad (3.44)
$$

in units of $[cm]$. The derivatives are the transfered from the interface levels to the midpoint level by

$$
\frac{1}{R_E \cos\lambda}\frac{d\Phi}{d\phi}(\phi, \lambda, z) = \frac{1}{2}g\frac{1}{R_E \cos\lambda}\left[\frac{dz^*}{d\phi}(\phi, \lambda, z) + \frac{dz^*}{d\phi}(\phi, \lambda, z + \Delta z)\right]
$$
$$
(3.45)
$$
$$
\frac{1}{R_E}\frac{d\Phi}{d\lambda}(\phi, \lambda, z) = \frac{1}{2}g\frac{1}{R_E}\left[\frac{dz^*}{d\lambda}(\phi, \lambda, z) + \frac{dz^*}{d\lambda}(\phi, \lambda, z + \Delta z)\right] \qquad (3.46)
$$

which is in $[cm/s^2]$. The periodic points are set to zero.

The final term is the vertical advection term $-W^{t+\Delta t}\frac{du_n^{t+\Delta t}}{dZ}$ and $-W^{t+\Delta t}\frac{dv_n^{t+\Delta t}}{dZ}$. The terms are added to the left hand side matrix $\mathbf{P}$ and $\mathbf{R}$ in $[1/s]$

$$
\mathbf{P}^3 = \mathbf{P}^2 + e^{-z}\begin{pmatrix} -\frac{W^{mid,t+\Delta t}}{2\Delta z} & 0 \\ 0 & -\frac{W^{mid,t+\Delta t}}{2\Delta z} \end{pmatrix} \qquad (3.47)
$$

$$
\mathbf{R}^3 = \mathbf{R}^2 + e^{-z}\begin{pmatrix} \frac{W^{mid,t+\Delta t}}{2\Delta z} & 0 \\ 0 & i\frac{W^{mid,t+\Delta t}}{2\Delta z} \end{pmatrix} \qquad (3.48)
$$

The lower boundary is taken into account by extrapolating the values of the matrix $\mathbf{P}$

$$
\mathbf{P}(z_{bot} - \frac{1}{2}\Delta z)\mathbf{v}(z_{bot} - \frac{1}{2}\Delta z) = 2\mathbf{P}(z_{bot})\mathbf{v}_{LB} - \mathbf{P}(z_{bot} + \frac{1}{2}\Delta z)\mathbf{v}(z_{bot} + \frac{1}{2}\Delta z)
$$
$$
(3.49)
$$

with $z_{bot} + \frac{1}{2}\Delta z$ on the midpoint level having the height index 1. The value $\mathbf{P}(z_{bot})$ is set to $\mathbf{P}(z_{bot} + \frac{1}{2}\Delta z)$, and the neutral velocity at the lower boundary

is $\mathbf{v}(z_{bot}) = \mathbf{v}_{LB}$. Therefore, substituting the lower boundary condition into the equation leads to

$$\mathbf{Q}(z_{bot} + \frac{1}{2}\Delta z)^* = \mathbf{Q}(z_{bot} + \frac{1}{2}\Delta z) - \mathbf{P}(z_{bot} + \frac{1}{2}\Delta z) \tag{3.50}$$

$$\mathbf{RHS}(z_{bot} + \frac{1}{2}\Delta z)^* = \mathbf{RHS}(z_{bot} + \frac{1}{2}\Delta z) - 2\mathbf{P}(z_{bot} + \frac{1}{2}\Delta z)\mathbf{v}_{LB} \tag{3.51}$$

$$\mathbf{P}(z_{bot} + \frac{1}{2}\Delta z) = 0 \tag{3.52}$$

At the upper boundary it's assumed that

$$\mathbf{R}(z_{top} - \frac{1}{2}\Delta z)\mathbf{v}(z_{top} + \frac{1}{2}\Delta z) = \mathbf{R}(z_{top} - \frac{1}{2}\Delta z)\mathbf{v}(z_{top} - \frac{1}{2}\Delta z) \tag{3.53}$$

with $z_{top} - \frac{1}{2}\Delta z$ on the midpoint level corresponds to the height index $nlev$. This which leads to

$$\mathbf{Q}(z_{top} - \frac{1}{2}\Delta z)^* = \mathbf{Q}(z_{top} - \frac{1}{2}\Delta z) - \mathbf{R}(z_{top} - \frac{1}{2}\Delta z) \tag{3.54}$$

$$\mathbf{R}(z_{top} - \frac{1}{2}\Delta z)^* = 0 \tag{3.55}$$

A tridiagional solver is called in `subroutine trsolv`. It solve the generic equation

$$p(k,i) * v(k-1,i) + q(k,i) * v(k,i) + r(k,i) * t(k+1,i) = rhs(k,i) \tag{3.56}$$

with $p(k,i)$ being the (i,j) element of the matrix $\mathbf{P}$, $q(k,i)$ of the matrix $\mathbf{Q}$, $r(k,i)$ of the matrix $\mathbf{R}$, $rhs(k,i)$ of the matrix $\mathbf{RHS}$, and $v(k,i)$ of the neutral velocity vector $\mathbf{v}_n$. The lower boundary at $z_{bot} = z_{LB}$ of the neutral velocity is stored at the top level $nlev + 1$ since this height is above the upper boundary anyway. The upper boundary pressure level is -7 which corresponds to z_{top}. The neutral velocity is only calculated from $z_{bot} + \frac{1}{2}\Delta z$ to $z_{top} - \frac{1}{2}\Delta z$. Note that the lower boundary is at $p - lev = -7$, and all the other values of the neutral velocity are on the midpoints which means at $p - lev = -6.75, -6.25, -5.75....5.75, 6.25, 6.75$.

The calculated values for the neutral velocity $\mathbf{u}_n^{upd,t+\Delta t}$ and $\mathbf{v}_n^{upd,t+\Delta t}$ are smoothed by a Fast Fourier transformation. All the wave numbers larger than a predefined value at each latitude are removed. The wave numbers

are defined in the module `cons.F`. The values of the neutral velocity at the timestep t are also updated by using

$$u_n^{upd,t} = \frac{1}{2}(1 - c_{smo})(u_n^{t-\Delta t} + u_{n,smo}^{upd,t+\Delta t}) + c_{smo}u_n^t \qquad (3.57)$$

$$v_n^{upd,t} = \frac{1}{2}(1 - c_{smo})(v_n^{t-\Delta t} + v_{n,smo}^{upd,t+\Delta t}) + c_{smo}v_n^t \qquad (3.58)$$

with $c_{smo} = 0.95$

physical field	variable	unit	pressure level	timestep
neutral temperature	T_n	K	midpoints	t
neutral temperature	$T_n^{t-\Delta t}$	K	midpoints	$t - \Delta t$
neutral temperature	$T_n^{t+\Delta t}$	K	midpoints	$t + \Delta t$
neutral zonal velocity	u_n	cm/s	midpoints	t
neutral meridional velocity	v_n	cm/s	midpoints	t
neutral zonal velocity	$u_n^{t-\Delta t}$	cm/s	midpoints	$t - \Delta t$
neutral meridional velocity	$v_n^{t-\Delta t}$	cm/s	midpoints	$t - \Delta t$
dimenionsless vertical velocity	$W^{t-\Delta t}$	$1/s$	interfaces	$t + \Delta t$
geopotential height	z	cm	interfaces	$t + \Delta t$
zonal horizontal diffusion	$h_{d,u}$	cm/s^2	midpoints	$t - \Delta t$
meridional horizontal diffusion	$h_{d,v}$	cm/s^2	midpoints	$t - \Delta t$
zonal electrodynamic drift velocity	$v_{ExB,x}$	cm/s	interfaces	t
meridional electrodynamic drift velocity	$v_{ExB,y}$	cm/s	interfaces	t
ion drag coefficients (geographic direction)	$\lambda_{xx}, \lambda_{xy}, \lambda_{yy}, \lambda_{yx}$	$1/s$	interfaces	$t + \Delta t$
molecular viscosity	k_m	$\frac{g}{cms}$	interfaces	t
mean molecular weight	$\overline{m}$	g/mol	interfaces	$t + \Delta t$

Table 3.6: Input fields to `subroutine duv`

physical field	variable	unit	pressure level	timestep
neutral zonal velocity	$u_n^{upd,t+\Delta t}$	cm/s	midpoints	$t + \Delta t$
neutral meridional velocity	$v_n^{upd,t+\Delta t}$	cm/s	midpoints	$t + \Delta t$
neutral zonal velocity	$u_n^{upd,t}$	cm/s	midpoints	t
neutral meridional velocity	$v_n^{upd,t}$	cm/s	midpoints	t

Table 3.7: Output fields of `subroutine duv`

physical field	variable	unit	pressure level	timestep
neutral temperature	T_n	K	midpoints	t
neutral temperature	$T_n^{t-\Delta t}$	K	midpoints	$t - \Delta t$
neutral temperature	$T_n^{t+\Delta t}$	K	midpoints	$t + \Delta t$
geopotential height	z	cm	interfaces	$t + \Delta t$
mean molecular weight	$\overline{m}$	g/mol	interfaces	$t + \Delta t$

Table 3.8: Input fields to `subroutine glp`

physical field	variable	unit	pressure level	timestep
zonal derivative of geopotential	$\frac{1}{R_E \cos \lambda} \frac{\partial \Phi^{t+\Delta t *}}{\partial \phi}$	cm/s^2	midpoints	$t + \Delta t *$
meridional derivative of geopotential	$\frac{1}{R_E} \frac{\partial \Phi^{t+\Delta t}}{\partial \lambda}$	cm/s^2	midpoints	$t + \Delta t$

Table 3.9: Output fields of `subroutine glp` i.e. `subroutine dldp`

variable	value
Δz	0.5
wgt	0.225
$\frac{g}{R}$	$\frac{870 cm/s^2}{8.314e^7 erg/K/mol}$

Table 3.10: Parameters of `subroutine glp` i.e. `subroutine dldp`

Chapter 4

Neutral Thermodynamics

physical field	variable	unit	pressure level	timestep
neutral tempera-ture	T_n	K	midpoints	t_n
mass mixing ratio O_2	Ψ_{O_2}	–	midpoints	t_n
mass mixing ratio O	Ψ_O	–	midpoints	t_n

Table 4.1: Input fields to `subroutine cpktkm`

physical field	variable	unit	pressure level	timestep
specific heat	C_p	$ergs/(Kcm^3)$	interfaces	t_n+
molecular viscosity	μ	$gms/(cms)$	interfaces	t_n+
thermal conductiv-ity	K_T	$ergs/(cmKs)$	interfaces	t_n

Table 4.2: Output fields of `subroutine cpktkm`

4.1   Calculation of K_T, μ, C_p

The input to `subroutine cpktkm` is summarized in table 4.1. The output of `subroutine cpktkm` is summarized in table 4.2. The mean mass at the midpoint level is determined by

$$\overline{m} = \frac{1}{\frac{\Psi_{O_2}}{m_{O_2}} + \frac{\Psi_O}{m_O} + \frac{\Psi_{N_2}}{m_{N_2}}} \tag{4.1}$$

with $\Psi_{N_2} = 1 - \Psi_O - \Psi_{O_2}$. The following values are calculated

$$P(O_2) = \overline{m}\frac{\Psi_{O_2}}{m_{O_2}} \tag{4.2}$$

$$P(O) = \overline{m}\frac{\Psi_O}{m_O} \tag{4.3}$$

$$P(N_2) = \overline{m}\frac{\Psi_{N_2}}{m_{N_2}} \tag{4.4}$$

The molecular viscosity is

$$\mu = [4.03 \cdot P(O_2) + 3.42 \cdot P(N_2) + 3.9 \cdot P(O)]\, T_n^{0.69} \cdot 10^{-6} \tag{4.5}$$

The thermal conductivity is

$$K_T = [56 \cdot (P(O_2) + P(N_2)) + 75.9 \cdot P(O)] T_n^{0.69} \tag{4.6}$$

Note that the value T_0 is set to zero in the code. (This is a holdover from the original TGCM, which only calculated a temperature difference. T_0 was then added to this calcualtion to get the actual temperature for purposes like this.) The specific heat is

$$C_p = \frac{1}{2} R^* \left[\frac{7}{32} P(O_2) + \frac{7}{28} P(N_2) + \frac{5}{16} P(O) \right] \tag{4.7}$$

with R^* the gas constant. At the upper boundary the values are set to

$$K_T(z_{top} + \frac{1}{2}\Delta z) = [56 \cdot (P(O_2) + P(N_2)) + 75.9 \cdot P(O)]$$

$$T_n^{0.69}(z_{top} - \frac{1}{2}\Delta z) \tag{4.8}$$

$$\mu(z_{top} + \frac{1}{2}\Delta z) = [4.03 \cdot P(O_2) + 3.42 \cdot P(N_2) + 3.9 \cdot P(O)]$$

$$T_n^{0.69}(z_{top} - \frac{1}{2}\Delta z) \cdot 10^{-6} \tag{4.9}$$

and all the other values at $z_{top} + \frac{1}{2}\Delta z$, and only T_n at a level below $z_{top} - \frac{1}{2}\Delta z$. The values are then transferred to the interface level by averaging

$$K_T(z) = \frac{1}{2}(K_T(z + \frac{1}{2}\Delta z) + K_T(z - \frac{1}{2}\Delta z)) \tag{4.10}$$

$$\mu(z) = \frac{1}{2}(\mu(z + \frac{1}{2}\Delta z) + \mu(z - \frac{1}{2}\Delta z)) \tag{4.11}$$

$$C_p(z) = \frac{1}{2}(C_p(z + \frac{1}{2}\Delta z) + C_p(z - \frac{1}{2}\Delta z)) \tag{4.12}$$

with z having the height index k on the interface level, $z + \frac{1}{2}\Delta z$ has the index k, and $z - \frac{1}{2}\Delta z$ has the index $k - 1$ on the midpoint level. The lower boundary is extrapolated by

$$C_p(z_{bot} = 2C_p(z_{bot} + \frac{1}{2}\Delta z) - C_p(z_{bot} + \Delta z) \tag{4.13}$$

$$K_T(z_{bot} = 2K_T(z_{bot} + \frac{1}{2}\Delta z) - K_T(z_{bot} + \Delta z) \tag{4.14}$$

$$\mu(z_{bot} = 2\mu(z_{bot} + \frac{1}{2}\Delta z) - \mu(z_{bot} + \Delta z) \tag{4.15}$$

$$\tag{4.16}$$

physical field	variable	unit	pressure level	timestep
neutral tempera-ture	T_n	K	midpoints	t_n
neutral tempera-ture	$T_n^{t-\Delta t}$	K	midpoints	$t_n - \Delta t$
neutral zonal veloc-ity	u_n	cm/s	midpoints	t_n
neutral meridional velocity	v_n	cm/s	midpoints	t_n
mass mixing ratio O_2	Ψ_{O_2}	$-$	midpoints	t_n
mass mixing ratio O	Ψ_O	$-$	midpoints	t_n
mean molecular mass	$\overline{m}$	g/mol	interfaces	$t_n + \Delta t$
specific heat	C_p	$\frac{erg}{Kg}$	interfaces	t_n
molecular diffusion	k_t	$\frac{erg}{cmKs}$	interfaces	t_n
molecular viscosity	k_m	$\frac{g}{cms}$	interfaces	t_n
horizontal diffusion	$h_{d,T}$	$\frac{cm}{s^2}$	midpoints	$t_n - \Delta t$
Joule heating	$Q_{J,T}$	$\frac{erg}{K\,s}$	midpoints	t_n
implicit cooling	L_{imp}	$\frac{1}{s}$	midpoints	t_n
explicit cooling	L_{exp}	$\frac{erg}{K\,s}$	midpoints	t_n
dimenionsless verti-cal velocity	$W^{t+\Delta t}$	$1/s$	interfaces	$t + \Delta t$

Table 4.3: Input fields to `subroutine dt`

4.2   Thermodynamic equation

The input to `subroutine dt` is summarized in table 4.3. The output of `subroutine dt` is summarized in table 4.4. The module data of `subroutine dt` is summarized in table 4.5. The thermodynamic equation is solved to get the neutral temperature

$$
\begin{aligned}
\frac{\partial T_n}{\partial t} =& \frac{ge^z}{p_0 C_p} \frac{\partial}{\partial Z} \left\{ \frac{K_T}{H} \frac{\partial T_n}{\partial Z} + K_E H^2 C_p \rho \left[\frac{g}{C_p} + \frac{1}{H} \frac{\partial T}{\partial Z} \right] \right\} - \mathbf{v}_n \cdot \nabla T_n - \\
& W \left(\frac{\partial T_n}{\partial Z} + \frac{R^* T_n}{C_p \overline{m}} \right) + \frac{Q^{exp} - e^z\ L^{exp}}{C_p} - L^{imp}
\end{aligned}
\tag{4.17}
$$

physical field	variable	unit	pressure level	timestep
neutral tempera-ture	$T_n^{upd,t+\Delta t}$	K	midpoints	$t_n + \Delta t$
neutral tempera-ture	$T_n^{upd,t}$	K	midpoints	t_n

Table 4.4: Output fields of `subroutine dt`

physical field	variable	unit	pressure level	timestep
haeting from solar radiation	Q_{qrj}	$\frac{erg}{K\,s}$	interfaces	t_n

Table 4.5: Module data of `subroutine dt`

with T_n the neutral temperature, t the time, g the gravitational accelera-tion, C_p the specific heat per unit mass, p_0 the reference pressure, K_T is the molecular thermal conductivity, H is the pressure scale height, K_E is the eddy diffusion coefficient, ρ is the atmospheric mass density, $\mathbf{v}_n$ is the hori-zontal neutral velocity with the zonal and meridional components u_n and v_n, W is the dimensionless vertical velocity given by $W = \frac{dZ}{dt}$, R^* is the universal gas constant, $\overline{m}$ is the mean atmospheric mass, and Q and L are the heating and cooling terms.
The local time variation of the neutral temperature is determined by the heat-ing and cooling terms on the right hand side of the thermodynamic equation. The first term is the heat transfer by vertical molecular heat conduction and adiabatic heating or cooling due to eddy diffusion. The second term is the heat transfer due to horizontal advection, and the third term is the adiabetic heating and cooling caused by the vertical winds. The last terms in equation (4.17) account for all the other heating and cooling terms.

To make it more easy to compare with the code we write the thermody-

namic equation with implicit and explicit terms

$$
\frac{T_n^{t+\Delta t} - T_n^{t-\Delta t}}{2\Delta t} = \frac{ge^z}{p_0 C_p}\frac{\partial}{\partial Z}\left\{\left(\frac{K_T}{H} + \frac{K_E H^2 C_p \rho}{H}\right)\frac{\partial T_n^{t+\Delta t}}{\partial Z}\right\} +
$$

$$
\frac{ge^z}{p_0 C_p}\frac{\partial}{\partial Z}\left\{K_E H^2 C_p \frac{g}{C_p}\right\} - \mathbf{v}_n^t \cdot \nabla T_n^t - \tag{4.18}
$$

$$
W^{t+\Delta t}\frac{\partial T_n}{\partial Z} - W^{t+\Delta t}\frac{R^* T_n^{t+\Delta t}}{C_p \overline{m}} + \frac{Q^{exp}}{C_p} - \frac{e^z\ L^{exp}}{C_p} - L^{imp}T_n^{t+\Delta t}
$$

The terms are ordered now by left and right hand side, and the whole equation is multiplied by $\frac{C_p}{e^z}$.

$$
\frac{C_p}{e^z}\left\{-\frac{T_n^{t-\Delta t,smo}}{2\Delta t} + \mathbf{v}_n^t \cdot \nabla T_n^t + W^{t+\Delta t}\frac{\partial T_n}{\partial Z} - \frac{Q^{exp} - e^z\ L^{exp}}{C_p}\right\} =
$$

$$
\frac{\partial}{\partial Z}\left\{\frac{g}{Hp_0}\left(\frac{K_T}{H} + K_E H^2 C_p \rho\right)\frac{\partial T_n^{t+\Delta t}}{\partial Z}\right\} + \tag{4.19}
$$

$$
\frac{\partial}{\partial Z}\left\{\frac{g^2}{p_0}\frac{K_E H^2 \rho}{T_n^t}T_n^{t+\Delta t}\right\} + \frac{C_p}{e^z}\left\{-\frac{T_n^{t+\Delta t}}{2\Delta t} - w^{t+\Delta t}\frac{R^* T_n^{t+\Delta t}}{C_p \overline{m}} - L^{imp}T_n^{t+\Delta t}\right\}
$$

We first describe the known terms on the left hand side. The horizontal advection $\mathbf{v}_n^t \cdot \nabla T_n^t$ is calculated similar to the horizontal advection in the momentum equation in chapter 3.3 equation (3.3) and following.

The advection term is calculated in the `subroutine advec` by taking the fourth order stencil for the derivative. The average velocity is denoted by $u_n^{avg}(\phi,\lambda) = \frac{1}{2}(u_n(\phi+\Delta\phi,\lambda) + u_n(\phi-\Delta\phi,\lambda))$ and $u_n^{2avg}(\phi,\lambda) = \frac{1}{2}(u_n(\phi+2\Delta\phi,\lambda) + u_n(\phi-2\Delta\phi,\lambda))$. The same is done for the meridional velocity v_n which leads to $v_n^{avg}(\phi,\lambda) = \frac{1}{2}(v_n(\phi,\lambda+\Delta\lambda) + v_n(\phi,\lambda-\Delta\lambda))$ and $v_n^{2avg}(\phi,\lambda) = \frac{1}{2}(v_n(\phi,\lambda+2\Delta\lambda) + v_n(\phi,\lambda-2\Delta\lambda))$. The horizontal advection of the neutral temperature is

$$
\mathbf{v}_n^t \cdot \nabla T_n^t = \frac{1}{R_E cos\lambda}(\frac{2}{3\Delta\phi}u_n^{avg}(\phi,\lambda)\left[T_n^t(\phi+\Delta\phi,\lambda) - T_n^t(\phi-\Delta\phi,\lambda)\right] -
$$

$$
\frac{1}{12\Delta\phi}u_n^{2avg}(\phi,\lambda)\left[T_n^t(\phi+2\Delta\phi,\lambda) - T_n^t(\phi-2\Delta\phi,\lambda)\right]) +
$$

$$
\frac{1}{R_E}(\frac{2}{3\Delta\lambda}v_n^{avg}(\phi,\lambda)\left[T_n^t(\phi,\lambda+\Delta\lambda) - T_n^t(\phi,\lambda-\Delta\lambda)\right] -
$$

$$
\frac{1}{12\Delta\lambda}v_n^{2avg}(i,j)\left[T_n^t(\phi,\lambda+2\Delta\lambda) - T_n^t(\phi,\lambda-2\Delta\lambda)\right]) \tag{4.20}
$$

in unit of $[\frac{K}{s}]$ the values are determined at midpoints.

The vertical advection term $W^{t+\Delta t}\frac{\partial T_n}{\partial Z}$ is calculated by

$$\frac{1}{2\Delta z}(W^{t+\Delta t}(z)\left[T_n^t(z+\frac{1}{2}\Delta z) - T_n^t(z-\frac{1}{2}\Delta z)\right] +$$

$$W^{t+\Delta t}(z+\Delta z)\left[T_n^t(z+\frac{3}{2}\Delta z) - T_n^t(z+\frac{1}{2}\Delta z)\right]) =$$

$$\frac{1}{2}\left[W^{t+\Delta t}(z)\frac{\partial T_n^t(z)}{\partial Z} + W^{t+\Delta t}(z+\Delta z)\frac{\partial T_n^t(z+\Delta z)}{\partial Z}\right] =$$

$$W^{avg,t+\Delta t}(z+\frac{1}{2}\Delta z)\frac{\partial T_n^{avg,t}(z+\frac{1}{2}\Delta z)}{\partial Z} \tag{4.21}$$

It takes the average between the values at the level z and $z + \Delta z$. Note that T_n is on the midpoints levels $z + \frac{1}{2}\Delta z$ etc. The vertical advection is determined at midpoints and has the units $[\frac{K}{s}]$.

The next term is from the time derivative of the neutral temperature $-\frac{T_n^{t-\Delta t,smo}}{2\Delta t}$. The smoothed value is calculated similar as in the momentum equation in chapter 3.3 in equation (3.22).

$$f_{merid}^{smooth} = f(\phi, \lambda) - c_{shapiro}(f(\phi, \lambda + 2\Delta\lambda) + f(\phi, \lambda - 2\Delta\lambda) -$$
$$4\left[f(\phi, \lambda + \Delta\lambda) + f(\phi, \lambda - \Delta\lambda)\right] + 6f(\phi, \lambda)) \tag{4.22}$$

$$f_{zonal}^{smooth} = f_{merid}^{smooth} - c_{shapiro}(f_{merid}^{smooth}(\phi + 2\Delta\phi, \lambda) + f_{merid}^{smooth}(\phi - 2\Delta\phi, \lambda) -$$
$$4\left[f_{merid}^{smooth}(\phi + \Delta\phi, \lambda) + f_{merid}^{smooth}(\phi - \Delta\phi, \lambda)\right] + 6f_{merid}^{smooth}(\phi, \lambda)) \tag{4.23}$$

with $f = T_n^{t-\Delta t}$ which leads to $T_n^{t-\Delta t,smo}$.

The heating terms are added together. First the terms from the heating caused by solar radiation, which are calculated in `subroutine qrj`.

$$Q_{solar} = Q_{EUV} + Q_{SchR} + Q_o \tag{4.24}$$

$$\tag{4.25}$$

with $Q_{Solar}(z+\frac{1}{2}\Delta z) = \frac{1}{2}[Q_{Solar}(z) + Q_{Solar}(z+\Delta z)]$ to calculate the value on the midpoint level $z + \frac{1}{2}\Delta z$. The solar radiation has contributions from the EUV and from the Schuhman Runge bands and continuum, and the O????.

$$Q = Q_{Solar} + 1.5Q_{JH} + h_{d,T} + Q_{OR} + Q_{md} \tag{4.26}$$

$$\tag{4.27}$$

with the Joule heating term denoted by Q_{JH} which is multiplied by 1.5 to take the heating due to the small scale electric field into account. The horizontal diffusion term is denoted by $h_{d,T}$?????.

The heating due to atomic oxygen recombination is determined by ?????

$$Q_{OR} = f_T r_{km} \frac{N_A}{\overline{m}} \left[\frac{p_0 e^{-z\overline{m}}}{k_B T_n} \frac{\Psi_o}{m_o} \right]^2 \tag{4.28}$$

with the Boltzman constant $k_B = 1.38 \cdot 10^{-16} \frac{cm^2 g}{s^2 K}$, and $f_T = 5.11 eV = 5.11 \cdot 1.602 \cdot 10^{-12} ergs$, which is the surplus heating and set in `subroutine` `cons`. The loss of O to O_2 is captured by r_{km} and set in the source code file `chemrates.F` according to Dickinson et al. 1984.

The photoeletron heating is determined by

$$Q_{photo} = q_{ionize} 0.05 \times 35. N_A \frac{1.602 \cdot 10^{-12}}{\overline{m}} \tag{4.29}$$

where q_{ionize} is the ionization rate.
The heating resulting from ion chemistry is of the type

$$Q_i^{chem} = N_A 1.602 \cdot 10^{-12} n_{neutral} r_k n_i q_{heat} \tag{4.30}$$

where $n_{neutral}$ is the number density of the neutral species, n_i is the number density of the ion species, r_k is the reaction rate, and q_{heat} is the heat emitted by the reaction.
The heating resulting from neutral chemistry of the minor species is

$$Q_i^{chem} = N_A 1.602 \cdot 10^{-12} n_{neutral} \beta n_{neutral} q_{heat} \tag{4.31}$$

where β is the reaction rate.
The heating from electron-neutral and electron-ion collisions are

$$Q_{en}^{chem} = L_{en}(T_e - T_n) \frac{N_A}{\overline{m}} \tag{4.32}$$

$$Q_{ei}^{chem} = L_{ei}(T_e - T_i) \frac{N_A}{\overline{m}} \tag{4.33}$$

The loss term due to NO cooling is

$$L_{NO} = 4.956 \cdot 10^{-12} N_A n_{NO} \frac{ANO}{ANO + 13.3} e^{\frac{-2700}{T_n}} \tag{4.34}$$

where $ANO = \bar{m} N_A 5 \cdot 10^{-4} e^{-z} (6.5 \cdot 10^{-11} \frac{n_o}{m_o} + 2.4 \cdot 10^{-14} \frac{n_{o2}}{m_{o2}})/(R T_n)$

The loss due to CO_2 cooling is

$$L_{CO2_{cool}} = 2.65 \cdot 10^{-13} n_{CO2} e^{\frac{-960}{T_n}} N_A ((\frac{n_{O2}}{m_{O2}} + \frac{n_{N2}}{m_{N2}}) ACO2 + \frac{n_O}{m_O} BCO2) \tag{4.35}$$

where

$$
\begin{aligned}
ACO2 =& 2.5 \cdot 10^{-15} & T_n < 200K \\
& 2.5 \cdot 10^{-15} (1 + 0.03(T_n - 200)) & T_n > 200K \\
BCO2 =& 1. \cdot 10^{-12} & T_n < 300K \\
& 1. \cdot 10^{-12} \frac{T_n}{300} & T_n > 300K
\end{aligned}
$$

The loss due to $O(^3P)$ cooling is

$$L_{O(^3P)_{cool}} = \frac{ANO3P(1) \times XO(k) \frac{N_A}{m_o} n_o e^{\frac{-BNO3P(1)}{T_n}}}{1 + ANO3P(2) e^{\frac{-BNO3P(2)}{T_n}} + ANO3P(3) e^{\frac{-BNO3P(3)}{T_n}}} \tag{4.36}$$

with XO is a pressure level dependent set of coefficients. $XO = (3 \times 0.01, 0.05, 0.1, 0.2, 0.4, 0.55, 0.7, 0.75, 15 \times 0.0)$. $ANO3P$ is a 3 element array of constants $ANO3P = (1.67 \cdot 10^{-18}, 0.6, 0.2)$. $BNO3P$ is a three element array of constants $BNO3P = (228, 228, 325)$.

The heating due to molecular diffusion is determined by

$$Q_{md} = \frac{g^2 \bar{m} K_m^{mid}}{p_0 R^* e^{-z} T_n^t} \left\{ \left(\frac{\partial u_n}{\partial Z} \right)^2 + \left(\frac{\partial v_n}{\partial Z} \right)^2 \right\} = \tag{4.37}$$

$$\frac{e^z g \bar{m} K_m^{mid}}{p_0 H} \left\{ \left(\frac{\partial u_n}{\partial Z} \right)^2 + \left(\frac{\partial v_n}{\partial Z} \right)^2 \right\} \tag{4.38}$$

with the gas constant $R^* = 8.314 10^7 \frac{ergs}{Kmol}$ and $\frac{1}{H} = \frac{g\bar{m}}{R^* T_n}$. The vertical change in the neutral velocity is calculated by

$$\frac{du_n}{dZ}(z + \frac{1}{2}\Delta z) = \frac{u_n(z + \frac{3}{2}\Delta z) - u_n(z - \frac{1}{2}\Delta z)}{2\Delta z} \tag{4.39}$$

$$\frac{dv_n}{dZ}(z + \frac{1}{2}\Delta z) = \frac{v_n(z + \frac{3}{2}\Delta z) - v_n(z - \frac{1}{2}\Delta z)}{2\Delta z} \tag{4.40}$$

At the lower boundary the derivative is determined by

$$\frac{du_n}{dZ}(z_{LB}) = \frac{1}{\Delta z}\left(u_n(z_{LB} + \frac{1}{2}\Delta z) + \frac{1}{3}u_n(z_{LB} + \frac{3}{2}\Delta z) - \frac{4}{3}u_n(z_{LB})\right) \quad (4.41)$$

$$\frac{dv_n}{dZ}(z_{LB}) = \frac{1}{\Delta z}\left(v_n(z_{LB} + \frac{1}{2}\Delta z) + \frac{1}{3}v_n(z_{LB} + \frac{3}{2}\Delta z) - \frac{4}{3}v_n(z_{LB})\right) \quad (4.42)$$

At the top the derivatives are set to

$$\frac{du_n}{dZ}(z_{top} - \Delta z) = \frac{1}{3}\frac{du_n}{dZ}(z_{top} - 2\Delta z) \quad (4.43)$$

$$\frac{dv_n}{dZ}(z_{top} - \Delta z) = \frac{1}{3}\frac{dv_n}{dZ}(z_{top} - 2\Delta z) \quad (4.44)$$

All the terms of the right hand side are added together which leads to

$$RHS = \frac{C_p}{e^z}\left[\mathbf{v}_n^t \cdot \nabla T_n^t + W^{t+\Delta t}\frac{\partial T}{\partial Z} - \frac{1}{2\Delta t}T_n^{t-\Delta t,smo}\right] - e^{-z}Q^{exp} + L^{exp}$$

$$(4.45)$$

Next we discuss the terms on the left hand side starting with the second derivative terms $\frac{\partial}{\partial Z}\left\{\frac{g}{Hp_0}\left(\frac{K_T}{H} + K_E H^2 C_p \rho\right)\frac{\partial T_n^{t+\Delta t}}{\partial Z}\right\}$. In the source code and in this description we substitute for simplicity $g_c = \frac{g}{Hp_0}\left(\frac{K_T}{H} + K_E H^2 C_p \rho\right)$. First the mass density ρ and the scale height H are calculated. The neutral temperature at the interface level is

$$T_n^t(z) = \frac{1}{2}\left[T_n^t(z - \frac{1}{2}\Delta z) + T_n^t(z + \frac{1}{2}\Delta z)\right] \quad (4.46)$$

and the scale height H is

$$H(z) = \frac{R^* T_n^t(z)}{\overline{m}(z)g} \quad (4.47)$$

and the mass density ρ

$$\rho(z) = \frac{p_0 e^{-z}\overline{m}(z)}{e^{-0.5\Delta z}R^* T_n^t(z)} = \frac{p}{H(z)g} \quad (4.48)$$

with the pressure $p = p_0 e^{-\int_o^z dz'/H}$. At the boundaries the values are set to

$$T_n^t(z_{LB}) = T_{n,LB}^t \tag{4.49}$$

$$T_n^t(z_{top}) = T_n^t(z_{top} - \frac{1}{2}\Delta z) \tag{4.50}$$

$$gH(z_{LB}) = \frac{RT_n^t(z_{LB})}{\overline{m}(z_{LB})} \tag{4.51}$$

$$gH(z_{top}) = \frac{R^*T_n^t(z_{top})}{\overline{m}(z_{top})} \tag{4.52}$$

$$\rho_{LB} = \frac{p_0 e^{-z_{LB}}}{e^{-0.5\Delta z}} \frac{1}{H(z_{LB})g} \tag{4.53}$$

$$\rho_{top} = \frac{p_0 e^{-z_{top}}}{e^{-0.5\Delta z}} \frac{1}{H(z_{top})g} \tag{4.54}$$

The second derivative $\frac{\partial}{\partial Z}\left\{g_c \frac{\partial T_n^{t+\Delta t}}{\partial Z}\right\}$ is approximated at midpoint level by

$$\frac{\partial}{\partial Z}\left\{g_c \frac{\partial T_n^{t+\Delta t}}{\partial Z}(z + \frac{1}{2}\Delta z)\right\} \approx \frac{1}{\Delta z^2}[T_n^{t+\Delta t}(z - \frac{1}{2}\Delta z)g_c(z)+$$

$$T_n^{t+\Delta t}(z + \frac{1}{2}\Delta z)\left\{-g_c(z + \Delta z) - g_c(z)\right\}+$$

$$T_n^{t+\Delta t}(z + \frac{3}{2}\Delta z)g_c(z + \Delta z)] \tag{4.55}$$

Note that g_c are calculated at the interface levels $z, z + \Delta z...$ and the neutral temperature is on the midpoint level. For a derivation of the discrete second order derivative we refer to chapter 3.3 equation (3.26).

The first order derivative $\frac{\partial}{\partial Z}\left\{\frac{g^2}{p_0}\frac{K_E H^2 \rho}{T_n^t}T_n^{t+\Delta t}\right\}$ is expanded by $\frac{T_n^{t+\Delta t}}{T_n^t}$. The term $\frac{g^2}{p_0}\frac{K_E H^2 \rho}{T_n^t}$ is substituted by f_c with f in the source code denotes $f = \frac{f_c}{2\Delta z}$. The first order derivative is determined by

$$\frac{\partial}{\partial Z}\left\{f_c T_n^{t+\Delta t}\right\}(z + \frac{1}{2}\Delta z) \approx \frac{1}{2\Delta z}[-T_n^{t+\Delta t}(z - \frac{1}{2}\Delta z)f_c(z)+$$

$$T_n^{t+\Delta t}(z + \frac{1}{2}\Delta z)\left\{f_c(z + \Delta z) - f_c(z)\right\}+$$

$$T_n^{t+\Delta t}(z + \frac{3}{2}\Delta z)f_c(z + \Delta z)] \tag{4.56}$$

Note that f_c is on the interface level, and the neutral temperature on the midpoint level. The first order derivative derived from

$$\frac{\partial f T_n^{t+\Delta t}}{\partial Z}(z + \frac{1}{2}\Delta z) = \frac{f(z + \Delta z)T_n^{t+\Delta t}(z + \Delta z) - f(z)T_n^{t+\Delta t}(z)}{\Delta z} \quad (4.57)$$

with the values at the interface level $T_n^{t+\Delta t}(z) = \frac{1}{2}(T_n^{t+\Delta t}(z - \frac{1}{2}\Delta z) + T_n^{t+\Delta t}(z + \frac{1}{2}\Delta z))$ and $T_n^{t+\Delta t}(z + \Delta z) = \frac{1}{2}(T_n^{t+\Delta t}(z + \frac{3}{2}\Delta z)T_n^{t+\Delta t}(z + \frac{1}{2}\Delta z))$.
The tridiagonal solver need the equation in the following form:

$$P(k,i)T_n^{t+\Delta t}(k-1,i) + Q(k,i)T_n^{t+\Delta t}(k,i) +$$
$$R(k,i)T_n^{t+\Delta t}(k+1,i) = RHS(k,i) \quad (4.58)$$

with the height index k for $z + \frac{1}{2}\Delta z$, $k+1$ for $z + \frac{3}{2}\Delta z$, and $k-1$ for $z - \frac{1}{2}\Delta z$.
The longitude index is denoted by i. Note that the equation is solved at each latitude λ with the index j.
The left hand side terms discussed above are sorted according to the height index which leads to

$$P(k,i) = g_c(k,i) - f_c(k,i) \quad (4.59)$$
$$Q^*(k,i) = -g_c(k+1,i) - g_c(k,i) - f_c(k,i) + f(k+1,i) \quad (4.60)$$
$$R = g_c(k+1,i) + f(k+1,i) \quad (4.61)$$

At the upper boundary the values are set to

$$R(z_{top} - \frac{1}{2}\Delta z) = 0 \quad (4.62)$$

$$P(z_{top} - \frac{1}{2}\Delta z) = g_c(z_{top} - \frac{1}{2}\Delta z) - f(z_{top} - \frac{1}{2}\Delta z) \quad (4.63)$$

$$Q(z_{top} - \frac{1}{2}\Delta z) = -g_c(z_{top} - \frac{1}{2}\Delta z) - f(z_{top} - \frac{1}{2}\Delta z) \quad (4.64)$$

The right hand side is

$$RHS = C_p^{mid}e^{-z}\left[\mathbf{v}_n^t\nabla T_n^t + w^{t+\Delta t}\frac{\partial T_n^t}{\partial Z} - \frac{1}{2\Delta t}T_n^{t-\Delta t,smo}\right] -$$
$$e^{-z}Q^{exp} + L^{exp} \quad (4.65)$$

At the height level k the following terms are added to Q

$$Q(k,i) = Q^*(k,i) + C_p^{mid}\left\{\frac{1}{2\Delta t} + L^{imp}\right\} + w^{mid}\frac{R}{m} \quad (4.66)$$

with the values at the midpoint level $C_p^{mid}(z + \frac{1}{2} + \Delta z) = C_p(z) + C_p(z + \Delta z)$ and $w^{mid}(z + \frac{1}{2} + \Delta z) = w(z) + w(z + \Delta z)$. At the lower boundary the following condition is used

$$P(z_{bot} - \frac{1}{2}\Delta z)T_n(z_{bot} - \frac{1}{2}\Delta z) = 2P(z_{bot})T_n(z_{LB}) - P(z_{bot} + \frac{1}{2}\Delta z)T_n(z_{bot} + \frac{1}{2}\Delta z)$$
(4.67)

$$P(z_{bot} + \frac{1}{2}\Delta z) = 0$$
(4.68)

with $z_{bot} + \frac{1}{2}\Delta z$ corresponding to the midpoint level and the height index $k = 1$. $P(z_{bot})$ is set to $P(z_{bot} + \frac{1}{2}\Delta z)$, and $T_n(z_{bot})$ is equal to the lower boundary with the value $T_n(z_{LB})$. This which leads to

$$Q^*(z_{bot} + \frac{1}{2}\Delta z) = Q(z_{bot} + \frac{1}{2}\Delta z) - P(z_{bot} + \frac{1}{2}\Delta z)$$
(4.69)

$$RHS^*(z_{bot} + \frac{1}{2}\Delta z) = RHS(z_{bot} + \frac{1}{2}\Delta z) - 2P(z_{bot} + \frac{1}{2}\Delta z)T_n^t(z_{LB})$$ (4.70)

$$P^*(z_{bot} + \frac{1}{2}\Delta z) = 0$$
(4.71)

Solving for the neutral temperature at each latitude leads to the updated neutral temperature $T_n^{upd,t_n+\Delta t}$ at the midpoints. The lower boundary of the neutral temperature is stored at the top level with the height index $nlev + 1$ which is above the upper boundary of the model with pressure level -7. Note that the lower boundary is at pressure level -7 which is z_{bot} or z_{LB}, however all the other values of the neutral temperature are on the midpoints which means at the pressure levels $-6.75, -6.25, -5.75....5.75, 6.25, 6.75$. The calculated values for the neutral temperature $T_n^{upd,t+\Delta t}$ are smoothed by a Fast Fourier transformation. All the wave numbers larger than a predefined value at each latitude are removed. The wave numbers are defined in the module `cons.F`. The values of the neutral temperature at the timestep t_n are also updated by using

$$T_n^{upd,t} = \frac{1}{2}(1 - c_{smo})(T_n^{t-\Delta t} + T_{n,smo}^{upd,t+\Delta t}) + c_{smo}T_n^t$$
(4.72)

with $c_{smo} = 0.95$

Chapter 5

Chemistry

5.1   Calculation of chemical reaction rates

The chemical reaction rates can be found in [22], and [23] In this module the time independent reaction rates are set as module data. The time dependent rates are calculated in the `subroutine chemrates_tdep`. First we describe the time independent rates for the ion chemistry:

5.1.1   Module data

$$O_2^+ + N(^4S) \xrightarrow{k_4} NO^+ + O + 4.21eV \qquad\qquad k_4 = 1 \cdot 10^{-10} \qquad (5.1)$$

$$O_2^+ + NO \xrightarrow{k_5} NO^+ + O_2 + 2.813eV \qquad\qquad k_5 = 4.4 \cdot 10^{-10} \qquad (5.2)$$

$$N^+ + O_2 \xrightarrow{k_6} O_2^+ + N(^4S) + 2.486eV \qquad\qquad k_6 = 4. \cdot 10^{-10} \qquad (5.3)$$

$$N^+ + O_2 \xrightarrow{k_7} NO^+ + O + 6.669eV \qquad\qquad k_7 = 2. \cdot 10^{-10} \qquad (5.4)$$

$$N^+ + O \xrightarrow{k_8} O^+ + N + 0.98eV \qquad\qquad k_8 = 1 \cdot 10^{-12} \qquad (5.5)$$

$$N_2^+ + O_2 \xrightarrow{k_9} O_2^+ + N_2 + 3.52eV \qquad\qquad k_9 = 6. \cdot 10^{-11} \qquad (5.6)$$

$$O^+ + N(^2D) \xrightarrow{k_{10}} N^+ + O + 1.45eV \qquad\qquad k_{10} = 1.3 \cdot 10^{-10} \qquad (5.7)$$

$$O^+(^2P) + N_2 \xrightarrow{k_{16}} N_2^+ + O + 3.02eV \qquad\qquad k_{16} = 4.8 \cdot 10^{-10} \qquad (5.8)$$

$$O^+(^2P) + N_2 \xrightarrow{k_{17}} N^+ + NO + 0.7eV \qquad\qquad k_{17} = 1.0 \cdot 10^{-10} \qquad (5.9)$$

$$O^+(^2P) + O \xrightarrow{k_{18}} O^+ + O + 5.2eV \qquad\qquad k_{18} = 4.0 \cdot 10^{-10} \qquad (5.10)$$

$$O^+(^2P) \xrightarrow{k_{21}} O^+ + h\nu(2470\text{Å}) \qquad\qquad k_{21} = 0.047 \qquad (5.11)$$

$$O^+(^2P) \xrightarrow{k_{22}} O^+ + h\nu(7320\text{Å}) \qquad\qquad k_{22} = 0.171 \qquad (5.12)$$

$$O^+(^2D) + N_2 \xrightarrow{k_{23}} N_2^+ + O + 1.33eV \qquad\qquad k_{23} = 8.0 \cdot 10^{-10} \qquad (5.13)$$

$$O^+(^2D) + O \xrightarrow{k_{24}} O^+(^4S) + e + 3.31eV \qquad\qquad k_{24} = 5.0 \cdot 10^{-12} \qquad (5.14)$$

$$O^+(^2D) + O_2 \xrightarrow{k_{26}} O_2 + O + 4.865eV \qquad\qquad k_{26} = 7.0 \cdot 10^{-10} \qquad (5.15)$$

$$\xrightarrow{k_{27}} \qquad\qquad k_{27} = 7.7 \cdot 10^{-5} \qquad (5.16)$$

The time independent rates for the neutral chemistry are

$$N(^2D) + O_2 \xrightarrow{\beta_2} NO + O(^1D) + 1.84eV \qquad \beta_2 = 5. \cdot 10^{-12} \qquad (5.17)$$

$$N(^2D) + O \xrightarrow{\beta_4} N(^4S) + O + 2.38eV \qquad \beta_4 = 7. \cdot 10^{-13} \qquad (5.18)$$

$$N(^2D) + NO \xrightarrow{\beta_6} N_2 + O + 5.63eV \qquad \beta_6 = 7. \cdot 10^{-11} \qquad (5.19)$$

$$N(^2D) \xrightarrow{\beta_7} N(^4S) + h\nu \qquad \beta_2 = 1.06 \cdot 10^{-5} \qquad (5.20)$$

$$(5.21)$$
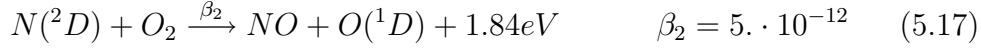
The temperature dependent rates are calculated at every timestep and every latitude. For the ion chemistry these reaction rates are:

$$O^+ + O_2 \xrightarrow{k_1} O + O_2^+ + 1.555eV \qquad (5.22)$$

$$O^+ + N_2 \xrightarrow{k_2} NO^+ + N(^4S) + 1.0888eV \qquad (5.23)$$

$$N_2^+ + O \xrightarrow{k_3} NO^+ + N(^2D) + 0.7eV \qquad (5.24)$$

$$NO^+ + e \xrightarrow{a_1} 0.2[N(^4S) + O + 2.75eV] \qquad (5.25)$$
$$0.8[N(^2D) + O + 0.38eV])$$

$$O_2^+ + e \xrightarrow{a_2} 0.15[O + O + 6.95eV] \qquad (5.26)$$
$$0.85[O + O + 4.98eV])$$

$$N_2^+ + e \xrightarrow{a_3} 0.1[N(^4S) + N(^4S) + 5.82eV] \qquad (5.27)$$
$$0.9[N(^2D) + N(^2D) + 3.44eV])$$

$$(5.28)$$
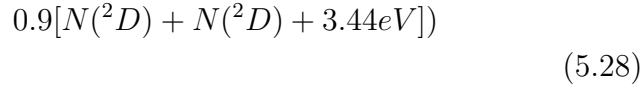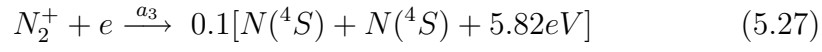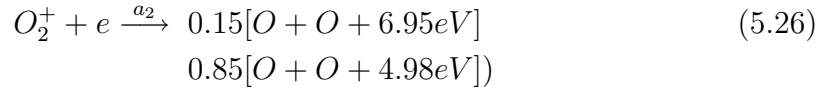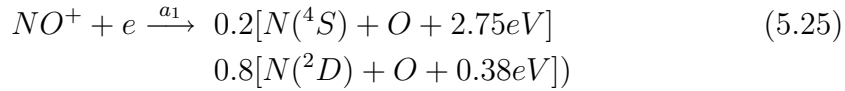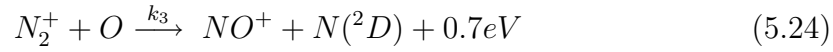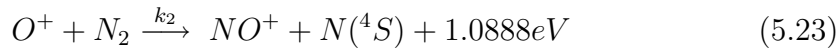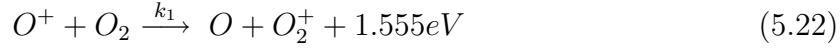
The time dependent reactions for the neutral chemistry are

$$N(^4S) + O_2 \xrightarrow{\beta_1} NO + O + 1.4eV \tag{5.29}$$

$$N(^4S) + NO \xrightarrow{\beta_3} N_2 + O + 3.25eV \tag{5.30}$$

$$N(^2D) + e \xrightarrow{\beta_5} N(^4S) + e + 2.38eV \tag{5.31}$$

$$NO + h\nu \xrightarrow{\beta_8} N(^4S) + O \tag{5.32}$$

$$NO + h\nu|_{Ly-\alpha} \xrightarrow{\beta_9} NO^+ + e \tag{5.33}$$

$$\xrightarrow{\beta_{9n}} \tag{5.34}$$

$$\xrightarrow{\beta_{17}} \tag{5.35}$$

$$O^+(^2P) + e \xrightarrow{k_{19}} O^+(^4S) + e + 5.0eV \tag{5.36}$$

$$O^+(^2P) + e \xrightarrow{k_{20}} O^+(^2O) + e + 1.69eV \tag{5.37}$$

$$O^+(^2D) + e \xrightarrow{k_{25}} O^+(^4S) + e + 3.31eV \tag{5.38}$$

$$O + O + N_2 \xrightarrow{k_{m12}} O_2 + N_2 + 5.0eV \tag{5.39}$$
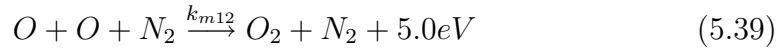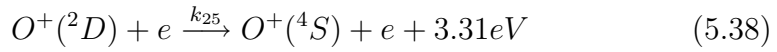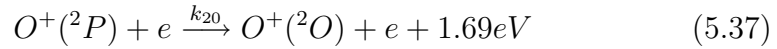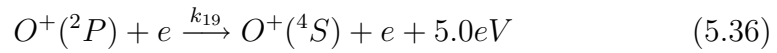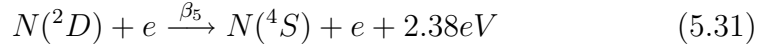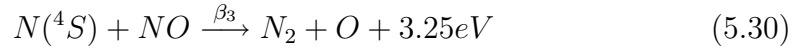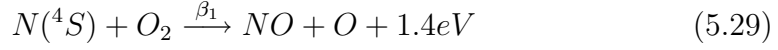
5.1.2   Calculation of time dependent reaction rates

The time dependent rates, mentioned in the previous section 5.1.1 are calculated in the `subroutine chemrates_tdep`. The temperatures are set by

$$T_1 = \frac{1}{300}(\frac{2}{3}T_i + \frac{1}{3}T_n)$$
$$T_2 = \frac{1}{300}(0.6363T_i + 0.3637T_n)$$
$$T_3 = \frac{1}{2}\frac{1}{300}(T_i + T_n) \tag{5.40}$$

with T_i, T_e and T_n denoting the ion, electron and neutral temperature, respectively.

$$k_1 = 1.6 \cdot 10^{-11} T_1^{-0.52} + 5.5 \cdot 10^{-11} e^{-22.85/T_1} \tag{5.41}$$

$$k_2^* = (8.6 \cdot 10^{-11} T - 2 - 5.92 \cdot 10^{-13}) T_2 + 1.533 \cdot^{-12} \tag{5.42}$$

$$e^t = e^{-3353/t_n}$$

$$k_2 = [(\{[(270.e^t + 220.)e^t + 85]e^t + 38\}e^t +$$
$$1) k_2^* e^t + k_2^*](1 - e^t) \tag{5.43}$$

$$k_3 = 5.2 \cdot 10^{-11} T_3^{0.2} \text{for} \frac{1}{2}(T_i + T_n) > 1500K$$

$$k_3 = 1.4 \cdot 10^{-10} T_3^{-0.44} \text{for} \frac{1}{2}(T_i + T_n) \leq 1500K \tag{5.44}$$

$$k_{19} = 4.10^{-8} \sqrt{300/T_e} \tag{5.45}$$

$$k_{20} = 1.510^{-7} \sqrt{300/T_e} \tag{5.46}$$

$$k_{25} = 6.610^{-8} \sqrt{300/T_e} \tag{5.47}$$

$$k_{m,12} = 9.5910^{-34} e^{480/T_n} \tag{5.48}$$

$$a_1 = 4.210^{-7} (300/T_e)^{0.85} \tag{5.49}$$

$$a_2 = 1.610^{-7} (300/T_e)^{0.55} \ T_e \geq 1200K$$

$$a_2 = 2.710^{-7} (300/T_e)^{0.7} \ T_e < 1200K \tag{5.50}$$

$$a_3 = 1.810^{-7} (300/T_e)^{0.39} \tag{5.51}$$

$$\beta_1 = 1.510^{-11} e^{-3600/T_n} \tag{5.52}$$

$$\beta_3 = 3.410^{-11} \sqrt{T_n/300} \tag{5.53}$$

$$\beta_5 = 3.610^{-10} \sqrt{T_e/300} \tag{5.54}$$

$$\beta_8 = 4.5^{-6}(1 + 0.11 \frac{F_{10.7} - 65}{165}) e^{-110^{-8} fnO_2^{0.38}} fls \tag{5.55}$$

with FnO_2 the O_2 line integral from `chapman.F`, $FNvO_2$ the column number density of O_2 from `chapman.F`, and fls denotes the flux variation due to orbital excentricity (from `init_module`. The 10.7 cm flux is denoted by

$F_{10.7}$.

$$\beta_9 = 2.9110^{11}(1 + 0.2\frac{F_{10.7} - 65}{100})210^{-18}e^{1-8.10^{-21}FnO_2}fls \tag{5.56}$$

$$\beta_{9n} = 510^9(1 + 0.2\frac{F_{10.7} - 65}{100})210^{-18}e^{1-8.10^{-21}FnvO_2}fls \tag{5.57}$$

$$\tag{5.58}$$

physical field	variable	unit	pressure level	timestep
neutral tempera-ture	T_n	K	midpoints	t_n
mass mixing ratio O_2	Ψ_{O_2}	–	midpoints	t_n
mass mixing ratio O	Ψ_O	–	midpoints	t_n
mean molecular mass	$\overline{m}$	g/mol	interfaces	$t_n + \Delta t$
number density of O^+	$n(O^+)$	$\#/cm^3$	midpoints	t_n
number density of $O^{+,t_n+\Delta t}$	$n(O^+)$	$\#/cm^3$	midpoints	t_n
number density of $N(^2D)$	$n(N(^2D))$	$\#/cm^3$	midpoints	t_n
number density of NO	$n(NO)$	$\#/cm^3$	midpoints	t_n
number density of $N(^4S)$	$n(N(^4S))$	$\#/cm^3$	midpoints	t_n
number density of $XIO^+(^2P)$	$n(XIO^+(^2P))$	$\#/cm^3$	midpoints	$t_n + \Delta t$
number density of $XIO^+(^2D)$	$n(XIO^+(^2D))$	$\#/cm^3$	midpoints	$t_n + \Delta t$

Table 5.1: Input fields to `subroutine elden`

5.2 Calculation of electron density N_e, N^+, N_2^+, NO^+

The input to `subroutine elden` is summarized in table 5.1. The output of `subroutine settei` is summarized in table 5.2. The module data of `subroutine elden` is summarized in table 5.3.

The electron density is calculated by

$$N_e = n(O^+) + n(N_2^+) + n(N^+) + n(O_2^+) + n(NO^+) \qquad (5.59)$$

physical field	variable	unit	pressure level	timestep
number density of N^+	$n(N^+)$	$\#/cm^3$	midpoints	$t_n + \Delta t$
number density of N_2^+	$n(N_2^+)$	$\#/cm^3$	midpoints	$t_n + \Delta t$
number density of NO^+	$n(NO^+)$	$\#/cm^3$	midpoints	$t_n + \Delta t$
number density of O_2^+	$n(O_2^+)$	$\#/cm^3$	midpoints	$t_n + \Delta t$
electron density	N_e	$\#/cm^3$	midpoints	$t_n + \Delta t$

Table 5.2: Output fields of `subroutine elden`

physical field	variable	unit	pressure level	timestep
QRJ: production due to N^+	$Q(N^+)$	$cm^{-3}s^{-1}$	interfaces	t_n
QRJ: production due to NO^+	$Q(NO^+)$	$cm^{-3}s^{-1}$	interfaces	t_n
CHEMRATES: reaction rates	k_i	cm^3s^{-1}	midpoints	–
CHEMRATES: N) production coefficient	β_9	s^{-1}	interface	–

Table 5.3: Module data of `subroutine elden`

with

$$n(O^+) = F \tag{5.60}$$

$$n(N_2^+) = \frac{D}{E' + \alpha_3 N_e} \tag{5.61}$$

$$n(N^+) = G \tag{5.62}$$

$$n(O_2^+) = \frac{B + \frac{HD}{E' + \alpha_3 N_e}}{C + \alpha_2 N_e} \tag{5.63}$$

$$n(NO^+) = \left[A + \frac{E'D - HD}{E' + \alpha_3 N - e} + \frac{C}{C + \alpha_2 N - e} \frac{B + HD}{E' + \alpha_3 N_e} \right] \frac{1}{\alpha_1 N_e} \tag{5.64}$$

This leads to an fourth order equation

$$a_4 N_e^4 + a_3 N_e^3 + a_2 N_e + a_1 N_e + a_0 = 0 \tag{5.65}$$

with

$$
\begin{aligned}
a_4 &= \alpha_1 \alpha_2 \alpha_3 & (5.66)\\
a_3 &= \alpha_1 (\alpha_2 E' + \alpha_3 C) - \alpha_1 \alpha_2 \alpha_3 (F + G) & (5.67)\\
a_2 &= \alpha_1 E' C - \alpha_1 (\alpha_2 E' + \alpha_3 C)(F + G) - \alpha_1 \alpha_2 D - \alpha_2 \alpha_3 A - \alpha_1 \alpha_3 B & (5.68)\\
a_1 &= -\alpha_1 \left[E' C(F + G) + DC + BE' + HD \right] - \\
&\quad \alpha_2 \left[E'(A + D) - HD \right] - \alpha_3 C(A + B) & (5.69)\\
a_0 &= -E' C(A + B + D) & (5.70)
\end{aligned}
$$

and

$$
\begin{aligned}
A &= Q(NO^+) + k_2 n(O^+) n(N_2) + k_7 n(N^+) n(O_2) + \beta_9 n(NO) & (5.71)\\
B &= Q(O_2^+) + k_1 n(O^+) + n(O_2) + k_6 n(N^+) n(O_2) + \\
&\quad k_{26} n(O_2) n(xiO^+(^2D)) & (5.72)\\
C &= k_4 n(N(^4S)) + k_5 n(NO) & (5.73)\\
D &= Q(N_2^+) + n(N_2) \left[k_{16} n(xiO^+(^2P) + k_{23} n(xiO^+(^2D)) \right] & (5.74)\\
E &= k_3 n(O) & (5.75)\\
F &= n(O^+) & (5.76)\\
G &= n(N^+) & (5.77)\\
H &= k_9 n(O_2) & (5.78)\\
E' &= E + H & (5.79)
\end{aligned}
$$

Then the electron density is

$$
\begin{aligned}
N_e = F + \frac{D}{E' + \alpha_3 N_e} + G + \frac{B}{C + \alpha_2 N_e} + \frac{HD}{(E' + \alpha_3 N_e)(C + \alpha_2 N_e)} + \\
\frac{1}{\alpha_1 N_e} \left[A + \frac{E'D - HD}{E' + \alpha_3 N_e} + \frac{CB}{C + \alpha_2 N_e} + \frac{CHD}{(E' + \alpha_3 N_e)(C + \alpha_2 N_e)} \right]
\end{aligned} \tag{5.80}
$$

The values A, B, C, D, E, F, G and H are evaluated at midpoint level

$$A(z + \frac{1}{2}\Delta z) = \frac{1}{2}(Q(NO^+)(z) + Q(NO^+)(z + \Delta z)) +$$

$$N\overline{m}\left[k_2 n(O^+)^{t+\Delta t}\frac{\Psi_{N_2}}{m_{N_2}} + k_7 n(N^+)\frac{\Psi_{O_2}}{m_{O_2}}\right] +$$

$$\frac{1}{2}\left[\beta_9(z) + \beta_9(z + \Delta z)\right]\frac{\Psi_{NO}}{m_{NO}} \tag{5.81}$$

$$B(z + \frac{1}{2}\Delta z) = \frac{1}{2}(Q(O_2^+)(z) + Q(O_2^+)(z + \Delta z)) +$$

$$N\overline{m}[k_1 n(O^+)^{T+\Delta t} + k_6 n(N^+) +$$

$$k_{26} n(xiO^+(^2D))]\frac{\Psi_{O_2}}{m_{O_2}} \tag{5.82}$$

$$C(z + \frac{1}{2}\Delta z) = N\overline{m}\left[k_4\frac{\Psi_{N(^4S)}}{m_{N(^4S)}} + k_5\frac{\Psi_{NO}}{m_{NO}}\right] \tag{5.83}$$

$$D(z + \frac{1}{2}\Delta z) = frac12\left[Q(N_2^+)(z) + Q(N_2^+)(z + \Delta z)\right] +$$

$$N\overline{m}\frac{\Psi_{N_2}}{m_{N_2}}\left[k_{16} n(xiO^+(^2P) + k_{23} n(xiO^+(^2D)))\right] \tag{5.84}$$

$$E'(z + \frac{1}{2}\Delta z) = N\overline{m}\left[k_3\frac{\Psi_O}{m_O} + k_9\frac{\Psi_{O_2}}{m_{O_2}}\right] \tag{5.85}$$

$$(F + G)(z + \frac{1}{2}\Delta z) = n(O^+) + n(N^+) \tag{5.86}$$

$$H(z + \frac{1}{2}\Delta z) = N\overline{m}k_9\frac{\Psi_{O_2}}{m_{O_2}} \tag{5.87}$$

First the conversion factor from mass mixing ratio to number density is calculated at the midpoint level

$$N\overline{m}(z + \frac{1}{2}\Delta z) = \frac{p_o e^{-z - \frac{1}{2}\Delta z}\overline{m}(z + \Delta z)}{k_B T_n(z + \Delta z)} \tag{5.88}$$

The mass mixing ratio of N_2 at the midpoint level is determined by

$$\Psi(N_2)(z + \frac{1}{2}\Delta z) = 1 - \Psi(O_2)(z + \frac{1}{2}\Delta z) - \Psi(O)(z + \frac{1}{2}\Delta z) \tag{5.89}$$

The number density of N^+ is

$$n(N^+) = \frac{Q(N^+) + k_{10} n(O^+) n(N(^2D))}{(k_6 + k_7) n(O_2) + k_8 n(O)} \tag{5.90}$$

which is calculated at the midpoint level in the code by

$$n(N^+)(z + \frac{1}{2}\Delta z) = \frac{\frac{1}{2}[Q(N^+)(z) + Q(N^+)(z + \Delta z)] + k_{10}n(O^+)N\overline{m}\frac{\Psi(N(^2D))}{m_{N(^2D)}}}{N\overline{m}(k_6 + k_7)\frac{\Psi(O_2)}{m_{O_2}} + k_8\frac{\Psi(O)}{m_O}}$$

$$(5.91)$$

The quadric solver solves for the electron density N_e, with $N_e \geq 3 \cdot 10^3$. Then, the number densities of N_2^+, O_2^+ and NO^+ can be determined on the midpoint level

$$n(N_2^+) = \frac{D}{E' + \alpha_3 N_e} \tag{5.92}$$

$$n(O_2^+) = \left[B + \frac{HD}{E' + \alpha_3 N_e}\right]\frac{1}{C + \alpha_2 N_e} \tag{5.93}$$

$$n(NO^+) = \frac{A + \frac{D(E'-H)}{E'+\alpha_3 N_e} + C\left(B + \frac{HD}{E'+\alpha_3 N_e}\right)}{C + \alpha_2 N_e}\frac{1}{\alpha_1 N_e} \tag{5.94}$$

with N_e still on the midpoint level. The electron density at the interface level is determined by

$$N_e(z) = \sqrt{N_e(z - \frac{1}{2}\Delta z)N_e(z + \frac{1}{2}\Delta z)} \tag{5.95}$$

with the midpoint level $z - \frac{1}{2}\Delta z$ denoted by index k, $z + \frac{1}{2}\Delta z$ then by the height index $k + 1$, and on the interface level z has the index $k + 1$. The upper and lower boundary are set by

$$N_e(z_{bot}) = \sqrt{\frac{N_e^3(z_{bot} + \frac{1}{2}\Delta z)}{N_e(z_{bot} + \frac{3}{2}\Delta z)}} \tag{5.96}$$

$$N_e(z_{top}) = \sqrt{\frac{N_e^3(z_{top} - \frac{1}{2}\Delta z)}{N_e(z_{top} - \frac{3}{2}\Delta z)}} \tag{5.97}$$

physical field	variable	unit	pressure level	timestep
neutral temperature	T_n	K	midpoints	t_n
mass mixing ratio O_2	$\Psi(O_2)$	–	midpoints	t_n
mass mixing ratio O	$\Psi(O)$	–	midpoints	t_n
mass mixing ratio X	$\Psi(X)^{t_n}$	–	midpoints	t_n
mass mixing ratio X	$\Psi(X)^{t_n+\Delta t}$	–	midpoints	$t_n + \Delta t$
upward number flux at upper boundary	$F_x^{upw,top}$	$\#/cm^3$	z_{top}	$t_n + \Delta t$
diffusive vector	D_v	???	midpoints??	t_n??
molecular weight of species X	m_X	$g/mole$	-	–
thermal diffusion coefficient	D_T	???	midpoints???	t_n???
loss of X	L_X	???	midpoints???	t_n????
production of X	P_X	???	midpoints???	t_n???
???coefficient of upward flux A, B, C	$A\frac{\partial \Psi_X}{\partial Z} + B\Psi_X + C = 0$	???	z_{bot}	$t_n + \Delta t$

Table 5.4: Input fields to `subroutine minor`

5.3   Calculation minor species $N(^4S)$ and NO, (and HOx in TIMEGCM)

The input to `subroutine minor` is summarized in table 5.4. The output of `subroutine minor` is summarized in table 5.5. The module data of `subroutine minor` is summarized in table 5.6. Since the minor species $N(^4S)$ and NO (and HOx in TIMEGCM) have longer life times, the neutral wind transport effects have to taken into account. The governing equation

physical field	variable	unit	pressure level	timestep
mass mixing ratio of species X	$\Psi(X)^{t_n,upd}$	–	interfaces???	t_n
mass mixing ratio of species X	$\Psi(X)^{t_n+\Delta t,upd}$	–	interfaces???	$t_n + \Delta t$

Table 5.5: Output fields of `subroutine minor`

physical field	variable	unit	pressure level	timestep
background eddy diffusion	K_E	???	interfaces	–

Table 5.6: Module data of `subroutine minor`

is (see [24]) Roble et al. 1988

$$\frac{\partial \Psi}{\partial t} = - e^z \frac{\partial}{\partial Z}\left[A\left(\frac{\partial}{\partial Z} - E\right)\Psi\right]$$
$$+ S\Psi - R - \left[\mathbf{v}_n \cdot \nabla\Psi + W_n \frac{\partial \Psi}{\partial Z}\right]$$
$$+ e^z \left[e^{-z}K_E\left(\frac{\partial}{\partial Z} + \frac{1}{\overline{m}}\frac{\partial \overline{m}}{\partial Z}\right)\Psi\right] + H_{sub} \qquad (5.98)$$

with

$$\tilde{E} = \left(1 - \frac{m}{\overline{m}} - \frac{1}{\overline{m}}\frac{\partial \overline{m}}{\partial Z}\right) - \tilde{\alpha}\frac{1}{T_n}\frac{\partial T_n}{Z} + \tilde{F}\tilde{\Psi} \qquad (5.99)$$

The vertical molecular diffusion coefficient is A, the production term is S, the loss term is R, the term E includes the effects of gravity, thermal diffusion and friction with the major species on the vertical profile of the two species (O_x, O_2). The matrix operator for frictional interaction is $\tilde{F}$, the thermal diffusion coefficient is α, and the mean molecular mass is $\overline{m}$, and Ψ stands for the mass mixing ratio of either NO, $N(4S)$ or HOx. In TIEGCM O_x is simply O, whereas in TIMEGCM, it is O_3+O. The horizontal diffusion caused by sub-grid processes which cannot be resolved by the model is added in by H_{sub}, and calculated in `subroutine hdif`

The temporal change in the mass mixing ratio on the left hand side of eq.(5.98) is equal to the vertical molecular diffusion which is denoted by

the first term on the right hand side, the production and loss of the minor species (term two and three in eq.(5.98)), the horizontal and vertical nonlinear advection term (fourth term), and the vertical eddy diffusion (fifth term). The temporal term and all terms dependent with Z derivatives are treated implicit. The solver needs the equation in the following from

$$P_k \Psi_{k-1}^{t+\Delta t} + Q_k \Psi_k^{t+\Delta t} + R_k \Psi_{k+1}^{t+\Delta t} = f_k \qquad (5.100)$$

where P_k, Q_k, R_k, and f_k are deterimned at timestep t at midpoints. $\Psi_{k-1,k+1}^{t+\Delta t}$ are also at midpoints but at the next timestep $t + \Delta t$, k stands for the index of the vertical grid. The equation 5.98) can be rearranged and multiplied by e^{-z} which will lead to

$$e^{-z} \frac{\Psi_n^{t+\Delta t}}{2\Delta t} + \frac{\partial}{\partial Z}\left[A_n \frac{\partial}{\partial Z} - E_n \Psi_n^{t+\Delta t}\right]$$

$$- e^{-z} S \Psi_n^{t+\Delta t} + e^{-z} W_n \frac{\partial \Psi^{t+\Delta t}}{\partial Z} - \frac{\partial}{\partial Z}\left\{ e^{-z} K_E \frac{\partial}{\partial Z} + \frac{1}{m}\frac{\partial \overline{m}}{\partial Z}\Psi^{t+\Delta t}\right\} =$$

$$- e^{-z} R - e^{-z}\left\{ \mathbf{v}_n \cdot \nabla \Psi^t\right\} + e^{-z}\frac{\Psi^{t-\Delta t}}{2\Delta t} + e^{-z} H_{sub} \qquad (5.101)$$

The second term is discretized by

$$\frac{\partial}{\partial Z}\left[A_n \frac{\partial}{\partial Z}\Psi_n^{t+\Delta t}\right] = \frac{1}{\Delta z^2}\{A_n(z - \frac{1}{2}\Delta z)\Psi^{t+\Delta t}(z - \Delta z)-$$

$$\left[A_n(z + \frac{1}{2}\Delta z) + A_n(z - \frac{1}{2}\Delta z)\right]\Psi^{t+\Delta t}(z)+$$

$$A_n(z + \frac{1}{2}\Delta z)\Psi^{t+\Delta t}(z + \Delta z)\} \qquad (5.102)$$

The third term by

$$- \frac{\partial}{\partial Z}\left[A_n E_n \Psi_n^{t+\Delta t}\right] = \frac{1}{\Delta z}\{-A_n(z - \frac{1}{2}\Delta z)E_n(z - \frac{1}{2}\Delta z)\Psi^{t+\Delta t}(z - \Delta z)-$$

$$\left[-A_n(z + \frac{1}{2}\Delta z)E_n(z + \frac{1}{2}\Delta z) + A_n(z - \frac{1}{2}\Delta z)E_n(z - \frac{1}{2}\Delta z)\right]\Psi^{t+\Delta t}(z)+$$

$$A_n(z + \frac{1}{2}\Delta z)E_n(z + \frac{1}{2}\Delta z)\Psi^{t+\Delta t}(z + \Delta z)\} \qquad (5.103)$$

The fifth term is discretized by

$$e^{-z}W_n\frac{\partial \Psi^{t+\Delta t}}{\partial Z} = \frac{1}{2\Delta z}e^{-z}W_n(z)\Psi^{t+\Delta t}(z+\Delta z)-$$
$$\frac{1}{2\Delta z}e^{-z}W_n(z)\Psi^{t+\Delta t}(z-\Delta z) \qquad (5.104)$$

the sixth term by

$$-\frac{\partial}{\partial Z}\left[e^{-z}K_E\frac{\partial}{\partial Z}\Psi^{t+\Delta t}\right] = -\frac{1}{\Delta z^2}[e^{-z+\frac{1}{2}\Delta z}K_E(z-\frac{1}{2}\Delta z)\Psi^{t+\Delta t}(z-\Delta z)-$$
$$\left\{e^{-z-\frac{1}{2}\Delta z}K_E(z+\frac{1}{2}\Delta z)+e^{-z+\frac{1}{2}\Delta z}K_E(z-\frac{1}{2}\Delta z)\right\}\Psi^{t+\Delta t}(z)+$$
$$e^{-z-\frac{1}{2}\Delta z}K_E(z+\frac{1}{2}\Delta z)\Psi^{t+\Delta t}(z+\Delta z)] \qquad (5.105)$$

and the seventh term is

$$-\frac{\partial}{\partial Z}e^{-z}K_E\frac{1}{\overline{m}}\frac{\partial \overline{m}}{\partial Z}\Psi^{t+\Delta t} = -\frac{1}{\Delta z^2}[$$
$$e^{-z+\frac{1}{2}\Delta z}K_E(z-\frac{1}{2}\Delta z)\frac{m(z-\Delta z)}{\overline{m}(z-\frac{1}{2}\Delta z)}\Psi^{t+\Delta t}(z-\Delta z)-$$
$$\{e^{-z-\frac{1}{2}\Delta z}K_E(z+\frac{1}{2}\Delta z)\frac{m(z)}{\overline{m}(z+\frac{1}{2}\Delta z)}+$$
$$e^{-z+\frac{1}{2}\Delta z}K_E(z-\frac{1}{2}\Delta z)\frac{m(z)}{\overline{m}(z-\frac{1}{2}\Delta z)}\}\Psi^{t+\Delta t}(z)+$$
$$e^{-z-\frac{1}{2}\Delta z}K_E(z+\frac{1}{2}\Delta z)\frac{m(z+\Delta z)}{\overline{m}(z+\frac{1}{2}\Delta z)}\Psi^{t+\Delta t}(z+\Delta z)] \qquad (5.106)$$

and

$$-e^{-z}S\Psi^{t+\Delta t}(z) \qquad (5.107)$$

Rearranging according to eq. (5.100) leads to the coefficients

$$P = \frac{1}{\Delta^2 z}\tilde{A}(z) + \frac{1}{\Delta z}\tilde{A}(z)\tilde{E}(z) - \frac{1}{2\Delta z}e^{-z}W(z + \frac{1}{2}\Delta z) -$$
$$\frac{1}{\Delta^2 z}e^{-z+\Delta z}K_E(z) - \frac{1}{\Delta^2 z}e^{-z+\Delta z}K_E(z)\frac{m(z - \frac{1}{2}\Delta z)}{\overline{m}(z)} \tag{5.108}$$

$$R = \frac{1}{\Delta^2 z}\tilde{A}(z + \Delta z) - \frac{1}{\Delta z}\tilde{A}(z + \Delta z)\tilde{E}(z + \Delta z) +$$
$$\frac{1}{2\Delta z}e^{-z}W(z + \frac{1}{2}\Delta z) - \frac{1}{\Delta^2 z}e^{-z}K_E(z + \Delta z) -$$
$$\frac{1}{\Delta^2 z}e^{-z}K_E(z + \Delta z)\frac{m(z - \frac{3}{2}\Delta z)}{\overline{m}(z + \Delta z)} \tag{5.109}$$

$$Q = \frac{e^{-z}}{2\Delta t} - \frac{1}{\Delta^2 z}[\tilde{A}(z + \Delta z) + \tilde{A}(z)] +$$
$$\frac{1}{\Delta z}[\tilde{A}(z + \Delta z)\tilde{E}(z + \Delta z) + \tilde{A}(z)\tilde{E}(z)] - e^{-z}S +$$
$$- \frac{1}{\Delta^2 z}[e^{-z}K_E(z + \Delta z) + e^{-z+\Delta z}K_E(z)]$$
$$- \frac{1}{\Delta^2 z}[e^{-z}K_E(z + \Delta z)\frac{m(z + \frac{1}{2}\Delta z)}{\overline{m}(z + \Delta z)} +$$
$$e^{-z+\frac{1}{2}\Delta z}K_E(z)\frac{m(z + \frac{1}{2}\Delta z)}{\overline{m}(z)}] \tag{5.110}$$

$$f = -e^{-z}R - e^{-z}\mathbf{v}_n \cdot \Psi^{t_n} + e^{-z}\frac{\Psi^{t_n-\Delta t}}{2\Delta t} \tag{5.111}$$

The lower boundary condition is ???? not used in the code?????

$$\frac{1}{2}(\Psi(z_{bot} - \Delta z) + \Psi(z_{bot} + \Delta z)) = \Psi(z_{bot}) \tag{5.112}$$

which leads to

$$\Psi(z_{bot} - \Delta z) = 2\Psi(z_{bot}) - \Psi(z_{bot} + \Delta z) \tag{5.113}$$

Inserting into the equation (5.100)

$$\{-P(z_{bot}) + Q(z_{bot})\}\,\Psi(z_{bot}) + R(z_{bot})\Psi(z_{bot} + \Delta z) =$$
$$f(z_{bot}) - 2\Psi(z_{bot})P(z_{bot}) \tag{5.114}$$

The upper boundary is ???? not used in the code ?????

$$\frac{\partial}{\partial Z}\Psi = \epsilon\Psi \tag{5.115}$$

which leads to

$$\frac{\Psi(z_{top}) - \Psi(z_{top} - \Delta z)}{\Delta z} = \frac{\epsilon(z_{top} - \frac{1}{2}\Delta z)}{2}\left(\Psi(z_{top}) + \Psi(z_{top} - \Delta z)\right) \tag{5.116}$$

and the value for $\Psi(z_{top})$

$$\Psi(z_{top}) = \frac{1 + \Delta z\frac{\epsilon(z_{top} - \frac{1}{2}\Delta z)}{2}}{1 - \Delta z\frac{\epsilon(z_{top} - \frac{1}{2}\Delta z)}{2}}\Psi(z_{top} - \Delta z) \tag{5.117}$$

Inserting into the equation (5.100)

$$P(z_{top} - \Delta z)\Psi(z_{top} - 2\Delta z) + \{Q(z_{top} - \Delta z) +$$

$$R(z_{top} - \Delta z)\}\frac{1 + \Delta z\frac{\epsilon(z_{top} - \frac{1}{2}\Delta z)}{2}}{1 - \Delta z\frac{\epsilon(z_{top} - \frac{1}{2}\Delta z)}{2}}\Psi(z_{top} - \Delta z) = f(z_{top} - \Delta z) \tag{5.118}$$

In the code first the thermal diffusion coefficient $\tilde{\alpha}$ is set with the diffusion vector $\Phi_1 = (0, 1.35, 1.11)$ and $\Phi_2 = (0.673, 0, 0.769)$ independent of the species, and the vector Φ_x depending on the species.

$$\begin{aligned}\alpha_{12} &= \Phi_{12} - \Phi_{13} \\ \alpha_{21} &= \Phi_{21} - \Phi_{23} \\ \alpha_{x1} &= \Phi_{x1} - \Phi_{x3} \\ \alpha_{x2} &= \Phi_{x2} - \Phi_{x13}\end{aligned} \tag{5.119}$$

The values $\Psi_x^{t_n - \Delta t}$ are smoothed with the Shapiro smoother, first in latitude,

$$\Psi_x^{t_n - \Delta t, lat} = \Psi_x^{t_n - \Delta t} - 0.003[\Psi_x^{t_n - \Delta t}(\phi, \lambda - 2\Delta\lambda) + \Psi_x^{t_n - \Delta t}(\phi, \lambda + 2\Delta\lambda) -$$

$$4\left(\Psi_x^{t_n - \Delta t}(\phi, \lambda + \Delta\lambda) + \Psi_x^{t_n - \Delta t}(\phi, \lambda - \Delta\lambda)\right) + 6\Psi_x^{t_n - \Delta t}(\phi, \lambda)] \tag{5.120}$$

and then in longitude

$$\Psi_x^{t_n - \Delta t, smo} = \Psi_x^{t_n - \Delta t, lat} - 0.003[\Psi_x^{t_n - \Delta t, lat}(\phi - 2\Delta\phi, \lambda) +$$

$$\Psi_x^{t_n - \Delta t, lat}(\phi + 2\Delta\phi, \lambda) - 4(\Psi_x^{t_n - \Delta t, lat}(\phi - \Delta\phi, \lambda) +$$

$$\Psi_x^{t_n - \Delta t, lat}(\phi + \Delta\phi, \lambda)) + 6\Psi_x^{t_n - \Delta t, lat}(\phi, \lambda)] \tag{5.121}$$

The horizontal advection $\mathbf{v}_n \cdot \nabla \Psi_x$ is calculated in `subroutine advec`, with

$$u_n^\phi(\phi, \lambda) = \frac{1}{2}[u_n(\phi + \Delta\phi, \lambda) + u_n(\phi - \Delta\phi, \lambda)]$$

$$u_n^{2\phi}(\phi, \lambda) = \frac{1}{2}[u_n(\phi + 2\Delta\phi, \lambda) + u_n(\phi - 2\Delta\phi, \lambda)]$$

$$v_n^\lambda(\phi, \lambda) = \frac{1}{2}[v_n(\phi, \lambda + \Delta\lambda) + v_n(\phi, \lambda - \Delta\lambda)]$$

$$v_n^{2\lambda}(\phi, \lambda)e = \frac{1}{2}[v_n(\phi, \lambda + 2\Delta\lambda) + v_n(\phi, \lambda - 2\Delta\lambda)] \qquad (5.122)$$

and the terms

$$T_1(\phi, \lambda) = \frac{1}{R_E \cos\lambda}\{\frac{2}{3\Delta\phi}u_n^\phi(\phi, \lambda)\left[\Psi_x(\phi + \Delta\phi, \lambda) - \Psi_x(\phi - \Delta\phi, \lambda)\right] -$$

$$\frac{1}{12\Delta\phi}u_n^{2\phi}(\phi, \lambda)\left[\Psi_x(\phi + 2\Delta\phi, \lambda) - \Psi_x(\phi - 2\Delta\phi, \lambda)\right]\} \qquad (5.123)$$

$$T_2(\phi, \lambda) = \frac{1}{R_E}\{\frac{2}{3\Delta\lambda}v_n^\lambda(\phi, \lambda)\left[\Psi_x(\phi, \lambda + \Delta\lambda) - \Psi_x(\phi, \lambda - \Delta\lambda)\right] -$$

$$\frac{1}{12\Delta\lambda}v_n^{2\lambda}(\phi, \lambda)\left[\Psi_x(\phi, \lambda + 2\Delta\lambda) - \Psi_x(\phi, \lambda - 2\Delta\lambda)\right]\} \qquad (5.124)$$

The advection $\mathbf{v}_n \cdot \nabla \Psi_x$ is then

$$\mathbf{v}_n \cdot \nabla\Psi_x = T_1 + T_2 \qquad (5.125)$$

At the lower boundary the following values are set ??? which level$z_{bot} - \frac{1}{2}\Delta z$ such that it fits afterward????

$$\Psi(O_2)(z_{bot} - \frac{1}{2}\Delta z) = b_{11}\Psi(O_2)(z_{bot} + \frac{1}{2}\Delta z) +$$

$$b_{12}\Psi(O)(z_{bot} - \frac{1}{2}\Delta z) + F_b(1) \qquad (5.126)$$

$$\Psi(O)(z_{bot} - \frac{1}{2}\Delta z) = b_{21}\Psi(O_2)(z_{bot} + \frac{1}{2}\Delta z) +$$

$$b_{22}\Psi(O)(z_{bot} - \frac{1}{2}\Delta z) + F_b(2) \qquad (5.127)$$

with $b_{11}, b_{12}, b_{22}, b_{21}$ and $\mathbf{F}_b$ from the file `bndry.F` and `subroutine bndcmp`. The mean molecular mass is

$$\overline{m}(z_{bot} - \frac{1}{2}\Delta z) = [\frac{\Psi(O_2)}{m_{O_2}}(z_{bot} - \frac{1}{2}\Delta z) + \frac{\Psi(O)}{m_O}(z_{bot} - \frac{1}{2}\Delta z) +$$

$$\frac{1 - \Psi(O_2) - \Psi(O)}{m_{N_2}}(z_{bot} - \frac{1}{2}\Delta z)]^{-1} \qquad (5.128)$$

The N_2 number density is

$$\Psi(N_2)(z + \frac{1}{2}\Delta z) = 1 - \Psi(O_2)(z + \frac{1}{2}\Delta z) - \Psi(O)(z + \frac{1}{2}\Delta z) \qquad (5.129)$$

and the mean molecular mass is

$$\overline{m}(z + \frac{1}{2}\Delta z) = [\frac{\Psi(O_2)}{m_{O_2}}(z + \frac{1}{2}\Delta z) + \frac{\Psi(O)}{m_O}(z + \frac{1}{2}\Delta z) +$$
$$\frac{\Psi(N_2)}{m_{N_2}}(z + \frac{1}{2}\Delta z)]^{-1} \qquad (5.130)$$

At the lower boundary the following quantities are calculated

$$\overline{m}(z_{bot}) = \frac{1}{2}[\overline{m}(z_{bot} - \frac{1}{2}\Delta z) + \overline{m}(z_{bot} - \frac{1}{2}\Delta z)] \qquad (5.131)$$

$$\frac{d\overline{m}}{dz}(z_{bot}) = \frac{\overline{m}(z_{bot} + \frac{1}{2}\Delta z) - \overline{m}(z_{bot} - \frac{1}{2}\Delta z)}{\Delta z} \qquad (5.132)$$

$$\Psi(O)(z_{bot}) = \frac{1}{2}[\Psi(O)(z_{bot} - \frac{1}{2}\Delta z) + \Psi(O)(z_{bot} + \frac{1}{2}\Delta z)] \qquad (5.133)$$

$$\Psi(O_2)(z_{bot}) = \frac{1}{2}[\Psi(O_2)(z_{bot} - \frac{1}{2}\Delta z) + \Psi(O_2)(z_{bot} + \frac{1}{2}\Delta z)] \qquad (5.134)$$

$$\frac{d\Psi(O)}{dz}(z_{bot}) = \frac{\Psi(O)(z_{bot} + \frac{1}{2}\Delta z) - \Psi(O)(z_{bot} - \frac{1}{2}\Delta z)}{\Delta z} \qquad (5.135)$$

$$\frac{d\Psi(O_2)}{dz}(z_{bot}) = \frac{\Psi(O_2)(z_{bot} + \frac{1}{2}\Delta z) - \Psi(O_2)(z_{bot} - \frac{1}{2}\Delta z)}{\Delta z} \qquad (5.136)$$

At all other levels these quantities are

$$\overline{m}(z) = \frac{1}{2}[\overline{m}(z + \frac{1}{2}\Delta z) + \overline{m}(z - \frac{1}{2}\Delta z)] \qquad (5.137)$$

$$\frac{d\overline{m}}{dz}(z) = \frac{\overline{m}(z + \frac{1}{2}\Delta z) - \overline{m}(z - \frac{1}{2}\Delta z)}{\Delta z} \qquad (5.138)$$

$$\Psi(O)(z) = \frac{1}{2}[\Psi(O)(z + \frac{1}{2}\Delta z) + \Psi(O)(z - \frac{1}{2}\Delta z)] \qquad (5.139)$$

$$\Psi(O_2)(z_{bot}) = \frac{1}{2}[\Psi(O_2)(z + \frac{1}{2}\Delta z) + \Psi(O_2)(z - \frac{1}{2}\Delta z)] \qquad (5.140)$$

$$\frac{d\Psi(O)}{dz}(z) = \frac{\Psi(O)(z + \frac{1}{2}\Delta z) - \Psi(O)(z - \frac{1}{2}\Delta z)}{\Delta z} \qquad (5.141)$$

$$\frac{d\Psi(O_2)}{dz}(z) = \frac{\Psi(O_2)(z + \frac{1}{2}\Delta z) - \Psi(O_2)(z - \frac{1}{2}\Delta z)}{\Delta z} \qquad (5.142)$$

The neutral temperature at the interfaces is set by

$$
\begin{aligned}
T_n(z_{bot}) &= T_n(z_{LB}) \\
T_n(z_{top}) &= T_n(z_{top} - \frac{1}{2}\Delta z) \\
T_n(z) &= \frac{1}{2}[T_n(z + \frac{1}{2}\Delta z) + T_n(z - \frac{1}{2}\Delta z)]
\end{aligned}
\tag{5.143}
$$

The production is calculated by

$$
P_0 = P_x \frac{m_x k_B T_n(z + \frac{1}{2}\Delta z}{p_0 e^{-z - \frac{1}{2}\Delta z}\overline{m}(z + \frac{1}{2}\Delta z)}
\tag{5.144}
$$

and stored in s0prod. The production P_x for the specie x is input to the subroutine, and is multiplied by $\frac{m_x}{N\overline{m}}$. ???? does this make sense????? The final thermal diffusion coefficients are determined ?????

$$
\begin{aligned}
\alpha_{11,f} &= -[\phi_{13} + \alpha_{12}\Psi(O)(z)] \\
\alpha_{12,f} &= -\alpha_{12}\Psi(O_2)(z) \\
\alpha_{21,f} &= -[\alpha_{21}\Psi(O)(z) \\
\alpha_{22,f} &= -[\phi_{23} + \alpha_{21}\Psi(O_2)(z)]
\end{aligned}
\tag{5.145}
$$

The quantity $1 - \frac{\tilde{m}}{m} - \frac{1}{m}\frac{\overline{m}}{\partial Z} + \tilde{F}\tilde{\Psi}$ is calculated and stored in the variable ex ?????

$$
\begin{aligned}
T_{ex} = &\{(\alpha_{x1}\alpha_{22,f} - \alpha_{x2}\alpha_{21,f})\left[\frac{d\Psi(O_2)}{dZ} - \left(1 - \frac{m_{O_2} + \frac{d\overline{m}}{dZ}}{\overline{m}}\right)\Psi(O_2)\right] + \\
&(\alpha_{x2}\alpha_{11,f} - \alpha_{x1}\alpha_{12,f})\left[\frac{d\Psi(O)}{dZ} - \left(1 - \frac{m_O + \frac{d\overline{m}}{dZ}}{\overline{m}}\right)\Psi(O)\right]\} \\
&\frac{1}{\alpha_{11,f}\alpha_{22,f} - \alpha_{12,f}\alpha_{21,f}} + 1 - \frac{m_X + \frac{d\overline{m}}{dZ}}{\overline{m}}
\end{aligned}
\tag{5.146}
$$

The vertical molecular diffusion coefficient $\tilde{A}$ is determined by

$$
\tilde{A} = -\frac{\overline{m}(z)}{\tau m_{N_2}}\left(\frac{T_0}{T_n(z)}\right)^{0.25}\{\phi_{x3} + \alpha_{x1}\Psi(O_2)(z) + \alpha_{x2}\Psi(O)\}^{-1}
\tag{5.147}
$$

with $\tau = 1.86 \cdot 10^3$, and $T_0 = 273K$. The value is stored in the variable `ax` in the source code. The effects of gravity, thermal diffusion and the frictional interaction with the major species is expressed by the variable $\tilde{E}$ given by eq. (5.99)

$$T_{thdiff}(z) = T_{ex} - \alpha_X \frac{T_n(z + \Delta z) - T_n(z - \Delta z)}{2\delta z T_n(z)} \tag{5.148}$$

and T_{ex} given by the expression in eq. (5.146). The quantity T_{thdiff} is stored in the variable `thdiff` in the source code. At the lower boundary the value is

$$T_{thdiff}(z_{bot}) = T_{ex}(z_{bot}) - \alpha_X \frac{T_n(z_{bot} + \Delta z) - T_n(z_{bot}}{\Delta z T_n(z_{bot})}$$

$$T_{thdiff}(z_{top}) = T_{ex}(z_{top}) - \alpha_X \frac{T_n(z_{top}) - T_n(z_{top} - \Delta z)}{\Delta z T_n(z_{top})} \tag{5.149}$$

If the INPUT flag `difhor` is set ($\lambda 0$) then the horizontal variation of the eddy diffusion and thermal conductivity ???? is set by

$$|\lambda_r| \geq 40^o \quad d_{fac} = hor(\lambda) + 1.0$$

$$|\lambda_r| < 40^o \quad d_{fac} = hor(\lambda) + \frac{1}{2}\left(1 + \sin \Pi \frac{|\lambda_r| - \frac{\Pi}{9}}{\Pi/4.5}\right) \tag{5.150}$$

with λ_r going from the south pole to the north pole???? check $|\lambda_r|$?????

The coefficients for the equation (5.100) which is solved for the mass mixing ratio are ???? check the pressure levels and with the equation at the beginning??????

$$P = \frac{\tilde{A}(k)}{\Delta z}\left(\frac{1}{\Delta z} + \frac{1}{2}T_{thdiff(k)}\right) - $$

$$e^{-z - \frac{1}{2}\Delta z}[e^{\frac{1}{2}\Delta z}K_E(k)d_{fac}\left\{\frac{1}{\Delta z} - \frac{1}{2}\frac{d\overline{m}}{dz}(k)\right\} +$$

$$\frac{1}{4}\{W(z) + W(z + \Delta z)\}]\frac{1}{\Delta z} \tag{5.151}$$

$$R = \frac{\tilde{A}(k+1)}{\Delta z}\left(\frac{1}{\Delta z} - \frac{1}{2}T_{thdiff(k+1)}\right) -$$

$$e^{-z-\frac{1}{2}\Delta z}[e^{-\frac{1}{2}\Delta z}K_E(k+1)d_{fac}\left\{\frac{1}{\Delta z} + \frac{1}{2}\frac{d\overline{m}}{dz}(k+1)\right\} -$$

$$\frac{1}{4}\left\{W(z) + W(z+\Delta z)\right\}]\frac{1}{\Delta z} \tag{5.152}$$

$$Q = -\left\{\frac{\tilde{A}(k)}{\Delta z}\left(\frac{1}{\Delta z} - \frac{1}{2}T_{thdiff(k)} + \frac{\tilde{A}(k+1)}{\Delta z}\left(\frac{1}{\Delta z} + \frac{1}{2}T_{thdiff(k+1)}\right)\right\} +$$

$$e^{-z-\frac{1}{2}\Delta z}(e^{\frac{1}{2}\Delta z}K_E(k)d_{fac}\left\{\frac{1}{\Delta z} + \frac{1}{2}\frac{d\overline{m}}{dz}(k)\right\} +$$

$$e^{-\frac{1}{2}\Delta z}K_E(k+1)d_{fac}\left\{\frac{1}{\Delta z} - \frac{1}{2}\frac{d\overline{m}}{dz}(k)\right\})\frac{1}{\Delta z} - L(l) + \frac{1}{2\Delta t}\} \tag{5.153}$$

$$f = e^{-z-\frac{1}{2}\Delta z}\left\{\frac{\Psi_X^{t-\Delta t,smo}}{2\Delta t} - \mathbf{v}_n \cdot \nabla\Psi(k) + R(k)\right\} \tag{5.154}$$

At the lower boundary

$$Q^*(k_{bot}) = Q(k_{bot}) + P(k_{bot})\frac{F(1) + 0.5F(2)\Delta z}{F(1) - 0.5F(2)\Delta z}$$

$$f^*(k_{bot}) = f(k_{bot}) - P(k_{bot})\frac{F(3)\Delta z}{F(1) - 0.5F(2)\Delta z}$$

$$P^*(k_{bot}) = 0 \tag{5.155}$$

with F the coefficient A, B, C of the upward flux which are input to the subroutine minor. The upper boundary is set by

$$P^*(k_{top}) = 1 + \frac{1}{2}\Delta z T_{thdiff}(k_{top})$$

$$Q^*(k_{top}) = P^*(k_{bot}) - 2.$$

$$R^*(k_{top}) = 0.$$

$$f^*(k_{top}) = -\frac{gm_x F_x^{upw,top}\Delta z}{p_0\tilde{A}N_A} \tag{5.156}$$

with $F_x^{upw,top}$ the upward number flux at the upper boundary which is input to `subroutine minor`.

Solving for the mass mixing ratio Ψ at each latitude leads to the updated mass mixing ratio $\Psi^{upd,t_n+\Delta t}$ at the midpoints. The calculated values for the mass mixing ration $\Psi^{upd,t+\Delta t}$ are smoothed by a Fast Fourier transformation, which is part of the `minor module`. All the wave numbers larger than a predefined value at each latitude are removed. The wave numbers are defined in the `subroutine minor`. The values of the mass mixing ration at the time step t_n are also updated by using

$$\Psi^{upd,t_n} = \frac{1}{2}(1 - c_{smo})(\Psi^{t_n-\Delta t} + \Psi_{smo}^{upd,t_n+\Delta t}) + c_{smo}\Psi^{t_n} \qquad (5.157)$$

with $c_{smo} = 0.95$. All the values of Ψ^{upd,t_n} and $\Psi^{upd,t_n+\Delta t}$ have to be at least as larger as 10^{-12}

physical field	variable	unit	pressure level	timestep
mass mixing ratio O_2	$\Psi(O_2)$	$-$	midpoints	t_n
mass mixing ratio O	$\Psi(O)$	$-$	midpoints	t_n
mass mixing ratio NO	$\Psi(NO)$	$-$	midpoints	t_n
electron density	Ne	$1/cm^3$	interfaces	t_n
number density O^+	$n(O^+)$	$1/cm^3$	midpoints	t_n
number density $N(^2P)$	$n(N(^2P))$	$1/cm^3$	midpoints	t_n
number density NO^+	$n(NO^+)$	$1/cm^3$	midpoints	t_n
conversion factor	$N\overline{m}$	$\#/cm^3 g/mole$	midpoints	t_n

Table 5.7: Input fields to `subroutine comp_n2d`

physical field	variable	unit	pressure level	timestep
mass mixing ratio $N(^2D)$	$\Psi(N(^2D))$	$-$	midpoints	$t_n + \Delta t$

Table 5.8: Output fields of `subroutine comp_n2d`

5.4   Calculation of Minor species $N(^2D)$, $N(^4S)$, and NO

5.4.1   Calculation of $N(^2D)$

The input to `subroutine comp_n2d` is summarized in table 5.7. The output of `subroutine comp_n2d` is summarized in table 5.8. $N(^2D)$ is assumed to be in photochemical equilibrium, such that the production $P(N(^2D))$ and loss rate $L(N(^2D))$ of $N(^2D)$ is balanced.

$$n(N(^2D)) = \frac{P(N(^2D))}{L(N(^2D))} \tag{5.158}$$

The production is due to solar EUV photodissociation of N_2, and ion and neutral chemistry

$$P(N(^2D))(z + \frac{1}{2}\Delta z) = \frac{1}{2}\left[Q_{tef}(z) + Q_{tef}(z + \Delta z)\right] br_{N^2D} +$$
$$k_3 n(N_2^+) N\overline{m}\frac{\Psi(O)}{m_o} + (\alpha_1 n(NO^+)0.85 +$$
$$\alpha_3 n(N_2^+)0.9)\sqrt{Ne(z)Ne(z + \Delta z)} \qquad (5.159)$$

with the branching ratio of producing $N(^2D)$ which is set to 0.6. The chemical reaction rates are α and k defined in the `chemrates_module`. The total production rate due to solar radiation and auroral particle precipitation is denoted by Q_{tef} which is calculated in `subroutine qrj`.
The loss term $L(N(^2D))$ is determined by

$$L(N(^2D))(z + \frac{1}{2}\Delta z) = N\overline{m}\left[\beta_2\frac{\Psi(O_2)}{m_{O_2}} + \beta_4\frac{\Psi(O)}{m_O} + \beta_6\frac{\Psi(NO)}{m_{NO}}\right] +$$
$$\beta_7 + \beta_5\sqrt{Ne(z)Ne(z + \Delta z)} + k_{10}n(O^+) \quad (5.160)$$

The chemical rates β are defined in the module `chemrates_module`.
The number density $n(N(^2D))$ is converted to the mass mixing ratio by

$$\Psi(N(^2D) = \frac{m_{N^2D}}{N\overline{m}}\frac{P(N(^2D))}{L(N(^2D))} \qquad (5.161)$$

5.4.2   Calculation of $N(^4S)$

The input to `subroutine comp_n4s` is summarized in table 5.9. The output of `subroutine comp_n4s` are the factor which define the lower boundary calculated in `subroutine minor` by solving $A\frac{dX}{dZ} + BX + C = 0$. Also the upward flux at the upper boundary is defined, and the production P and loss rate L of $N(^4S)$. These values are stored in module data of the module `comp_n4s`. After `subroutine comp_n4s` the `subroutine minor_n4s` is called to calculate the mass mixing ratio of $N(^4S)$. `Subroutine minor_n4s` is not described here since it just calls `subroutine minor`. For information about `subroutine minor` please see chapter 5.3. The input to `subroutine minor` is described in table 5.4 and the output in table 5.5, subsituting the species X by $N(^4S)$.

physical field	variable	unit	pressure level	timestep
mass mixing ratio O_2	$\Psi(O_2)$	–	midpoints	t_n
mass mixing ratio O	$\Psi(O)$	–	midpoints	t_n
mass mixing ratio NO	$\Psi(NO)$	–	midpoints	t_n
mass mixing ratio $N(^2D)$	$\Psi(N(^2(D)))$	–	midpoints	t_n
electron density	Ne	$1/cm^3$	interfaces	t_n
number density O_2^+	$n(O_2^+)$	$1/cm^3$	midpoints	t_n
number density O^+	$n(O^+)$	$1/cm^3$	midpoints	t_n
number density N_2^+	$n(N_2^+)$	$1/cm^3$	midpoints	t_n
number density N^4	$n(N^4)$	$1/cm^3$	midpoints	t_n
number density NO^+	$n(NO^+)$	$1/cm^3$	midpoints	t_n
neutral temperature	Tn	K	midpoints	t_n
mean molecular mass	$\overline{m}$	$g/mole$????	midpoints	t_n
conversion factor	$N\overline{m}$	$\#/cm^3 g/mole$	midpoints	t_n

Table 5.9: Input fields to `subroutine comp_n4s`

$N(^4S)$ has longer life time and is therefore influenced by the neutral winds.

The lower boundary is given by photochemical equilibrium. The factors A, B, and C for the equation solved in `subroutine minor` $A\frac{d\Psi(N(^4S))}{dZ} + B\Psi(N(^4S)) + C = 0$ are

$$A = 0$$
$$B = 1.$$
$$C = (N(^4S)) = \frac{P(N(^4S))}{L(N(^4S))} \tag{5.162}$$

The conversion factor from number density to mass mixing ratio $N\overline{m}(z_{LB})$

at the lower boundary is

$$N\overline{m}(z_{LB}) = p_0 e^{-z_{bot}-1/2\Delta z} e^{1/2\Delta z} \frac{\overline{m}(z_{bot})}{k_B T_n(z_{bot})} \tag{5.163}$$

The mass mixing ratio ????? or number density at the lower boundary is then

$$C = n(N(^4S))(z_{lbc}) = \frac{m_{n(^4S)}}{N\overline{m}}[Q_{tef}(1-br_{N^2D})\frac{1}{N\overline{m}(z_{bot})}+$$

$$\frac{\Psi(N(^2D))}{m_{N^2D}}(\beta_4 N\overline{m}(z_bot)\frac{\Psi(NO)}{m_o} + \beta_5 Ne + \beta_7) + \beta_8\frac{\Psi(NO)}{m_{NO}}]$$

$$\frac{1}{\beta_1\frac{\Psi(O_2)}{m_{O_2}} + \beta_3\frac{\Psi(NO}{m_{NO}} + N\overline{m}\beta_{17}\frac{\Psi(O)}{m(O)}\frac{\Psi(N_2)}{m_{N_2}}} \tag{5.164}$$

At the upper boundary the upward diffusive flux is set

$$n(N(^4S))(z_{ubc}) = 0. \tag{5.165}$$

The production rate P of $N(^4S)$ is

$$P(N(^4S)) = \frac{1}{2}(Q_{tef}(z) + Q_{tef}(z+\Delta z))(1-br_{N^2D})+$$

$$N\overline{m}[\frac{\Psi(N^2D)}{m_{N^2D}}\left\{\beta_5\frac{1}{2}(Ne(z) + Ne(z+\Delta z) + \beta_7\right\}+$$

$$\frac{1}{2}(\beta_8(z) + \beta_8(z+\Delta z))\frac{\Psi(NO)}{m_{NO}}]+$$

$$N\overline{m}[k_2 n(O^+)\frac{\Psi(xN_2)}{m_{N_2}} + k_6 n(N^+)\frac{\Psi(O_2)}{m_{O_2}}k_8 n(N^+)\frac{\Psi(O)}{m_O}+$$

$$\sqrt{Ne(z)\cdot Ne(z+\Delta z)}(\alpha_1 n(NO^+)0.15 + \alpha_3 n(N_2^+)1.1)] \tag{5.166}$$

and the loss rate L of $N(^4S)$ is

$$L(N(^4S)) = -N\overline{m}\left[\beta_1\frac{\Psi(O_2)}{m_{O_2}} + \beta_3\frac{\Psi(NO)}{m_{NO}} + N\overline{m}\beta_{17}\frac{\Psi(O)}{m_O}\frac{\Psi(xN_2)}{m_{N_2}}\right]-$$

$$k_4 n(O_2^+) \tag{5.167}$$

physical field	variable	unit	pressure level	timestep
mass mixing ratio O_2	$\Psi(O_2)$	–	midpoints	t_n
mass mixing ratio O	$\Psi(O)$	–	midpoints	t_n
mass mixing ratio $N(^4S)$	$\Psi(N(^4S))$	–	midpoints	t_n
mass mixing ratio $N(^2D)$	$\Psi(N(^2(D)))$	–	midpoints	t_n
electron density	Ne	$1/cm^3$	interfaces	t_n
number density O_2^+	$n(O_2^+)$	$1/cm^3$	midpoints	t_n
neutral temperature	Tn	K	midpoints	t_n
mean molecular mass	$\overline{m}$	$g/mole????$	midpoints	t_n
conversion factor	$N\overline{m}$	$\#/cm^3 g/mole$	midpoints	t_n

Table 5.10: Input fields to `subroutine comp_no`

5.4.3   Calculation of NO

The input to `subroutine comp_no` is summarized in table 5.10. The output of `subroutine comp_no` are the factors A, B, and C which define the lower boundary condition of NO , the upper boundary upward diffusive flux, and the production P and loss rate L of NO. These values are stored in module data of the module `comp_no`. After `subroutine comp_no` the `subroutine minor_no` is called to calculate the mass mixing ratio of NO. Subroutine `minor_no` is not described here since it just calls `subroutine minor`. For information about `subroutine minor` please see chapter 5.3. The input to `subroutine minor` is described in table 5.4 and the output in table 5.5, subsituting the species X by NO.

NO has longer life time and is therefore influenced by the neutral winds. The lower boundary is given by photochemical equilibrium. The factors A, B, and C for the equation solved in `subroutine minor` $A\frac{d\Psi(N(^4S))}{dZ} +$

$B\Psi(N(^4S)) + C = 0$ are

$$A = 0$$
$$B = 1.$$
$$C = ???\Psi(NO) = -\frac{n(NO)(z_{LB})m_{NO}k_B T_n(z_{LBC})}{p_0 e^{1/2\Delta z}e^{-z-1/2\Delta z}\overline{m}(z_{LBC}}$$
(5.168)

with $n(NO)(z_{LB}) = 4\cdot 10^6$. At the upward diffusive flux at the upper boundary is set to zero

$$n(N(^4S))(z_{ubc}) = 0.$$
(5.169)

The production rate P of NO is

$$P(NO) = (N\overline{m})^2 \frac{\Psi(O_2)}{m_{O_2}}\left(+\beta_2 \frac{\Psi(N(^2D))}{m_{N^2D}}\right) +$$
$$(N\overline{m})^3 \beta_{17} \frac{\Psi(N_2)}{m_{N_2}} \frac{\Psi(N(^4S))}{m_{N^4S}}$$
(5.170)

and the loss rate L of NO is

$$L(NO) = - N\overline{m}\left[\beta_3 \frac{\Psi(N(^4S))}{m_{N(^4S)}} + \beta_6 \frac{\Psi(N(^2D))}{m_{N(^2D)}}\right] - \frac{1}{2}\left(\beta_8(z) + \beta_8(z + \Delta z)\right) +$$
$$\frac{1}{2}\left(\beta_9(z) + \beta_9(z + \Delta z)\right) - k_9 n(O_2^+)\frac{1}{2}\left(\beta_{9n}(z) + \beta_{9n}(z + \Delta z)\right)$$
(5.171)

physical field	variable	unit	pressure level	timestep
mass mixing ratio O_2	$\Psi(O_2)$	−	midpoints	t_n
mass mixing ratio O	$\Psi(O)$	−	midpoints	t_n
electron density	Ne	$1/cm^3$	interfaces	t_n
number density O^+	$n(O^+)$	$1/cm^3$	midpoints	t_n
number density N_2^+	$n(N_2^+)$	$1/cm^3$	midpoints	t_n
number density NO^+	$n(NO^+)$	$1/cm^3$	midpoints	t_n
number density NO	$n(NO)$	$1/cm^3$	midpoints	t_n
number density $N(^4S)$	$n(N(^4S))$	$1/cm^3$	midpoints	t_n
number density N^+	$n(N^+)$	$1/cm^3$	midpoints	t_n

Table 5.11: Input fields to `subroutine comp_o2o`

physical field	variable	unit	pressure level	timestep
matrix coefficients for rhs?	fs	−	midpoints?	$t_n + \Delta t$

Table 5.12: Output fields of `subroutine comp_o2o`

5.5 Calculation of Major species O_2, and O ,

5.5.1 Calculation of source and sinks for O_2 and O

The input to `subroutine comp_O2O` is summarized in table 5.11. The output of `subroutine comp_o2o` is summarized in table 5.12. The module data of `subroutine comp_o2o` is summarized in table 5.13. The source and sink terms for the neutral composition are calculated in this subroutine, and stored in the coefficient matrix fs, which is module data of `chemrates_module`.

Firstly, the total dissociation frequency and the production rates are

transferred from the interface level to the midpoint level.

$$rj(z + \frac{1}{2}\Delta z) = \frac{1}{2}[rj(z) + rj(z + \Delta z)]$$

$$Q(O_2^+)(z + \frac{1}{2}\Delta z) = \frac{1}{2}[Q(O_2^+)(z) + Q(O_2^+)(z + \Delta z)]$$

$$Q(O^+)(z + \frac{1}{2}\Delta z) = \frac{1}{2}[Q(O^+)(z) + Q(O^+)(z + \Delta z)] \tag{5.172}$$

The conversion factor $N\overline{m}$ from number density to mass mixing ratio is evaluated at the midpoint level

$$N\overline{m}(z + \frac{1}{2}\Delta z) = \frac{p_0 e^{-z-1/2\Delta z}}{k_B T_n(z + 1/2\Delta z)}\left(\frac{\Psi(O_2)}{m_{O_2}} + \frac{\Psi(O)}{m_O} + \frac{\Psi(N_2)}{m_{N_2}}\right) \tag{5.173}$$

with $\Psi(N_2) = 1 - \Psi(O_2) - \Psi(O)$, and $1/\overline{m}(z + \frac{1}{2}\Delta z) = \frac{\Psi(O_2)}{m_{O_2}} + \frac{\Psi(O)}{m_O} + \frac{\Psi(N_2)}{m_{N_2}}$.
The O_x production is

$$P(O_x) = (N\overline{m})^2\left[\beta_3\frac{n(N^4S)}{m_{N^4S}}\frac{n(NO)}{m_{NO}} + \beta_6\frac{n(N^2D)}{m_{N^2D}}\frac{n(NO)}{m_{NO}}\right] +$$

$$\frac{1}{2}(\beta_8(z) + \beta_8(z + \Delta z))\frac{n(NO)}{m_{NO}}N\overline{m}(z + \frac{1}{2}\Delta z) +$$

$$N\overline{m}(z + \frac{1}{2}\Delta z)\left[k_4 n(O_2^+)\frac{n(N^4S)}{m_{N^4S}} + k_4 n(O^+)\frac{n(N^2D)}{m_{N^2D}}\right] +$$

$$\sqrt{Ne(z)Ne(z + \Delta z)}(a_1 n(NO^+) = 2a_2 n(O_2^+)) \tag{5.174}$$

???? what is mass mixing ratio and what number density ??? and

$$P(O_{x2}) = (N\overline{m})(z + \frac{1}{2}\Delta z)\left[\beta_1\frac{n(N^4S)}{m_{N^4S}} + \beta_2\frac{n(N^2D)}{m_{N^2D}}\right] +$$

$$k_1 n(O^+) + k_7 n(N^+) + 2rj(z + \frac{1}{2}\Delta z) \tag{5.175}$$

The O_x loss rates are

$$L(O_{x1}) = 2k_{m12}N\overline{m}\frac{1}{\frac{1}{2}(\overline{m}(z) + \overline{m}(z + \Delta z))} \tag{5.176}$$

$$L(O_{x2}) = k_3 n(N_2^+) + k_8 n(N^+) \tag{5.177}$$

$$L(O_{x3}) = Q(O^+)(z + \frac{1}{2}\Delta z) \tag{5.178}$$

The O_2 production rates are

$$P(O_2)_1 = k_{m12} \frac{N\overline{m}(z + \frac{1}{2}\Delta z)}{\frac{1}{2}(\overline{m}(z) + \overline{m}(z + \Delta z))} \tag{5.179}$$

$$P(O_2)_2 = 0 \tag{5.180}$$

$$P(O_2)_3 = k_5 \frac{n(NO)}{m_{NO}} n(O_2^+) N\overline{m}(z + \frac{1}{2}\Delta z) \tag{5.181}$$

The O_2 loss rates are

$$L(O_2)_1 = N\overline{m}(z + \frac{1}{2}\Delta z) \left[\beta_1 \frac{n(N^4 S)}{m_{N^4 S}} + \beta_2 \frac{n(N^2 D)}{m_{N^2 D}} \right] +$$
$$k_1 n(O^+) + (k_6 + k_7) n(N^+) + k_9 n(N_2^+) + rj \tag{5.182}$$

$$l(O_2)_2 = Q(O_2^+)(z + \frac{1}{2}\Delta z) \tag{5.183}$$

The coefficients of the matrix (fs) are then

$$fs_{11} = -L(O_2) \tag{5.184}$$

$$fs_{12} = N\overline{m}(z + \frac{1}{2}\Delta z) P(O_2)_1 \frac{\Psi(O)}{m_O} \frac{m_{O_2}}{m_O} \tag{5.185}$$

$$fs_{21} = P(O_x)_2 \frac{m_O}{} m_{O_2} \tag{5.186}$$

$$fs_{22} = -L(O_x)_2 - L(O_x)_1 \frac{\Psi(O)}{m_O} N\overline{m}(z + \frac{1}{2}\Delta z) \tag{5.187}$$

$$fs_{10} = (P(O_2)_3 - L(O_2)_2) \frac{m_{O_2}}{N\overline{m}} \tag{5.188}$$

$$fs_{20} = (P(O_x)_1 - L(O_x)_3) \frac{m_O}{N\overline{m}} \tag{5.189}$$

$$\tag{5.190}$$

5.5.2 Calculation of major species O_2 and O

The input to subroutine comp is summarized in table 5.14. The output of subroutine comp is summarized in table 5.15. The module data of subroutine comp is summarized in table 5.16. The calculation of the composition is explained in [4] The major neutral constituents of the thermosphere

are O_2, O, and N_2. The mass mixing ratio of these are

$$\Psi_i = n_i m_i \left(\sum_{j=1}^{3} n_j m_j \right)^{-1} \tag{5.191}$$

with n_i the number density of the *ith* species, with $i = 1, 2,$ and 3 corresponding to O_2, O, and N_2. The molecular mass of the *ith* species is m_i. The vector of mass mixing ratios is defined by

$$\mathbf{\Psi} = \left(\begin{array}{c} \Psi_{O_2} \\ \Psi_O \end{array} \right) \tag{5.192}$$

The N_2 mass mixing ratio is determined by

$$\Psi_{N_2} = 1 - \Psi_{O_2} - \Psi_O \tag{5.193}$$

The coupled vector equation for the mass mixing ratio vector [4]

$$\frac{\partial}{\partial t}\mathbf{\Psi} = -e^z \tau^{-1} \frac{\partial}{\partial z} \left[\frac{\overline{m}}{m_{N_2} \left(\frac{T_{00}}{T_n} \right)^{0.25}} \alpha^{-1} \mathbf{L} \mathbf{\Psi} \right] +$$
$$e^z \frac{\partial}{\partial z} \left(K(z) e^{-z} \frac{\partial}{\partial z} \mathbf{\Psi} \right) -$$
$$\left(\mathbf{v}_n \cdot \nabla \mathbf{\Psi} + W \frac{\partial}{\partial z} \mathbf{\Psi} \right) + \mathbf{S} - \mathbf{R} \tag{5.194}$$

with time t, the vertical coordinate $z = ln(p_0/p)$, the pressure p and p_0 the reference pressure. The diffusion time scale is $\tau = (p_0 H_0 / p_{00} D_0) = 1.86 10^3 s$, with H_0 the characteristic molecular nitrogen scale height at $T_{00} = 273K$, $p_{00} = 10^5 Pa$, the characteristic diffusion coefficient at p_{00} and temperature T_{00} is $D_0 = 2 10^{-5} m^2/s$. The mean molecular mass is $\overline{m}$, the molecular mass of each species is m_i. The horizontal neutral velocity is $\mathbf{v}_n$, and the "vertical" velocity is $W = \frac{dz}{dt}$. $K(z)$ is the eddy diffusion coefficient, the effective mass source is $\mathbf{S}$, and the removal rate is $\mathbf{R}$.

The matrix α varies as the inverse of the diffusion coefficients according to

$$\begin{aligned} \alpha_{11} &= - \left[\phi_{13} + (\phi_{12} - \phi_{13})\Phi_2 \right] \\ \alpha_{22} &= - \left[\phi_{23} + (\phi_{21} - \phi_{23})\Phi_1 \right] \\ \alpha_{12} &= (\phi_{12} - \phi_{13})\Phi_1 \\ \alpha_{21} &= (\phi_{12} - \phi_{13})\Phi_2 \end{aligned} \tag{5.195}$$

where $i = 1, 2,$ and3 denotes O_2, O, and N_2 respectively. The value ϕ_{ij} is determined by

$$\phi_{ij} = \frac{D}{D_{ij}}\frac{m_3}{m_j} \tag{5.196}$$

with D_{ij} is the mutual diffusion coefficient for gases i and j with D_{12}, D_{13}, D_{23}, and D_0 being 0.26, 0.18, 0.26 [2], and $0.2 \times 10^{-4} m^2/s$, respectively. D is the characteristic diffusion coefficient, which has the same temperature and pressure dependence as D_{ij}

$$D = D_0\frac{P_{00}}{P}\left(\frac{P}{T_{00}}\right)^{1.75} \tag{5.197}$$

The matrix operator $\mathbf{L}$ is diagonal with elements

$$\mathbf{L} = \delta_{ij}\left(\frac{\delta}{\delta z} - \epsilon_{ii}\right) \tag{5.198}$$

and

$$\epsilon_{ii} = 1 - \frac{m_i}{m} - \frac{1}{m}\frac{\partial}{\partial z} \tag{5.199}$$

The matrix $\mathbf{L}$ defines diffusive equilibrium through $\mathbf{L\Phi} = 0$. at the upper boundary diffusive equilibrium is assumed, so that $\mathbf{L\Phi} = 0$. At the lower boundary the atomic oxygen concentration $n(O)$ peaks, which was observed, and therefore it is assumed $\partial n(O)/\partial z = 0$. Together with the the conservation of total oxygen atoms, this assumption leads to the following condition at the lower boundary

$$\frac{\partial}{\partial z}\Psi_2 = \Psi_2$$
$$\Psi_1 + \Psi_2 = constant \tag{5.200}$$

In the source code in `comp.F` first the values ϕ_{ij} from equation (5.195) are set

$$\phi_{21} = \frac{0.2}{0.26}\frac{28}{32} = \qquad\qquad 0.673$$

$$\phi_{12} = \frac{0.2}{0.26}\frac{28}{10} = \qquad\qquad 1.35$$

$$\phi_{13} = \frac{0.2}{0.18}\frac{28}{28} = \qquad\qquad 1.11$$

$$\phi_{23} = \frac{0.2}{0.26}\frac{28}{28} = \qquad\qquad 0.769 \tag{5.201}$$

The diffusive time scale τ is set to $1.86 \times 10^3 s$, and the standard temperature $T_{00} = 273K$. A δ matrix is set up as the identity matrix

$$\delta = \begin{pmatrix} 1 & 0 \\ 0 & 1 \end{pmatrix} \tag{5.202}$$

The horizontal advection term $\mathbf{v}_n \cdot \nabla \Psi$ is determined in the `subroutine advecl` which is part of the file `comp.F`. The input to the `subroutine advecl` is the mass mixing ratios $\Psi(O_2)^{tn}$ and $\Psi(O)^{tn}$, as well as the horizontal neutral velocities u_n and v_n.

$$\mathbf{v}_n \cdot \Psi_i = \frac{1}{2} \frac{1}{R_e \cos \lambda} [\frac{2}{3\Delta\phi} (\Psi_i(\phi + \Delta\phi, \lambda) - \Psi_i(\phi - \Delta\phi, \lambda))$$
$$(u_n(\phi + \Delta\phi, \lambda) + u_n(\phi - \Delta\phi, \lambda)) -$$
$$\frac{1}{12\Delta\phi} (\Psi_i(\phi + 2\Delta\phi, \lambda) - \Psi_i(\phi - 2\Delta\phi, \lambda)) (u_n(\phi + 2\Delta\phi, \lambda) + u_n(\phi - 2\Delta\phi, \lambda))] +$$
$$\frac{1}{2} \frac{1}{R_e} [\frac{2}{3\Delta\lambda} (\Psi_i(\phi, \lambda + \Delta\lambda) - \Psi_i(\phi, \lambda - \Delta\lambda)) (v_n(\phi, \lambda + \Delta\lambda) + v_n(\phi, \lambda - \Delta\lambda)) -$$
$$\frac{1}{12\Delta\lambda} (\Psi_i(\phi, \lambda + 2\Delta\lambda) - \Psi_i(\phi, \lambda - 2\Delta\lambda)) (v_n(\phi, \lambda\Delta\lambda) + v_n(\phi, \lambda - 2\Delta\lambda))] \tag{5.203}$$

for $i = 1, 2$ which corresponds to O_2 and O, respectively. The mass mixing ratios at timestep $t_n - \Delta t$ are smoothed with a two part Shapiro smoother. The smoothing in latitude is

$$\Psi_i^{t-\Delta t, \lambda_s} = \Psi_i^{t-\Delta t} - 0.03 \{\Psi_i^{t-\Delta t}(\phi, \lambda + 2\Delta\lambda) + \Psi_i^{t-\Delta t}(\phi, \lambda - 2\Delta\lambda) -$$
$$4[\Psi_i^{t-\Delta t}(\phi, \lambda + \Delta\lambda) + \Psi_i^{t-\Delta t}(\phi, \lambda - \Delta\lambda) + 6\Psi_i^{t-\Delta t}(\phi, \lambda)]\} \tag{5.204}$$

and afterwards a zonal smoothing is applied

$$\Psi_i^{t-\Delta t, smo} = \Psi_i^{t-\Delta t, \lambda_s} - 0.03 \{\Psi_i^{t-\Delta t, \lambda_s}(\phi + 2\Delta\phi, \lambda+) + \Psi_i^{t-\Delta t, \lambda_s}(\phi - 2\Delta\phi, \lambda) -$$
$$4[\Psi_i^{t-\Delta t, \lambda_s}(\phi + \Delta\phi, \lambda) + \Psi_i^{t-\Delta t, \lambda_s}(\phi - \Delta\phi, \lambda) + 6\Psi_i^{t-\Delta t, \lambda_s}(\phi, \lambda)]\} \tag{5.205}$$

for $i = 1, 2$ which corresponds to O_2 and O, respectively. The horizontal diffusion factor is set by

$$
\begin{aligned}
|\lambda| > 40^o &\qquad d_{fac} = 0.25 + 1.0 \\
|\lambda| \leq 40^o &\qquad d_{fac} = 0.25 + \frac{1}{2}\left(1 + \sin(\frac{\Pi(|\lambda| - 20^o)}{40^o})\right) \tag{5.206}
\end{aligned}
$$

If the input flag $DIFHOR$ is set to zero, in the input file then $d_{fac} = 0$. The mean molecular mass $\overline{m}$ is calculated at the midpoint level

$$\overline{m}(z + \frac{1}{2}\Delta z) = \left(\frac{\Psi(O_2)}{m_{O_2}} + \frac{\Psi(O)}{m_O} + \frac{\Psi(N_2)}{m_{N_2}} \right)^{-1} \qquad (5.207)$$

with $\Psi(N_2) = 1 - \Psi(O_2) - \Psi(O)$. Note that the mass mixing ratios are also on the midpoint levels.

The lower boundary values for the mass mixing ratios are set by

$$\Psi_i(z_{LB}) = b(i,1)\Psi(O_2)(z_{LB} + \frac{1}{2}\Delta z) + b(i,2)\Psi(O)(z_{LB} + \frac{1}{2}\Delta z) + f_b(i) \qquad (5.208)$$

for $i = 1, 2$ which corresponds to O_2 and O, respectively. The values $b(i,1)$, $b(i,2)$ and $f_b(i)$ are set in the `boundary_module`. With the mass mixing ratios at the lower boundary the mean molecular mass can be determined at the lower boundary

$$\overline{m}(z_{LB}) = \left(\sum_{i=1}^{3} \frac{\Psi_i}{m_i}(z_{LB}) \right)^{-1} \qquad (5.209)$$

for $i = 1, 2 \text{and} 3$ which corresponds to O_2, O and N_2, respectively. The term $\frac{1}{\overline{m}}\frac{\partial \overline{m}}{\partial z}$ at the bottom is determined

$$wk_4 = \frac{1}{\overline{m}(z_{LB}) + \overline{m}(z_{LB} + \frac{1}{2}\Delta z)} \frac{\overline{m}(z_{LB} + \frac{1}{2}\Delta z) + \overline{m}(z_{LB})}{\Delta z} \qquad (5.210)$$

???? where is the factor of $1/2$ and $1/2$ in wk_4 which level. Is the LB below the LB level???????. The *epsilon* terms $1 - \frac{1}{\overline{m}}[m_i + \frac{\partial \overline{m}}{\partial z}]$ are

$$\epsilon_i(k_m) = 1 - \frac{2}{\overline{m}(z_{LB}) + \overline{m}(z_{LB} + \frac{1}{2}\Delta z)}[m_i + \frac{\overline{m}(z_{LB} + \frac{1}{2}\Delta z) - \overline{m}(z_{LB})}{\Delta z}] \qquad (5.211)$$

for $i = 1, 2$ which corresponds to O_2 and O, respectively, and $k_m = 2$. The value

$$zz_1(k_m) = zz_1(k_m) = 0 \qquad (5.212)$$

??? how does the algorithm goes????. Next the matrix α at the height level $z + 0.25\Delta z$ is determined

$$\alpha_{1,1}^*(k_m) = \alpha_{22} = -\Delta_{11}[\phi_{2,3} + \{\phi_{2,1} - \phi_{2,3}\}$$
$$\frac{1}{2}\{\Psi_1(z_{LB}) + \Psi_1(z_{LB} + \frac{1}{2}\Delta z)\}] \tag{5.213}$$

$$\alpha_{1,2}^*(k_m) = -\alpha_{12} = [1 - \Delta_{12}][\phi_{1,2} - \phi_{1,3}]$$
$$\frac{1}{2}\{\Psi_1(z_{LB}) + \Psi_1(z_{LB} + \frac{1}{2}\Delta z)\}] \tag{5.214}$$

$$\alpha_{2,2}^*(k_m) = \alpha_{11} = -\Delta_{22}[\phi_{1,3} + \{\phi_{1,2} - \phi_{1,3}\}$$
$$\frac{1}{2}\{\Psi_2(z_{LB}) + \Psi_2(z_{LB} + \frac{1}{2}\Delta z)\}] \tag{5.215}$$

$$\alpha_{2,1}^*(k_m) = -\alpha_{21} = [1 - \Delta_{22}][\phi_{2,2} - \phi_{2,3}]$$
$$\frac{1}{2}\{\Psi_2(z_{LB}) + \Psi_2(z_{LB} + \frac{1}{2}\Delta z)\}] \tag{5.216}$$

Note, that the indices in the source code already take into account the inverse of the matrix with $\alpha^{-1} = \alpha^*/det|\alpha|$, and therefore the diagonal values are switches and the off-diagonal terms have an minus sign. The determinant $det|\alpha|$ is the same as $det|\alpha^*(k_m)| = \alpha_{1,1}^*(k_m)\alpha_{2,2}^*(k_m) - \alpha_{1,2}^*(k_m)\alpha_{2,1}^*(k_m)$. The matrix α^* is multiplied by the factor $\frac{1}{\tau}\frac{m}{m_{N_2}}\left(\frac{T_{00}}{T_n}\right)^{0.25}\frac{1}{det|\alpha^*|}$

$$wk_1 = \frac{1}{\tau}\frac{1}{2}[\overline{m}(z_{LB} + \overline{m}(z_{LB} + \frac{1}{2}\Delta z)]\frac{1}{m_{N_2}}\left(\frac{T_{00}}{T_n(z_{LB})}\right)^{0.25}\frac{1}{det|\alpha^*(k_m)|} \tag{5.217}$$

which lead to the quantity defined as $A = \frac{1}{\tau}\frac{\overline{m}}{m_{N_2}}\left(\frac{T_{00}}{T_n}\right)^{0.25}\alpha^{-1}$. The value γ at the bottom are set to

$$\gamma_{ij}(k = 1) = 0. \tag{5.218}$$

for $i = 1, 2$ and $j + 1, 2$, which corresponds to O_2 and O, respectively.

After setting all the values at the bottom of the model, the height loops starts from the bottom to the top of the model ($k = 1/z = -6.75$ to $k =$

$nlev - 1/z = 6.75$). The *epsilon*terms $1 - \frac{1}{m}[m_i + \frac{\partial \overline{m}}{\partial z}]$ are set at z by

$$\epsilon_i(k_p) = 1 - \frac{2}{\overline{m}(z - \frac{1}{2}\Delta z) + \overline{m}(z + \frac{1}{2}\Delta z)}[m_i + \frac{\overline{m}(z + \frac{1}{2}\Delta z) - \overline{m}(z - \frac{1}{2}\Delta z)}{\Delta z}]$$

(5.219)

for $i = 1, 2$ which corresponds to O_2 and O, respectively, and $k_p = 1$. Note that before the value $\epsilon_i(k_m)$ was determined, with $k_m = 2$. The values of k_m and k_p are alternating between 1 and 2 to get the values at the previous height level $k_m = k - 1$, and the height level $k_p = k + 1$. The α is determined at k_p/z by

$$\alpha_{1,1}^*(k_p) = \alpha_{22} = -\Delta_{11}[\phi_{2,3} + \{\phi_{2,1} - \phi_{2,3}\}$$
$$\frac{1}{2}\{\Psi_1(z - \frac{1}{2}\Delta z) + \Psi_1(z + \frac{1}{2}\Delta z)\}]$$

(5.220)

$$\alpha_{1,2}^*(k_p) = -\alpha_{12} = [1 - \Delta_{12}][\phi_{1,2} - \phi_{1,3}]$$
$$\frac{1}{2}\{\Psi_1(z - \frac{1}{2}\Delta z) + \Psi_1(z + \frac{1}{2}\Delta z)\}]$$

(5.221)

$$\alpha_{2,2}^*(k_p) = \alpha_{11} = -\Delta_{22}[\phi_{1,3} + \{\phi_{1,2} - \phi_{1,3}\}$$
$$\frac{1}{2}\{\Psi_2(z - \frac{1}{2}\Delta z) + \Psi_2(z + \frac{1}{2}\Delta z)\}]$$

(5.222)

$$\alpha_{2,1}^*(k_p) = -\alpha_{21} = [1 - \Delta_{22}][\phi_{2,2} - \phi_{2,3}]$$
$$\frac{1}{2}\{\Psi_2(z - \frac{1}{2}\Delta z) + \Psi_2(z + \frac{1}{2}\Delta z)\}]$$

(5.223)

The matrix α^* is multiplied by the factor $\frac{1}{\tau}\frac{\overline{m}}{m_{N_2}}\left(\frac{T_{00}}{T_n}\right)^{0.25}\frac{1}{det|\alpha^*|}$

$$wk_1 = \frac{1}{\tau}\frac{1}{2}[\overline{m}(z - \frac{1}{2}\Delta)\overline{m}(z + \frac{1}{2}\Delta z)]\frac{1}{m_{N_2}}\left(\frac{T_{00}}{T_n(z)}\right)^{0.25}\frac{1}{det|\alpha^*(k_p)|} \quad (5.224)$$

which lead to the quantity defined as $A = \frac{1}{\tau}\frac{\overline{m}}{m_{N_2}}\left(\frac{T_{00}}{T_n}\right)^{0.25}\alpha^{-1}$. The term $\frac{1}{m}\frac{\partial \overline{m}}{\partial z}$ at is determined, but first the value wk_4 which holds the value for k_p/z is copied into wk_3 which holds the value for $k_m/z - \Delta z$.

$$wk_4 = \frac{1}{\overline{m}(z - \frac{1}{2}\Delta z) + \overline{m}(z + \frac{1}{2}\Delta z)}\frac{\overline{m}(z + \frac{1}{2}\Delta z) + \overline{m}(z - \frac{1}{2}\Delta z)}{\Delta z} \quad (5.225)$$

???? where is the factor of 1/2 and 1/2 in wk_4 which level. ???????.

The discretizied equation can be written as

$$\mathbf{P}_k \mathbf{\Psi}_{k-1}^{t_n+\Delta t} + \mathbf{Q}_k \mathbf{\Psi}_k^{t_n+\Delta t} + \mathbf{R}_k \mathbf{\Psi}_{k+1}^{t_n+\Delta t} = \mathbf{f}_k \qquad (5.226)$$

with

$$P_k = \frac{A(k_m)}{\Delta z}\left(\frac{1}{\Delta z} + \frac{\epsilon(k_m)}{2}\right) - \frac{e^{-z}K(k_m)}{\Delta^2 z} - \frac{e^{-z}W(k)}{2\Delta z} \qquad (5.227)$$

$$R_k = \frac{A(k_p)}{\Delta z}\left(\frac{1}{\Delta z} + \frac{\epsilon(k_p)}{2}\right) - \frac{e^{-z}K(k_p)}{\Delta^2 z} + \frac{e^{-z}W(k)}{2\Delta z} \qquad (5.228)$$

$$Q_k = -\left[\frac{A(k_m)}{\Delta z}\left(\frac{1}{\Delta z} - \frac{\epsilon(k_m)}{2}\right)\right. \qquad (5.229)$$

$$\frac{A(k_p)}{\Delta z}\left(\frac{1}{\Delta z} + \frac{\epsilon(k_p)}{2}\right) - \frac{e^{-z}K(k_m)}{\Delta^2 z} - \frac{e^{-z}K(k_p)}{\Delta^2 z} + JSe^{-z} - \frac{e^{-z}}{2\Delta t}\right]$$

$$f_k = e^{-z}\left[\frac{\Psi^{t_n-\Delta t}(k)}{2\Delta t} - \mathbf{v}_n \cdot \nabla\Psi^{t_n}(k)\right] \qquad (5.230)$$

In the source code the values are

$$P_k(i,j) = [A(k_m)(i,j)\left(\frac{1}{\Delta z} + \frac{\epsilon(k_m)(j)}{2}\right)$$

$$- e^{-(z+\frac{1}{2}\Delta z)}(e^{\frac{1}{2}\Delta z}K(k???z - \frac{1}{2}\Delta z)d_{fac}(\frac{1}{\Delta z} - wk_3) +$$

$$0.25(W(z) + W(z+\Delta z)))\Delta(i,j)]\frac{1}{\Delta z} \qquad (5.231)$$

$$R_k(i,j) = [A(k_p)(i,j)\left(\frac{1}{\Delta z} - \frac{\epsilon(k_p)(j)}{2}\right)$$

$$- e^{-(z+\frac{1}{2}\Delta z)}(e^{-\frac{1}{2}\Delta z}K(k+1/z + \frac{1}{2}\Delta z)d_{fac}(\frac{1}{\Delta z} + wk_4) -$$

$$0.25(W(z) + W(z+\Delta z)))\Delta(i,j)]\frac{1}{\Delta z} \qquad (5.232)$$

$$Q_k(i,j) = -\frac{1}{\Delta z}[A(k_m)(i,j)\left(\frac{1}{\Delta z} - \frac{\epsilon(k_m)(j)}{2}\right) + A(k_p)(i,j)\left(\frac{1}{\Delta z} + \frac{\epsilon(k_p)(j)}{2}\right)$$

$$+ e^{-(z+\frac{1}{2}\Delta z)}(\{e^{\frac{1}{2}\Delta z}K(k+1/z+\frac{1}{2}\Delta z)(\frac{1}{\Delta z} - wk_4)-$$

$$e^{-\frac{1}{2}\Delta z}K(k/z - \frac{1}{2}\Delta z)(\frac{1}{\Delta z} + wk_3)\}\frac{d_{fac}}{\Delta z} + \frac{1}{2\Delta t}$$

$$)\Delta(i,j) - fs(i,j)] \tag{5.233}$$

The right hand side is assembled in the following

$$f_k(i) = e^{-(z+\frac{1}{2}\Delta z)}[\frac{\Psi_i^{t_n - \Delta t, smo}}{2\Delta t} - \mathbf{v}_n \cdot \nabla\Psi_i + f_{s,0}(i) + h_{d,i}] \tag{5.234}$$

for $i = 1, 2$ corresponding to O_2 and O, respectively.

At the lower boundary the coefficients are adjusted ??? what's the condition there???

$$Q_k^*(i,j)(z_{bot}) = Q_k(i,j)(z_{bot}) + P_k(i,1)(z_{bot})b(1,j) + P_k(i,2)(z_{bot})b(2,j) \tag{5.235}$$

with $z_{bot} = -6.75$ or $z_{bot} = z_{LB} + \frac{1}{2}\Delta z$, and $i = 1, 2$ and $j = 1, 2$ corresponding to O_2 and O, respectively. The updated right hand side is

$$f_k^*(i)(z_{bot}) = f_k(i)(z_{bot}) - P_k(i,1)(z_{bot})fb(1) - P_k(i,2)(z_{bot})fb(2) \tag{5.236}$$

with $i = 1, 2$ corresponding to O_2 and O, respectively.

At the upper boundary we set $\frac{\partial}{\partial z}\boldsymbol{\Psi} = \epsilon\boldsymbol{\Psi}$ which leads to

$$\frac{\Psi(k+1) - \Psi(k)}{\Delta z} = \frac{\epsilon(z+\frac{1}{2}\Delta z)}{2}(\Psi(k+1) + \Psi(k))) \tag{5.237}$$

with $k = nlev1 - 1$ and $k+1 = nlev$ corresponding to $z_{ub} - \frac{3}{2}\Delta z = 6.25$ and $z_{ub} - \frac{1}{2}\Delta z = 6.75$, respectively. The coefficient equation looks like

$$P_k\Psi(k-1) + [Q_k + R_k\frac{1 + 0.5\epsilon(k+1/2)\Delta z}{1 - 0.5\epsilon(k+1/2)\Delta z}]\Psi(k) = f_k \tag{5.238}$$

??? make matrix out of the equation????

$$Q_k^*(i,j)(z_{ub} - \frac{3}{2}\Delta z) = Q_k(i,j)(z_{ub} - \frac{3}{2}\Delta z)+$$

$$\frac{1 + 0.5\epsilon(k+1/2)\Delta z}{1 - 0.5\epsilon(k+1/2)\Delta z}R_k(i,j)(z_{ub} - \frac{3}{2}\Delta z) \qquad (5.239)$$

$$R_k^*(i,j)(z_{ub} - \frac{3}{2}\Delta z) = 0 \qquad (5.240)$$

with $i = 1,2$ and $j = 1,2$ corresponding to O_2 and O, respectively. For solving the equation the following values are needed ??? is this Newton iteration??? How does it work????

$$Q_k'(i,j) = Q_k(i,j) - P_k(i,1) * \gamma(1,j)(k) - P_k(i,2) * \gamma(2,j)(k) \quad (5.241)$$

$$wk_1 = det|Q_k'| \qquad (5.242)$$

$$wk_{m1}(1,j) = \frac{1}{wk_1}[\Delta(1,j)Q_k(2,2) - (1 - \Delta(1,j))Q_k(1,j)] \qquad (5.243)$$

$$wk_{m1}(2,j) = \frac{1}{wk_1}[\Delta(2,j)Q_k(1,1) - (1 - \Delta(2,j))Q_k(2,j)] \qquad (5.244)$$

$$wk_{v1}(i) = f_k(i) - \sum_{j=1}^{2} P_k(i,j)zz(k)(j) \qquad (5.245)$$

$$\gamma(k+1)(1,j) = \sum_{m=1}^{2} wk_{m1}(1,m)R_k(m,j) \qquad (5.246)$$

$$\gamma(k+1)(2,j) = \sum_{m=1}^{2} wk_{m1}(2,m)R_k(m,j) \qquad (5.247)$$

$$zz(k+1)(i) = \sum_{m=1}^{2} wk_{m1}(i,m)wk_{v1}(m) \qquad (5.248)$$

Hereby end the height loop from the bottom to the top of the model. The values at the top ($k = nlev + 1$ or $z_{UB} + \frac{1}{2}\Delta z = 7.25$) are set

$$\Psi_i^{t_n+\Delta t}(z_{UB} + \frac{1}{2}\Delta z) = 0 \qquad (5.249)$$

with $i = 1,2$ corresponding to O_2 and O, respectively. The updated value is

$$upd_i(z_{UB} + \frac{1}{2}\Delta z) = 0 \qquad (5.250)$$

Then the downward sweep begins

$$upd_i(k) = zz(k+1)(i) \tag{5.251}$$

$$upd_i(k) = upd_i(k) - \sum_{j=1}^{2} \gamma(k+1)(i,j)upd_j(k+1) \tag{5.252}$$

$$\Psi_i^{t_n+\Delta t}(k) = upd_i(k) \tag{5.253}$$

with k and $k+1$ corresponding to $z - \frac{1}{2}\Delta z$ and $z + \frac{1}{2}\Delta z$, respectively, and with $i = 1, 2$ and $j = 1, 2$ corresponding to O_2 and O, respectively.

The upper boundary is set by

$$\Psi_i^{t_n+\Delta t}(lev1) = \frac{1 + 0.5\epsilon_i(k_p)\Delta z}{1 - 0.5\epsilon_i(k_p)\Delta z}\Psi_i^{t_n+\Delta t}(lev1 - 1) \tag{5.254}$$

with $i = 1, 2$ and corresponding to O_2 and O, respectively.
The calculated values for the mass mixing ratio $\Psi_i^{upd,t+\Delta t}$ are smoothed by a Fast Fourier transformation. All the wave numbers larger than a predefined value at each latitude are removed. The wave numbers are defined in the module cons.F. The values of the mass mixing ratio at the timestep t_n are also updated by using

$$\Psi_i^{upd,t_n} = \frac{1}{2}(1 - c_{smo})(\Psi_i^{t_n-\Delta t} + \Psi_{i,smo}^{upd,t_n+\Delta t}) + c_{smo}\Psi_i^{t_n} \tag{5.255}$$

with $c_{smo} = 0.95$, and $i = 1, 2$ and corresponding to O_2 and O, respectively. Non negative values are assured by

$$\Psi_i^{upd,t_n} < 1 \times 10^{-6} \qquad \Psi_i^{upd,t_n} = 1 \times 10^{-6} \tag{5.256}$$

$$\Psi_i^{upd,t_n+\Delta t} < 1 \times 10^{-6} \qquad \Psi_i^{upd,t_n+\Delta t} = 1 \times 10^{-6} \tag{5.257}$$

$$1 - \sum_{i=1}^{2} \Psi_i^{upd,t_n+\Delta t} < 1 \times 10^{-6} \qquad \Psi_i^{upd,t_n+\Delta t} = \Psi_i^{upd,t_n+\Delta t}\frac{1 - 10^{-6}}{\sum_{i=1}^{2} \Psi_i^{upd,t_n+\Delta t}} \tag{5.258}$$

$$1 - \sum_{i=1}^{2} \Psi_i^{upd,t_n} < 1 \times 10^{-6} \qquad \Psi_i^{upd,t_n} = \Psi_i^{upd,t_n}\frac{1 - 10^{-6}}{\sum_{i=1}^{2} \Psi_i^{upd,t_n}} \tag{5.259}$$

physical field	variable	unit	module	timestep
inverse of molecular mass O_2	$1/m_{O_2}$	$mole/g$	cons	$-$
inverse of molecular mass O	$1/m_O$	$mole/g$	cons	$-$
inverse of molecular mass N_2	$1/m_{N_2}$	$mole/g$	cons	$-$
reference pressure	p_0	???	cons	$-$
-	e^z	$-$	cons	$-$
Boltzman constant	k_B	$-$	cons	$-$
molecular mass NO	m_{NO}	$g/mole$	cons	$-$
molecular mass $N(^4S)$	m_{N^4S}	$g/mole$	cons	$-$
molecular mass $N(^2D)$	m_{N^2D}	$g/mole$	cons	$-$
molecular mass O_2	m_{O_2}	$g/mole$	cons	$-$
molecular mass O	m_O	$g/mole$	cons	$-$
total O_2 dissociation frequency	rj	$1/s$	qrj	*interface*
O_2^+ production rate	$Q(O_2^+)$	??	qrj	*interface*
O^+ production rate	$Q(O^+)$	??	qrj	*interface*
chemical reaction rates	k_i	???	chemrates	$-$
chemical reaction rates	β_i	???	chemrates	$-$
chemical reaction rates	a_i	???	chemrates	$-$
coefficient matrix	fs	???	chemrates	$-$

Table 5.13: Module data used in `subroutine comp_o2o`

physical field	variable	unit	pressure level	timestep
mass mixing ratio O_2	$\Psi(O_2)$	–	midpoints	t_n
mass mixing ratio O	$\Psi(O)$	–	midpoints	t_n
mass mixing ratio O_2	$\Psi(O_2)$	–	midpoints	$t_n - \Delta t$
mass mixing ratio O	$\Psi(O)$	–	midpoints	$t_n - \Delta t$
neutral temperature	T_n	K	midpoints	t_n
neutral zonal velocity	u_n	cm/s	midpoints	t_n
neutral meridional velocity	v_n	cm/s	midpoints	t_n
neutral "vertical" velocity	W	$1/s$	interfaces	t_n
horizontal diffusion of O_2	$h_a(O_2)$	??	midpoints ???	t_n
horizontal diffusion of O	$h_d(O)$	??	midpoints ???	t_n

Table 5.14: Input fields to `subroutine comp`

physical field	variable	unit	pressure level	timestep
updated mass mixing ratio O_2	$\Psi(O_2)^{upd}$	–	midpoints	t_n
updated mass mixing ratio O	$\Psi(O)^{upd}$	–	midpoints	t_n
updated mass mixing ratio O_2	$\Psi(O_2)^{upd}$	–	midpoints	$t_n + \Delta t$
updated mass mixing ratio O	$\Psi(O)^{upd}$	–	midpoints	$t_n + \Delta t$

Table 5.15: Output fields of `subroutine comp`

physical field	variable	unit	module	timestep
inverse of molecular mass O_2	$1/m_{O_2}$	$mole/g$	cons	—
inverse of molecular mass O	$1/m_O$	$mole/g$	cons	—
inverse of molecular mass N_2	$1/m_{N_2}$	$mole/g$	cons	—
-	$e^{-z-\frac{1}{2}\Delta z}$	—	cons	—
-	$e^{-\frac{1}{2}\Delta z}$	—	cons	—
-	$e^{\frac{1}{2}\Delta z}$	—	cons	—
molecular mass O_2	m_{O_2}	$g/mole$	cons	—
molecular mass O	m_O	$g/mole$	cons	—
	Π	—	cons	—
	$\frac{1}{2\Delta t}$		cons	—
smoothing factor	$f_{smo} = 0.95$		cons	—
	$\frac{1}{2}(1-0.95)$		cons	—
background eddy diffusion	d_k		cons	—
wave filtering	k_{ut5}		cons	—
matrix coefficients with source and sinks	**fs**		chemrates	—

Table 5.16: Module data used in `subroutine comp`

Chapter 6

Ionospheric processes

6.1   Joule heating calculation

For the Joule heating calculation we assume that the electric field $\mathbf{E}$ is perpendicular to the geomagnetic field. The heating rate per unit mass Q_J [erg/s/g] is

$$Q_J = \frac{\mathbf{J}\perp \cdot (\mathbf{E} + \mathbf{v}_n \times \mathbf{B})}{\rho} = \frac{\sigma_P(\mathbf{E} + \mathbf{v}_n \times \mathbf{B})^2}{\rho} = \lambda_1(\mathbf{v}_{ExB} - \mathbf{v}_{n\perp})^2 \quad (6.1)$$

where $\mathbf{v}_n$ is is the neutral wind, $textbf{v}_{n,\perp}$ is the component of $\mathbf{v}_n$ perpendicular to the geomagnetic field $\mathbf{B}$, σ_P is the Pedersen conductivity, ρ is the atmospheric mass density, $\mathbf{v}_{ExB}$ is the electrodynamic drift velocity $\frac{\mathbf{E}\times\mathbf{B}}{B^2}$, and λ_1 is the Pedersen ion drag coefficient $\frac{\sigma_P B^2}{\rho}$.

The Joule heating is used in calculating the ion and neutral temperatures (see chapter 4.2 and 6.3).

In the heat equation for the neutrals there is no explicit term for the energy transfer from the ion to the neutrals, since we assume that eventually the whole Joule heating will go into the neutral temperature.

$$Q_J^{T_n} = \lambda_1(\mathbf{v}_{ExB} - \mathbf{v}_{n\perp})^2 \tag{6.2}$$

According to [25] only part of the Joule heating contributes to the ion temperature

$$Q_J^{T_i} = \frac{\overline{m}_n}{\overline{m}_n + \overline{m}_i}\lambda_1(\mathbf{v}_{ExB} - \mathbf{v}_{n\perp})^2 \tag{6.3}$$

This approximation is valid above approx. 100 km where the contributions from the electron neutral collisions to the Pedersen conductivity σ_P is small.

6.1.1   Joule heating calculation for ion temperature

The input to `subroutine qjoule_ti` is summarized in table 6.1. The output of `subroutine qjoule_ti` is summarized in table 6.2. The mean molecular mass of the ions $\overline{m}_{ion}$ at the midpoints in [g/mol] is calculated by

$$\overline{m}_{ion} = \frac{N_{O^+}m_O + N_{O_2^+}m_{O_2} + N_{N^+}m_{N^{4s}} + N_{N_2^+}m_{N_2} + N_{NO^+}m_{NO}}{N_{O^+} + N_{O_2^+} + N_{N^+} + N_{N_2^+} + N_{NO^+}} \tag{6.4}$$

and the mean molecular mass of the neutrals $\overline{m}_n$ at the midpoints in [g/mol] is

$$\overline{m}_n(z + \frac{1}{2}\Delta z) = 0.5 * (\overline{m}_n(z) + \overline{m}_n(z + \Delta z) \tag{6.5}$$

physical field	variable	unit	pressure level	timestep
neutral tempera-ture	T_n	K	midpoint	t_n
mean molecular mass	$\overline{m}$	$\frac{g}{mole}$	interface	t_{n+1}
mass mixing ratio of O_2	Ψ_{O_2}	mmr	midpoint	t_n
number density of ions	$N_{O_2^+}$	$1/cm^3$	midpoint	t_n
	N_{O^+}	$1/cm^3$	midpoint	t_n
	N_{NO^+}	$1/cm^3$	midpoint	t_n
	N_{N^+}	$1/cm^3$	midpoint	t_n
ion drag coefficient	λ_1	$1/s$	interface	t_n
$\mathbf{E} \times \mathbf{B}$ velocity	$\mathbf{v}_{ExB}$	cm/s	interface	t_n
dimensionless verti-cal velocity	W	$1/s$	interface	t_n
neutral velocity	$\mathbf{v}_n$	cm/s	midpoints	t_n

Table 6.1: Input fields to `subroutine qjoule_ti`

physical field	variable	unit	pressure level	timestep
Joule heating of ion temperature	$Q_J^{T_i}$	$\frac{ergs}{sg}$	midpoints	t_n t_{n+1}

Table 6.2: Output fields of `subroutine qjoule_ti`

with $\overline{m}_n$ on the interface level with z correspond to the height index k, $z+\Delta z$ to $k + 1$, and on the midpoint level $z + \frac{1}{2}$ correspond to the height index k. The scale height H [cm] at midpoints is

$$H = \frac{R^* T_n}{\overline{m}_n g} \tag{6.6}$$

since T_n and $\overline{m}_n$ are on the midpoint level. Note that the gas constant R^* is in units of [erg/K/mol] and the mean molecular mass in units of [g/mol]. The vertical neutral velocity w in [cm/s] is

$$w = WH \tag{6.7}$$

with the dimensionless vertical velocity W. The dimensionless vertical veloc-ity at the midpoints is determined by averaging the values at the height level

variable	physical name	value
N_A	Avogadro number	$6.023 \times 10^{23} \#/mol$
g	gravitational acceleration at lower boundary	cm/s^2
R^*	gas constant	$8.314 \times 10^7 erg/K/mol$
m_i	molecular weight species i	g/mol

Table 6.3: Global parameters used in `subroutine qjoule_ti`

k and $k+1$ to get the midpoint level k, i.e. $W(z+\frac{1}{2}) = 0.5[W(z)+W(z+\Delta z)]$. The $\mathbf{E} \times \mathbf{B}$ drift velocity $\mathbf{v}_{ExB}$ in [cm/s] at the midpoints is $\mathbf{v}_{ExB}(z+\frac{1}{2}\Delta z) = 0.5(\mathbf{v}_{ExB}(z) + \mathbf{v}_{ExB}(z + \Delta z))$, and the Pedersen ion drag coefficient λ_1 in [1/s] is averaged in the same way to get the midpoint values.

physical field	variable	unit	pressure level	timestep
neutral tempera-ture	T_n	K	midpoint	t_n
mean molecular mass	$\overline{m}$	$\frac{g}{mole}$	interface	t_{n+1}
mass mixing ratio of molecular oxygen	Ψ_{O_2}	-	midpoint	t_n
mass mixing ratio of atomic oxygen	Ψ_O	-	midpoint	t_n
ion temperature	T_i	K	midpoint	t_n
electron tempera-ture	T_e	K	midpoint	t_n
number density of ions	$N_{O_2^+}$	$1/cm^3$	midpoint	t_n
	N_{O^+}	$1/cm^3$	midpoint	t_n
	N_{NO^+}	$1/cm^3$	midpoint	t_n

Table 6.4: Input fields to `subroutine lamdas`

6.2 Ion drag calculation

The input to `subroutine lamdas` is summarized in table 6.4.

The output of `subroutine lamdas` is summarized in table 6.5. First the factor

$$\frac{q_e}{B} \quad \text{in} \left[\frac{C}{T} \frac{cm^3}{m^3} \right] \tag{6.8}$$

physical field	variable	unit	pressure level	timestep
ion drag coefficients geographic direc-tion	$\lambda_{xx}, \lambda_{yy}, \lambda_{xy}, \lambda_{yx},$	$1/s$	interface	t_n
Pedersen	λ_1	$1/s$	interface	t_n
conductivities	σ_H, σ_P	S/m	midpoint	t_n

Table 6.5: Output fields of `subroutine lamdas`

variable	physical name	value
q_e	electron charge	$1.602 \times 10^{-19}C$
$\frac{q_e}{10 m_e}$		$1.7588028 \times 10^7 C/g$
$\frac{q_e}{10 N_a}$		$9.6489 \times 10^3 C/mol$
m_{NO^+}	molecular weight of NO^+	$30 g/mol$

Table 6.6: Local parameters used in `subroutine lamdas`

is calculated. The gyro frequencies Ω in units of $[\frac{CT}{kg} = s^1]$ are

$$\Omega_{O^+} = \frac{q_e B}{N_a m_{O^+}} \tag{6.9}$$

$$\Omega_{O_2^+} = \frac{q_e B}{N_a m_{O_2^+}} \tag{6.10}$$

$$\Omega_{NO^+} = \frac{q_e B}{N_a m_{NO^+}} \tag{6.11}$$

$$\Omega_e = \frac{q_e B}{m_e} \tag{6.12}$$

The collision frequencies ν in units of $[s^{-1}]$ are determined by, e.g. [25]

$$\frac{1}{N_{O_2}}\nu_{O_2^+-O_2} = 2.59 \times 10^{-11}\sqrt{\frac{T_i+T_e}{2}}\left[1-0.73log_{10}\sqrt{\frac{T_i+T_e}{2}}\right]^2 \quad (6.13)$$

$$\frac{1}{N_{O_2}}\nu_{O^+-O_2} = 6.64 \times 10^{-10} \quad (6.14)$$

$$\frac{1}{N_{O_2}}\nu_{NO^+-O_2} = 4.27 \times 10^{-10} \quad (6.15)$$

$$\frac{1}{N_O}\nu_{O^+-O} = 3.67 \times 10^{-11}\sqrt{\frac{T_i+T_e}{2}}[1-0.064log_{10}\sqrt{\frac{T_i+T_e}{2}}]^2 f_{cor} \quad (6.16)$$

$$\frac{1}{N_O}\nu_{NO^+-O} = 2.44 \times 10^{-10} \quad (6.17)$$

$$\frac{1}{N_O}\nu_{O_2^+-O} = 2.31 \times 10^{-10} \quad (6.18)$$

$$\frac{1}{N_{N_2}}\nu_{O_2^+-N_2} = 4.13 \times 10^{-10} \quad (6.19)$$

$$\frac{1}{N_{N_2}}\nu_{NO^+-N_2} = 4.34 \times 10^{-10} \quad (6.20)$$

$$\frac{1}{N_{N_2}}\nu_{O^+-N_2} = 6.82 \times 10^{-10} \quad (6.21)$$

with N_n the number density for the neutral n in units of $[1/cm^3]$, and the temperature in $[K]$. The collisions frequencies for $\nu_{O_2^+-O_2}$ and ν_{O^+-O} are resonant, all other are nonresonant. The Burnside factor f_{cor} multiplies the ν_{O^+-O} collision frequency, and has the default value 1.5, which has been found to improve agreement between calculated winds and electron densities in the upper thermosphere in other models. The quantity xnmbar, which is the neutral number density N in cm^{-3} times the mean mass $\overline{m}_{mid}$ in $[g/mole]$ at the midpoints of the height level, is calculated by

$$N\overline{m}_{mid} = \frac{p_o e^{-Z}\overline{m}_{mid}}{k_B T_n} \quad (6.22)$$

where $p_o e^{-Z}$ is the pressure at the midpoints in $[dyn/cm^2]$ with Z the dimensionless variable at midpoints. The mean molecular weight at midpoints is averaged by $\overline{m}_{mid}(z+\frac{1}{2}\Delta z) = 0.5*(\overline{m}(z)+\overline{m}(z+\Delta z))$ with the height index on the interface level k corresponds to z, $k+1$ to $z+\Delta z$, and on the

midpoint level corresponds $z + \frac{1}{2}\Delta z$ to the k index level. The Boltzmann constant is denoted by k_B in [erg/K] and the neutral temperature T_n is in units of [K].

The number densities in $[1/cm^3]$ are

$$N_{O_2} = \frac{N\overline{m}_{mid}\Psi_{O_2}}{m_{O_2}} \tag{6.23}$$

$$N_O = \frac{N\overline{m}_{mid}\Psi_O}{m_O} \tag{6.24}$$

$$N_{N_2} = \frac{N\overline{m}_{mid}\Psi_{N_2}}{m_{N_2}} \tag{6.25}$$

with Ψ the mass mixing ratio. The mass mixing ratio of N_2 is determined by $\Psi_{N_2} = 1 - \Psi_{O_2} - \Psi_O$ with $\frac{\Psi_{N_2}}{m_{N_2}} \geq 1. \times 10^{-20}\frac{mol}{g}$.

The collision frequencies in $[1/s]$ are

$$\nu_{O_2^+} = \nu_{O_2^+-O_2} + \nu_{O_2^+-O} + \nu_{O_2^+-N_2} \tag{6.26}$$

$$\nu_{O^+} = \nu_{O^+-O_2} + \nu_{O^+-O} + \nu_{O^+-N_2} \tag{6.27}$$

$$\nu_{NO^+} = \nu_{NO^+-O_2} + \nu_{NO^+-O} + \nu_{NO^+-N_2} \tag{6.28}$$

$$\begin{aligned}
\nu_{en} = {} & 2.33 \times 10^{-11} N_{N_2} T_e (1 - 1.21 \times 10^{-4} T_e) + \\
& 1.82 \times 10^{-10} N_{O_2}\sqrt{T_e}(1 + 3.6 \times 10^{-2}\sqrt{T_e}) + \\
& 8.9 \times 10^{-11} N_O\sqrt{T_e}(1 + 5.7 \times 10^{-4} T_e)
\end{aligned} \tag{6.29}$$

The ratios r between collision frequency ν and gyro frequency Ω are

$$r_{O_2^+} = \frac{\nu_{O_2^+}}{\Omega_{O_2^+}} \tag{6.30}$$

$$r_{O^+} = \frac{\nu_{O^+}}{\Omega_{O^+}} \tag{6.31}$$

$$r_{NO^+} = \frac{\nu_{NO^+}}{\Omega_{NO^+}} \tag{6.32}$$

$$r_e = \frac{\nu_{en}}{\Omega_e} \tag{6.33}$$

with the gyro frequency for ions $\Omega_i = eB/m_i$ and for electrons $\Omega_e = eB/m_e$.

The Pedersen conductivity in $[S/m]$ is

$$
\begin{aligned}
\sigma_P =& \frac{q_e}{B}[N_{O^+}\frac{r_{O^+}}{1+r_{O^+}^2} + N_{O_2^+}\frac{r_{O_2^+}}{1+r_{O_2^+}^2}+ \\
& N_{NO^+}\frac{r_{NO^+}}{1+r_{NO^+}^2} + N_e\frac{r_e}{1+r_e^2}]
\end{aligned}
\tag{6.34}
$$

The Hall conductivity in $[S/m]$ is

$$
\begin{aligned}
\sigma_H =& \frac{q_e}{B}[-N_{O^+}\frac{1}{1+r_{O^+}^2} - N_{O_2^+}\frac{1}{1+r_{O_2^+}^2}- \\
& N_{NO^+}\frac{1}{1+r_{NO^+}^2} + N_e\frac{1}{1+r_e^2}]
\end{aligned}
\tag{6.35}
$$

with $N_e = N_{O^+} + N_{O_2^+} + N_{NO^+}$ assuming charge equilibrium. The Pedersen and Hall ion drag coefficients are

$$
\lambda_1 = \frac{\sigma_P B^2}{\rho}
\tag{6.36}
$$

$$
\lambda_2 = \frac{\sigma_H B^2}{\rho}
\tag{6.37}
$$

with $\rho = \frac{\overline{m}}{N_A}$, and N_A the Avagadro number. The ion drag coefficients are transferred to interfaces by

$$
\lambda_1(z) = \sqrt{\lambda_1(z + \frac{1}{2}\Delta z) * \lambda_1(z - \frac{1}{2}\Delta z)}
\tag{6.38}
$$

$$
\lambda_2(z) = \sqrt{\lambda_2(z + \frac{1}{2}\Delta z) * \lambda_2(z - \frac{1}{2}\Delta z)}
\tag{6.39}
$$

with the height index k at the z interface level, and $k+1$ at $z+\Delta z$. On the midpoint level the index k corresponds to $z + \frac{1}{2}\Delta z$. For the top and bottom

boundary the values are calculated by

$$\lambda_1(z_{top}) = \sqrt{\lambda_1^3(z_{top} - \frac{1}{2}\Delta z)/\lambda_1(z_{top} - \frac{3}{2}\Delta z)} \tag{6.40}$$

$$\lambda_2(z_{top}) = \sqrt{\lambda_2^3(z_{top} - \frac{1}{2}\Delta z)/\lambda_2(z_{top} - \frac{3}{2}\Delta z))} \tag{6.41}$$

$$\lambda_1(z_{bot}) = \sqrt{\lambda_1^3(z_{bot} + \frac{1}{2}\Delta z))/\lambda_1(z_{bot} + \frac{3}{2}\Delta z)} \tag{6.42}$$

$$\lambda_2(z_{bot}) = \sqrt{\lambda_2^3(z_{bot} + \frac{1}{2}\Delta z)/\lambda_2(z_{bot} + \frac{3}{2}\Delta z)} \tag{6.43}$$

with z_{top} on the interface level corresponds to the index $nlev$, and $z_{top} - \frac{1}{2}\Delta z$ is on the midpoint level and has the index $nlev-1$. At the bottom boundary z_{bot} corresponds to the index 1 on the interface level, and $z_{bot} + \frac{1}{2}\Delta z$ corresponds to the index 1 on the midpoint level. The ion drag tensor in magnetic direction $\underline{\lambda}^{mag}$ is

$$\underline{\lambda}^{mag} = \begin{pmatrix} \lambda_{xx}^{mag} & \lambda_{xy}^{mag} \\ \lambda_{yx}^{mag} & \lambda_{yy}^{mag} \end{pmatrix} = \begin{pmatrix} \lambda_1 & \lambda_2 sinI \\ -\lambda_2 sinI & \lambda_1 sin^2 I \end{pmatrix} \tag{6.44}$$

with the x–direction in magnetic east, and y–direction magnetic north. The inclination of the geomagnetic field lines is I. Note that in the code lyxnorot $[= \lambda_{yx}^{mag}]$ has the wrong sign, but is not used, being replaced by -lxynorot $[= -\lambda_{xy}^{mag}]$. The ion drag tensor can be rotated in geographic direction by using the rotation matrix $\mathbf{R}$

$$\mathbf{R} = \begin{pmatrix} \cos D & \sin D \\ -\sin D & \cos D \end{pmatrix} \tag{6.45}$$

with the declination D of the geomagnetic field. Applying the rotation to the ion drag tensor $\mathbf{R}\underline{\lambda}^{mag}\mathbf{R}^{-1}$ leads to

$$\Lambda = \begin{pmatrix} \lambda_{xx} & \lambda_{xy} \\ \lambda_{yx} & \lambda_{yy} \end{pmatrix} = \tag{6.46}$$

$$\begin{pmatrix} \lambda_{xx}^{mag} cos^2 D + \lambda_{yy}^{mag} sin^2 D & \lambda_{xy}^{mag} + (\lambda_{yy}^{mag} - \lambda_{xx}^{mag})\sin D \cos D \\ -\lambda_{xy}^{mag} + (\lambda_{yy}^{mag} - \lambda_{xx}^{mag})\sin D \cos D & \lambda_{yy}^{mag} \cos^2 D + \lambda_{xx}^{mag} \sin^2 D \end{pmatrix} \tag{6.47}$$

physical field	variable	unit	pressure level	timestep
neutral tempera-ture	T_n	K	midpoints	t_n
mass mixing ratio O_2	Ψ_{O_2}	–	midpoints	t_n
mass mixing ratio O	Ψ_O	–	midpoints	t_n
mean molecular mass	$\overline{m}$	g/mol	interfaces	$t_n + \Delta t$
Joule heating of ions	$Q_J^{T_i}$	$\frac{erg}{sg}$	midpoints	t_n
electron density	N_e	$\#/cm^3$	interfaces	t_n
electron tempera-ture	T_e	K	midpoints	t_n
ion temperature	T_i	K	midpoints	t_n
number density O^+	N_{O^+}	$\#/cm^3$	interfaces	t_n?
number density O_2^+	$N_{O_2^+}$	$\#/cm^3$	interfaces	t_n?
number density NO^+	N_{NO^+}	$\#/cm^3$	interfaces	t_n?

Table 6.7: Input fields to `subroutine setei`

6.3 Calculation of electron and ion temperature

The input to `subroutine settei` is summarized in table 6.7. The output of `subroutine settei` is summarized in table 6.8. The module data of `subroutine settei` is summarized in table 6.9. The general energy conservation equation without chemical and viscous heating of electron gas

$$\frac{3}{2} N_e k_B \frac{\partial T_e}{\partial t} = - N_e k_B T_e \nabla \cdot \mathbf{u}_e - \frac{3}{2} N_e k_B \mathbf{u}_e \cdot \nabla T_e - \nabla \cdot q_e +$$
$$\sum Q_e - \sum L_e \tag{6.48}$$

with the electron bulk velocity $\mathbf{u}_e$, the electron heat flow vector q_e, the sum of all local electron heating rates are $\sum Q_e$, and the sum of all local cooling

physical field	variable	unit	pressure level	timestep
electron tempera-ture	$T_e^{t_n+\Delta t}$	K	midpoints	$t_n + \Delta t$
ion temperature	$T_i^{t_n+\Delta t}$	K	midpoints	$t_n + \Delta t$

Table 6.8: Output fields of `subroutine settei`

physical field	variable	unit	pressure level	timestep

Table 6.9: Module data of `subroutine settei`

rates are $\sum L_e$. The electron heat vector is

$$q_e = -\beta_e \mathbf{J} - K^e \nabla_\parallel T_e \tag{6.49}$$

with β_e is the thermalelectric transport coefficient, $\mathbf{J}$ is the electric current density, and K^e is the electron thermal conductivity parallel to the magnetic field. K^e in $[\frac{ergs}{cm \ s \ K}]$ is calculated according to [Rees & Roble 1975]

$$K^e = \frac{7.5 \cdot 10^5 T_e^{2.5}}{1 + 3.22 \cdot 10^4 \frac{T_e^2}{N_e} (d_1 N_{N_2} + d_2 N_{O_2} + d_3 N_O)} \tag{6.50}$$

with

$$d_1 = 2.82 \cdot 10^{-17} - 3.41 \cdot 10^{-21} T_e \tag{6.51}$$

$$d_2 = 2.2 \cdot 10^{-16} - 7.92 \cdot 10^{-18} \sqrt{T_e} \tag{6.52}$$

$$d_3 = 1.1 \cdot 10^{-16}(1 + 5.7 \cdot 10^{-4} T_e) \tag{6.53}$$

We assume a quasi-steady state and neglect thermalelectric heat flux, horizontal gradients of T_e and N_e, and adiabatic expansion and heat advection. With these assumptions the general electron energy conservation equation is simplified to

$$\sin^2 I \frac{\partial}{H \partial Z} \left(K^e \frac{\partial T_e}{H \partial Z} \right) + \sum Q_e - \sum L_e = 0 \tag{6.54}$$

The heating sources are solar EUV radiation, deactivation of excited neutral and ion species, dissociative recombination of electrons with ions, energetic

particle precipitation, and Joule heating. Only the solar EUV radiation and the energetic particle precipitation are considered, all other contributions are neglectable small.

We substitute

$$K^e = K^0 T^{5/2} \tag{6.55}$$

$$L_e = L_{on}(T_e - T_n) + L_{oi}(T_e - T_i) \tag{6.56}$$

with $G = T_e^{7/2}$ the derivative is

$$\frac{\partial G}{\partial Z} = \frac{7}{2} T_e^{5/2} \frac{\partial T_e}{\partial Z} \tag{6.57}$$

and, therefore

$$\frac{K^e}{H} \frac{\partial T_e}{\partial Z} = \frac{2}{7} \frac{K^0}{H} \frac{\partial G}{\partial Z} \tag{6.58}$$

and the loss terms are

$$L_e = \frac{L_{on} + L_{oi}}{T_e^{5/2}} G - L_{on} T_n - L_{oi} T_i \tag{6.59}$$

The energy conservation equation reads

$$\sin^2 I \frac{\partial}{H \partial Z} \left(\frac{2}{7} \frac{K^0}{H} \frac{\partial G}{\partial Z} \right) - \left(\frac{L_{on} + L_{oi}}{T_e^{5/2}} \right) G = -L_{on} T_n - L_{oi} T_i - Q_e \tag{6.60}$$

The heat flux from the topside ionosphere is F_e with

$$F_{eD} = F_{10.7}^* 1.2 [-5 \cdot 10^7 A - 4 \cdot 10^7] \tag{6.61}$$

for the daytime, and for the nighttime

$$F_{eD} = \frac{F_e D}{2} \tag{6.62}$$

with $F_{10.7^*} = F_{10.7}$ and $F_{10.7^*} \leq 235$. The factor A is set to

$$\text{for } |\lambda_m| \geq 40^o \qquad A = 1 \tag{6.63}$$

$$\text{for } |\lambda_m| < 40^o \qquad A = \frac{1}{2}[1 + \sin(\Pi \frac{|\lambda_m| - 20}{40})] \tag{6.64}$$

The aurora contribution is added

$$F_{eDA} = F_{eD} + Q_{aurora} \tag{6.65}$$

$$F_{eNA} = F_{eN} + Q_{aurora} \tag{6.66}$$

For solar zenith angles $\psi \geq 90^o$ the flux is $F_e = F_{eNA}$, and for $\psi < 90^o$ the flux is $F_e = F_{eDA}$

for $80^o < \psi < 100$
$$F_e = \frac{1}{2}(F_{eDA+F_{eNA}} + \frac{1}{2}(F_{eDA-F_{eNA}})\cos(\Pi\frac{\psi - 80}{20}) \tag{6.67}$$

for $\psi \leq 80$ $\quad or \quad \psi \geq 100$ $\quad F_e$ $\tag{6.68}$

For $|\lambda_m| > 60^o$ a polar contribution is added $Q_{aurora} = 3 \cdot 10^9$. The values of the neutral temperature T_n, the mass mixing ratio Ψ_{O_2} and Ψ_o, and the electron temperature T_e at the interfaces are calculated by averaging the values from the height level $z+\frac{1}{2}\Delta z$ and $z-\frac{1}{2}\Delta z$ to get the value at the level z, with the height index k corresponding to z, and k and $k+1$ corresponding to $z - \frac{1}{2}\Delta z$ and $z + \frac{1}{2}\Delta z$ respectively on the midpoint level; e.g. for the electron temperature

$$T_e(z) = \frac{1}{2}(T_e(z + \frac{1}{2}\Delta z) + T_e(z - \frac{1}{2}\Delta z)) \tag{6.69}$$

The bottom value is extrapolated for T_e, T_n, Ψ_O, and Ψ_{O_2}, as shown for the electron temperature

$$T_e(z_{bot}) = \frac{1}{2}(3T_e(z_{bot} + \frac{1}{2}\Delta z) - T_e(z_{bot} + \frac{3}{2}\Delta z)) \tag{6.70}$$

with the height index $k = 1$ for the midpoint level $z_{bot}+\frac{1}{2}\Delta z$, and the interface height index $k = 1$ for z_{bot}. Note that even for the neutral temperature the values are extrapolated although a lower boundary value exist. The value at the top are also extrapolated for T_e, T_n, Ψ_O, and Ψ_{O_2}, as shown for the electron temperature

$$T_e(z_{top}) = \frac{1}{2}(3T_e(z_{top} - \frac{1}{2}\Delta z) - T_e(z_{top} - \frac{3}{2}\Delta z)) \tag{6.71}$$

The mass mixing ratio of N_2 is calculated by

$$\Psi_{N_2} = 1 - \Psi_O - \Psi_{O_2} \quad with \quad \Psi_{N_2} \geq 0 \tag{6.72}$$

The mass mixing ratios Ψ_i are converted to number densities N_i. First the exponentials e^{-z} are set

$$e^{-Z} = e^{\frac{1}{2}\Delta Z}e^{-Z-\frac{1}{2}\Delta Z} \tag{6.73}$$

$$e^{-Z_{top}} = e^{\frac{1}{2}\Delta Z}e^{-Z_{top}-\frac{1}{2}\Delta Z} \tag{6.74}$$

For the conversion from mass mixing ratio to number density the following factor $N\overline{m}$ is calculated

$$N\overline{m} = \frac{p_0 e^{-Z}\overline{m}(z)}{k_B T_n(z)} = \frac{p\overline{m}(z}{k_B T_n(z)} \tag{6.75}$$

The number densities at the interface level are

$$N_{O_2} = N\overline{m}\frac{\Psi_{O_2}}{m_{O_2}} \tag{6.76}$$

$$N_O = N\overline{m}\frac{\Psi_O}{m_O}N_{N_2} = N\overline{m}\frac{\Psi_{N_2}}{m_{N_2}} \tag{6.77}$$

The scale height H in $[cm]$ is determined on midpoint level and interface level

$$H = \frac{R^* T_n}{g} \tag{6.78}$$

with R^* the gas constant, g the gravitational acceleration, and T_n the neutral temperature either on midpoint or interface level. A minimum inclination magnitude is assumed, which is initially set to the variable dipmin (0.17 radians for the low-resolution TIEGCM or 0.24 radians for the high-resolution TIEGCM), but then increased to $arcsin\sqrt{0.1}$ (= 0.322 radians = 18.4°). Below, we call the modified inclination angle I^*.

The term $\sin^2 I \frac{\partial}{H\partial Z}\left(\frac{2}{7}\frac{K^0}{H}\frac{\partial G}{\partial Z}\right)$ of the electron energy conservation equation is first determined. The derivative is calculated by

$$\frac{\partial}{\partial Z}\left(f\frac{\partial Y}{\partial Z}\right)(z + \frac{1}{2}\Delta z) = \frac{1}{\Delta z}\left[f(z + \Delta z)\frac{\partial Y}{\partial Z}(z + \Delta z) - f(z)\frac{\partial Y}{\partial Z}(z)\right] =$$

$$\frac{1}{\Delta z^2}[f(z)Y(z - \frac{1}{2}\Delta z) + Y(z + \frac{1}{2}\Delta z)(-f(z + \Delta z) - f(z)) + \tag{6.79}$$

$$f(z + \Delta z)Y(z + \frac{3}{2}\Delta z)]$$

with $f = \frac{2K^o}{7H}$ and $Y = G$. The solver needs the equation in the following form

$$P(z + \frac{1}{2}\Delta z)G(z - \frac{1}{2}\Delta z) + Q(z + \frac{1}{2}\Delta z)G(z + \frac{1}{2}\Delta z) +$$

$$R(z + \frac{1}{2}\Delta z)G(z + \frac{3}{2}\Delta z) = RHS(z + \frac{1}{2}\Delta z) \qquad (6.80)$$

Therefore, from the derivative the following values can be set

$$P(z + \frac{1}{2}\Delta z) = \frac{2\sin^2 I^*}{7\Delta^2 z H(z + \frac{1}{2}\Delta z)}\frac{K^o(z)}{H(z)} \qquad (6.81)$$

$$R((z + \frac{1}{2}\Delta z) = \frac{2\sin^2 I^*}{7\Delta^2 z H(z + \frac{1}{2}\Delta z)}\frac{K^o(z + \Delta z)}{H(z + \Delta z)} \qquad (6.82)$$

$$Q((z + \frac{1}{2}\Delta z) = \frac{2\sin^2 I^*}{7\Delta^2 z H(z + \frac{1}{2}\Delta z)}\left[-\frac{K^o(z + \Delta z)}{H(z + \Delta z)} - \frac{K^o(z)}{H(z)}\right] \qquad (6.83)$$

At the bottom of the model we set $T_e(z_{bot}) = T_n(z_{bot})$ which leads to $G = T_n^{7/2}$. The boundary is then

$$G(z_{bot}) = T_n^{7/2}(z_{bot}) = \frac{1}{2}[G(z_{bot} - \frac{1}{2}\Delta z) + G(z_{bot} + \frac{1}{2}\Delta z)] \qquad (6.84)$$

which leads to

$$G(z_{bot} - \frac{1}{2}\Delta z) = 2T_n^{7/2}(z_{bot}) - G(z_{bot} + \frac{1}{2}\Delta z) \qquad (6.85)$$

and is inserted into

$$P(z_{bot} + \frac{1}{2}\Delta z)G(z_{bot} - \frac{1}{2}\Delta z) + Q(z_{bot} + \frac{1}{2}\Delta z)G(z_{bot} + \frac{1}{2}\Delta z) +$$

$$R(z_{bot} + \frac{1}{2}\Delta z)G(z_{bot} + \frac{3}{2}\Delta z) = RHS(z_{bot} + \frac{1}{2}\Delta z) \qquad (6.86)$$

and gives

$$P(z_{bot} + \frac{1}{2}\Delta z)\left[2T_n^{7/2}(z_{bot}) - G(z_{bot} + \frac{1}{2}\Delta z)\right] +$$

$$Q(z_{bot} + \frac{1}{2}\Delta z)G(z_{bot} + \frac{1}{2}\Delta z) + R(z_{bot} + \frac{1}{2}\Delta z)G(z_{bot} + \frac{3}{2}\Delta z) = \qquad (6.87)$$

$$RHS(z_{bot} + \frac{1}{2}\Delta z)$$

Therefore at the lower boundary the coefficients are

$$Q^*(z_{bot} + \frac{1}{2}\Delta z) = Q(z_{bot} + \frac{1}{2}\Delta z) - P(z_{bot} + \frac{1}{2}\Delta z) \tag{6.88}$$

$$RHS^*(z_{bot} + \frac{1}{2}\Delta z) = RHS(z_{bot} + \frac{1}{2}\Delta z) - 2P(z_{bot} + \frac{1}{2}\Delta z)T_n^{7/2}(z_{bot} \tag{6.89}$$

$$P^*(z_{bot} + \frac{1}{2}\Delta z) = 0 \tag{6.90}$$

At the upper boundary the flux is set

$$\frac{2K^o}{7H}\frac{\partial G}{\partial Z} = F_e \tag{6.91}$$

which leads to $\frac{\partial G}{\partial Z} = \frac{7H}{2K^o}F_e$. So the top level value can be set by using

$$\frac{G(z_{bot} + \frac{1}{2}\Delta z) - G(z_{bot} - \frac{1}{2}\Delta z)}{\Delta z} = \left(\frac{7H}{2K^o}F_e\right)(z_{top}) \tag{6.92}$$

and solving for $G(z_{bot} + \frac{1}{2}\Delta z)$. Inserting it into

$$P(z_{top} - \frac{1}{2}\Delta z)G(z_{top} - \frac{3}{2}\Delta z) + Q(z_{top} - \frac{1}{2}\Delta z)G(z_{top} - \frac{1}{2}\Delta z) +$$
$$R(z_{top} - \frac{1}{2}\Delta z)G(z_{top} + \frac{1}{2}\Delta z) = RHS(z_{top} - \frac{1}{2}\Delta z) \tag{6.93}$$

leads to

$$P(z_{top} - \frac{1}{2}\Delta z)G(z_{top} - \frac{3}{2}\Delta z) + Q(z_{top} - \frac{1}{2}\Delta z)G(z_{top} - \frac{1}{2}\Delta z) +$$
$$R(z_{top} - \frac{1}{2}\Delta z)\left[\left(\frac{7H}{2K^o}F_e\right)(z_{top})\Delta z + G(z_{bot} - \frac{1}{2}\Delta z)\right] = \tag{6.94}$$
$$RHS(z_{top} - \frac{1}{2}\Delta z)$$

Therefore at the upper boundary the coefficients are

$$Q^*(z_{top} - \frac{1}{2}\Delta z) = Q(z_{top} + \frac{1}{2}\Delta z) + R(z_{top} - \frac{1}{2}\Delta z) \tag{6.95}$$

$$RHS^*(z_{top} - \frac{1}{2}\Delta z) = RHS(z_{top} - \frac{1}{2}\Delta z) -$$
$$R(z_{top} + \frac{1}{2}\Delta z)\left(\frac{7H}{2K^o}F_e\right)(z_{top})\Delta z \tag{6.96}$$

$$R^*(z_{top} - \frac{1}{2}\Delta z) = 0 \tag{6.97}$$

The flux F_e was set before see eq. (6.61)

The heating rate is

$$\sum Q_e = \left[Q_{O_2^+} + Q_{O^+} + Q_{N_2^+} + Q_{NO^+} + Q_{N^+} + Q_{O^+(2D)} + Q_{O^+(2p)} \right] \epsilon \tag{6.98}$$

with ϵ the heat efficiency. In the code first $\sum Q_e / \epsilon$ is calculated at the interface level. The values of $\sum Q_e / \epsilon$ at the midpoint level are calculated by

$$\frac{\sum Q_e}{\epsilon}(z + \frac{1}{2}\Delta z) = \sqrt{\frac{\sum Q_e}{\epsilon}(z) \frac{\sum Q_e}{\epsilon}(z + \Delta z)} \tag{6.99}$$

In the same way the electron density is determined at the midpoint level

$$N_e(z + \frac{1}{2}\Delta z) = \sqrt{N_e(z)N_e(z + \Delta z)} \quad \text{with} \quad N_e \geq 100. \tag{6.100}$$

For the conversion from mass mixing ratio to number density $N\overline{m}$ at the midpoint level is determined

$$N\overline{m}(z + \frac{1}{2}\Delta z) = \frac{p_0 e^{-z - \frac{1}{2}\Delta z}\overline{m}(z + \frac{1}{2}\Delta z)}{k_B T_n(z + \frac{1}{2}\Delta z)} \tag{6.101}$$

The number densities N_i at the midpoint level are

$$N_{O_2}(z + \frac{1}{2}\Delta z) = N\overline{m}(z + \frac{1}{2}\Delta z)\frac{\Psi_{O_2}(z + \frac{1}{2}\Delta z}{m_{O_2}} \tag{6.102}$$

$$N_O(z + \frac{1}{2}\Delta z) = N\overline{m}(z + \frac{1}{2}\Delta z)\frac{\Psi_O(z + \frac{1}{2}\Delta z)}{m_O} \tag{6.103}$$

$$N_{N_2}(z + \frac{1}{2}\Delta z) = N\overline{m}(z + \frac{1}{2}\Delta z)\frac{\Psi_{N_2}(z + \frac{1}{2}\Delta z)}{m_{N_2}} \tag{6.104}$$

with $\Psi_{N_2} = 1 - \Psi_{O_2} - \Psi_O$ and $\Psi_{N_2} \geq 0$. The heat efficiency ϵ at the midpoint level is then

$$\epsilon = exp\left[-\left(12.75 + 6.941R + 1.166R^2 + 0.08043R^3 + 0.001996R^4 \right) \right] \tag{6.105}$$

with

$$R = \ln \frac{N_e}{N_{O_2} + 0.1 \cdot N_O + N_{N_2}} \tag{6.106}$$

Therefore, the following term is added to the right hand side

$$RHS = \frac{\sum Q_e}{\epsilon}(z + \frac{1}{2}\Delta z) \tag{6.107}$$

The cooling term due to vibrational excitation $L(e, N_2)_{vib}$ of N_2 is given by

$$\frac{L(e, N_2)_{vib}}{N_e} = N_{N_2} 1.3 \cdot 10^{-4} A \frac{-3200}{T_e T_n} \frac{1 - exp\left[3200\left(\frac{1}{T_e} - \frac{1}{T_n}\right)\right]}{3200\left(\frac{1}{T_e} - \frac{1}{T_n}\right)} \tag{6.108}$$

with the value of A

$$A = 5.7 \cdot 10^{-8} exp(\frac{-3352.6}{T_e}) \quad \text{for } T_e < 1000K$$

$$A = 2. \cdot 10^{-7} exp(\frac{-4605.2}{T_e}) \quad \text{for } 1000K \leq T_e \leq 2000K$$

$$A = 2.53 \cdot 10^{-6} \sqrt{T_e} exp(\frac{-17620}{T_e}) \quad \text{for } 2000K < T_e$$

The rotational excitation of N_2 and the cooling rates due to elastic electron-neutral collisions are $L(e, N_2)_{elast} + L(e, N_2)_{rot}$

$$\frac{L(e, N_2)_{elast} + L(e, N_2)_{rot}}{N_e} =$$

$$N_{N_2}\left[1.77 \cdot 10^{-19}\left\{1 - 1.21 \cdot 10^{-4}T_e\right\}T_e + 2.9 \cdot 10^{-14}\frac{1}{\sqrt{T_e}}\right] \tag{6.109}$$

The elastic, vibrational and rotational excitation of O_2 is

$$\frac{L(e, O_2)_{elast} + L(e, O_2)_{vib} + L(e,)_2)_{rot}}{N_e} = \tag{6.110}$$

$$N_{O_2}\left[1.21 \cdot 10^{-18}\left(1 + 3.6 \cdot 10^{-2}\sqrt{T_e}\right)\sqrt{T_e} + 3.125 \cdot 10^{-21}T_e^2 + 6.9 \cdot 10^{-14}\frac{1}{\sqrt{T_e}}\right]$$

due to elastic electron neutral collision and due to fine structure excitation of O is

$$\frac{L(e,O)_{elast} + L(e,O)_{fs}}{N_e} = \tag{6.111}$$

$$N_O \left[7.9 \cdot 10^{-19} \left(1 + 5.7 \cdot 10^{-4} T_e \right) \sqrt{T_e} + 3.4 \cdot 10^{-12} \frac{1 - 7 \cdot 10^{-5} T_e}{T_n} \left(\frac{150}{T_e} + 0.4 \right) \right]$$

All the loss terms together are $L(e,n)$

$$\frac{L(e,n)}{N_e} = \frac{L(e,N_2)_{vib}}{N_e} + \frac{L(e,O_2)_{elast} + L(e,O_2)_{vib} + L(e,O_2)_{rot}}{N_e} +$$

$$\frac{L(e,O)_{elast} + L(e,O)_{fs}}{N_e} \tag{6.112}$$

and is multiplied by the electron density on the midpoint level. The cooling rate due to mixture of the electrons with ions is $L(e,i)$

$$L(e,i) = 3.2 \cdot 10^{-8} \frac{N_e}{T_e^{3/2}} 15 \left(N_{O^+} + 0.5 N_{O_2} + 0.53 N_{NO^+} \right) \tag{6.113}$$

The cooling due to ion neutral collision is $L(i,n)$ in $\left[\frac{erg}{s\, cm^3} \right]$

$$L(i,n) = N_{O^+} \left(6.6 \cdot 10^{-14} N_{N_2} + 5.8 \cdot 10^{-14} N_{O_2} + 0.21 \cdot 10^{-14} N_O \sqrt{2 T_n} \right) +$$

$$N_{O^+} \left(5.45 \cdot 10^{-14} N_{O_2} + 5.9 \cdot 10^{-14} N_{N_2} + 4.5 \cdot 10^{-14} N_O \right) +$$

$$N_{O_2^+} \left(5.8 \cdot 10^{-14} N_{N_2} + 4.4 \cdot 10^{-14} N_O + 0.14 \cdot 10^{-14} N_{O_2} \sqrt{2 T_n} \right) \tag{6.114}$$

The coefficients are updated by

$$Q^* = Q - \frac{L(e,n) + L(e,i)}{T_e^{5/2}} \tag{6.115}$$

$$RHS^* = RHS - L(e,n) T_n - L(e,i) T_i \tag{6.116}$$

Note that the temperatures T_n, T_i and T_e are at timestep t_n and midpoints height level. The tridiagonal solver solve eq. (6.88) which gives G and the updated electron temperatures

$$T_e(t_n + \Delta t) = G^{2/7} \quad \text{with} \quad T_e(t_n + \Delta t) \geq T_n(t_n) \tag{6.117}$$

The ion temperature T_i at timestep $t_n + \Delta t$ is determined from

$$L(e, i)(T_e - T_i) + \rho Q_J^{T_i} = L(i, n)(T_i - T_n) \qquad (6.118)$$

which leads to

$$T_i = \frac{L(e, i)T_e(t_n + \Delta t) + L(i, n)T_n(t_n) + \rho Q_J^{T_i}}{L(e, i) + L(i, n)} \qquad (6.119)$$

with $\rho = \frac{N\overline{m}}{N_A}$ in $[g/cm^3]$, and N_A is the Avogadro number. The ion temperature has to be larger than the neutral temperature $T_i \geq T_n$.

For the thermodynamic equation an addition to the heating term is determined.

$$Q(en, ei) = Q(e, n) + Q(e, i) = \frac{N_A}{N\overline{m}} \left[L(e, n)(T_e^{t_n} - T_n^{t_n}) + L^*(e, i)(T_e^{t_n} - T_i^{t_n}) \right]$$
$$(6.120)$$

with

$$L^*(e, i) = L(e, i)(T_e^{t_n} - T_i^{t_n}) \qquad \text{for } T_e^{t_n} - T_i^{t_n} > 0 \qquad (6.121)$$
$$L^*(e, i) = 0 \qquad \text{for } T_e^{t_n} - T_i^{t_n} \leq 0 \qquad (6.122)$$

with $L^*(e, i)$ in $[ergs/cm^3/s/K]$. The term is added to the total heating term Q_{tot} at the interface level

$$Q_{tot}^*(z) = Q_{tot}(z) + \frac{1}{2}(Q(en, ei)(z + \frac{1}{2}\Delta z) + Q(en, ei)(z - \frac{1}{2}\Delta z)) \quad (6.123)$$

The upper and lower boundary are extrapolated

$$Q_{tot}^*(z_{bot}) = Q_{tot}(z_{bot}) + \frac{3}{2}Q(en, ei)(z + \frac{1}{2}\Delta z)$$
$$- Q(en, ei)(z_{bot} + \frac{3}{2}\Delta z)) \qquad (6.124)$$
$$Q_{tot}^*(z_{top}) = Q_{tot}(z_{top}) + \frac{3}{2}Q(en, ei)(z_{top} - \frac{1}{2}\Delta z)$$
$$- Q(en, ei)(z_{top} - \frac{3}{2}\Delta z)) \qquad (6.125)$$

6.4   Calculation of O^+ number density

The input to `subroutine oplus` is summarized in table 6.10. The output of `subroutine oplus` is summarized in table 6.11. The module data of `subroutine oplus` is summarized in table 6.12. Most major species are in photochemical equilibrium below $1000 km$, and can be simply calculated by balancing the production and loss rates. However, O^+ is determined by considering diffusion, along the magnetic field line and the $\mathbf{E} \times \mathbf{B}$ transport. In the following for simplicity the variable n is used for the O^+ number density $n(O^+)$.

$$\frac{\partial n}{\partial t} - Q + Ln = -\nabla \cdot (n\mathbf{v}_i) \tag{6.126}$$

with n the O^+ number density, Q the production rate of O^+, L the loss rate of O^+. The right hand side is the transport due $\mathbf{E} \times \mathbf{B}$ drift and the field aligned ambipolar diffusion. The ion velocity $\mathbf{v}_i$ is given by

$$\mathbf{v}_i = \mathbf{v}_{i,\parallel} + \mathbf{v}_{i,\perp} \tag{6.127}$$

with the parallel and perpendicular velocity with respect to the geomagnetic field

$$\mathbf{v}_{i,\parallel} = \left[\mathbf{b} \cdot \frac{1}{\nu_{in}} \left(\mathbf{g} - \frac{1}{\rho_i}\nabla(P_i + P_e) \right) + \mathbf{b} \cdot \mathbf{v}_n \right] \mathbf{b} \tag{6.128}$$

$$\mathbf{v}_{i,\perp} = \frac{\mathbf{E} \times \mathbf{B}}{|B|} \tag{6.129}$$

The parallel velocity is caused by ambipolar diffusion and the perpendicular velocity by $\mathbf{E} \times \mathbf{B}$ drift velocity. The unit vector along the geomagnetic field line is $\mathbf{b}$, ν_{in} is the O^+ ion-neutral collision frequency, $\mathbf{g}$ the gravitational acceleration due to gravity, ρ_i is the ion mass density, P_i and P_e are the ion and electron pressure, $\mathbf{v}_n$ is the neutral velocity, $|B|$ is the geomagnetic field strength, and $\mathbf{E}$ is the electric field.

Inserting the parallel (6.128) and perpendicular (6.129) velocity into the O^+

transport equation (6.126) leads to

$$
\begin{aligned}
&\frac{\partial n}{\partial t} - Q + Ln + [(\mathbf{b}_h \cdot \nabla_h) K b_z] \left[\left(\frac{1}{H} \frac{\partial}{\partial Z} (2T_p n) + \frac{mg}{k_B} n \right) \right] \\
&- (\mathbf{b}_h \cdot \nabla_h)(\mathbf{b} \cdot v_n n) + \left(b_z \frac{1}{H} \frac{\partial}{\partial Z} + \nabla \cdot \mathbf{b} \right) K b_z \left(\frac{1}{H} \frac{\partial}{\partial Z} (2T_p n) + \frac{mg}{k_B} n \right) - \\
&\left(b_z \frac{1}{H} \frac{\partial}{\partial Z} + \nabla \cdot \mathbf{b} \right) (\mathbf{b} \cdot v_n n) - \left[B^2 \mathbf{v}_{ExB,h} \cdot \nabla \left(\frac{n}{B^2} \right) \right]_H - \\
&B^2 \mathbf{v}_{ExB,z} \frac{1}{H} \frac{\partial}{\partial Z} \left(\frac{n}{B^2} \right) + (\mathbf{b}_H \cdot \nabla_H) K (\mathbf{b}_H \cdot \nabla_H) (2nT_p) + \\
&K b_z (\mathbf{b}_H \cdot \nabla_H) \left(\frac{1}{H} \frac{\partial}{\partial Z} (2T_p n) + \frac{mg}{k_B} n \right) + \\
&\left(b_z \frac{1}{H} \frac{\partial}{\partial Z} + \nabla \cdot \mathbf{b} \right) K (\mathbf{b}_H \cdot \nabla_H (2nT_p)) = 0
\end{aligned}
\tag{6.130}
$$

where the ambipolar diffusion coefficient is $K = D_A + K_E$ with K_E the eddy diffusion coefficient in the lower thermosphere, and D_A the molecular diffusion coefficient. The geomagnetic unit vector, the horizontal vector and vertical component are $\mathbf{b}$, $\mathbf{b}_H$ and b_z respectively. The scale height is denoted by H, $\mathbf{v}_{ExB,h}$ is the horizontal drift vector, and $\mathbf{v}_{ExB,z}$ the vertical component. The horizontal derivative of ∇ is ∇_H. The plasma pressure is $T_p = \frac{1}{2}(T_e + T_i)$.

The fourth, eleventh, and sixth term are the contributions of the vertical component of ambipolar diffusion to the plasma transport due to respectively, the horizontal variation of the diffusion coefficient and b_z, the horizontal variation of the vertical ambipolar diffusion, and the vertical variation of the vertical ambipolar diffusion. The tenth term is the contribution of the horizontal component of the ambipolar diffusion due to variations in the vertical and horizontal direction. The fifth and seventh term are the neutral wind effects on the O^+ distribution, and the eight and ninth terms are the effects of the $\mathbf{E} \times \mathbf{B}$ transport.

The flux at the upper boundary is determined in the `subroutine oplus_flux`. The transport from and to the plasmasphere is specified by the flux Φ. The

latitudinal variation of the flux is specified by the factor A

$$A = 1 \qquad\qquad\qquad\qquad \text{for} |\lambda_m| \geq \frac{\Pi}{24}$$

$$A = \frac{1}{2}\left(1 + \sin\Pi\frac{|\lambda_m| - \frac{\Pi}{48}}{\Pi/24}\right) \qquad\qquad \text{for} |\lambda_m| < \frac{\Pi}{24} \qquad (6.131)$$

with $A \geq 0.05$, and λ_m the geomagnetic latitude. The daytime flux is Φ_D^o and upward, and the nighttime flux Φ_N^o which is downward

$$\Phi_D^o = 2 \cdot 10^8$$
$$\Phi_N^o = -2 \cdot 10^8 \qquad\qquad\qquad (6.132)$$

and the flux variation during the day– and nighttime is given by

$$F_{eD} = \Phi_D^o A$$
$$F_{eN} = \Phi_N^o A \qquad\qquad\qquad (6.133)$$

The solar zenith angle ψ determines which flux F^{O^+} is used

$$F^{O^+} = F_{eN} \quad \text{for} \quad \psi \geq 80^o$$
$$F^{O^+} = F_{eD} \quad \text{for} \quad \psi < 100^o \qquad\qquad (6.134)$$

with

$$F^{O^+} = \frac{1}{2}[F_{eD} + F_{eN}] + \frac{1}{2}[F_{eD} - F_{eN}]\cos(\Pi\frac{\psi - 80}{20}) \quad \text{for} \quad 80^o < \psi < 100^o \qquad (6.135)$$

The divergence of the geomagnetic field vector $\mathbf{b}$ is determined in `subroutine divb`. Since variation in height of the geomagnetic field is neglected the divergence also varies only with latitude and longitude.

$$\nabla \cdot \mathbf{b} = \frac{b_x(\phi + \Delta\phi, \lambda) - b_x(\phi - \Delta\phi, \lambda)}{2\Delta\phi R_E \cos\lambda} +$$
$$\frac{\cos\lambda + \Delta\lambda b_y(\phi, \lambda + \Delta\lambda) - \cos\lambda - \Delta\lambda b_y(\phi, \lambda - \Delta\lambda)}{2\Delta\lambda R_E \cos\lambda} +$$
$$\frac{2b_z(\phi, \lambda)}{R_E} \qquad\qquad\qquad (6.136)$$

with b_y the northward, b_x the eastward, and b_z the upward component of the unit geomagnetic field vector $\frac{\mathbf{B}}{|B|}$. The divergence is stored in the value `dvb`.

In the first latitudinal scan the plasma pressure is determined at $\lambda - \Delta\lambda$, λ and , $\lambda + \Delta\lambda$, e.g. at λ

$$T_p(\phi, \lambda, z + \frac{1}{2}\Delta z) = \frac{1}{2}(T_i + T_e) \tag{6.137}$$

The values in the code are stored in the variable `tpj`.

In `subroutine rrk` the diffusion coefficient are determined. The values are stored in the variable `dj` in the source code at $\lambda - \Delta\lambda$, λ and , $\lambda + \Delta\lambda$.

$$D_A = \frac{1.42 \cdot 10^{17} k_B T_n}{p\overline{m}\left[\frac{\Psi_O}{m_O}\sqrt{T_p}(1 - 0.064 log_{10}T_p)^2 C_f + 18.6\frac{\Psi_{N_2}}{m_{N_2}} + 18.1\frac{\Psi_{O_2}}{m_{O_2}}\right]} \tag{6.138}$$

with the pressure $p(z + \frac{1}{2}\Delta) = p_0 e^{-z - \frac{1}{2}\Delta z}$, the number density of N_2 is $\Psi_{N_2} = 1 - \Psi_{O_2} - \Psi_O$, the factor is $C_f = 1.5$, and $N = \frac{p_0 e^{-z - \frac{1}{2}\Delta z}}{k_B T_n}$. The value D_A is determined at half pressure levels e.g. $z + \frac{1}{2}\Delta z$. The variable `tpj` holds $2T_p$ at the midpoint pressure level $z + \frac{1}{2}\Delta z$ and at the latitudes $\lambda - \Delta\lambda$, λ and , $\lambda + \Delta\lambda$. The scale height is also determined at the midpoint pressure level, and the latitudes $\lambda - \Delta\lambda$, λ and , $\lambda + \Delta\lambda$.

$$H = \frac{R^* T_n}{\overline{m}g} \tag{6.139}$$

The scale height is stored in the variable `hj`. The dot product $\mathbf{b} \cdot \mathbf{v}_n n$ is stored in `bvel` and calculated also on the midpoint pressure level, and the latitudes $\lambda - \Delta\lambda$, λ and , $\lambda + \Delta\lambda$.

$$\mathbf{b} \cdot \mathbf{v}_n n = \left[b_x u_n + b_y v_n + b_z \frac{W(z) + W(z + \frac{1}{2}\Delta z)}{2}H(z + \frac{1}{2}\Delta z)\right]n \tag{6.140}$$

In `subroutine diffus` the term $\left[2\frac{\partial T_p n}{H\partial Z} + \frac{m_O + g}{R^*}n\right]$ at the midpoint pressure level is determined

$$F(z + \frac{1}{2}\Delta z) = \frac{1}{2H(z + \frac{1}{2}\Delta z)\Delta z}[2T_p(z + \frac{3}{2}\Delta z)n(z + \frac{3}{2}\Delta z) -$$

$$2T_p(z - \frac{1}{2}\Delta z)n(z - \frac{1}{2}\Delta z)] + \frac{m_O + g}{R^*}n(z + \frac{1}{2}\Delta z) \tag{6.141}$$

The term is stored in the variable `diffj`. The upper and lower boundary values are set by

$$
F(z_{bot} + \frac{1}{2}\Delta z) = \frac{1}{H(z_{bot} + \frac{1}{2}\Delta z)\Delta z}[2T_p(z_{bot} + \frac{3}{2}\Delta z)n(z_{bot} + \frac{3}{2}\Delta z) -
$$

$$
(6.142)
$$

$$
2T_p(z_{bot} + \frac{1}{2}\Delta z)n(z_{bot} + \frac{1}{2}\Delta z)] + \frac{m_{O^+}g}{R^*}n(z_{bot} + \frac{1}{2}\Delta z)
$$

$$
F(z_{top} - \frac{1}{2}\Delta z) = \frac{1}{H(z_{top} - \frac{1}{2}\Delta z)\Delta z}[2T_p(z_{top} - \frac{1}{2}\Delta z)n(z_{top} - \frac{1}{2}\Delta z) -
$$

$$
(6.143)
$$

$$
2T_p(z_{top} - \frac{3}{2}\Delta z)n(z_{top} - \frac{3}{2}\Delta z)] + \frac{m_{O^+}g}{R^*}n(z_{top} - \frac{1}{2}\Delta z)
$$

The value $2nT_p$ is determined at midpoint level, and the latitudes $\lambda - \Delta\lambda$, λ and , $\lambda + \Delta\lambda$. The value overwrites the variable `tpj`. The latitudinal smoothed value of $n(O^+)^{t_n-\Delta t}$ are determined by

$$
n(O^+)^{smo\lambda,t_n-\Delta t} = n(O^+)^{t_n-\Delta t} - f_{smo}[n(O^+)^{t_n-\Delta t}(\lambda + 2\Delta\lambda) +
$$
$$
n(O^+)^{t_n-\Delta t}(\lambda - 2\Delta\lambda) - 4(n(O^+)^{t_n-\Delta t}(\lambda + \Delta\lambda) +
$$
$$
n(O^+)^{t_n-\Delta t}(\lambda - \Delta\lambda)) + 6n(O^+)^{t_n-\Delta t}(\lambda)] \qquad (6.144)
$$

and stored in `optm1_smooth`, and $f_{smo} = 0.003$.

The second latitudinal scan starts with calculating the value of $\mathbf{b} \cdot \nabla_H$ in `subroutine bdotdh` at the midpoint level. The output variable is `bdotdh_op`. The input is the term from eq. (6.141) $F = \left[2\frac{\partial T_p n}{H\partial Z} + \frac{m_{O^+}g}{R^*}n\right]$, which leads to $(\mathbf{b} \cdot \nabla_H)\left[2\frac{\partial T_p n}{H\partial Z} + \frac{m_{O^+}gn}{R^*}\right]$

$$
T1 = \frac{1}{R_E}[\frac{b_x}{2\Delta\phi\cos\lambda}\left\{F(\phi + \Delta\phi, \lambda) - F(\phi - \Delta\phi, \lambda)\right\} +
$$
$$
b_y\frac{F(\phi, \lambda + \Delta\lambda) - F(\phi, \lambda - \Delta\lambda)}{2\Delta\lambda}] \qquad (6.145)
$$

The term is multiplied by the diffusion coefficient D_A from `subroutine rrk`, which leads to

$$
D_A(z + \frac{1}{2}\Delta z)b_z(\mathbf{b} \cdot \nabla_H)\left[2\frac{\partial T_p n}{H\partial Z} + \frac{m_{O^+}g}{R^*}n\right] \qquad (6.146)
$$

The same subroutine `bdotdh` is used to calculate $\mathbf{b} \cdot \nabla_H [2T_p n]$. Using eq. (6.145) with $F = 2T_p n$. The values are determined at the midpoint pressure level, and at the latitudes $\lambda - \Delta\lambda$, λ and , $\lambda + \Delta\lambda$. Afterwards the value is multiplied by

$$D_A(z + \frac{1}{2}\Delta z)\mathbf{b} \cdot \nabla_H [2T_p n] \tag{6.147}$$

and stored in the variable `bdotdh_opj`.

The third latitudinal scan starts with calling the subroutine `bdotdh` for the term in eq. (6.147) $F = D_A\mathbf{b} \cdot \nabla_H [2T_p n]$, which leads to (see eq. (6.145))

$$\mathbf{b} \cdot \nabla_H \left(D_A\mathbf{b} \cdot \nabla_H [2T_p n] \right) \tag{6.148}$$

evaluated at the midpoint pressure level, and stored in the variable `bdotdh_diff`.

The subroutine `bdzdvb` calculates the term $\left(b_z \frac{1}{H} \frac{\partial}{\partial Z} + \nabla \cdot \mathbf{b} \right) G$, with the input into the subroutine $\nabla \cdot \mathbf{B}$, and $G = D_A\mathbf{b} \cdot \nabla_H [2T_p n]$.

$$T3(z + \frac{1}{2}\Delta z)) = \frac{b_z}{2H(z + \frac{1}{2}\Delta z)\delta z} \left\{ G(z + \frac{3}{2}\Delta z) - G(z - \frac{1}{2}\Delta z) \right\} +$$
$$\nabla \cdot \mathbf{b} G(z + \frac{1}{2}\Delta z) \tag{6.149}$$

At the upper and lower boundary the values are set to

$$T3(z_{top} - \frac{1}{2}\Delta z)) = \frac{b_z}{2H(z_{top} - \frac{1}{2}\Delta z)\delta z} \left\{ G(z_{top} - \frac{1}{2}\Delta z) - G(z_{top} - \frac{3}{2}\Delta z) \right\} +$$
$$\nabla \cdot \mathbf{b} G(z_{top} - \frac{1}{2}\Delta z) \tag{6.150}$$

$$T3(z_{bot} + \frac{1}{2}\Delta z)) = \frac{b_z}{2H(z_{bot} + \frac{1}{2}\Delta z)\delta z} \left\{ G(z_{bot} + \frac{3}{2}\Delta z) - G(z_{bot} + \frac{1}{2}\Delta z) \right\} +$$
$$\nabla \cdot \mathbf{b} G(z_{bot} + \frac{1}{2}\Delta z) \tag{6.151}$$

All the explicit terms are added together from eq. (6.146), (6.147), and

(6.149) which leads to

$$
\begin{aligned}
T_{1,explicit} = & - D_A(z + \frac{1}{2}\Delta z)b_z(\mathbf{b}\cdot\nabla_H)\left[2\frac{\partial T_p n}{H\partial Z} + \frac{m_{O^+}g}{R^*}n\right] \\
& - \mathbf{b}\cdot\nabla_H\left(D_A\mathbf{b}\cdot\nabla_H\left[2T_p n\right]\right) \\
& - \left(b_z\frac{1}{H}\frac{\partial}{\partial Z} + \nabla\cdot\mathbf{b}\right)\left(D_A\mathbf{b}\cdot\nabla_H\left[2T_p n\right]\right) \qquad (6.152)
\end{aligned}
$$

In addition the term $(\mathbf{b}_H\cdot\nabla_H)(\mathbf{b}\cdot\mathbf{v}_{n,H})$ and $\left[b^2 v_{ExB,H}\cdot\nabla(\frac{n}{B^2})\right]_H$ are treated as explicit terms which leads to

$$
\begin{aligned}
T_{2,explicit} =& T_{1,explicit} + \frac{1}{2R_E}[\frac{b_x}{\Delta\phi\cos\lambda}\left(\mathbf{b}\cdot\mathbf{v}_n(\phi+\Delta\phi,\lambda) - \mathbf{b}\cdot\mathbf{v}_n(\phi-\Delta\phi,\lambda)\right) + \\
& v_{ExB,x}(z+\frac{1}{2}\Delta z)B^2(\phi,\lambda)\left(\frac{n(\phi+\Delta\phi,\lambda)}{B^2(\phi+\Delta\phi,\lambda)} - \frac{n(\phi-\Delta\phi,\lambda)}{B^2(\phi-\Delta\phi,\lambda)}\right) \\
& + \frac{1}{\Delta\lambda}(b_y\left(\mathbf{b}\cdot\mathbf{v}_n(\phi,\lambda+\Delta\lambda) - \mathbf{b}\cdot\mathbf{v}_n(\phi,\lambda-\Delta\lambda)\right) + \\
& v_{ExB,y}(z+\frac{1}{2}\Delta z)B^2(\phi,\lambda)\left(\frac{n(\phi,\lambda+\Delta\lambda)}{B^2(\phi,\lambda+\Delta\lambda)} - \frac{n(\phi,\lambda-\Delta\lambda)}{B^2(\phi,\lambda-\Delta\lambda)}\right))]
\end{aligned}
$$
$$(6.153)$$

Afterwards the following values are set

$$
\frac{\nabla\cdot\mathbf{b}}{b_z} \qquad (6.154)
$$

$$
\frac{1}{\Delta z H} \qquad (6.155)
$$

$$
T_p = \frac{1}{2}(T_e + T_i) \qquad (6.156)
$$

at the midpoint pressure level and stored in the variables `dvb`, `srchdz`, and `tp` respectively.

The term $2T_p\frac{1}{H\Delta z} \pm \frac{gm}{2R^*}$ are determined

$$
S_p(z+\frac{3}{2}\Delta z) = 2T_p(z+\frac{3}{2}\Delta z)\frac{1}{H(z+\Delta z)\Delta z} + \frac{gm}{2R^*} \qquad (6.157)
$$

$$
S_m(z+\frac{3}{2}\Delta z) = 2T_p(z+\frac{1}{2}\Delta z)\frac{1}{H(z+\Delta z)\Delta z} - \frac{gm}{2R^*} \qquad (6.158)
$$

and stored in the variable `tphdz1` for S_p and `tphdz0` for S_m respectively. The lower boundaries are set by

$$S_p(z_{bot} + \frac{1}{2}\Delta z) = 2T_p(z_{bot} + \frac{1}{2}\Delta z)$$

$$\left[\frac{1.5}{H(z_{bot} + \frac{1}{2}\Delta z)\Delta z} - \frac{0.5}{H(z_{bot} + \frac{3}{2}\Delta z)\Delta z} \right] + \frac{gm}{2R^*} \quad (6.159)$$

$$S_m(z_{bot} + \frac{1}{2}\Delta z) = 2 \cdot \left[2T_p(z_{bot} + \frac{1}{2}\Delta z) - T_p(z_{bot} + \frac{3}{2}\Delta z) \right]$$

$$\left[\frac{1.5}{H(z_{bot} + \frac{1}{2}\Delta z)\Delta z} - \frac{0.5}{H(z_{bot} + \frac{3}{2}\Delta z)\Delta z} \right] - \frac{gm}{2R^*} \quad (6.160)$$

and stored in `tphdz1(lev0)` and `tphdz0(lev0)`, respectively, with $lev0$ corresponding to $z_{bot} + \frac{1}{2}\Delta z$ on the midpoint pressure level. The upper boundary values are

$$S_p(z_{top} + \frac{1}{2}\Delta z) = 2 \cdot \left[2T_p(z_{top} - \frac{1}{2}\Delta z) - T_p(z_{top} - \frac{3}{2}\Delta z) \right]$$

$$\left[\frac{1.5}{H(z_{top} - \frac{1}{2}\Delta z)\Delta z} - \frac{0.5}{H(z_{top} - \frac{3}{2}\Delta z)\Delta z} \right] + \frac{gm}{2R^*}$$
$$(6.161)$$

$$S_m(z_{top} + \frac{1}{2}\Delta z) = 2T_p(z_{top} - \frac{1}{2}\Delta z)$$

$$\left[\frac{1.5}{H(z_{top} - \frac{1}{2}\Delta z)\Delta z} - \frac{0.5}{H(z_{top} - \frac{3}{2}\Delta z)\Delta z} \right] - \frac{gm}{2R^*}$$
$$(6.162)$$

and stored in `tphdz1(lev1)` and `tphdz0(lev1)`, respectively, with the index $lev1 = nlev + 1$ corresponding to $z_{top} + \frac{1}{2}\Delta z$.

The diffusion coefficient D_A are calculated at the interface pressure level $z, z + \Delta z, ...$ by averaging

$$D_A(z) = \frac{1}{2} \left(D_A(z + \frac{1}{2}\Delta z) + D_A(z - \frac{1}{2}\Delta z) \right) \quad (6.163)$$

and stored in the variable `djint`. The upper and lower boundary values are

determined by extrapolation

$$D_A(z_{bot}) = \frac{1}{2}\left(3D_A(z_{bot} + \frac{1}{2}\Delta z) - D_A(z_{bot} + \frac{3}{2}\Delta z)\right) \qquad (6.164)$$

$$D_A(z_{top}) = \frac{1}{2}\left(3D_A(z_{top} - \frac{1}{2}\Delta z) - D_A(z_{top} - \frac{3}{2}\Delta z)\right) \qquad (6.165)$$

The term $T_4 = \frac{\nabla \cdot \mathbf{b}}{b_z} + \frac{\mathbf{b}_H \cdot \nabla_H(D_A b_z)}{R_E D_A b_z^2}$ is determined at the midpoint pressure level, and stored in the variable `divbz`

$$
\begin{aligned}
T_4(z + \frac{1}{2}\Delta z) = &\frac{\nabla \cdot \mathbf{b}}{b_z}(\phi, \lambda) + \frac{1}{R_E D_A(\phi, \lambda, z + \frac{1}{2}\Delta z)b_z^2}[\\
&\frac{b_x(\phi, \lambda)}{\cos \lambda}(\frac{D_A(\phi + \Delta\phi, \lambda, z + \frac{1}{2}\Delta z)b_z(\phi + \Delta\phi, \lambda)}{2\Delta\phi} - \\
&\frac{D_A(\phi - \Delta\phi, \lambda, z + \frac{1}{2}\Delta z)b_z(\phi - \Delta\phi, \lambda)}{2\Delta\phi}) + \\
&b_y(\phi, \lambda)(\frac{D_A(\phi, \lambda + \Delta\lambda, z + \frac{1}{2}\Delta z)b_z(\phi, \lambda + \Delta\lambda)}{2\Delta\lambda} - \\
&\frac{D_A(\phi, \lambda - \Delta\lambda, z + \frac{1}{2}\Delta z)b_z(\phi, \lambda - \Delta\lambda)}{2\Delta\lambda})]
\end{aligned}
\qquad (6.166)
$$

The periodic points for T_4 are set to zero.

The term $T_5 = b_z^2(\frac{1}{H\Delta z} \pm \frac{1}{2}T_4)$ are calculated, with $T_4 = \frac{\nabla \cdot \mathbf{b}}{b_z} + \frac{\mathbf{b}_H \cdot \nabla_H(D_A b_z)}{R_E D_A b_z^2}$, see above in eq.(6.166)

$$T_{5p}(z + \frac{1}{2}\Delta z) = b_z^2\left[\frac{1}{H\Delta z} + \frac{1}{2}\left(\frac{\nabla \cdot \mathbf{b}}{b_z} + \frac{\mathbf{b}_H \cdot \nabla_H(D_A b_z)}{R_E D_A b_z^2}(z + \frac{1}{2}\Delta z)\right)\right] \qquad (6.167)$$

$$T_{5m}(z + \frac{1}{2}\Delta z) = b_z^2\left[\frac{1}{H\Delta z} - \frac{1}{2}\left(\frac{\nabla \cdot \mathbf{b}}{b_z} + \frac{\mathbf{b}_H \cdot \nabla_H(D_A b_z)}{R_E D_A b_z^2}(z + \frac{1}{2}\Delta z)\right)\right] \qquad (6.168)$$

and stored in the variables $hdzpbz$ and $hdzmdz$ respectively.

The smoothing of $n(O^+)^{t_n - \Delta t}$ is finished with a longitudinal smoothing.

See eq. (6.144) for the latitudinal smoothing

$$n(O^+)^{smo,t_n-\Delta t} = n(O^+)^{smo\lambda,t_n-\Delta t} - f_{smo}[n(O^+)^{smo\lambda,t_n-\Delta t}(\phi+2\Delta\phi,\lambda)+$$
$$n(O^+)^{smo\lambda,t_n-\Delta t}(\phi-2\Delta\phi,\lambda) - 4(n(O^+)^{smo\lambda,t_n-\Delta t}(\phi+\Delta\phi,\lambda)+$$
$$n(O^+)^{smo\lambda,t_n-\Delta t}(\phi-\Delta\phi,\lambda)) + 6n(O^+)^{t_n-\Delta t}(\phi+\Delta\phi,\lambda)] \qquad (6.169)$$

with $f_{smo} = 0.003$. The smoothed number density is added to the explicit term $T_{2,explicit}$

$$T_{3,explicit} = T_{2,explicit} - \frac{n(O^+)^{smo,t_n-\Delta t}}{2\Delta t} \qquad (6.170)$$

The tridiagonal solver need the equation in the following form:

$$P(k,i)n^{t+\Delta t}(k-1,i)+Q(k,i)n^{t+\Delta t}(k,i)+$$
$$R(k,i)n^{t+\Delta t}(k+1,i) = T_{explicit}(k,i) \qquad (6.171)$$

with the height index k for $z+\frac{1}{2}\Delta z$, $k+1$ for $z+\frac{3}{2}\Delta z$, and $k-1$ for $z-\frac{1}{2}\Delta z$. The longitude index is denoted by i. Note that the equation is solved at each latitude λ with the index j.

The fourth and sixth term of the O^+ transport equation eq.(6.130) are treated implicit with the fourth term being

$$[(\mathbf{b}_h \cdot \nabla_h)Kb_z]\left[\left(\frac{1}{H}\frac{\partial}{\partial Z}(2T_p n) + \frac{mg}{k_B}n\right)\right]$$

and the sixth term

$$\left(b_z\frac{1}{H}\frac{\partial}{\partial Z} + \nabla\cdot\mathbf{b}\right)Kb_z\left(\frac{1}{H}\frac{\partial}{\partial Z}(2T_p n) + \frac{mg}{k_B}n\right)$$

$$P_1((z+\frac{1}{2}\Delta z),\phi) = T_{5m}(z+\frac{1}{2}\Delta z,\phi)D_A(z,\phi)S_m(z+\frac{1}{2}\Delta z,\phi) \qquad (6.172)$$
$$Q_1((z+\frac{1}{2}\Delta z),\phi) = -(T_{5p}(z+\frac{1}{2}\Delta z,\phi)D_A(z+\Delta z,\phi)S_m(z+\frac{3}{2}\Delta z,\phi)+$$
$$T_{5m}(z+\frac{1}{2}\Delta z,\phi)D_A(z,\phi)S_p(z+\frac{1}{2}\Delta z,\phi)) \qquad (6.173)$$
$$R_1((z+\frac{1}{2}\Delta z),\phi) = T_{5p}(z+\frac{1}{2}\Delta z,\phi)D_A(z+\Delta z,\phi)S_p(z+\frac{3}{2}\Delta z,\phi) \quad (6.174)$$

for the terms please see equations (6.158),(6.157), (6.163),(6.168),and (6.167). The term $\mathbf{b} \cdot \mathbf{v}_n$ is determined

$$
\begin{aligned}
T_6(z + \frac{1}{2}\Delta z) = & b_x u_n(z + \frac{1}{2}\Delta z) + b_y v_n(z + \frac{1}{2}\Delta z) + \\
& H(z + \frac{1}{2}\Delta z)b_z W(z + \frac{1}{2}\Delta z)
\end{aligned}
\tag{6.175}
$$

Note that the dimensionless vertical velocity W is on the interface level $z, z + \Delta z, ...$

Part of the seventh term in eq. (6.130) which is

$$
(b_z \frac{1}{H}\frac{\partial}{\partial Z})(\mathbf{b} \cdot \mathbf{v}_n)
$$

and the ninth term

$$
B^2 \mathbf{v}_{ExB,z}\frac{1}{H}\frac{\partial}{\partial Z}\left(\frac{n}{B^2}\right)
$$

are treated implicit leading to ??? who is this done???

$$
\begin{aligned}
P_2((z + \frac{1}{2}\Delta z), \phi) = & P_1 + b_z \mathbf{b} \cdot \mathbf{v}_n((z + \frac{1}{2}\Delta z), \phi) + \\
& \mathbf{v}_{ExB,z}((z + \frac{3}{2}\Delta z), \phi)\frac{1}{2H(z + \frac{3}{2}\Delta z), \phi)\Delta z}
\end{aligned}
\tag{6.176}
$$

$$
Q_2((z + \frac{1}{2}\Delta z), \phi) = Q_1 - \mathbf{v}_{ExB,z}((z + \frac{1}{2}\Delta z), \phi)\frac{6}{R_E}
\tag{6.177}
$$

$$
\begin{aligned}
R_2((z + \frac{1}{2}\Delta z), \phi) = & R_1 - b_z mathbfb \cdot \mathbf{v}_n((z + \frac{3}{2}\Delta z), \phi) + \\
& \mathbf{v}_{ExB,z}((z + \frac{1}{2}\Delta z), \phi)\frac{1}{2H(z + \frac{1}{2}\Delta z), \phi)\Delta z}
\end{aligned}
\tag{6.178}
$$

The coefficients at the upper and lower boundary are set to

$$P_2^*((z_{bot} + \frac{1}{2}\Delta z), \phi) = P_2((z_{bot} + \frac{1}{2}\Delta z), \phi) + b_z[2\mathbf{b} \cdot \mathbf{v}_n((z_{bot} + \frac{1}{2}\Delta z), \phi)$$

$$- \mathbf{b} \cdot \mathbf{v}_n((z_{bot} + \frac{3}{2}\Delta z), \phi)] \tag{6.179}$$

$$+ \mathbf{v}_{ExB,z}((z_{bot} + \frac{1}{2}\Delta z), \phi)\frac{1}{2H(z_{bot} + \frac{1}{2}\Delta z), \phi)\Delta z}$$

$$Q_2^*((z_{top} - \frac{1}{2}\Delta z), \phi) = Q_2((z_{top} - \frac{1}{2}\Delta z), \phi)$$

$$- \mathbf{v}_{ExB,z}((z_{top} - \frac{1}{2}\Delta z), \phi)\frac{6}{R_E} \tag{6.180}$$

$$R_2^*((z_{top} - \frac{1}{2}\Delta z), \phi) = R_2(z_{top} - \frac{1}{2}\Delta z), \phi) - + ??b_z[2\mathbf{b} \cdot \mathbf{v}_n((z_{top} - \frac{1}{2}\Delta z), \phi)$$

$$- \mathbf{b} \cdot \mathbf{v}_n((z_{top} - \frac{3}{2}\Delta z), \phi)] \tag{6.181}$$

$$+ \mathbf{v}_{ExB,z}((z_{top} - \frac{1}{2}\Delta z), \phi)\frac{1}{2H(z_{top} - \frac{1}{2}\Delta z), \phi)\Delta z}$$

We add the other part of the seventh term in the transport equation (6.130)?? check b_z where does it come from???

$$(\nabla \cdot \mathbf{b})(\mathbf{b} \cdot v_n n)$$

and the time derivative of the number density of $n(O^+)$ to the Q–coefficient

$$Q_3((z + \frac{1}{2}\Delta z), \phi) = Q_2 - (b_z \nabla \cdot \mathbf{b}(\phi))(\mathbf{b} \cdot \mathbf{v}_n((z + \frac{1}{2}\Delta z), \phi)) - \frac{1}{2\Delta t} \tag{6.182}$$

The upper boundary condition is defined by

$$-b_z^2 D_a \left(T_p \frac{\partial}{H \partial Z} + \frac{mg}{R^*} \right) n = F^{O^+} \tag{6.183}$$

with F^{O^+} the flux of O^+ from and to the plasmasphere, which was defined in eq. (6.134) and (6.135).

$$B = - b_z^2 D_a(z_{top}) S_m(z_{top} + \frac{1}{2}\Delta z) \tag{6.184}$$

$$A = - b_z^2 D_a(z_{top}) S_p(z_{top} + \frac{1}{2}\Delta z) \tag{6.185}$$

with $S_m = 2T_p \frac{\partial}{H\partial Z} + \frac{mg}{R^*}$ from eq. (6.162) leading to

$$Q_3^*((z_{top} - \frac{1}{2}\Delta z), \phi) = Q_3((z_{top} - \frac{1}{2}\Delta z), \phi) + \frac{B}{A}R_2^*((z_{top} - \frac{1}{2}\Delta z), \phi)$$
$$(6.186)$$

and for the right hand side

$$T_{3,explicit}^*((z_{top} - \frac{1}{2}\Delta z), \phi) = T_{3,explicit}((z_{top} - \frac{1}{2}\Delta z), \phi) -$$
$$F^{O^+} R_2^*((z_{top} - \frac{1}{2}\Delta z), \phi)\frac{1}{A} \qquad (6.187)$$

The source and sink terms are calculated

$$n(XIO^+(^2P)) = \frac{1}{2}\left(Q(O^+(^2P))(z) + Q(O^+(^2P))(z + \frac{1}{2}\Delta z)\right)$$
$$\frac{1}{(k_{16} + k_{17})n(N_2) + k_{18}n(O) + (k_{19} + k_{20})N_e(z??) + k_{21} + k_{22}}$$
$$(6.188)$$

$$n(XIO^+(^2D)) = \frac{1}{2}\left(Q(O^+(^2D))(z) + Q(O^+(^2D))(z + \frac{1}{2}\Delta z)\right) +$$
$$\frac{(k_{20}N_e(z??) + k_{22})n(XIO^+(^2P))}{k_{23}n(N_2) + k_{24}n(O) + k_{26}n(O_2)} \qquad (6.189)$$

$$L^{O^+} = k_1 n(O_2) + k_2 n(N_2) + k_{10n(N(^2D))} \qquad (6.190)$$

The loss term L^{O^+} is added to the left hand side

$$Q_4((z + \frac{1}{2}\Delta z), \phi) = Q_3((z + \frac{1}{2}\Delta z), \phi) - L^{O^+} \qquad (6.191)$$

The right hand side is updated by

$$T_{4,explicit}((z + \frac{1}{2}\Delta z), \phi) = T_{3,explicit}((z + \frac{1}{2}\Delta z), \phi) - Q(O^+) -$$
$$(k_{19}N_e(z) + k_{21})n(XIO^+(^2P)) -$$
$$(k_{25}N_e(z) + k_{27})n(XIO^+(^2D)) -$$
$$(k_{18}n(XIO^+(^2P)) + k_{24}n(XIO^+(^2D)))n(O)$$
$$(6.192)$$

The lower boundary condition is specified by photochemical equilibrium $n = \frac{Q}{L}$ leading to

$$Q_4^*((z_{bot} + \frac{1}{2}\Delta z), \phi) = Q_4((z_{bot} + \frac{1}{2}\Delta z), \phi) - P_2((z_{bot} + \frac{1}{2}\Delta z), \phi) \quad (6.193)$$

$$T_{4,explicit}^*((z_{bot} + \frac{1}{2}\Delta z), \phi) = T_{4,explicit}((z_{bot} + \frac{1}{2}\Delta z), \phi) -$$
$$2P_2((z_{bot} + \frac{1}{2}\Delta z), \phi)\frac{Q(O^+)}{1.5L^{O^+}(z_{bot} + \frac{1}{2}\Delta z) - 0.5L^{O^+}(z_{bot} + \frac{3}{2}\Delta z)} \quad (6.194)$$

$$P_2^*((z_{bot} + \frac{1}{2}\Delta z), \phi) = 0 \quad (6.195)$$

Solving for the number density of O^+ at each latitude leads to the updated number densities $n(O^+)^{upd,t_n + \Delta t}$ at the midpoints. The calculated values for the number density of $n(O^+)^{upd,t+\Delta t}$ are smoothed by a Fast Fourier transformation leading to $n(O^+)_{smo}^{upd,t+\Delta t}$. All the wave numbers larger than a predefined value at each latitude are removed. The wave numbers are defined in the module `cons.F`???. The values of the number densities at the timestep t_n are also updated by using

$$n(O^+)^{upd,t} = \frac{1}{2}(1 - c_{smo})(n(O^+)^{t-\Delta t} + n(O^+)_{smo}^{upd,t+\Delta t}) + c_{smo}n(O^+)^{t_n} \quad (6.196)$$

with $c_{smo} = 0.95$ The upper boundary values are set to zero

$$n(O^+)^{upd,t_n}(z_{top} - \frac{1}{2}\Delta z) = 0 \quad (6.197)$$

$$n(O^+)_{smo}^{upd,t_n}(z_{top} - \frac{1}{2}\Delta z) = 0 \quad (6.198)$$

and the number density is set such that it has a minimum value of $1 \cdot 10^{-5}$.

$$n(O^+)^{upd,t_n}(z + \frac{1}{2}\Delta z) \geq 1 \cdot 10^{-5} \quad (6.199)$$

$$n(O^+)_{smo}^{upd,t_n}(z + \frac{1}{2}\Delta z) \geq 1 \cdot 10^{-5} \quad (6.200)$$

physical field	variable	unit	pressure level	timestep
neutral tempera-ture	T_n	K	midpoints	t_n
neutral zonal veloc-ity	u_n	cm/s	midpoints	t_n
neutral meridional velocity	v_n	cm/s	midpoints	t_n
dimenionsless verti-cal velocity	$W^{t+\Delta t}$	$1/s$	interfaces	$t + \Delta t$
mass mixing ratio O_2	Ψ_{O_2}	$-$	midpoints	t_n
mass mixing ratio O	Ψ_O	$-$	midpoints	t_n
mean molecular mass	$\overline{m}$	g/mol	interfaces	$t_n + \Delta t$
electron tempera-ture	T_e	K	midpoints	t_n
ion temperature	T_i	K	midpoints	t_n
electron density	N_e	$\#/cm^3$	interfaces	t_n
number density of $N_2(D)$??	$n(N_2(D))$??	$\#/cm^3$	midpoints	t_n
electrodynamic drift velocity	$v_{ExB,x}$	cm/s	interface	t_n
electrodynamic drift velocity	$v_{ExB,y}$	cm/s	interfaces	t_n
electrodynamic drift velocity	$v_{ExB,z}$	cm/s	interfaces	t_n
conversion factor mmr to $\#/cm^3$	$N\overline{m}$	$\frac{\#g}{cm^3mole}$	midpoints???	t_n
number density of O^+	$n(O^+)^{t_n}$	$\#/cm^3$	midpoints???	t_n
number density of O^+	$n(O^+)^{t_n-\Delta t}$	$\#/cm^3$	midpoints???	$t_n - \Delta t$

Table 6.10: Input fields to `subroutine oplus`

physical field	variable	unit	pressure level	timestep
number density of O^+	$n(O^+)^{upd,t_n}$	$\#/cm^3$	midpoints???	t_n
number density of O^+	$n(O^+)^{upd,t_n+\Delta t}$	$\#/cm^3$	midpoints???	$t_n + \Delta t$

Table 6.11: Output fields of `subroutine oplus`

physical field	variable	unit	pressure level	timestep
heating from solar radiation ???	$Q(^2P)$	$\frac{erg}{K\,s}$???	interfaces	t_n
heating from solar radiation	$Q(O^+(^2D))$	$\frac{erg}{K\,s}$???	interfaces	t_n
heating from solar radiation ????	$Q(O^+)$	$\frac{erg}{K\,s}$???	interfaces	t_n
chemical reaction rates	k_i	??	-	$-$???

Table 6.12: Module data of `subroutine oplus`

Chapter 7

Electrodynamics

7.1   Steady–State Electrodynamic Equations

The basic equations of the steady state electrodynamo are shown in this chapter. If an equation is taken from [20]. then the additional equation number refers to the equation number in [20]. In the following the presentation of the equations is based on the coding in the source code and might not look straight forward in many places. For the location in the source code of the equations it is referred to the `subroutine names`.

For longer time scales it is valid to assume steady state electrodynamics with a divergence free current density $\mathbf{J}$. It is also assumed that the conductivity along the magnetic field line is very high, thus there is no electric field component in this direction. Therefore the electrodynamo equation can be reduced to a two dimensional equation.

The current density is divergence free

$$\nabla \cdot \mathbf{J} = 0 \tag{7.1}$$

The current density has an ohmic component transverse to the magnetic field and parallel to the magnetic field line $\mathbf{J}_{||}$ and a non–ohmic magnetospheric component $\mathbf{J}_M$. In the TIEGCM only the ohmic component transverse to the magnetic field is considered by default. The other two components can be added by the user which is discussed later in chapter 7.6.4 and 7.6.4. The total current density is expressed by (eq. 2.1 in [20])

$$\mathbf{J} = \sigma_P(\mathbf{E} + \mathbf{u} \times \mathbf{B}) + \sigma_H \mathbf{b} \times (\mathbf{E} + \mathbf{u} \times \mathbf{B}) + \mathbf{J}_{||} + \mathbf{J}_M \tag{7.2}$$

with σ_P and σ_H the Pedersen and Hall conductivities. The neutral wind is denoted by $\mathbf{u}$, the electric field by $\mathbf{E}$ and the geomagnetic field by $\mathbf{B}$ with $\mathbf{b}$ the unit vector parallel to $\mathbf{B}$.

The following relations are used to derive the electrodynamo equation. For details it is referred to [20]. Apex coordinates are used with two sets of base vectors $\mathbf{e}_i$ and $\mathbf{d}_j$ which are calculated in `subroutine apxparm` (see chapter 7.3). The directions of $\mathbf{e}_1$ and $\mathbf{d}_1$ are more or less in magnetic eastward, $\mathbf{e}_2$ and $\mathbf{d}_2$ in downward or equatorward, and $\mathbf{e}_3$ and $\mathbf{d}_3$ in field line

direction. (eq. 3.11- 3.13 in [20])

$$\mathbf{e}_1 = \mathbf{d}_2 \times \mathbf{d}_3 \tag{7.3}$$
$$\mathbf{e}_2 = \mathbf{d}_3 \times \mathbf{d}_1 \tag{7.4}$$
$$\mathbf{e}_3 = \mathbf{d}_1 \times \mathbf{d}_2 \tag{7.5}$$

with (eq. 3.8- 3.10 in [20])

$$\mathbf{d}_1 = R_0 cos\lambda_m \nabla\phi_m \tag{7.6}$$
$$\mathbf{d}_2 = -R_0 sinI_m \nabla\lambda_m \tag{7.7}$$
$$\mathbf{d}_3 = \frac{\mathbf{b_0}}{|\mathbf{d}_1 \times \mathbf{d}_2|} \tag{7.8}$$

The geomagnetic longitude and apex latitude are ϕ_m and λ_m, I_m is the inclination of the geomagnetic field, R_0 the radius to the reference height $R_E + h_0$, and b_0 the unit vector in the direction of the geomagnetic field. The neutral wind $\mathbf{u}$ and the electric field $\mathbf{E}$ can be expressed in terms of the base vectors which has the advantage that the components are constant along a magnetic field line (eq. 4.5 in [20]).

$$\mathbf{u} = u_{e1}\mathbf{e}_1 + u_{e2}\mathbf{e}_2 \quad \text{with} \quad u_{ei} = \mathbf{u} \cdot \mathbf{d}_i \tag{7.9}$$
$$\mathbf{E} = E_{d1}\mathbf{d}_1 + E_{d2}\mathbf{d}_2 \quad \text{with} \quad E_{di} = \mathbf{E} \cdot \mathbf{e}_i \tag{7.10}$$

The geomagnetic field $\mathbf{B}$ is approximated by the main field $\mathbf{B}_0$. We are using the International Geomagnetic Reference Field (IGRF2000) in TIEGCM and ignore the magnetic perturbation $\Delta\mathbf{B}$ due to the external currents (eq. 3.10, 3.15, 4.4 in [20]).

$$\mathbf{B}_0 = \mathbf{B}_{e3}\mathbf{e}_3 \tag{7.11}$$
$$\mathbf{b}_0 = \mathbf{d}_3 D \quad \text{with} \quad D = |\mathbf{d}_1 \times \mathbf{d}_2| \tag{7.12}$$

The current density can be expressed by

$$\mathbf{J} = \sum_{i=1}^{3} J_{ei}\mathbf{e}_i \text{ with } J_{ei} = \mathbf{J} \cdot \mathbf{d}_i \tag{7.13}$$

Using all the equations from above leads to the current density components J_{e1} and J_{e2} (eq. 5.7, 5.8 in [20])

$$J_{e1} = \sigma_P d_1^2 (E_{d1} + u_{e2}B_{e3}) + (\sigma_H \mathbf{d}_1 \cdot \mathbf{d}_2 - \sigma_H D)(E_{d2} - u_{e1}B_{e3}) \tag{7.14}$$
$$J_{e2} = (\sigma_P \mathbf{d}_1 \cdot \mathbf{d}_2 + \sigma_H D)(E_{d1} + u_{e2}B_{e3}) + \sigma_P d_2^2 (E_{d2} - u_{e1}B_{e3}) \tag{7.15}$$

The height integrated current density in magnetic eastward and downward/equatorward direction are $K_{m\phi}$ and $K_{m\lambda}$. Knowing the current density $\mathbf{J}$ the height integrated components can be calculated by (eq. 5.1, 5.2 in [20])

$$K_{m\phi} = |sinI_m| \int_{s_L}^{s_U} \frac{J_{e1}}{D} ds \tag{7.16}$$

$$K_{m\lambda} = \mp \int_{s_L}^{s_U} \frac{J_{e2}}{D} ds \tag{7.17}$$

with the index $(\cdot)_m$ standing for modified apex (see chapter 7.3). The integration is done along the field line and s_L and s_U are the lower and upper boundary of the ionosphere, i.e. in the TIEGCM v 1.7 model 90 km to the top of the model. The electrostatic field is the gradient of the electric potential. Therefore the component of the electric field are (eq. 5.9, 5.10 in [20])

$$E_{m\phi} = E_{d1} = -\frac{1}{Rcos\lambda_m} \frac{\partial \Phi}{\partial \phi_m} \tag{7.18}$$

$$E_{m\lambda} = -E_{d2}sinI_m = -\frac{1}{R} \frac{\partial \Phi}{\partial \lambda_m} \tag{7.19}$$

Inserting equations (7.18) and (7.19) into the current density component expressions (7.14) and (7.15), which then can be used to calculate the height integrated current density in equations (7.16) and (7.17). This leads to (eq. 5.11, 5.12 in [20])

$$K_{m\phi} = \Sigma_{\phi\phi}E_{m\phi} + \Sigma_{\phi\lambda}E_{m\lambda} + K_{m\phi}^D \tag{7.20}$$

$$K_{m\lambda} = \Sigma_{\lambda\phi}E_{m\phi} + \Sigma_{\lambda\lambda}E_{m\lambda} + K_{m\lambda}^D \tag{7.21}$$

The terms $K_{m\phi}^D$ and $K_{m\lambda}^D$ are the wind driven height integrated current densities which are the driving forces (eq. 5.19, 5.20 in [20]).

$$K_{m\phi}^D = B_{e3}|sinI_m| \int_{s_L}^{s_U} \left[\frac{\sigma_P d_1^2}{D} u_{e2} + \left(\sigma_H - \frac{\sigma_P \mathbf{d}_1 \cdot \mathbf{d}_2}{D}\right) u_{e1}\right] ds \tag{7.22}$$

$$K_{m\lambda}^D = \mp B_{e3} \int_{s_L}^{s_U} \left[\left(\sigma_H + \frac{\sigma_P \mathbf{d}_1 \cdot \mathbf{d}_2}{D}\right) u_{e2} - \frac{\sigma_P d_2^2}{D} u_{e1}\right] ds \tag{7.23}$$

The conductances in the equations (7.20) and (7.21) are (eq. 5.13–5.18 in

[20])

$$\Sigma_{\phi\phi} = |sinI_m| \int_{s_L}^{s_U} \frac{\sigma_P d_1^2}{D} ds \tag{7.24}$$

$$\Sigma_{\lambda\lambda} = \frac{1}{|sinI_m|} \int_{s_L}^{s_U} \frac{\sigma_P d_2^2}{D} ds \tag{7.25}$$

$$\Sigma_H = \int_{s_L}^{s_U} \sigma_H ds \tag{7.26}$$

$$\Sigma_C = \int_{s_L}^{s_U} \frac{\sigma_P \mathbf{d}_1 \cdot \mathbf{d}_2}{D} ds \tag{7.27}$$

$$\Sigma_{\phi\lambda} = \pm(\Sigma_H - \Sigma_C) \tag{7.28}$$

$$\Sigma_{\lambda\phi} = \mp(\Sigma_H + \Sigma_C) \tag{7.29}$$

$$\tag{7.30}$$

Since current continuity applies, the divergence of the horizontal current $K_{m\phi}$ and $K_{m\lambda}$ has to be balanced by an upward current density J_{mr} at the top of the ionospheric current sheet layer. (eq. 5.3 in [20])

$$J_{mr} = \frac{-1}{R cos\lambda_m} \left(\frac{\partial K_{m\phi}}{\partial\phi_m} + \frac{\partial K_{m\lambda} cos\lambda_m}{\partial\lambda_m} \right) \tag{7.31}$$

Inserting the height integrated current densities (7.20) and (7.21) into equation (7.31) and assuming that in the closed field line region the field lines are equipotential leads to (eq. 5.23 in [20])

$$\frac{\partial}{\partial\phi_m} \left(\frac{\Sigma_{\phi\phi}^T}{cos\lambda_m} \frac{\partial\Phi}{\partial\phi_m} + \Sigma_{\phi\lambda}^T \frac{\partial\Phi}{\partial|\lambda_m|} \right) + \frac{\partial}{\partial|\lambda_m|} \left(\Sigma_{\lambda\phi}^T \frac{\partial\Phi}{\partial\phi_m} + \Sigma_{\lambda\lambda}^T cos\lambda_m \frac{\partial\Phi}{\partial|\lambda_m|} \right)$$
$$= R\frac{\partial K_{m\phi}^{DT}}{\partial\phi_m} + R\frac{\partial K_{m\lambda cos\lambda_m}^{DT}}{\partial|\lambda_m|} + R^2 cos\lambda_m J_{Mr} \tag{7.32}$$

with $\frac{\partial}{\partial|\lambda_m|} = -\frac{\partial^{SH}}{\partial\lambda_m} = \frac{\partial^{NH}}{\partial\lambda_m}$ and $J_{Mr} = J_{mr}^{SH} + J_{mr}^{NH}$. The values $(\cdot)^T$ denote the sum of the values from northern $(\cdot)^{NH}$ and southern $(\cdot)^{SH}$ hemisphere

(eq. 5.24–5.29 [20])

$$\Sigma_{\phi\phi}^{T} = \Sigma_{\phi\phi}^{NH} + \Sigma_{\phi\phi}^{SH} \tag{7.33}$$

$$\Sigma_{\lambda\lambda}^{T} = \Sigma_{\lambda\lambda}^{NH} + \Sigma_{\lambda\lambda}^{SH} \tag{7.34}$$

$$\Sigma_{\lambda\phi}^{T} = \Sigma_{\lambda\phi}^{NH} - \Sigma_{\lambda\phi}^{SH} \tag{7.35}$$

$$\Sigma_{\phi\lambda}^{T} = \Sigma_{\phi\lambda}^{NH} - \Sigma_{\phi\lambda}^{SH} \tag{7.36}$$

$$K_{m\phi}^{DT} = K_{m\phi}^{D,NH} + K_{m\phi}^{D,SH} \tag{7.37}$$

$$K_{m\lambda}^{DT} = K_{m\lambda}^{D,NH} - K_{m\lambda}^{D,SH} \tag{7.38}$$

In the source code the electrodynamo equation (7.32) is divided by $\frac{\partial \lambda_m}{cos\lambda_0 \partial \lambda_0}$ with λ_0 the equally spaced distribution in modified apex latitudes λ_m which is irregular spaced. The latitudinal distribution is explained in more detail in section 7.4.

physical field	variable	unit	pressure level	timestep
neutral zonal wind	u_n	$\frac{cm}{s}$	half	t_n
neutral meridional wind	v_n	$\frac{cm}{s}$	half	t_n
dimensionless vertical wind	W	$\frac{1}{s}$	full	t_n
geopotential height	z	cm	full	$t_n + \Delta t$
Pedersen conductivity	σ_P	S/m	half	t_n
Hall conductivity	σ_H	S/m	half	t_n
mean molecular mass	$\overline{m}$	$\frac{g}{mole}$	full	$t_n + \Delta t$
neutral temperature	T_n	K	half	t_n

Table 7.1: Input fields to `subroutine prep-dynamo`

7.2 Input to the Electrodynamo

In `subroutine prep-dynamo` fields are prepared for the electrodynamo calculation. The preparation includes reversing the order of the indexing, as well as gathering the fields from the different processors to the master processor. The electrodynamo part is still serial and therefore a gathering of all the subdomains at the beginning and a distribution of the fields to all the subdomains at the end has to be done.

The input to `subroutine prep-dynamo` is summarized in table 7.1. To calculate the vertical neutral velocity w_n the pressure scale height H in $[cm]$ is determined at first, assuming hydrostatic equilibrium for timescales longer than a few minutes.

$$H = \frac{R^* T_n}{\overline{m} g} \tag{7.39}$$

with R^* the gas constant in $[\frac{erg}{moleK}]$, T_n the neutral temperature in $[K]$, $\overline{m}$ the mean molecular mass in $[\frac{g}{mole}]$ and g acceleration of gravity in $[\frac{cm}{s^2}]$. The dimensionless vertical wind W is

$$W = -\frac{1}{p}\frac{dp}{dt} \tag{7.40}$$

which is used to get the vertical wind at a constant pressure level by

$$w_n = HW \tag{7.41}$$

with the pressure p and $\frac{dp}{dt}$ the time rate of change following the fluid motion.

7.3 Apex Coordinates

The apex and modified apex coordinate system is described in [20]. The apex latitude λ_A is constant along a field line with an apex height h_A.

$$\lambda_A = \pm cos^{-1}(1 + \frac{h_A}{R_{eq}})^{-1/2} \tag{7.42}$$

with R_{eq} denoting the Earth radius at the equator and the $\pm$ sign for the location of the field line foot point in the northern / southern geomagnetic hemisphere. In the electrodynamo part of TIEGCM modified apex coordinates are used. Modified apex coordinates λ_m have a reference height h_R associated with them.

$$\lambda_m = \pm cos^{-1} \left(\frac{R_E + h_R}{R_E + h_A} \right)^{-1/2} \tag{7.43}$$

The mean Earth radius is denoted by R_E assuming a spherical Earth. The reference height h_R is assumed to be the bottom boundary of the ionosphere at $h_R = h_0 = 90km$. One of the advantages for using modified apex latitudes λ_m is that the field line foot point latitudes are continuous at the 90 km (for TIEGCM) lower boundary of the model. Apex latitudes, in contrast, would have a gap at low latitudes since only field line with an apex of at least 90 km could be used for the field line integration. The apex longitude ϕ_A and the modified apex longitude ϕ_m are the same. The apex routines are called once per model run from `program tgcm`. The only input to the calculation of the apex coordinate system in `subroutine apxparm` is the model year. If the electric potential is not calculated in TIEGCM (input flag **dynamo==0**) the magnetic field information as well as the information needed for the mapping to and from the geographic to the geomagnetic grid is read from an existing NetCDF–file. Note that even if the electric potential is not calculated a potential pattern at high latitude can be prescribed.

In the `subroutine apxparm` the apex coordinates as well as the geomagnetic main field and the base vectors are determined which are summarized in table 7.2 and later used for the electrodynamo calculation. For each geographic grid point λ_g, ϕ_g the modified apex latitude and longitude λ_m, ϕ_m is calculated. The north–, east– and downward component, respectively, B_x, B_y and B_z, of the main field $\mathbf{B}_0$ and the components of the base vector $\mathbf{d}_1$ and $\mathbf{d}_2$ are determined. The base vectors $\mathbf{d}_1$ and $\mathbf{d}_2$ are more or less in

variable	description	unit
λ_m, ϕ_m	modified apex coordinates	radian
$B_{e3}(h_0)$	magnetic field component in $\mathbf{e}_3$ direction	nT
$B_z(h_0)$	downward magnetic field component	Gauss
$B_0(h_0)$	main magnetic field strength	Gauss
$\mathbf{d}_1(h_0)$	base vector approx. mag. eastward	-
$\mathbf{d}_2(h_0)$	base vector approx. mag. down–/equatorward	-
$D(h_0)$	$\|\mathbf{d}_1 \times \mathbf{d}_2\|$	-

Table 7.2: Apex quantities calculated in `subroutine apxparm` and used for the calculation of the electric potential

magnetic eastward and down–/equatorward direction. B_{e3} is the main field component in $\mathbf{e}_3$ direction. The vector $\mathbf{e}_3$ is in the direction of the magnetic field line and decreases with increasing altitude. In addition the quantity D is calculated with $D = |\mathbf{d}_1 \times \mathbf{d}_2|$.

The magnetic field quantities $B_z(h_0)$ and $B_0(h_0)$ are in units of [Gauss], $B_{e3}(h_0)$ is in [nT] and the coordinates λ_m and ϕ_m in [rad] with h_0 the reference height (90 km). The mapping from the geographic to the geomagnetic grid and vice versa is done by bilinear interpolation. For each grid point the surrounding grid points of the other grid are determined and the weighting factor for each of these corner grid points are calculated.

7.4 Latitudinal modified apex grid

Within TIEGCM the distribution of the geomagnetic latitudinal grid points is expressed in two different ways. One is the irregular distribution of modified apex latitudes λ_m^* which gives a better distribution of the latitudinal grid points by having more grid points close to the geomagnetic equator and therefore resolves the equatorial electrojet better. The second expression of latitudinal grid point distribution is equally spaced in modified apex latitude λ_m^* and is denoted by λ_0. The relation between the two is expressed by

$$tan\lambda_m^* = \frac{r_1}{R_0}tan\lambda_0 + \frac{tan\lambda_0^{2(\alpha+1))}}{(1+tan^2\lambda_0)^\alpha}^{1/2} \tag{7.44}$$

with $\alpha = 1.668$ and $r_1 = 1.06e7$. The radius R_0 is the radius to the lower boundary of the model at height h_0. For each equally spaced λ_0 the latitude
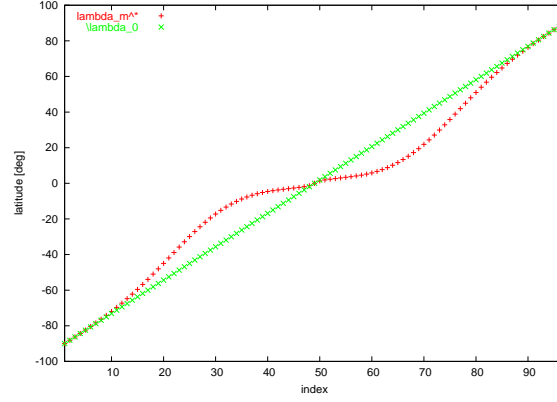
Figure 7.1: Distribution of modified apex latitude points for λ_0 (crosses) and λ_m^* (pluses)

λ_m^* is calculated. In addition a look up table is set up for equally one degree spaced latitudes λ_m^* with the corresponding λ_0 determined by using Newton's methods. All the arrays are set up in subroutine consdyn. Figure 7.1 shows the distribution of the grid points for λ_0 and λ_m^* for 97 latitudinal grid points.

7.5 Mapping from and to the geomagnetic grid

The fields in table 7.3 are mapped from the geographic grid to the geomagnetic grid in subroutine transf. Subroutine transf is called from subroutine dynamo once per timestep. The lower boundary of the TIEGCM model (up to version 1.8) is at 97 km, however the field line integration starts at $h_0 = 90$ km altitude, where the lower boundary of the ionosphere is assumed to lie. Therefore the fields in table 7.3 needed for the field line integration have to be extended downward. Three additional height levels (k=-2 to 0) are introduced with k being the height index. The geopotential height z is linearly extrapolated and the conductivities are assumed to vary

variable	description	unit	dimension
σ_P	Pedersen conductivity	S/m	3D
σ_H	Hall conductivity	S/m	3D
z	geopotential height	cm	3D
$sinI_m(h_0)$	inclination angle	-	2D
$B_{e3}(h_0)$	magnetic field component	T	2D
$\frac{\mathbf{d_1 \cdot d_2}}{D}(h_0)$	base vector quantity	-	2D
$\frac{\mathbf{d_1 \cdot d_1}}{D}(h_0)$	base vector quantity	-	2D
$\frac{\mathbf{d_2 \cdot d_2}}{D}(h_0)$	base vector quantity	-	2D
u_{e1}, u_{e2}	neutral wind components	$\frac{m}{s}$	3D

Table 7.3: Mapped fields in `subroutine transf`

exponentially.

$$z(k) = h_0 + (k+2)\left(\frac{z(k=1) - h_0}{3}\right) \qquad \text{for k=0 to -2 by -1}$$

(7.45)

$$\sigma_P(k') = \sigma_P(k'=1)exp\left(\frac{z(k+\frac{1}{2}) - z(k=1\frac{1}{2})}{fac_{ped}}\right) \quad \text{for k' =0 to -2 by -1}$$

(7.46)

$$\sigma_H(k') = \sigma_H(k'=1)exp\left(\frac{z(k+\frac{1}{2}) - z(k=1\frac{1}{2})}{fac_{hall}}\right) \quad \text{for k' =0 to -2 by -1}$$

(7.47)

Note that the geopotential height is saved on full pressure levels (k) and the conductivities on half pressure levels ($k' = k + \frac{1}{2}$). Therefore the geopotential height z for the conductivity extension (eq. 7.46 and 7.47) is calculated at half pressure levels denoted by e.g. $k' = k + \frac{1}{2}$. The factors at which the conductivities are assumed to decay below the lower boundary of the model are $fac_{ped} = 5. \times 10^5$ and $fac_{hall} = 3. \times 10^5$

The neutral winds **u** are assumed to be constant between h_0=90 to 97 km and can be expressed by

$$\mathbf{u} = \mathbf{e}_1 u_{e1} + \mathbf{e}_2 u_{e2} \qquad (7.48)$$

with the base vectors $\mathbf{e}_i$ (see [20]). The base vectors $\mathbf{d}_i$ and $\mathbf{e}_i$ satisfy $\mathbf{d}_i\mathbf{e}_j = \delta_{ij}$ with δ_{ij} the Kronecker delta. The components u_{e1} in magnetic eastward

and u_{e2} in down–/equatorward direction at altitude h are calculated by

$$u_{e1}(h) = \mathbf{d}_1(h) \cdot \mathbf{u}(h) \tag{7.49}$$
$$u_{e2}(h) = \mathbf{d}_2(h) \cdot \mathbf{u}(h) \tag{7.50}$$

The height variation of $\mathbf{d}_1(h)$ and $\mathbf{d}_1(h)$ is determined by

$$\mathbf{d}_1(h) = \left[\frac{R_E + h_0}{R_E + h)}\right]^{3/2} \mathbf{d}_1(h_0) \tag{7.51}$$

$$\mathbf{d}_2(h) = \left[\frac{R_E + h_0}{R_E + h)}\right]^{3/2} \sqrt{\frac{4. - 3.cos^2\lambda_m(h_0)}{(4. - 3.\frac{R_E+h_0}{R_E+h}cos^2\lambda_m(h_0)}} \mathbf{d}_2(h_0) \tag{7.52}$$

with $\lambda_m(h_0)$ the modified apex value at height h_0 which is kept constant vertically and thus representing the quasi–dipole latitude. In addition the following quantities are calculated

$$\frac{\mathbf{d}_1 \cdot \mathbf{d}_1}{D} \tag{7.53}$$

$$\frac{\mathbf{d}_2 \cdot \mathbf{d}_2}{D} \tag{7.54}$$

$$\frac{\mathbf{d}_1 \cdot \mathbf{d}_2}{D} \tag{7.55}$$

These values are calculated at height h_0. The values at the pole need special treatment since we have different longitudinal grid points for one spatial point. Therefore the pole values are extrapolated from the longitudinal averaged values next to the pole.

$$x(l_{pole}) = \frac{9\sum_{lon} x(l_{pole} \pm 1) - \sum_{lon} x(l_{pole} \pm 2)}{8\ nlon} \tag{7.56}$$

with the latitudinal index of the pole l_{pole} and $x(l_{pole} \pm 1)$ denoting the values one grid point off the south– and northpole respectively. The number of geographic longitudinal grid points is $nlon$ and $\sum_{lon}$ denotes the sum over all longitudinal grid points. The following fields are processed: $z(h)$, $\sigma_P(h)$, $\sigma_H(h)$, $u_{e1}(h)$, $u_{e2}(h)$, $\frac{\mathbf{d}_1 \cdot \mathbf{d}_1}{D}$, $\frac{\mathbf{d}_2 \cdot \mathbf{d}_2}{D}$, $\frac{\mathbf{d}_1 \cdot \mathbf{d}_2}{D}$, $sinI_m$, B_{e3}. In addition, periodic points for these fields are added.

The mapping from the geographic to the geomagnetic grid is done for each latitude separately right before the integration along the field line which foot point at this latitude. The field line integration is described in section 7.7.

The geomagnetic equatorial values $\sigma_{P,eq}(h)$, $\sigma_{H,eq}(h)$, $u_{e1,eq}(h)$, $u_{e2,eq}(h)$ have to be known at each geomagnetic latitude and therefore are calculated before the field line integration is done. The mapping from the geographic to the geomagnetic grid is done by a bilinear interpolation. The surrounding geographic grid points for each geomagnetic grid point and the weighting factors for each of the geographic points are determined in `subroutine apxparm`.

7.6 High Latitude Input

7.6.1 Weimer

To use the high latitude potential as defined by Weimer the flag **POTEN-TIAL_MODEL = WEIMER** in the input file of a TIEGCM has to be set. The Weimer high latitude potential was not working to estimate the convection radius under Bz positive conditions in version 1.7 and 1.8 of TIEGCM. Additional problems concerning the crossover between the high latitude electric fields and the calculated dynamo fields for active conditions with relatively large convection radii theta0 were finally fixed in version 1.94 with the replacement of the constant cross-over co-latitudes with dynamic cross-over co-latitudes described in section 7.6.3.

7.6.2 Heelis

At high latitude the electric potential pattern can be prescribed as determined by Heelis. The calculation of the electric potential due to Heelis is not described since we didn't work on this part of the code. The Heelis potential pattern is the default if the flag **POTENTIAL_MODEL** is not specified. The Heelis model is also the basis for the high latitude modifications described in the following sections. Therefore when using these modifications the flag **POTENTIAL_MODEL = HEELIS** should be set in the input file.

7.6.3 Dynamics cross-over co-latitudes

The TIEGCM uses an imposed electric field model such as the Weimer (2005) [30] or Heelis (1982) [9] electric potential models at high magnetic latitudes above a critical magnetic co-latitude called `crit(1)`. This is set at 15 degrees co-latitude, or at 75 geomagnetic latitude. Below a second magnetic co-latitude called `crit(2)`, the dynamo model calculates the electric field in the TIEGCM. This is set at 30 degrees co-latitude, or at 60 geomagnetic latitude. Between 60 and 75 geomagnetic latitude, there is a linear variation of the combined dynamo solution and the imposed high latitude solution. **Crit** is set as a real parameter in `cons.F` .
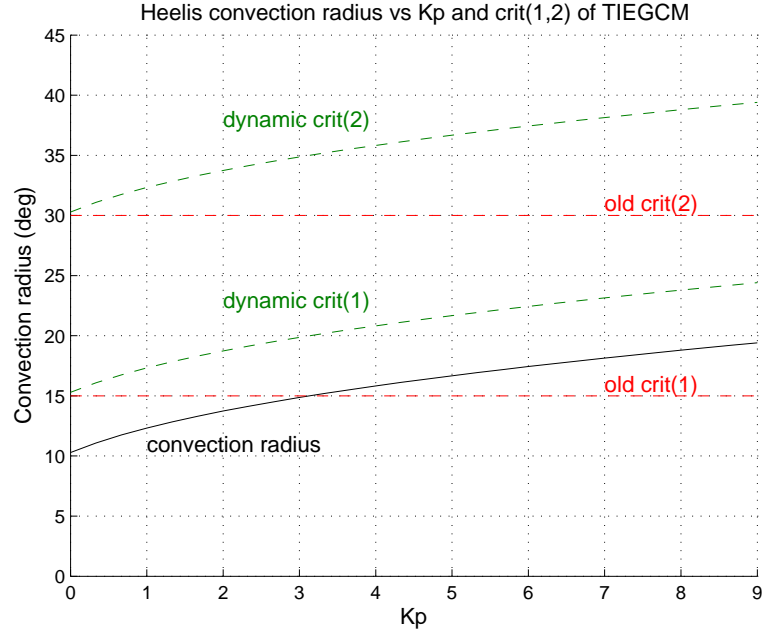
Figure 7.2: Heelis convection radius over Kp

The convection radius increases as a function of magnetic activity, and is offset towards 0 MLT from the magnetic pole by 1.1 degree for the Heelis (1982) [9] convection model, and by 4.2 degrees for the Weimer (2005) [30] convection model. Assuming the convection is centered on the magnetic pole, the following figure 7.2 shows how the convection radius increases for the Heelis model in the TIEGCM as a function of Kp and also plots `crit(1)` and `crit(2)` lines. The red dashed lines are the present constant crit(1) and crit(2) values, while the dashed green lines are the proposed 'dynamic' crit(1) and crit(2) values. The dynamic values are always equatorwards of the radius of convection, where crit(1) is set to be 5 degrees larger than the convection radius and crit(2) is 15 degrees larger. This distance from the convection radius is actually a function of MLT because of the offset of the convection pattern towards 0 MLT.

The Heelis convection radius maximizes at 19 degrees for Kp 9, and thus is never more than 5 degrees equatorwards of the constant crit(1) and crit(2) values from the 4 degrees at Kp 9 (19-15=4) and the additional 1.1 de-

grees offset towards 0 MLT. However, the Weimer (2005) convection radius is approximately 20-25 degrees in active periods, and with the additional 4.2 degree offset towards 0 MLT can be 10-15 degrees equatorwards of the constant crit(1) at 0 MLT, which is at the location of crit(2) and the dynamo only solution. We found insufficient TEC magnitudes for 06348 between 16-22 UT using the constant crit values and Weimer (2005) potential patterns driven by 5-min IMF, but good TEC magnitudes when using dynamic crit values. Other tests showed NmF2 values on active days are generally improved in both the Weimer (2005) and Heelis (1982) convection cases using dynamic crit values.

However, we have not finished our testing, especially since the Heelis NmF2 improved for all stations except the station closest to the crit(2) value for the WHI (Whole Heliosphere Interval: March 20, 2008 to April 16, 2008 - Solar Carrington Rotation 2068) period. Thus we have some more testing to determine where we should best place the dynamic crit values with respect to the convection radius and to each other.

7.6.4 Modification of the high latitude input

In the electrodynamo equation (7.32) we neglected so far the current part J_{Mr} between the ionosphere and magnetosphere. The current from the magnetosphere can be influenced by the electric field distribution, however the mechanism is not fully understood. The total field-aligned current between ionosphere and magnetosphere can be described as the divergence of a magnetospheric current $\mathbf{K}^M$

$$J_{Mr} = \frac{1}{R_0 cos\lambda_m}\Big(\frac{\partial K_\phi^M}{\partial \phi_m} + \frac{\partial K_{|\lambda|}^M cos\lambda_m}{\partial |\lambda_m|}\Big) \tag{7.57}$$

The height integrated current density $\mathbf{K}^M$ doesn't have to be realistic, but the divergence, i.e. the current J_{Mr}, should be. Using the divergence assures that the integrated field-aligned current over both hemispheres vanishes, and therefore there is no net current into the ionosphere. The two components of the field-aligned current K_ϕ^M and $K_{|\lambda|}^M$, eastward and poleward/ upward, can be differently defined depending on the acting region and the mimicking mechanism. The different contributions are described in the following three subsections. Note that in the default code non of these options is used. To

use them one or all of the flags **mod_heelis**, **J_rR** and **eqMgCnd** have to
be set to `.true.` in the `dynamo_module`.

Field–aligned current

This part has not been tested yet, however the source code can be found
in `subroutine calrhs_jrr`. To use the field–aligned part the flag `J_rR =`
`.true.` in `dynamo_module` has to be set. The magnetospheric current com-
ponents K_ϕ^M and $K_{|\lambda|}^M$ for the field–aligned current can be derived from a
reference potential Φ_R which we assume is the Heelis potential for now. Us-
ing the Heelis potential leads to realistic magnitudes and directions in the
current, but might not represent correctly the field-aligned current in the
region 1.

$$K_\phi^M = \frac{1}{R_0}\Big(\frac{\Sigma_{\phi\phi}^T}{cos\lambda_m}\frac{\partial\Phi_R}{\partial\phi_m} + \Sigma_{\phi\lambda}^T\frac{\partial\Phi_R}{\partial|\lambda_m|}\Big) \tag{7.58}$$

$$K_{|\lambda|}^M = \frac{1}{R_0 cos\lambda_m}\Big(\Sigma_{\lambda\phi}^T\frac{\partial\Phi_R}{\partial\phi_m} + \Sigma_{\lambda\lambda}^T cos\lambda_m\frac{\partial\Phi_R}{\partial|\lambda_m|}\Big) \tag{7.59}$$

The current components in equations (7.58) and (7.59) are calculated in
a similar way as the left hand side of the electrodynamo equation, which is
described in section 7.9. The conductance expressions in equation (7.151)–
(7.154) are used to calculate the current components in equations (7.58)
and (7.59), and therefore these conductances are input to the `subroutine`
`calrhs_jrr` where the current components eq. (7.151)–(7.154) are calcu-
lated. The finite difference stencil for the partial derivatives in equations
(7.58) and (7.59) is set up in `subroutine nsstencil`. In comparison to the
set up of the finite difference stencil in section 7.9 for the left hand side of the
electrodynamo equation, here, it's done for both hemispheres and without
upwinding technique. Once the finite difference stencil is calculated the elec-
tric potential Φ_R is inserted, which is done in `subroutine insert_pot`, to
calculate the current components. Although the calculation is done for both
hemisphere, it is not necessary since the used Heelis potential is symmet-
ric about the equator and the coefficients of the conductances in equations
(7.151)–(7.154) are already the sum of the two hemispheres. After calcu-
lating the current it is added to the right hand side of the electrodynamo
equation (7.32).

Equivalent magnetospheric conductances

The magnetospheric field-aligned current can be influenced by the electric field distribution in the ionosphere, and therefore depend on the electric potential. The region 2 current with the shielding effect of strong electric fields from high to low latitude is an example of this magnetosphere–ionosphere interaction. The region 2 current can be approximated by a Hall conductor. In addition, the magnetospheric ion loss can be simulated by adding a zonal Pedersen conductance. In TIEGCM we adopt the concept from [16] by using equivalent magnetospheric conductances $\Sigma_{\phi\phi}^M$ and Σ_H^M. The magnetospheric current in eq. (7.57) can be replaced by

$$K_\phi^M = \frac{-1}{R_0}\Big(\frac{\Sigma_{\phi\phi}^M}{cos\lambda_m}\frac{\partial\Phi}{\partial\phi_m} + \Sigma_H^M\frac{\partial\Phi}{\partial|\lambda_m|}\Big) \tag{7.60}$$

$$K_{|\lambda|}^M = \frac{\Sigma_H^M}{R_0 cos\lambda_m}\frac{\partial\Phi_R}{\partial\phi_m} \tag{7.61}$$

with $\Sigma_{\phi\phi}^M$ and Σ_H^M being the equivalent magnetospheric zonal Pedersen and Hall conductances. The values of $\Sigma_{\phi\phi}^M$ and Σ_H^M are taken from figure 4 in [16] and plotted in figure 7.3. In `subroutine set_cicr` the equivalent magnetospheric conductances are set up and added to the conductances due to solar ionization and particle precipitation in `subroutine add_cicr`. In figure 7.3 the equivalent magnetospheric conductances start at 72° magnetic latitude which is the convection reversal boundary for this specific case. However, the convection reversal boundary varies with the geomagnetic conditions and the location is determined in the `aurora module`. The contributions to the electrodynamo equation due to the equivalent magnetospheric conductances are calculated in a similar way as described in section 7.7 for the left hand side of the electrodynamo equation. The conductances are calculated on the irregular spaced grid λ_m^*, but for the finite differencing the regular grid λ_0 in λ_m^* is used. Therefore, the difference in the partial derivatives due to the change from λ_m^* to λ_0 have to be taken into account, as described in table 7.5. The conductance quantities are then prepared for the finite differencing as shown in eq. (7.151) and (7.153) and added to the conductances due to solar ionization and particle precipitation. To use the equivalent magnetospheric conductances, the flag **eqMgCnd** has to be set to `.true.` in the `dynamo_module`.
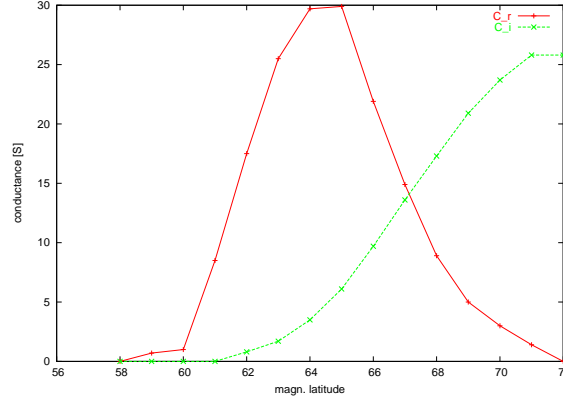
Figure 7.3: Latitudinal variation of equivalent magnetospheric conductances $\Sigma_{\phi\phi}^{M}$ (C_r) and Σ_{H}^{M} (C_i) for the convection reversal boundary at 72°.

Modified reference potential

In the region 1 the magnetospheric current in eq.(7.57) can be represented by the combination of a field–aligned current described in section 7.6.4 and a reference electric potential distribution Φ^{R}. The later is described in the following. The contribution to the magnetospheric current from a reference potential can be specified by

$$K_{\phi}^{M} = \frac{\Sigma^{R}}{R_0 cos\lambda_m}\frac{\partial(\Phi^{R} - \Phi)}{\partial\phi_m} \qquad (7.62)$$

$$K_{|\lambda|}^{M} = \frac{\Sigma^{R}}{R_0}\frac{\partial(\Phi^{R} - \Phi)}{\partial\phi_m} \qquad (7.63)$$

The reference conductance Σ^{R} is not a physical conductance, but determines how strongly the calculated electric potential Φ reflects the reference potential Φ^{R}. The reference conductance is set to

$$\Sigma^{R} = \min\left(\Sigma_{max}^{R}, \Sigma_b[e^{|\lambda_m - \lambda_{crb}|\frac{2}{\alpha_t}} - 1]\right) \quad \text{for} \quad |\lambda_m| \geq \lambda_m^{crb} \qquad (7.64)$$

$$\Sigma^{R} = 0 \quad \text{for} \quad |\lambda_m| < \lambda_m^{crb} \qquad (7.65)$$

with α_t being the width of the transition zone, here 3°, equatorward of the convection reversal boundary λ_m^{crb}. The maximum reference conductance Σ_{max}^{R} is set to $10,000$ S and the base conductance Σ_b is 5 S. In the polar cap region the electric potential should be the reference potential. In the source

code the Heelis potential is used for the reference potential Φ^R. The convection reversal boundary is denoted by λ_m^{crb}, which varies with the geomagnetic conditions, and is set in the `aurora module`. In figure 7.4 the latitudinal variation of the reference conductance Σ^R is shown for $\lambda_m^{crb} = 72^o$.

In the source code the calling tree is the following

```
subroutine dynamo
...
if (mod_heelis) then
   if(istep = 1 ) then call set_zigmar
   call add_zigmar
   call diff_rimr
   call add_rimr
endif
...
```

To use the modified reference potential the flag **mod_heelis** in the `dynamo_module` has to be set to `.true.`. The current in the equations (7.62) and (7.63) are calculated like the left hand side of the electrodynamo equation which is described in section 7.9. The reference conductances Σ^R are calculated according to eq. (7.64) and (7.65) in `subroutine set_zigmar`. The coefficients of the reference conductance are added in `subroutine add_zigmar` to the conductances $\Sigma_{\phi\phi}$ and $\Sigma_{\lambda\lambda}$ of the electrodynamo equation. The finite difference stencil is set up in `subroutine diff_rimr` by `subroutine nsstencil`. In comparison to the set up of the stencil for the left hand side of the electrodynamo equation, in section 7.9, the stencil is calculated for both hemispheres and no upwinding technique are used. Once the finite difference stencil is calculated the electric potential Φ_R is inserted to calculate the additional current for the right hand side of the electrodynamo equation in `subroutine insert_pot`. Although the additional current is determined for both hemisphere separately, this is not necessary since the reference potential and the coefficients of Σ^R are symmetric about the equator.
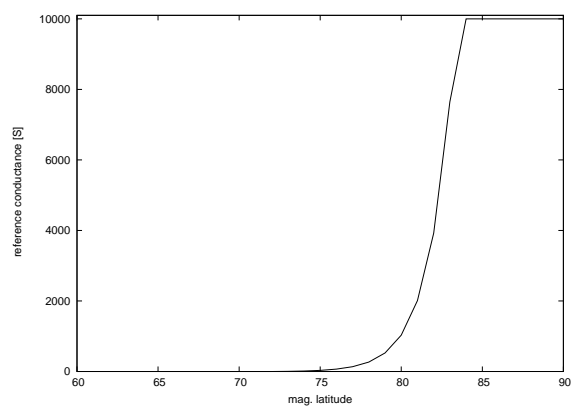
Figure 7.4: Latitudinal variation of reference conductance Σ^R for $\lambda_m^{crb} = 72^o$
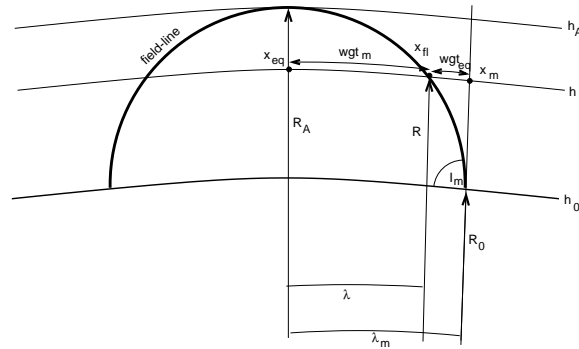
Figure 7.5: Sketch of geometry for the field–line integration

7.7 Field line Integration

This section refers to the `subroutine fieldline_integrals` in TIEGCM.

The electrodynamo equation is reduced to two dimensions assuming that the field–lines are equipotential due to the high conductivity along the field–line. The variable along the field line is s, and s_L and s_U are the lower and upper boundary of the line–integration. The inclination of the geomagnetic field–line at the reference height h_0 on an assumed spherical Earth is I_m, and B_{e3} is the component of the geomagnetic field along the field–line. Note that all value,s except the geopotential height z, are stored on half pressure levels to make the integration more convenient.

Approximation of field line values   The correct way to do the field line integration would be to trace points along the field line. However, the geomagnetic grid in TIEGCM is not oriented along the field line, and therefore the tracking would involve a two dimensional search and an interpolation to calculate the value on the field line. This can be computational expensive and therefore an approximation, which should be close to the true field line integration, is used. The field line integration is approximated by a height integration combined with an interpolation between the height-varying values at the foot point of the field line $(\lambda_m,\ h)$ and the magnetic equator $(\lambda_m = 0, h)$ (see. figure 7.5). Hence, only the height varying values at the foot point location (λ_m, h) are needed. Figure 7.5 shows schematically a field

line with the foot point latitude λ_m at the reference height h_0. The value x_{fl} at height h on the field line is approximated by the value x_{eq} at the equator and height h and the value x_m at foot point latitude λ_m and height h.

$$x_{fl} = wgt_{eq}x_{eq} + wgt_m x_m \tag{7.66}$$

with the weights wgt_{eq} for the equator value and wgt_m for the foot point value. From figure 7.5 the weight can be found as

$$wgt_{eq} = \frac{\lambda_m - \lambda}{\lambda_m} \approx \frac{sin(\lambda_m - \lambda)}{\lambda_m} \tag{7.67}$$

assuming that the difference $\lambda_m - \lambda$ is small, which is true close to the foot point of the field line. Note that determining λ would involve searching for the point on the field line at height h which is time consuming, thus the sinus is used. For field lines which foot point is at mid– and height latitude the value on the field line is essentially the height–varying value at the foot point, since the field line is almost vertical. Close to the magnetic equator the approximation is not so good anymore but the inaccuracy can be neglected when compared to the total field line integration. The term $sin(\lambda_m - \lambda)$ can be substituted by

$$sin(\lambda_m - \lambda) = sin\lambda_m cos\lambda - cos\lambda_m sin\lambda \tag{7.68}$$

and since for a dipolar field $R = R_A cos^2\lambda$ the $cos\lambda$ and $sin\lambda$ in equation (7.68) can be substituted by

$$cos\lambda = \sqrt{\frac{R}{R_A}}; \quad sin\lambda = \sqrt{1 - \frac{R}{R_A}}; \tag{7.69}$$

$$cos\lambda_m = \sqrt{\frac{R_0}{R_A}}; \quad sin\lambda_m = \sqrt{1 - \frac{R_0}{R_A}}; \tag{7.70}$$

with R_A the radius of the field–line apex (see figure 7.5). The weighting factors are

$$wgt_{eq} \approx \frac{1}{\lambda_m}\sqrt{1 - \frac{R_0}{R_A}}\sqrt{\frac{R}{R_A}} - \sqrt{\frac{R_0}{R_A}}\sqrt{1 - \frac{R}{R_A}} \tag{7.71}$$

$$wgt_m = 1 - wgt_{eq} \tag{7.72}$$

The quantities on the field–line at (h, λ) are therefore approximated by

$$\sigma_P(h, \lambda) = wgt_{eq}(h, \lambda_{eq})\sigma_P(h, \lambda_{eq}) + wgt_m(h, \lambda_m)\sigma_P(h, \lambda_m) \tag{7.73}$$

$$\sigma_H(h, \lambda) = wgt_{eq}(h, \lambda_{eq})\sigma_H(h, \lambda_{eq}) + wgt_m(h, \lambda_m)\sigma_H(h, \lambda_m) \tag{7.74}$$

$$u_{e1}(h, \lambda) = wgt_{eq}u_{e1}(h, \lambda_{eq})(h, \lambda_{eq}) + wgt_m(h, \lambda_m)u_{e1}(h, \lambda_m) \tag{7.75}$$

$$u_{e2}(h, \lambda) = wgt_{eq}u_{e2}(h, \lambda_{eq})(h, \lambda_{eq}) + wgt_m(h, \lambda_m)u_{e2}(h, \lambda_m) \tag{7.76}$$

Height variation of $\mathbf{d}_1$ and $\mathbf{d}_2$ The apex values $\frac{d_1^2}{D}$, $\frac{d_2^2}{D}$ and $\frac{\mathbf{d}_1 \cdot \mathbf{d}_2}{D}$ are referenced to height h_0 (see section 7.3). The height variation of these values are small, but should be taken into account. The values $\mathbf{d}_1$, $\mathbf{d}_2$ and D vary with height like

$$\mathbf{d}_1^2(h) = \left[\frac{R_0}{R}\right]^3 \mathbf{d}_1^2(h_0) \tag{7.77}$$

$$\mathbf{d}_2^2(h) = \left[\frac{R_0}{R}\right]^3 \left[\frac{4 - 3cos^2\lambda}{4 - 3\frac{R_0}{R}cos^2\lambda}\right] \mathbf{d}_2^2(h_0) \tag{7.78}$$

$$D(h) = \mathbf{d}_1 \cdot \mathbf{d}_2 = \left(\frac{R_0}{R}\right)^3 \left(\frac{4 - 3cos^2\lambda}{4 - 3\frac{R_0}{R}cos^2\lambda}\right)^{1/2} D(h_0) \tag{7.79}$$

Using the dipole approximation $cos^2\lambda = \frac{R}{R_A}$ we can approximate the height variation by

$$\frac{\mathbf{d}_1^2(h)}{D(h)} = \left(\frac{R_A - \frac{3}{4}R_0}{R_A - \frac{3}{4}R}\right)^{1/2} \frac{\mathbf{d}_1^2(h_0)}{D(h_0)} = \frac{1}{h_{fac}}\frac{\mathbf{d}_1^2(h_0)}{D(h_0)} \tag{7.80}$$

$$\frac{\mathbf{d}_2^2(h)}{D(h)} = \left(\frac{R_A - \frac{3}{4}R}{R_A - \frac{3}{4}R_0}\right)^{1/2} \frac{\mathbf{d}_2^2(h_0)}{D(h_0)} = h_{fac}\frac{\mathbf{d}_2^2(h_0)}{D(h_0)} \tag{7.81}$$

Approximation of ds along the field line   Since the integration is done in height rather than along the field–line ds in equations (7.24)–(7.29) is expressed in terms of height h.

$$ds = \frac{dh}{|sinI|} \tag{7.82}$$

However, $sinI$ is going to zero at the magnetic equator and ds would be infinite. Therefore, we have to approximate the relation in equation (7.82).

Starting from the calculation of $sinI$ and using the dipole approximation $cos^2\lambda = \frac{R}{R_A}$ leads to

$$sinI = \frac{2sin\lambda}{\sqrt{4 - 3cos^2\lambda}} = 2\sqrt{\frac{h_A - h}{R_E + 4h_A - 3h}} \qquad (7.83)$$

The numerator $\sqrt{h_A - h}$ varies more than the denominator. Therefore equation (7.82) is written as

$$ds = \frac{dh}{|sinI|} = -A(h)d\sqrt{h_A - h} = \frac{A(h)dh}{2\sqrt{h_A - h}} \qquad (7.84)$$

with $A(h)$ is the area at height h. The minus sign is introduced since ds should increase with increasing height. From equation (7.84) follows that the area A(h) and $A(h_0)$ at the reference height is

$$A(h) = \frac{2\sqrt{h_A - h}}{|sinI|}; \quad A(h_0) = \frac{2\sqrt{h_A - h_0}}{|sinI_m|}; \qquad (7.85)$$

Thus, the height varying factor is

$$\frac{A(h)}{A(h_0)} = \frac{2\sqrt{h_A - h}}{|sinI|}\frac{|sinI_m|}{2\sqrt{h_A - h_0}} = \sqrt{\frac{R_A - \frac{3}{4}R}{R_A - \frac{3}{4}R_0}} \qquad (7.86)$$

substituting the inclination angle $sinI$ and $sinI_m$ from equation (7.83). Inserting equation (7.85) for $A(h_0)$ in equation (7.84) will give

$$A(h) = \frac{2\sqrt{h_A - h_0}}{|sinI_m|}\sqrt{\frac{R_A - \frac{3}{4}R}{R_A - \frac{3}{4}R_0}} = A(h_0)h_{fac} \qquad (7.87)$$

The height varying factor $A(h)$ consists of two terms: a height dependent factor h_{fac} which was already defined in equation (7.81) and a height independent term $A(h_0)$.

The factor $-d\sqrt{h_A - h}$ in equation (7.82) at the pressure level k can be discretized as follows

$$-d_k\sqrt{h_A - h} = \sqrt{h_A - h_k} - \sqrt{h_A - h_{k+1}} \qquad (7.88)$$

with k being the index of the discrete pressure levels. Note that the geopotential height z is used for h which is stored at full pressure levels. The increment along the field line in eq. (7.84) can be written as

$$ds = -A(h_0)h_{fac}d\sqrt{h_A - h} \qquad (7.89)$$

quantity	name in source code	unit
$\frac{\Sigma_{\phi\phi}}{|sinI_m|}$	zigm11	S
$|sinI_m|\Sigma_{\lambda\lambda}$	zigm22	S
Σ_C	zigmc	S
Σ_H	zigm2	S
$\frac{K_{m\phi}^D}{|sinI_m|}$	rim(1)	A/m
$\pm K_{m\lambda}^D$	rim(2)	A/m

Table 7.4: Field line integrated quantities in `subroutine` `fieldline_integrals`

Field line integration   The following fields are calculated (see also equations 7.22, 7.23, 7.24, 7.25, 7.28, 7.29) using the field line integration

$$\frac{\Sigma_{\phi\phi}}{|sinI_m|} = \int_{s_L}^{s_U} \frac{\sigma_P \mathbf{d}_1^2}{D} ds \tag{7.90}$$

$$|sinI_m|\Sigma_{\lambda\lambda} = \int_{s_L}^{s_U} \frac{\sigma_P \mathbf{d}_2^2}{D} ds \tag{7.91}$$

$$\Sigma_C = \int_{s_L}^{s_U} \frac{\sigma_P \mathbf{d}_1 \cdot \mathbf{d}_2}{D} ds \tag{7.92}$$

$$\Sigma_H = \int_{s_L}^{s_U} \sigma_H ds \tag{7.93}$$

$$\frac{K_{m\phi}^D}{|sinI_m|} = B_{e3}(h_0) \int_{s_L}^{s_U} \left[\frac{\sigma_P \mathbf{d}_1^2}{D} u_{e2} + \left(\sigma_H - \frac{\sigma_P \mathbf{d}_1 \cdot \mathbf{d}_2}{D} \right) u_{e1} \right] ds \tag{7.94}$$

$$-K_{m\lambda}^D = \pm B_{e3}(h_0) \int_{s_L}^{s_U} \left[-\frac{\sigma_P \mathbf{d}_2^2}{D} u_{e1} + \left(\sigma_H + \frac{\sigma_P \mathbf{d}_1 \cdot \mathbf{d}_2}{D} \right) u_{e2} \right] ds \tag{7.95}$$

The field line integration is approximated by taking the sum over all pressure level k (k = -2 to `mlev`, with `mlev` the number of pressure levels). With the approximations of the field line integration in the previous section, the

integrals in equations (7.90)–(7.95) are calculated by

$$\frac{\Sigma_{\phi\phi}}{|sinI_m|} = -A(h_0)\frac{d_1^2}{D}(h_0) \sum_{k=-2}^{mlev} \sigma_{P,k} d_k \sqrt{h_A - h} \tag{7.96}$$

$$|sinI_m|\Sigma_{\lambda\lambda} = -A(h_0)\frac{d_2^2}{D}(h_0) \sum_{k=-2}^{mlev} \sigma_{P,k} h_{fac,k}^2 d_k \sqrt{h_A - h} \tag{7.97}$$

$$\Sigma_C = -A(h_0)\frac{\mathbf{d}_1 \cdot \mathbf{d}_2}{D}(h_0) \sum_{k=-2}^{mlev} \sigma_{P,k} h_{fac,k} d_k \sqrt{h_A - h} \tag{7.98}$$

$$\Sigma_H = -A(h_0) \sum_{k=-2}^{mlev} \sigma_{H,k} h_{fac,k} d_k \sqrt{h_A - h} \tag{7.99}$$

$$\frac{K_{m\phi}^D}{|sinI_m|} = -B_{e3}A(h_0) \sum_{k=-2}^{mlev} \Big[\sigma_{P,k}\frac{d_1^2}{D}(h_0)u_{e2,k} + \sigma_{H,k}u_{e1,k}h_{fac,k}-$$

$$\sigma_{P,k}\frac{\mathbf{d}_1 \cdot \mathbf{d}_2}{D}(h_0)u_{e1,k}h_{fac,k}\Big]d_k\sqrt{h_A - h}$$

$$-K_{m\lambda}^D = \pm B_{e3}A(h_0) \sum_{k=-2}^{mlev} \Big[\sigma_{H,k}u_{e2,k}f_{fac,k} + \sigma_{P,k}\frac{\mathbf{d}_1 \cdot \mathbf{d}_2}{D}(h_0)u_{e2,k}h_{fac,k}-$$

$$\sigma_{P,k}\frac{d_2^2}{D}(h_0)u_{e1,k}h_{fac,k}^2\Big]d_k\sqrt{h_A - h}$$
$$\tag{7.100}$$

After the field line integration is carried out the equatorial field line integral values are set, as well as the equatorial boundary condition is included. Finally, the coefficients of the partial differential equation are modified to take into account that the finite differencing is done with respect to the equally spaced grid with λ_0 which is a function of λ_m^*, although the derivatives are calculated on the irregular grid with λ_m^*. These tasks are carried out in `subroutine transf` of TIEGCM and described in the following.

Equatorial values The values at the geomagnetic equator are approximated since no field line integration can be performed. It is assumed that the average along a field line for a quantities which primarily depend on the Pedersen conductivity σ_P increase by a factor of four from one field line to

the next higher one. The average along a field line for quantities mainly dependent on Hall conductivity σ_H vary by 0.83 from one field line to the next higher one. The exact value should not be important for the electric potential calculation, as long as the values are physically reasonable and not too different than those of adjacent field lines. The factor of $\frac{1}{2}$ is introduced to take the adding of the two hemispheres into account, which is done later.

$$\frac{\Sigma_{\phi\phi,eq}}{|sinI_m|} = \frac{1}{2}\frac{1}{4}\frac{\Sigma_{\phi\phi,eq+\Delta\lambda_m}}{|sinI_m|} \tag{7.101}$$

$$|sinI_m|\Sigma_{\lambda\lambda,eq} = \frac{1}{2}\frac{1}{4}|sinI_m|\Sigma_{\lambda\lambda,eq+\Delta\lambda_m} \tag{7.102}$$

$$\Sigma_{C,eq} = \frac{1}{2}\frac{1}{4}\Sigma_{C,eq+\Delta\lambda_m} \tag{7.103}$$

$$\Sigma_{H,eq} = \frac{1}{2}0.12\Sigma_{H,eq+\Delta\lambda_m} \tag{7.104}$$

$$\frac{K^D_{m\phi,eq}}{|sinI_m|} = \frac{1}{2}0.12\frac{K^D_{m\phi,eq+\Delta\lambda_m}}{|sinI_m|} \tag{7.105}$$

$$K^D_{m\lambda,eq} = \frac{1}{2}0.12K^D_{m\lambda,eq+\Delta\lambda_m} \tag{7.106}$$

Equatorial boundary condition At the equator the northward height integrated current density has to vanish (see [20] eq. 5.30 or 5.31).

$$K_{m\lambda} = 0 \tag{7.107}$$

Solving equation (5.31) in [20] for $\frac{\partial\Phi}{\partial\lambda_m}$ leads to

$$\frac{\partial\Phi}{\partial\lambda_m} = \frac{1}{\Sigma_{\lambda\lambda}}\Big[R_0K^D_{m\lambda} - \frac{\Sigma_{\lambda\phi}}{cos\lambda_m}\frac{\partial\Phi}{\partial\phi_m}\Big] \tag{7.108}$$

which is substituted into the electrodynamo equation (7.32). Due to the special geometry at the geomagnetic equator with horizontal field lines we can use the Cowling conductivity

$$\Sigma_{Cowling} = \Sigma_{\phi\phi} - \frac{\Sigma_{\phi\lambda}\Sigma_{\lambda\phi}}{\Sigma_{\lambda\lambda}} \tag{7.109}$$

and get

$$\frac{\partial}{\partial\phi_m}\Big[\frac{\Sigma_{Cowling}}{cos\lambda_m}\frac{\partial\Phi}{\partial\phi_m}\Big] + \frac{\partial}{\partial|\lambda_m|}\Big[\Sigma_{\lambda\phi}\frac{\partial\Phi}{\partial\phi_m} + \Sigma_{\lambda\lambda}cos\lambda_m\frac{\partial\Phi}{\partial|\lambda_m|}\Big] =$$
$$R_0\frac{\partial}{\partial\phi_m}\Big[K^D_{m\phi} - \frac{\Sigma_{\phi\lambda}}{\Sigma_{\lambda\lambda}}K^D_{m\lambda}\Big] + R_0\frac{\partial K^{DT}_{m\lambda cos\lambda_m}}{\partial|\lambda_m|} \tag{7.110}$$

Therefore the value $\frac{\Sigma_{\phi\phi}}{|sinI_m|}$ (see table 7.4) at the geomagnetic equator has to be modified by

$$\frac{\Sigma_{\phi\phi}^{mod}}{|sinI_m|} = \left[\frac{\Sigma_{\phi\phi}}{|sinI_m|} - \frac{\Sigma_{\phi\lambda}\Sigma_{\lambda\phi}}{\Sigma_{\lambda\lambda}|sinI_m|} \right]_{eq} \qquad (7.111)$$

as well as the value $\frac{K_{m\phi}^{D}}{|sinI_m|}$ (see table 7.4) by

$$\frac{K_{m\phi,eq}^{D,mod}}{|sinI_m|} = \left[\frac{K_{m\phi}^{D}}{|sinI_m|} - \frac{\Sigma_{\phi\lambda}K_{m\lambda}^{D}}{\Sigma_{\lambda\lambda}|sinI_m|} \right]_{eq} \qquad (7.112)$$

Transformation from λ_m^* to λ_0   The geomagnetic latitudinal grid λ_m^* is irregular spaced in latitude. For convenience the derivatives are taken with respect to λ_0 which is equally spaced in λ_m^*. Therefore, the electrodynamo equation (see also eq. 7.32) can be written with $\lambda_m = \lambda_m^*$

$$\frac{\partial}{\partial\phi_m}\Big(\frac{\Sigma_{\phi\phi}}{cos\lambda_m^*}\frac{\partial\Phi}{\partial\phi_m} + \Sigma_{\phi\lambda}\frac{\partial\Phi}{\partial|\lambda_m^*|}\Big) + \frac{\partial}{\partial|\lambda_m^*|}\Big(\Sigma_{\lambda\phi}\frac{\partial\Phi}{\partial\phi_m} + \Sigma_{\lambda\lambda}cos\lambda_m^*\frac{\partial\Phi}{\partial|\lambda_m^*|}\Big)$$
$$= R\frac{\partial K_{m\phi}^{D}}{\partial\phi_m} + R\frac{\partial K_{m\lambda}^{D}cos\lambda_m^*}{\partial|\lambda_m^*|} + R^2cos\lambda_m^*J_{mr}$$
$$\qquad (7.113)$$

and has to be transformed to account for the change to λ_0. Note that the longitude is not changing. The whole equation is multiplied by $\frac{\partial\lambda_m^*}{\partial\lambda_0}$ which lead to

$$\frac{\partial\lambda_m^*}{\partial\lambda_0}\frac{\partial}{\partial\phi_m}\Big(\frac{\Sigma_{\phi\phi}}{cos\lambda_0}\frac{cos\lambda_0}{cos\lambda_m^*}\frac{\partial\Phi}{\partial\phi_m} + \Sigma_{\phi\lambda}\frac{\partial\lambda_0}{\partial\lambda_m^*}\frac{\partial\Phi}{\partial\lambda_0}\Big)+$$
$$\frac{\partial\lambda_m^*}{\partial\lambda_0}\frac{\partial}{\partial\lambda_m^*}\Big(\Sigma_{\lambda\phi}\frac{\partial\Phi}{\partial\phi_m} + \Sigma_{\lambda\lambda}cos\lambda_0\frac{cos\lambda_m^*}{cos\lambda_0}\frac{\partial\lambda_0}{\lambda_m^*}\frac{\partial\Phi}{\partial\lambda_0}\Big) \qquad (7.114)$$
$$= R_0\frac{\partial\lambda_m^*}{\partial\lambda_0}\frac{\partial K_{m\phi}^{D}}{\partial\phi_m} + R_0\frac{\partial K_{m\lambda}^{D}cos\lambda_0\frac{cos\lambda_m^*}{cos\lambda_0}}{\partial\lambda_0} + R_0^2cos\lambda_m\frac{\partial\lambda_m^*}{\partial\lambda_0}J_{mr}$$

The electrodynamo equation is multiplied by $\frac{\partial\lambda_m^*}{\partial\lambda_0}$ to avoid problems at the geomagnetic equator due to $\frac{1}{sinI_m}$ which is not defined at the equator, however $\frac{1}{sinI_m}\frac{\partial\lambda_0}{\partial\lambda_m^*}$ is defined at the equator. The quantities after the transformation are listed in table (7.5) with $(\cdot)(0)$ denoting the quantity $(\cdot)$ referenced to λ_0. The polar values of the conductances are calculated by extrapolated

quantity		name in source code	unit
$\Sigma_{\phi\phi}(0)$ $\qquad=$ $\Sigma_{\phi\phi}\frac{cos\lambda_0}{cos\lambda_m^*}\frac{\partial\lambda_m^*}{\partial\lambda_0}$		zigm11	S
$\Sigma_{\lambda\lambda}(0)$ $\qquad=$ $\Sigma_{\lambda\lambda}\frac{cos\lambda_m^*}{cos\lambda_0}\frac{\partial\lambda_0}{\partial\lambda_m^*}$		zigm22	S
$\Sigma_C(0) = \Sigma_C$		zigmc	S
$\Sigma_H(0) = \Sigma_H$		zigm2	S
$K_{m\phi}^D(0) = K_{m\phi}^D\frac{\partial\lambda_m^*}{\partial\lambda_0}$		rim(1)	A/m
$\pm K_{m\lambda}^D(0)$ $\qquad=$ $\pm K_{m\lambda}^D\frac{cos\lambda_m^*}{cos\lambda_0}$		rim(2)	A/m

Table 7.5: Quantities after the transformation at the end of `subroutine transf`

weighting e.g. for a quantity x the polar value is determined by

$$x(j_{pole}) = \frac{1}{3\text{nmlon}}\left[4.\sum_{i=1}^{nmlon} x(i, j_{pole} \mp 1) - \sum_{i=1}^{nmlon} x(i, j_{pole} \mp 2)\right] \qquad (7.115)$$

with *nmlon* the number of longitudes and j_{pole} the latitudinal index at the north / south pole and the $\mp$ sign referring to the poles respectively. The height integrated current densities $K_{m\phi}^D(0)$ and $K_{m\lambda}^D(0)$ are averaged over the pole. Note that the electrodynamo equation is not solved at the pole, however the polar values are needed for the finite differencing.

7.8 Gravity and plasma pressure driven current

7.8.1 Gravity Driven Current

This section refers to the subroutine magpres_grav in TIEGCM. Note that the units in this section are the units used in the source code of TIEGCM. By default the gravity driven current is calculated for a model run. To omit the gravity and plasma pressure driven current the flag **j_pg=.false.** in magpres_g_module has to be set.

The current driven by gravity can be calculated by

$$\mathbf{J}_g(h) = \frac{1}{\mathbf{B}(h)^2} \rho_{ion} \mathbf{g}(h) \times \mathbf{B}(h) \qquad (7.116)$$

with **B** [Gauss] the Earth main magnetic field, the ion density ρ_{ion} $[\frac{1}{cm^3}]$, and $\mathbf{g}(h)$ $[\frac{cm}{s^2}]$ the gravitational acceleration at height h. The gravitational field gets weaker with height and therefore the gravitational acceleration at reference height $h_0 = 90\ km$ is scaled by

$$\mathbf{g}(h) = \left(\frac{R_0}{R}\right)^2 \mathbf{g}(h_0) \qquad (7.117)$$

with $R = R_E + h$ and R_E the mean Earth radius. The radius of the reference height is $R_0 = R_E + h_0$. The ion density is determined by

$$\rho_{ion} = M_i \sum_i n_i m_i \quad \text{with} \quad i = O^+, O^{2+}, N^+, N^{2+}, NO^+ \qquad (7.118)$$

with the mass of a unit atomic weight M_i [g], n_i $[\frac{1}{cm^3}]$ the ion number density of the species i and m_i its corresponding atomic weight. Combining equations (7.117) and (7.118) and converting from $[\frac{g}{s^2 cm^2}]$ to $[\frac{kg}{s^2 m^2}]$ will introduce an additional factor of 10 (see equation 7.120).
The height variation of the Earth main magnetic field is approximated by

$$\mathbf{B}(h) = \left(\frac{R_0}{R}\right)^3 \mathbf{B}(h_0) \qquad (7.119)$$

with $\mathbf{B}(h_0)$ [Gaus] referenced to h_0. The components of the main field are $\mathbf{B} = (b_x, b_y, b_z)$ the north–, east– and downward components or $\mathbf{B} =$

$(b_{\phi_g}, b_{\lambda_g}, b_{z_g})$ with ϕ_g, λ_g and z_g the directions in geographic longitude, latitude and upward height respectively. The current in $[\frac{A}{cm^2}]$ due to the gravitational force is calculated at half pressure levels $k + \frac{1}{2}$ by

$$\mathbf{J}_{g,k+\frac{1}{2}} = 10\frac{R}{R_0}\frac{1}{\mathbf{B}_0^2}\rho_{ion}g(h_0)(b_x, -b_y, 0) \tag{7.120}$$

Note that in the TIEGCM code most quantities are evaluated at half levels $k+\frac{1}{2}$ and stored at level k' with $(\cdot)'$ denoting the half levels $(\cdot)+\frac{1}{2}$ in contrast to k which is the full pressure level k. Therefore R and ρ_{ion} in equation (7.120) must be evaluated at the half level $k + \frac{1}{2}$.

7.8.2 Plasma Pressure Gradient Driven Current

This section refers to the subroutine magpres_grav in TIEGCM. Note that the units in this section are the units used in the source code of TIEGCM. The plasma pressure gradient driven current is calculated by default for a model run. To omit the gravity and plasma pressure driven current the flag **j_pg=.false.** in magpres_g_module has to be set.

The current due to the plasma pressure gradient ∇p_p is

$$\mathbf{J}_p = -\frac{1}{\mathbf{B}(h)^2}\nabla p_p \times \mathbf{B}(h) \tag{7.121}$$

with the plasma pressure

$$\nabla p_p = k_B\nabla[(T_i + T_e)N_e] \tag{7.122}$$

The Boltzmann constant is denoted by k_B; T_i, T_e and N_e are the ion temperature [K], the electron temperature [K] and the electron density $[\frac{1}{cm^3}]$. The gradient ∇ is taken in the geographic direction $(\nabla_{\phi_g}, \nabla_{\lambda_g}, \nabla_{z_g})$.
The vertical gradient $\nabla_{z_g}p_p$ is approximated at the half pressure level $k + \frac{1}{2}$ by

$$\nabla_{z_g}p_{p,k+\frac{1}{2}} = 10k_B\left[\frac{N_{e,k+1} - N_{e,k}}{z_{k+1} - z_k}(T_i + T_e)_{k+\frac{1}{2}} + \frac{(T_i + T_e)_{k+1} - (T_i + T_e)_k}{z_{k+1} - z_k}N_{e,k+\frac{1}{2}}\right] \tag{7.123}$$

with the geopotential height z in [cm]. The factor of 10 takes the conversion from $[\frac{g}{s^2 cm^2}]$ to $[\frac{kg}{s^2 m^2}]$ into account.

The plasma pressure gradient in geographic eastward direction at the half pressure level $k + \frac{1}{2}$ and geographic longitude ϕ_g and geographic latitude λ_g is approximated by

$$
\nabla_{\phi_g} p_{p,k+\frac{1}{2}} = 10 k_B \frac{1}{2\Delta\phi R_{k+\frac{1}{2}} \cos\lambda_g} \Bigg[
$$
$$
\left(N_e(\phi_g + \Delta\phi_g) - N_e(\phi_g - \Delta\phi_g) \right)_{k+\frac{1}{2}} (T_i(\phi_g) + T_e(\phi_g))_{k+\frac{1}{2}} +
$$
$$
\left((T_i + T_e)(\phi_g + \Delta\phi_g) - (T_i + T_e)(\phi_g - \Delta\phi_g) \right)_{k+\frac{1}{2}} N(\phi_g)_{e,k+\frac{1}{2}} \Bigg]
$$
$$
(7.124)
$$

with $\Delta\phi_g$ the discrete step size in the eastward direction and the radius $R_{k+\frac{1}{2}}$ at the half pressure level.

The plasma pressure gradient in geographic north direction at the half pressure level $k + \frac{1}{2}$ and geographic longitude ϕ_g and geographic latitude λ_g is approximated by

$$
\nabla_{\lambda_g} p_{p,k+\frac{1}{2}} = 10 k_B \frac{1}{2\Delta\lambda R_{k+\frac{1}{2}}} \Bigg[
$$
$$
\left(N_e(\lambda_g + \Delta\lambda_g) - N_e(\lambda_g - \Delta\lambda_g) \right)_{k+\frac{1}{2}} (T_i(\lambda_g) + T_e(\lambda_g))_{k+\frac{1}{2}} +
$$
$$
\left((T_i + T_e)(\lambda_g + \Delta\lambda_g) - (T_i + T_e)(\lambda_g - \Delta\lambda_g) \right)_{k+\frac{1}{2}} N(\lambda_g)_{e,k+\frac{1}{2}} \Bigg]
$$
$$
(7.125)
$$

with $\Delta\lambda_g$ the discrete step size in the northward direction. At the geographic poles we set

$$
\nabla_{\lambda_g} p_{p,k+\frac{1}{2}}(\lambda_g = \pm 90°) = 0 \tag{7.126}
$$

Inserting the derivatives (7.123), (7.124) and (7.125) into equation (7.122) lead to

$$
\nabla p_p = 10 k_B \begin{pmatrix} \nabla_{\phi_g} \\ \nabla_{\lambda_g} \\ \nabla_{z_g} \end{pmatrix} [(T_i + T_e) N_e]_{\phi_g, \lambda_g, k+\frac{1}{2}} \tag{7.127}
$$

with ∇p_p in $[\frac{kg}{s^2m^2}]$. The cross product with the geomagnetic field vector from equation (7.121) can be written as

$$
\begin{aligned}
\mathbf{J}_{p,\phi_g,\lambda_g,k+\frac{1}{2}} &= -\frac{10k_B}{\mathbf{B}_0^2}\left(\frac{R}{R_0}\right)^3 \begin{pmatrix} \nabla_{\phi_g} \\ \nabla_{\lambda_g} \\ \nabla_{z_g} \end{pmatrix} \times \begin{pmatrix} b_y \\ b_x \\ -b_z \end{pmatrix} [(T_i + T_e)N_e]_{\phi_g,\lambda_g,k+\frac{1}{2}} \\
&= -\frac{10k_B}{\mathbf{B}_0^2}\left(\frac{R}{R_0}\right)^3 \begin{pmatrix} -\nabla_{\lambda_g} b_z - \nabla_{z_g} b_x \\ \nabla_z b_y + \nabla_{\phi_g} b_z \\ \nabla_{\phi_g} b_x - \nabla_{\lambda_g} b_y \end{pmatrix} [(T_i + T_e)N_e]_{\phi_g,\lambda_g,k+\frac{1}{2}}
\end{aligned}
$$
(7.128)

The height variation of the magnetic field is approximated by the factor $(\frac{R}{R_0})^3$. The calculated current vectors $\mathbf{J}_g$ and $\mathbf{J}_p$ have to be rotated to point in the geomagnetic direction.

$$
\frac{1}{D}J_{e1}^{p,g} = \frac{\mathbf{d}_1}{D} \cdot \mathbf{J}_{pg}
$$
(7.129)

$$
\frac{1}{D}J_{e2}^{p,g} = \frac{\mathbf{d}_2}{D} \cdot \mathbf{J}_{pg}
$$
(7.130)

with $\mathbf{d}_1$ and $\mathbf{d}_2$ denoting the vectors in quasi magnetic eastward and down/ equatorward direction. The quantity D varies with the strength of the geomagnetic field and the distortion of the geomagnetic field from a pure dipole field. The quantity D can be calculated by using the vectors $\mathbf{d}_1$ and $\mathbf{d}_2$

$$
D = |\mathbf{d}_1 \times \mathbf{d}_2|
$$
(7.131)

The vectors $\mathbf{d}_1(h_0)$ and $\mathbf{d}_2(h_0)$ as well as $D(h_0)$ are only calculated at the reference height h_0. The height variation is approximated by

$$
\mathbf{d}_1(h) = \mathbf{d}_1(h_0)\left(\frac{R_0}{R}\right)^{\frac{3}{2}}; \qquad \mathbf{d}_2(h) = \mathbf{d}_2(h_0)\left(\frac{R_0}{R}\right)^{\frac{3}{2}} \frac{\sqrt{4 - 3cos^2\lambda_m}}{\sqrt{4 - 3\frac{R_0}{R}cos^2\lambda_m}}
$$
(7.132)

Considering equation (7.131) the quantity $\frac{\mathbf{d}_1}{D}$ varies like $\frac{1}{\mathbf{d}_2}$ and $\frac{\mathbf{d}_2}{D}$ varies like $\frac{1}{\mathbf{d}_1}$. The current at top pressure level of the model is extrapolated using

$$
J_{e1,k_{max}+\frac{1}{2}}^{p,g} = \frac{3}{2}J_{e1,k_{max}-\frac{1}{2}}^{p,g} - \frac{1}{2}J_{e1,k_{max}-\frac{3}{2}}^{p,g}
$$
(7.133)

$$
J_{e2,k_{max}+\frac{1}{2}}^{p,g} = \frac{3}{2}J_{e2,k_{max}-\frac{1}{2}}^{p,g} - \frac{1}{2}J_{e2,k_{max}-\frac{3}{2}}^{p,g}
$$
(7.134)

with $k_{max} + \frac{1}{2}$ the index of the highest pressure level.

7.8.3   Field–line Integration

This section describes how the gravity and plasma pressure gradient driven current is added to forcing of the electrodynamo equation. The gravity and plasma pressure gradient driven current is therefore added to the current driven by the neutral wind. The current of the different sources are combined in subroutine fieldline_integrals, before the field line integration. The field line integration itself is described in section 7.7.

The height–integrated eastward current density $K_{m\phi}$, see eq. (7.22), is calculated and included on the right hand side of the electrodynamo equation (7.32). The current $J_{e1}^{p,g}$ due to gravity and plasma pressure gradient is added.

$$K_{m\phi} = |sinI_m| \int_{s_L}^{s_U} \frac{J_{e1}}{D} ds = B_{e3}|sinI_m| \int_{s_L}^{s_U} \left[\frac{J_{e1}^{D}}{D} + \frac{J_{e1}^{p,g}}{B_{e3}D} \right] ds \qquad (7.135)$$

with s the line–integral variable and s_L and s_U the lower and upper boundary of the line–integration. The inclination of the geomagnetic field line at the reference height h_0 on an assumed spherical Earth is I_m and B_{e3} the component of the geomagnetic field along the field–line. The eastward current J_{e1} has a contribution from the neutral winds J_{e1}^{D} and from the plasma pressure and gravity term $J_{e1}^{p,g}$.

The field–line integration is approximated by a height–integration combined with an interpolation between the height-varying values at the foot point of the field line (λ_m) and at the magnetic equator ($\lambda = 0$) which is described in section 7.7. Figure 7.5 shows schematically that for a field line with the foot point at the reference height h_0 and latitude λ_m the value x_{fl} at height h on the field line is approximated by the value x_{eq} at the equator and value x_m at foot point λ_m and height h. The calculation of the weighting factors x_{fl} and wgt_{eq} for the interpolation are described in section 7.7 equations (7.66) and (7.67).

Therefore the eastward current at (λ, h) on the field line is approximated by

$$J_{e1}^{p,g}(\lambda, h) = wgt_{eq}(h, \lambda_{eq})J_{e1,eq}^{p,g}(\lambda_{eq}, h) + wgt_m(\lambda_m, h)J_{e1,m}^{p,g}(\lambda_m, h) \quad (7.136)$$

Since the integration is done in height rather than along the field–line, ds in equation 7.135 is expressed in terms of height h. The conversion from field line integration to height is shown in section 7.7. The increment ds along the field line is substituted by eq. (7.89). The contribution $K_{m\phi}^{p,g}$ to the height

integrated eastward current is the sum over all pressure level k

$$\frac{K_{m\phi}^{p,g}}{|sinI_m|} = B_{e3}(h_0)A(h_0) \sum_k \left[\frac{10^4 J_{e1}^{p,g}(\lambda, h_{k+\frac{1}{2}})}{B_{e3}(h_0)D(h_{k+\frac{1}{2}})} \right] 10^{-2} h_{fac}(-d\sqrt{h_A - h_{k+\frac{1}{2}}})$$

(7.137)

The factor 10^4 converts the current from $[\frac{A}{cm^2}]$ to $[\frac{A}{m^2}]$ and the factor 10^{-2} converts ds from [cm] to [m]. The north–/upward height integrated current density is

$$K_{m\lambda} = \mp \int_{s_L}^{s_U} \frac{J_{e2}}{D} ds = \mp B_{e3} \int_{s_L}^{s_U} \left[\frac{J_{e2}^D}{D} + \frac{J_{e2}^{p,g}}{B_{e3}D} \right] ds \qquad (7.138)$$

With the above mentioned approximation of the field line integration the contribution from the plasma pressure gradient and the gravity driven current is the sum over all pressure level k

$$K_{m\lambda}^{p,g} = \pm B_{e3}(h_0)A(h_0) \sum_k \left[\frac{10^4 J_{e2}^{p,g}(\lambda, h_{k+\frac{1}{2}}])}{B_{e3}(h_0)D(h_{k+\frac{1}{2}})} \right] 10^{-2} h_{fac}(d\sqrt{h_A - h_{k+\frac{1}{2}}})$$

(7.139)

7.9   Finite Differencing

Hemispheric symmetry   As mentioned in section 7.1 we assume that the conductivity along the magnetic field line is very large, thus conjugate foot points are equipotential. To get a symmetric potential pattern we add the conductances and wind driven current densities of the two hemispheres together and solve for only one. The symmetry of the potential pattern is only valid at low– and mid–latitudes with closed field lines. At high latitudes the electric potential is specially treated as discussed in section 7.6.

The added together values from the northern and southern hemisphere are denoted by $(\cdot)^T$ (see equation (7.33)–(7.38)). In the source code in `subroutine dynamo` the following values are calculated

$$\Sigma_{\phi\phi}^{T}(0) = \Sigma_{\phi\phi}^{NH}(0) + \Sigma_{\phi\phi}^{SH}(0) \tag{7.140}$$

$$\Sigma_{\lambda\lambda}^{T}(0) = \Sigma_{\lambda\lambda}^{NH}(0) + \Sigma_{\lambda\lambda}^{SH}(0) \tag{7.141}$$

$$-\Sigma_{C}^{T}(0) = -(\Sigma_{C}^{NH}(0) - \Sigma_{C}^{SH}(0)) \tag{7.142}$$

$$\Sigma_{H}^{T}(0) = \Sigma_{H}^{NH}(0) - \Sigma_{H}^{SH}(0) \tag{7.143}$$

$$K_{m\phi}^{DT}(0) = K_{m\phi}^{D,NH}(0) + K_{m\phi}^{D,SH}(0) \tag{7.144}$$

$$K_{m\lambda}^{DT}(0) = K_{m\lambda}^{D,NH}(0) - K_{m\lambda}^{D,SH}(0) \tag{7.145}$$

Note that in the source code $-\Sigma_{C}^{T}(0)$ is put into ZIGMC, and that $-K_{m\lambda}^{D,SH}(0)$ was saved in RIM(2). The hemispherically added values are saved in the latitude indices of the northern hemisphere from $(nmlat + 1)/2$, which is the index for the equator, to the pole at $nmlat$. The number of magnetic latitudes is $nmlat$.

Differencing of the right hand side   In `subroutine rhspde` the right hand side is differentiated.

$$rhs = \frac{R_0}{cos\lambda_0}\Big[\frac{\partial K_{m\phi}^{DT}(0)}{\partial\phi_0} + \frac{\partial K_{m\lambda}^{DT}(0)cos\lambda_0}{\partial|\lambda_0|}\Big] \tag{7.146}$$

A central differencing scheme is used which leads to the derivative at the location $\phi(i)$, $\lambda_0(j)$

$$rhs(i,j) = \frac{R_0}{2\Delta\phi cos\lambda_0(j)}\left[K_{m\phi}^{DT}(0)(i+1,j) - K_{m\phi}^{DT}(0)(i-1,j)\right]+$$
$$\frac{R_0}{2\Delta\lambda_0 cos\lambda_0(j)}\left[K_{m\lambda}^{DT}(0)(i,j+1)cos\lambda_0(j+1)-\right.$$
$$\left.K_{m\lambda}^{DT}(0)(i,j-1)cos\lambda_0(j-1)\right]$$

(7.147)

with i, j the longitudinal and latitudinal index and the adjacent grid points $i \pm 1, j \pm 1$. The polar derivative is approximated by

$$rhs(i,j_{pole}) = -\frac{2R_0}{cos\lambda_0(j-1)mlon}\left[\sum_{i=1}^{mlon}K_{m\lambda}^{DT}(0)(i,j_{pole}-1)\right]$$

(7.148)

At the magnetic equator the northward current $K_{m\lambda}$ has to vanish see equation (7.107) or in [20] eq. (5.30) or (5.31). Therefore the right hand side derivatives are discretized by

$$rhs(i,j_{eq}) = \frac{R_0}{\Delta\phi cos\lambda_0(j_{eq})}\left[K_{m\phi}^{D,modT}(0)(i+\frac{1}{2},j_{eq}) - K_{m\phi}^{D,modT}(0)(i-\frac{1}{2},j_{eq})\right]+$$
$$\frac{2R_0}{\Delta\lambda_0}\left[K_{m\lambda}^{DT}(0)(i,j_{eq}+\frac{1}{2})cos\lambda_0(j_{eq}+\frac{1}{2})\right]$$

(7.149)

with $K_{m\phi}^{D,mod}$ the modified height integrated eastward current density due to neutral winds $K_{m\phi}^{D}$, see equation (7.112). It is referred to section 7.9 eq. (7.169)–(7.171) for explanation of the discrete boundary condition at the magnetic equator. At the geomagnetic equator $cos\lambda_0(j_{eq}) = 1$ and equation (7.149) can be written as

$$rhs(i,j_{eq}) = \frac{R_0}{2\Delta\phi_0}\left[K_{m\phi}^{D,modT}(0)(i+1,j_{eq}) - K_{m\phi}^{D,modT}(0)(i-1,j_{eq})\right]+$$
$$\frac{R_0}{\Delta\lambda_0}\left[K_{m\lambda}^{DT}(0)(i,j_{eq}+1)cos\lambda_0(j_{eq}+1) + K_{m\lambda}^{DT}(0)(i,j_{eq})\right]$$

(7.150)

The whole right hand side is multiplied by R_0 in [m] to get eq. (7.146).

Differencing of the left hand side   In this paragraph the finite differencing of the left hand side of the electrodynamo equation is discussed. In the source code the calling tree for the differencing is the following:

```
subroutine dynamo
...
if (isolve == 2) then
   call stencmd
        call htrpex
        call cnmmod
        call cnm
else
   call stencil
        call htrpex
        call cnm
endif
...
```

The flag **isolve**=2 means that at the finest grid level an additional coefficient matrix is set up without upwinding for terms violating the diagonal dominance (see paragraph further down in this section). The multigrid solver which is discussed in section 7.10 uses the coefficient matrix without upwinding to calculate the residual on the finest grid level. At all other grid levels the coefficient matrix with upwinding is used to solve for the residual. If **isolve**$\neq$ 2 the upwinding method is applied at all grid levels to solve for the electric potential. For more information about the different option with the multigrid solver we refer to section 7.10.

In `subroutine dynamo` the conductances are prepared for the finite differencing. The conductance coefficients represent

$$A = \frac{\Sigma_{\phi\phi}^T(0)}{cos\lambda_0\Delta\phi^2} \rightarrow zigm11 \tag{7.151}$$

$$B = \frac{\Sigma_{\lambda\lambda}^T(0)cos\lambda_0}{\Delta\lambda_0^2} \rightarrow zigm22 \tag{7.152}$$

$$C = \frac{\Sigma_{\phi\lambda}^T(0)}{4\Delta\lambda_0\Delta\phi} \rightarrow zigmc \tag{7.153}$$

$$D = \frac{\Sigma_{\phi\lambda}^T(0)}{4\Delta\lambda_0\Delta\phi} \rightarrow zigm2 \tag{7.154}$$

with `zigm11`, `zigm22`, `zigmc`, `zigm2` the variable names in the source code. Note that the factor of four is introduced due to the central differencing. Both hemisphere are already added together and the coefficients are stored in the index range of the "northern hemisphere" ((nmlat+1)/2 to nmlat). In the "southern hemisphere" index range (1 to (nmlat+1)/2), the same values are stored as in the northern range ((nmlat+1)/2 to nmlat) except of the two mixed terms which change sign.

$$zigmc(SH) \rightarrow -\frac{\Sigma_{\phi\lambda}^T(0)}{4\Delta\lambda_0\Delta\phi} \tag{7.155}$$

$$zigm2(SH) \rightarrow -\frac{\Sigma_{\phi\lambda}^T(0)}{4\Delta\lambda_0\Delta\phi} \tag{7.156}$$

The polar value of $\frac{\Sigma_{\phi\phi}^T(0)}{cos\lambda_0\Delta\phi^2}$ is set to zero to avoid floating point exception. The polar value is not used in the electrodynamo equation since the potential at the pole is prescribed.

The `subroutine stencmd` or `subroutine stencil` is called for each conductance term eq. (7.151)–(7.154) and the finite difference stencil is updated for the contributions of the corresponding conductance term. First the conductance is copied into a working array in `subroutine htrpex` and the longitudinal wrap around points, necessary for the longitudinal derivatives, are set. Note that there are 5 different grid levels and therefore there are 16 additional points on either side of the working array. The working array stores the values from the equator (index 1) to the pole (index (nmlat+1)/2).

The contributions to the stencil from the different conductances are determined in `subroutine cnmmod` and/or `subroutine cnm`. Subroutine `cnmmod`

is called if the flag **isolve**=2 is set, and then only for the finest grid level This subroutine sets up the coefficient stencil without upwinding method. At all the other grid levels upwinding may be used if necessary. For **isolve** $\neq$ 2 all the stencils are determined with upwinding methods if necessary, which is done in `subroutine cnm`. Please read section 7.10 for more information about the different solver types (flag **isolve**).

From equation (7.114) and the values in table 7.5 we get the following left hand side of the electrodynamo equation.

$$
\begin{aligned}
cos\lambda_0 \; lhs = & \frac{\partial}{\partial\phi_0}\Big(\frac{\Sigma^T_{\phi\phi}(0)}{cos\lambda_0}\frac{\partial\Phi}{\partial\phi_0} + \Sigma^T_{\phi\lambda}(0)\frac{\partial\Phi}{\partial\lambda_0}\Big) + \\
& \frac{\partial}{\partial\lambda_0}\Big(\Sigma^T_{\lambda\phi}(0)\frac{\partial\Phi}{\partial\phi_0} + \Sigma^T_{\lambda\lambda}(0)cos\lambda_0\frac{\partial\Phi}{\partial\lambda_0}\Big)
\end{aligned}
\tag{7.157}
$$

Note that the right hand side *rhs* in equation (7.146) is already divided by $cos\lambda_0$ therefore we have to include the $cos\lambda_0$ on the left hand side of eq. (7.157). Replacing the two terms in the brackets in eq. (7.157) by

$$
T_\phi = \frac{\Sigma^T_{\phi\phi}(0)}{cos\lambda_0}\frac{\partial\Phi}{\partial\phi_0} + \Sigma^T_{\phi\lambda}(0)\frac{\partial\Phi}{\partial\lambda_0}
\tag{7.158}
$$

$$
T_\lambda = \Sigma^T_{\lambda\phi}(0)\frac{\partial\Phi}{\partial\phi_0} + \Sigma^T_{\lambda\lambda}(0)cos\lambda_0\frac{\partial\Phi}{\partial\lambda_0}
\tag{7.159}
$$

leads to

$$
cos\lambda_0 \; lhs = \frac{\partial}{\partial\phi_0}T_\phi + \frac{\partial}{\partial\lambda_0}T_\lambda
\tag{7.160}
$$

For clarity we will omit the dependence on λ_0 shown by $(\cdot)(0)$ in the following e.g. we write $\Sigma^T_{\phi\lambda}$ instead off $\Sigma^T_{\phi\lambda}(0)$. Using central differencing for the finite differences gives

$$
cos\lambda_0 \; lhs = \frac{T_\phi(i+\frac{1}{2},j) - T_\phi(i-\frac{1}{2},j)}{\Delta\phi_0} + \frac{T_\lambda(i,j+\frac{1}{2}) - T_\lambda(i,j-\frac{1}{2})}{\Delta\lambda_0}
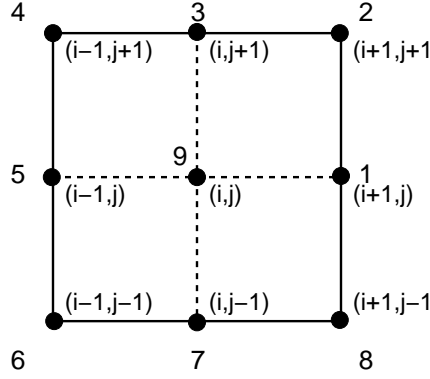\tag{7.161}
$$

Figure 7.6: Geometry for the 9 point stencil

with

$$
\begin{aligned}
T_\phi(i + \frac{1}{2}, j) =& \frac{\Sigma^T_{\phi\phi}(i + \frac{1}{2}, j)}{cos\lambda_0(j)} \frac{\Phi(i + 1, j) - \Phi(i, j)}{\Delta\phi_0} + \\
& \Sigma^T_{\phi\lambda}(i + \frac{1}{2}, j) \frac{\Phi(i + \frac{1}{2}, j + \frac{1}{2}) - \Phi(i + \frac{1}{2}, j - \frac{1}{2})}{\Delta\lambda_0} \\
T_\phi(i - \frac{1}{2}, j) =& \frac{\Sigma^T_{\phi\phi}(i - \frac{1}{2}, j)}{cos\lambda_0(j)} \frac{\Phi(i, j) - \Phi(i - 1, j)}{\Delta\phi_0} + \\
& \Sigma^T_{\phi\lambda}(i - \frac{1}{2}, j) \frac{\Phi(i - \frac{1}{2}, j + \frac{1}{2}) - \Phi(i - \frac{1}{2}, j - \frac{1}{2})}{\Delta\lambda_0} \\
T_\lambda(i, j + \frac{1}{2}) =& \Sigma^T_{\lambda\phi}(i, j + \frac{1}{2}) \frac{\Phi(i + \frac{1}{2}, j + \frac{1}{2}) - \Phi(i - \frac{1}{2}, j + \frac{1}{2})}{\Delta\phi_0} + \\
& \Sigma^T_{\lambda\lambda}(i, j + \frac{1}{2})cos\lambda_0(j + \frac{1}{2}) \frac{\Phi(i, j + 1) - \Phi(i, j)}{\Delta\lambda_0} \\
T_\lambda(i, j - \frac{1}{2}) =& \Sigma^T_{\lambda\phi}(i, j - \frac{1}{2}) \frac{\Phi(i + \frac{1}{2}, j - \frac{1}{2}) - \Phi(i - \frac{1}{2}, j - \frac{1}{2})}{\Delta\phi_0} + \\
& \Sigma^T_{\lambda\lambda}(i, j - \frac{1}{2})cos\lambda_0(j - \frac{1}{2}) \frac{\Phi(i, j) - \Phi(i, j - 1)}{\Delta\lambda_0}
\end{aligned}
\tag{7.162}
$$

The numbering of the nine point stencil can be seen in figure 7.6 with the index i denoting the longitude and the index j for the latitude. The values at half grid points e.g. $(i + \frac{1}{2}, j)$ are determined by averaging the values of the adjacent grid points, e.g.

$$
\Sigma^T_{\phi\phi}(i + \frac{1}{2}, j) = \frac{1}{2} \left[\Sigma^T_{\phi\phi}(i + 1, j) + \Sigma^T_{\phi\phi}(i, j) \right]
\tag{7.163}
$$

Accordingly, the values at $(i - \frac{1}{2}, j)$, $(i, j + \frac{1}{2})$ and $(i, j - \frac{1}{2})$ can be calculated. The difference at half points in latitude and longitude e.g. $(i + \frac{1}{2}, j + \frac{1}{2})$ is also resolved by averaging the values of the adjacent grid points which leads to e.g.

$$
\begin{aligned}
&\Phi(i + \frac{1}{2}, j + \frac{1}{2}) - \Phi(i + \frac{1}{2}, j - \frac{1}{2}) = \\
&\frac{1}{4}\big[\Phi(i + 1, j + 1) - \Phi(i + 1, j - 1) + \Phi(i, j + 1) - \Phi(i, j - 1)\big]
\end{aligned}
\tag{7.164}
$$

Accordingly, $\Phi(i - \frac{1}{2}, j + \frac{1}{2}) - \Phi(i - \frac{1}{2}, j - \frac{1}{2})$, $\Phi(i + \frac{1}{2}, j + \frac{1}{2}) - \Phi(i - \frac{1}{2}, j + \frac{1}{2})$ and $\Phi(i + \frac{1}{2}, j - \frac{1}{2}) - \Phi(i - \frac{1}{2}, j - \frac{1}{2})$ are discretized. The resulting contributions from the conductance terms to the nine point stencil in figure 7.6 are summarized in table 7.6. Therein, we are using the abbreviations A, B, C, D from equations (7.151)–(7.154) for the conductance quantities.

Upwinding   In the following the contributions to the stencil are denotes by the variable c, e.g. at node 9 the coefficient would be c(i,j). The stability is not preserved if the stencil coefficient of adjacent points of c(i,j) are changing sign e.g. $c(i + 1, j)c(i - 1, j) < 0$ or $c(i, j + 1)c(i, j - 1) < 0$. To avoid instabilities the diagonal dominance of the coefficient matrix has to be preserved. This can be done by using upwinding methods depending on the orientation of the flux (i.e. the sign of the stencil coefficients). The derivatives with respect to e.g. λ_0 for the central differencing is

$$
\frac{d\Phi(i + \frac{1}{2}, j)}{d\lambda_0} = \frac{1}{\Delta\lambda_0}\big[\Phi(i + \frac{1}{2}, j + \frac{1}{2}) - \Phi(i + \frac{1}{2}, j - \frac{1}{2})\big]
\tag{7.165}
$$

and the upwinding leads to

$$
\begin{aligned}
\frac{d\Phi(i + \frac{1}{2}, j)}{d\lambda_0} &= \frac{1}{2}\Big[\frac{d\Phi(i + 1, j)}{d\lambda_0} + \frac{d\Phi(i, j)}{d\lambda_0}\Big] \\
&= \frac{1}{2}\Big[\frac{\Phi(i + 1, j + 1) - \Phi(i + 1, j - 1)}{2\Delta\lambda_0} + \frac{\Phi(i, j + 1) - \Phi(i, j)}{\Delta\lambda_0}\Big] \\
\frac{d\Phi(i + \frac{1}{2}, j)}{d\lambda_0} &= \frac{1}{2}\Big[\frac{d\Phi(i + 1, j)}{d\lambda_0} + \frac{d\Phi(i, j)}{d\lambda_0}\Big] \\
&= \frac{1}{2}\Big[\frac{\Phi(i + 1, j + 1) - \Phi(i + 1, j - 1)}{2\Delta\lambda_0} + \frac{\Phi(i, j) - \Phi(i, j - 1)}{\Delta\lambda_0}\Big]
\end{aligned}
\tag{7.166}
$$

node	$A = \frac{\Sigma^T_{\phi\phi}}{\Delta\phi^2 cos\lambda_0}$	$B = \frac{\Sigma^T_{\lambda\lambda}(0)cos\lambda_0}{\Delta\lambda_0^2}$	$C = \frac{\Sigma^T_{\phi\lambda}(0)}{4\Delta\lambda_0\Delta\phi}$	$D = \frac{\Sigma^T_{\lambda\phi}(0)}{4\Delta\lambda_0\Delta\phi}$
1	$A(i+\frac{1}{2},j)$	-	-	$D(i,j+\frac{1}{2})-D(i,j-\frac{1}{2})$
2	-	-	$C(i+\frac{1}{2},j)$	$D(i,j+\frac{1}{2})$
3	-	$B(i,j+\frac{1}{2})$	$C(i+\frac{1}{2},j)-C(i-\frac{1}{2},j)$	-
4	-	-	$-C(i-\frac{1}{2},j)$	$-D(i,j+\frac{1}{2})$
5	$A(i-\frac{1}{2},j)$	-	-	$-D(i,j+\frac{1}{2})+D(i,j-\frac{1}{2})$
6	-	-	$C(i-\frac{1}{2},j)$	$D(i,j-\frac{1}{2})$
7	-	$B(i,j-\frac{1}{2})$	$-C(i+\frac{1}{2},j)+C(i-\frac{1}{2},j)$	-
8	-	-	$-C(i+\frac{1}{2},j)$	$-D(i,j-\frac{1}{2})$
9	$-A(i+\frac{1}{2},j)-A(i-\frac{1}{2},j)$	$-B(i,j+\frac{1}{2})-B(i,j-\frac{1}{2})$	-	-

Table 7.6: Contributions from conductance terms to nine point stencil using central differencing for all terms (see `subroutine cnm` and `subroutine cnmmod`)

node	$C = \frac{\Sigma_{\phi\lambda}^T(0)}{4\Delta\lambda_0\Delta\phi}$	$D = \frac{\Sigma_{\phi\lambda}^T(0)}{4\Delta\lambda_0\Delta\phi}$
1	-	$2D(i,j+\frac{1}{2}) - 2D(i,j-\frac{1}{2})$
3	$2C(i+\frac{1}{2},j) - 2C(i-\frac{1}{2},j)$	-
5	-	-
7	-	-
9	$-2C(i+\frac{1}{2},j) + 2C(i+\frac{1}{2},j)$	$-2D(i,j+\frac{1}{2}) + 2D(i,j-\frac{1}{2})$

Table 7.7: Modification to stencil due to upwinding with positive flux $f_l > 0$ in `subroutine cnm` and `subroutine cnmmod`

and for the derivative with respect to longitude ϕ the upwinding results in

$$\frac{d\Phi(i,j+\frac{1}{2})}{d\phi_0} = \frac{1}{2}\Big[\frac{d\Phi(i,j+1)}{d\phi_0} + \frac{d\Phi(i,j)}{d\phi_0}\Big]$$
$$= \frac{1}{2}\Big[\frac{\Phi(i+1,j+1) - \Phi(i-1,j+1)}{\Delta\phi_0} + \frac{\Phi(i+1,j) - \Phi(i,j)}{2\Delta\phi_0}\Big]$$
$$\frac{d\Phi(i,j+\frac{1}{2})}{d\phi_0} = \frac{1}{2}\Big[\frac{d\Phi(i,j+1)}{d\phi_0} + \frac{d\Phi(i,j)}{d\phi_0}\Big]$$
$$= \frac{1}{2}\Big[\frac{\Phi(i+1,j+1) - \Phi(i-1,j+1)}{2\Delta\phi_0} + \frac{\Phi(i,j) - \Phi(i-1,j)}{\Delta\phi_0}\Big]$$
$$\tag{7.167}$$

The flux at the center of the stencil (i, j) is determined by the flux average of the two adjacent points in the corresponding direction. Thus, the latitudinal flux at the center c(i,j) is $f_l = \frac{1}{2}[c(i,j+1) + c(i,j-1)]$ and the longitudinal flux is $f_l = \frac{1}{2}[c(i+1,j) + c(i-1,j)]$. For positive flux $f_l > 0$ the values in table 7.7 are used and for negative flux $f_l < 0$ the modifications in table 7.8 are applied. If the flux at the two adjacent points goes into the same direction $c(i+1,j)c(i-1,j) > 0$ or $c(i,j+1)c(i,j-1) > 0$ the central differencing in table 7.6 is used.

Equatorial boundary At the equator the coefficient stencil has to be modified to take into account the boundary condition which was described in section 7.7 eq. (7.107)–(7.112). The discrete modification to the right hand side was described in the paragraph on page 194 eq. (7.149) but the derivation will be explained in the following together with the left hand side. Including the equatorial boundary condition eq. (7.107) into the electrodynamo equation eq. (7.32) leads to eq. (7.110). The boundary condition can

node	$C = \frac{\Sigma^T_{\phi\lambda}(0)}{4\Delta\lambda_0\Delta\phi}$	$D = \frac{\Sigma^T_{\phi\lambda}(0)}{4\Delta\lambda_0\Delta\phi}$
1	-	-
3	-	-
5	-	$-2D(i,j+\frac{1}{2})+2D(i,j-\frac{1}{2})$
7	$-2C(i+\frac{1}{2},j)+2C(i-\frac{1}{2},j)$	-
9	$2C(i+\frac{1}{2},j)-2C(i+\frac{1}{2},j)$	$2D(i,j+\frac{1}{2})-2D(i,j-\frac{1}{2})$

Table 7.8: Modification to stencil due to upwinding with negative flux $f_l < 0$ in `subroutine cnm` and `subroutine cnmmod`

be rewritten as

$$\Sigma_{\lambda\phi}\frac{\partial\Phi}{\partial\phi_m} + \Sigma_{\lambda\lambda}cos\lambda_m\frac{\partial\Phi}{\partial|\lambda_m|} = R_0cos\lambda_m K^D_{m\lambda} \tag{7.168}$$

and from which in discrete form follows that

$$
\begin{aligned}
T_\lambda(i,j_{eq}+\frac{1}{2}) + T_\lambda(i,j_{eq}-\frac{1}{2}) =& R_0cos\lambda_0(j_{eq}+\frac{1}{2})K^D_{m\lambda}(i,j_{eq}+\frac{1}{2})+ \\
& R_0cos\lambda_0(j_{eq}-\frac{1}{2})K^D_{m\lambda}(i,j_{eq}-\frac{1}{2})
\end{aligned}
\tag{7.169}
$$

with T_λ defined in eq. (7.159). The electrodynamo equation at the equator (7.110)) is discretizied by

$$
\begin{aligned}
\frac{1}{cos\lambda_0(j_{eq})}&\left[\frac{T_\phi(i+\frac{1}{2},j_{eq})-T_\phi(i-\frac{1}{2},j_{eq})}{\Delta\phi_0} + \frac{T_\lambda(i,j_{eq}+\frac{1}{2})-T_\lambda(i,j_{eq}-\frac{1}{2})}{\Delta\lambda_0}\right] = \\
&\frac{R_0}{cos\lambda_0(j_{eq})\Delta\phi_0}\left[K^{D,modT}_{m\phi}(i+\frac{1}{2},j_{eq})-K^{D,modT}_{m\phi}(i-\frac{1}{2},j_{eq})\right]+ \\
&\frac{R_0}{cos\lambda_0(j_{eq})\Delta\lambda_0}\left[K^{DT}_{m\lambda}(i,j_{eq}+\frac{1}{2})cos\lambda_0(j_{eq}+\frac{1}{2})-K^{DT}_{m\lambda}(i,j_{eq}-\frac{1}{2})cos\lambda_0(j_{eq}-\frac{1}{2})\right]
\end{aligned}
\tag{7.170}
$$

Inserting equation (7.169) into the electrodynamo equation (7.170) the values $K^{DT}_{m\lambda}(i,j_{eq}-\frac{1}{2})$ and $T_\lambda(i,j_{eq}-\frac{1}{2})$ are substituted by $K^{DT}_{m\lambda}(i,j_{eq}+\frac{1}{2})$ and

node	$A = \frac{\Sigma^T_{\phi\phi}}{\Delta\phi^2 cos\lambda_0}$	$B = \frac{\Sigma^T_{\lambda\lambda}(0)cos\lambda_0}{\Delta\lambda_0^2}$	$C = \frac{\Sigma^T_{\phi\lambda}(0)}{4\Delta\lambda_0\Delta\phi}$	$D = \frac{\Sigma^T_{\phi\lambda}(0)}{4\Delta\lambda_0\Delta\phi}$
1	$A(i+\frac{1}{2},j)$	-	-	$D(i,j+\frac{1}{2})$
2	-	-	-	$D(i,j+\frac{1}{2})$
3	-	$B(i,j+\frac{1}{2})$	-	-
4	-	-	-	$-D(i,j+\frac{1}{2})$
5	$A(i-\frac{1}{2},j)$	-	-	$-D(i,j+\frac{1}{2})$
6	-	-	-	-
7	-	-	-	-
8	-	-	-	-
9	$-A(i+\frac{1}{2},j)-A(i-\frac{1}{2},j)$	$-B(i,j+\frac{1}{2})$	-	-

Table 7.9: Modification to stencil at the equator (see `subroutine cnm` or `subroutine cnmmod`)

$T_\lambda(i, j_{eq} + \frac{1}{2})$ which lead to

$$\frac{T_\phi(i+\frac{1}{2},j_{eq}) - T_\phi(i-\frac{1}{2},j_{eq})}{\Delta\phi_0} + \frac{2T_\lambda(i,j_{eq}+\frac{1}{2})}{\Delta\lambda_0} =$$

$$\frac{R_0}{\Delta\phi_0}\left[K_{m\phi}^{D,modT}(i+\frac{1}{2},j_{eq}) - K_{m\phi}^{D,modT}(i-\frac{1}{2},j_{eq})\right] + \qquad (7.171)$$

$$\frac{R_0}{\Delta\lambda_0}\left[2K_{m\lambda}^{DT}(i,j_{eq}+\frac{1}{2})cos\lambda_0(j_{eq}+\frac{1}{2})\right]$$

with $cos\lambda_0(j_{eq}) = 1$ and the value $T_\phi = \frac{\Sigma^{modT}_{\phi\phi}(0)}{cos\lambda_0}\frac{\partial\Phi}{\partial\phi_0}$ at the equator. Therefore the stencil has to be modified at the equator according to table 7.9 with $B(i,j-\frac{1}{2}) = 0$, $D(i,j-\frac{1}{2}) = 0$ and no $\Sigma_{\phi\lambda}$ contributions. The coefficients for A are not changing (see table 7.6).

Coefficient stencil   In table 7.10 the longitudinal and latitudinal dimensions of the 5 different grid levels are given. On the finest grid level the right hand side is stored in $c0(:,:,10)$. Therefore the dimension is 10 instead of 9, which is the size at all other grid levels. At the pole ($j = nmlat^*$) the off diagonal terms are set to zero and the diagonal terms to one $c^*(i,nmlat^*,9) = 1$ in `subroutine edges` with $(\cdot)^*$ denoting the different grid levels. The right hand side is set to one at the pole $c0(i,nmlat,10) = 1$. The left hand side *lhs* is finally divided by $cos\lambda_0$ in `subroutine divide`.

grid level	variable c^*	long.dimension	lat.dimension $nmlat^*$	"points" of stencil
0	c0	81	49	10
1	c1	41	25	9
2	c2	21	13	9
3	c3	11	7	9
4	c4	6	4	9

Table 7.10: Coefficient matrix name and dimensions at the different grid levels

7.10   Solving for the electric potential

In TIEGCM a multigrid solver is used which was developed by J. Adams. The source code and information can be found at http://www.scd.ucar.edu/css-/software/mudpack/. In the original mudpack solver the finite differencing and the setting of all the boundary conditions are part of solver package. For TIEGCM the stencil and the boundary conditions are already set up in the TIEGCM code, and therefore the multigrid solver was modified accordingly. We have three different solver options in TIEGCM which are all based on the mudpack multigrid package.

- **isolve=0** multigrid solver `mudcr2` (see section 7.10.1)

- **isolve=1** multigrid solver `muhcr2` as direct solver (see section 7.10.2)

- **isolve=2** modified multigrid solver `mudcr2` (see section 7.10.3)

7.10.1   Multigrid solver `mudcr2`

The `subroutine mud2cr` attempts to compute the second-order difference approximation to a two-dimensional linear nonseparable elliptic partial differential equation with cross derivative terms on a rectangle. The approximation is generated on a uniform grid covering the rectangle. The parameters used for the multigrid solver in TIEGCM are the following:

- **intl=0**: this is an input to the subroutine and is zero for the initial call to `mud2cr` to check for errors. After the initial call of `mud2cr` **intl=1** will be set and the PDE is solved.

- boundary conditions: with x being the longitudinal direction and y the latitudinal one from the equator to the pole.

    - **nxa =0** : flags boundary conditions on the edge x=xa. nxa = 0 means the boundary condition is periodic in x on [xa,xb].

    - **nxb =0**: flags boundary conditions on the edge x=xb. nxb = 0 means the boundary condition is periodic in x on [xa,xb].

    - **nyc =2**: flags boundary conditions on the edge y=yc (equator). nyc = 2 means that there are mixed derivative boundary conditions at y=yc.

- **nyd =1**: flags boundary conditions on the edge y=yd (pole). nyd=1 means that the boundary condition is specified and input thru the variable `phi`.

- defining the number of grid points in x (longitude) and y (latitude) direction

  - **ixp = 5**: ixp+1 is the number of points on the coarsest x grid visited during multigrid cycling.

  - **jyq = 3**: jyq+1 is the number of points on the coarsest y grid visited during multigrid cycling.

  - **iex = 5**: integer exponent of 2 used in defining the number of grid points in the x direction

  - **jey = 5**: integer exponent of 2 used in defining the number of grid points in the y direction

  - **nx**: number of equally spaced grid points in the interval [xa,xb]
    $nx = ixp\, 2^{iex-1} + 1$

  - **ny**: number of equally spaced grid points in the interval [yc,yd]
    $ny = jyq\, 2^{jey-1} + 1$

- **iguess = 0:** no initial guess is used forcing full multigrid cycling

- **tolmax = 0.01**: tolmax is the maximum relative error tolerance used to terminate the relaxation iterations. Assume Φ_1 and Φ_2 are the last two computed approximations at the finest grid level. If we define
  $\Phi_{diff} = max(|\Phi_2(i,j) - \Phi_1(i,j)|)$ for all i, j and
  $\Phi_{max} = max(|\Phi_2(i,j)|)$ for all i, j then convergence is considered to have occurred if and only if $\frac{\Phi_{diff}}{\Phi_{max}} < tolmax$

- **maxcy = 150**: if $tolmax > 0.0$ is input, which means error control is used, then maxcy is the limit on the number of cycles between the finest and coarsest grid levels. When the multigrid iteration is working correctly only a few cycles are required for convergence.

- **method = 3**: method of relaxation. If neither fx (the longitudinal second order derivative $\Sigma_{\phi\phi}/\Delta\phi^2$) or fy (the latitudinal second order derivative $\Sigma_{\lambda\lambda}/\Delta\lambda_0^2$) dominates over the solution region and they both vary considerably choose method = 3, which uses line relaxation in both the x and y direction

- **nwork**: length of work array
  $length = [7(nx + 2)(ny + 2) + 4(11 + isx + jsy)nx * ny]/3$

- **mgopt**: multigrid options the default values (2,2,1,3) in the vector `mgopt` were chosen for robustness.

    – **mgopt(1) = 2**: w cycling

    – **mgopt(2) = 2**: the number of pre–relaxation sweeps executed before the residual is restricted and cycling is invoked at the next coarser grid level

    – **mgopt(3) = 1**: the number of post–relaxation sweeps executed after the cycling has been invoked at the next coarser grid level and the residual correction has been transferred back

    – **mgopt(4) = 3**: multicubic prolongation (interpolation) is used to transfer residual corrections and the PDE approximation from the coarse to the fine grid within full multigrid cycling.

- output Φ: solution of PDE which is the electric potential

- output **ierror**: indicates invalid input arguments when returned positive and nonfatal warnings when returned negative.

If no convergence is reached with this version of the multigrid solver the direct solver described in section 7.10.2 is used.

7.10.2   Multigrid solver `muhcr2` as direct solver

This solver which is in `subroutine muh2cr` is originally a hybrid multigrid/direct method which approximates the same 2-d nonseparable elliptic PDE as the mudpack solver `mud2cr`. Using a direct method combines the efficiency of multigrid iteration with the certainty of a direct method. The basic algorithm is modified by using banded Gaussian elimination in place of relaxation whenever the coarsest subgrid is encountered within the multigrid cycling. The solver becomes a full direct method if grid size arguments are chosen so that the coarsest and finest grids coincide, i.e. choosing iex=jey=1 and ixp=nx-1, jyq=ny-1. This will set the Gaussian elimination on the finest grid. In this case, `subroutine muh2cr` produces a direct solution to the same nonseparable elliptic PDE. In TIEGCM we are using the solver `muhcr2` only as a direct solver.

7.10.3 Modified multigrid solver `mudcr2`

This solver is the same as the solver in section 7.10.1 only with the exception that the residual is calculated with the coefficient stencil without upwinding (see section 7.9). Therefore the solution converges toward the solution of the direct solver using the coefficient stencil without the upwinding method. In general upwinding introduces unwanted numerical dissipation. The unmodified coefficient stencil is stored in the array `cofum`. In comparison with the solver in section 7.10.1 the number of relaxation steps has to be increased to get convergence.

- **mgopt(2) = 3**: the number of pre–relaxation sweeps executed before the residual is restricted and cycling is invoked at the next coarser grid level

- **mgopt(3) = 2**: the number of post–relaxation sweeps executed after cycling has been invoked at the next coarser grid level and the residual correction has been transferred back

All the other parameters remain the same and can be found in section 7.10.1. If no convergence is reached with this multigrid solver the direct solver described in section 7.10.2 is called.

7.11   Electric Field

In `subroutine threed` the two and three dimensional electric field and the three dimensional electric potential is calculated from the two dimensional electric potential Φ. The components of the electric field E_{d1} and E_{d2} which are in more-or-less magnetic eastward and downward/equatorward direction are determined by

$$E_{d1} = -\frac{1}{R_0 cos\lambda_m}\frac{\partial\Phi}{\partial\phi_m} \tag{7.172}$$

$$E_{d2} = \frac{1}{R_0 sinI_m}\frac{\partial\Phi}{\partial\lambda_m} \tag{7.173}$$

In the code the equally spaced latitudinal grid point distribution λ_0 in λ_m^* is used to calculate the derivatives. Therefore the mapping factors from the irregular latitudinal spaced grid λ_m^* to λ_0 have to be taken into account. Including these factors the discrete derivatives are

$$E_{d1}(i,j) = -\frac{1}{R_0}\frac{cos\lambda_0(j)}{cos\lambda_m^*(j)}\frac{\Phi(i-1,j)-\Phi(i+1,j)}{2cos\lambda_0(j)\Delta\phi_m} \tag{7.174}$$

$$E_{d2}(i,j) = \frac{1}{R_0}\frac{\partial\lambda_0(j)}{|sinI_m(j)|\partial\lambda_m^*(j)}\frac{\Phi(i,j-1)-\Phi(i,j+1)}{2\Delta\lambda_0} \tag{7.175}$$

The polar values are averaged over the four surrounding points. At the equator a second order polynomial of the electric potential is fitted through the adjacent points and thus the derivative of the polynomial at the equator is determined.

The three dimensional electric potential and electric field is calculated assuming that the dipolar magnetic field lines are equipotential. At each grid point $(\phi(i), \lambda_m^*(j), h(k))$ the foot point of the magnetic field line going through this grid point is determined. Having found the foot point of the field line at height h_0 the values, i.e. electric potential and electric field, at this point can be determined by a two dimensional interpolation of the surrounding points. The polar values are determined by longitudinal averaging all the polar values.

7.12 Additional features

7.12.1 Magnetic perturbations

The magnetic perturbation from a TIEGCM model run can be determined by using the postprocessor program `MagIon`. The program is available upon request together a `MagIon` user guide, a model description is in preparation. The global magnetic perturbations at the ground and above the ionosphere at low orbiting satellite heights can be determined, or what a magnetometer would measure at the ground. For details about the calculation and the necessary assumption we refer to [19] and the `MagIon` user guide.

To calculate the magnetic perturbation the radial component of the field-aligned current J_{qr} and the height–integrated current densities $K_{m\phi}$ and $K_{m\lambda}$ have to be known. In addition, if the influence of gravity and plasma pressure gradient driven current should be included the height dependent $K_{m\phi}^{int}$ have to be determined with and without the current driven by gravity and plasma pressure gradient. The calculation of these currents is not the default in the TIEGCM source code, thus the flag **icalkqlam == 1** in the `module dynamo` has to be set. In the following the calculation of the different currents J_{qr}, $K_{q\phi}$ and $K_{q\lambda}$, which can be found in the file `current.F`, is described.

Field–aligned current J_{qr}

The field–aligned current can be determined from the electrodynamo equation (7.32) without the assumption of symmetrical hemispheres which leads to

$$\frac{\partial}{\partial \phi_m}\Big(\frac{\Sigma_{\phi\phi}}{cos\lambda_m}\frac{\partial \Phi}{\partial \phi_m} + \Sigma_{\phi\lambda}\frac{\partial \Phi}{\partial |\lambda_m|}\Big) + \frac{\partial}{\partial |\lambda_m|}\Big(\Sigma_{\lambda\phi}\frac{\partial \Phi}{\partial \phi_m} + \Sigma_{\lambda\lambda}cos\lambda_m\frac{\partial \Phi}{\partial |\lambda_m|}\Big)$$
$$= R\frac{\partial K_{m\phi}^{D}}{\partial \phi_m} + R\frac{\partial K_{m\lambda cos\lambda_m}^{D}}{\partial |\lambda_m|} + R^2 cos\lambda_m J_{mr}$$

$$\text{(7.176)}$$

Note that compared to the electrodynamo equation (7.32) the conductances and the wind driven current are different in the northern and southern hemisphere denoted by e.g. $\Sigma_{\phi\phi}$ instead of $\Sigma_{\phi\phi}^{T}$. Therefore we determine the finite difference coefficient stencil for both hemispheres instead of only one as described in section 7.9 on page 196. The set up of the finite difference stencil is analog to the one for only one hemisphere. The `subroutine nosocoef` sets up the coefficient stencil for both hemisphere and also saves the wind

driven current. The `subroutine nosocoef` is called shortly after the field line integrations i.e. before the conductances and wind driven currents are added together from the two hemispheres (see table 7.5). The conductances are prepared for the finite differencing and represent

$$A = \frac{\Sigma_{\phi\phi}(0)}{cos\lambda_0 \Delta\phi^2} \rightarrow nszigm11 \tag{7.177}$$

$$B = \frac{\Sigma_{\lambda\lambda}(0)cos\lambda_0}{\Delta\lambda_0^2} \rightarrow nszigm22 \tag{7.178}$$

$$C = \frac{\Sigma_{\phi\lambda}(0)}{4\Delta\lambda_0\Delta\phi} \rightarrow nszigmc \tag{7.179}$$

$$D = \frac{\Sigma_{\phi\lambda}(0)}{4\Delta\lambda_0\Delta\phi} \rightarrow nszigm2 \tag{7.180}$$

The set up of the stencil is analog to section 7.9 see table 7.6 and 7.9 with A, B, C and D from the definitions above eq. (7.177)–(7.180).

The calling tree is

```
...
call nsstencil
   call nscnm
...
```

Note that the stencil is only calculated on the finest grid. In addition no upwinding method to preserve the diagonal dominance is used since the finite difference stencil is not used for solving. The numbering of the nine node stencil for the southern hemisphere is the same as for the northern hemisphere, which is illustrated in figure 7.7 for both hemispheres. This means that e.g. points 6", 7" and 8" in the southern hemisphere are toward the poles and not toward the equator as for the northern hemisphere points 6, 7 and 8. This switch of the nodes 6, 7, 8 with 4, 3, 2 is reflected in the set up of the stencil in the southern hemisphere done in `subroutine nscnm`. The result is stored in the array `nscoef`. The wind driven currents of the right hand side are treated in the same way as in the dynamo equation in section 7.9 on page 194. The right hand side is saved in the array `nsrhs`.

Having set up the finite difference coefficient matrix $\bar{\mathbf{C}}$ of the left hand side, as described in the previous paragraph, and determined the wind driven

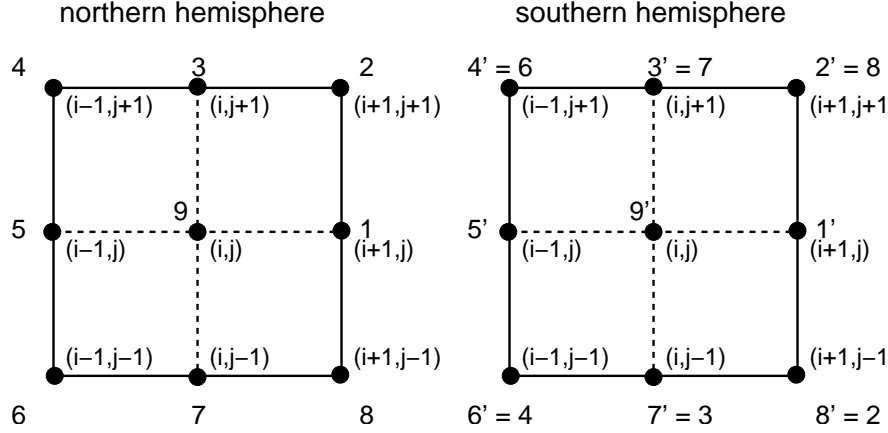northern hemisphere   southern hemisphere

Figure 7.7: Geometry for the 9 point stencil in the northern and southern hemisphere

current of the right hand side vector **rhs** we can insert the calculated electric potential vector $\mathbf{\Phi}$ into equation (7.176) to solve for the field aligned current vector $\mathbf{J}_{mr}$.

$$R_0^2 \frac{cos\lambda_m}{cos\lambda_0} \frac{\partial\lambda_0}{\partial\lambda_m^*} J_{mr} = \bar{C}\Phi - \text{rhs} \tag{7.181}$$

Note that the whole electrodynamo equation was multiplied by $\frac{1}{cos\lambda_0}\frac{\partial\lambda_0}{\partial\lambda_m^*}$ as mentioned on page 162. The current calculation is done in `subroutine nosocrrt`. For the polar values the average values at adjacent latitudinal point are extrapolated by

$$J_{mr}(j_{pole}) = \frac{1}{8\text{nmlon}} \Big[9 \sum_{i=1}^{nmlon} J_{mr}(i, j_{pole} \mp 1) - \sum_{i=1}^{nmlon} J_{mr}(i, j_{pole} \mp 2) \Big] \tag{7.182}$$

with *nmlon* the number of longitudes and j_{pole} the latitudinal index at the north / south pole and the $\mp$ sign referring to the poles respectively. Close to the magnetic equator there is no distinct allocation of the current to either the height integrated current density $K_{m\lambda}$ or the field–aligned current J_{mr} since the magnetic field lines are almost horizontal in this region. Therefore the allocation to either one of the two currents $K_{m\lambda}$ and J_{mr} depends strongly on the reference height h_0. Raising the reference height will shift the current from the field line to the ionospheric current sheet $K_{m\lambda}$. The exact distribution of the current at the equator can be neglected for the calculation of the

magnetic perturbations. Therefore we linearly interpolate the field–aligned current between $\pm 12^o$ latitude.

$$J_{mr}(j) = \frac{J_{mr}(\lambda_m^{max})J_{mr}(\lambda_m^{min})}{\lambda_m^{max} - \lambda_m^{min}}(\lambda_m - \lambda_m^{min}) + J_{mr}(\lambda_m^{min}) \qquad (7.183)$$

$$\text{for} \quad \lambda_m^{min} \leq \lambda_m \leq \lambda_m^{max} \qquad (7.184)$$

with $\lambda_m^{min} = -12^o$ and $\lambda_m^{max} = 12^o$. Due to the linear interpolation at each latitude higher frequency modes are introduced which are smoothed by a weighted average in longitude.

$$J_{mr}(j) = \frac{1}{5}[J_{mr}(i+1,j) + 3J_{mr}(i,j) + J_{mr}(i-1,j)] \qquad (7.185)$$

Since the field–aligned current J_{mr} is used to calculate the ionospheric equator– / downward current sheet contribution $K_{m\lambda}$ the total current system is adjusted automatically to satisfy that it is divergence free.

Eastward current J_{e1} and height integrated current densities $K_{q\phi}$, $K_{q\lambda}$

To calculate the eastward height integrated current density $K_{q\phi}$, see also eq. (7.4) in [20],

$$K_{q\phi} = \int_{h_l}^{h_u} \Big(\frac{R_E + h}{R_0}\Big)^{5/2} \frac{J_{e1}}{F} dh \qquad (7.186)$$

the eastward current J_{e1} has to be known. The eastward current J_{e1} is determined by, see also eq. (5.7) in [20],

$$\frac{J_{e1}}{D} = \sigma_P \frac{d_1^2}{D}(E_{d1} + u_{e2}B_{e3}) + (\sigma_P \frac{\mathbf{d}_1 \cdot \mathbf{d}_2}{D} - \sigma_H)(E_{d2} - u_{e1}B_{e3}) + \text{fac}\frac{J_{e1}^{p,g}}{D} \qquad (7.187)$$

The downward–/ equatorward current component J_{e2} is only calculated for postprocessing reasons.

$$\frac{J_{e2}}{D} = \sigma_P \frac{d_2^2}{D}(E_{d2} - u_{e1}B_{e3}) + (\sigma_P \frac{\mathbf{d}_1 \cdot \mathbf{d}_2}{D} + \sigma_H)(E_{d1} + u_{e2}B_{e3}) + \text{fac}\frac{J_{e2}^{p,g}}{D} \qquad (7.188)$$

with fac $= 10^4$ being the conversion factor from $\frac{1}{cm^2}$ to $\frac{1}{m^2}$. The current components are computed on the half pressure levels. The input quantities σ_H, σ_P, $\frac{d_1^2}{D}$, $\frac{\mathbf{d_1 \cdot d_2}}{D}$, u_{e1}, u_{e2} and B_{e3} are all stored at half pressure levels. Only the electric field E_{d1} and E_{d2} are at full pressure levels and have to be converted to half levels by

$$E_{d1}(k') = \frac{1}{2}(E_{d1}(k) + E_{d1}(k+1)) \qquad (7.189)$$

with k' denoting the half pressure level index $k' = k + \frac{1}{2}$. We assume that $\frac{d_2^2}{D} = 1$ everywhere which is approximately true. In addition to this simplification the height variation of the magnetic field component B_{e3} is neglected. The current contribution due to plasma pressure gradient and gravity $J_{e1}^{p,g}$ is

$$\frac{J_{e1}^{p,g}}{D} = \frac{\mathbf{J}_p \cdot \mathbf{d}_1 + \mathbf{J}_g \cdot \mathbf{d}_1}{D} \qquad (7.190)$$

with $\mathbf{J}_p$ determined in section 7.8.2 by eq. (7.121) and the gravity term $\mathbf{J}_g$ in section 7.8.1 by eq. (7.116). The gravity and plasma pressure gradient current is calculated in `subroutine magpres_grav` on the geographic grid and is mapped afterward to the geomagnetic grid. Both terms $\mathbf{J}_p$ and $\mathbf{J}_g$ are stored at half pressure levels.

Once the eastward current J_{e1} is determined the height integrated eastward current density $K_{m\phi}$ can be calculated by using eq. (7.186) with the dipole filed quantity F quantity, see also eq. (6.9) in [20],

$$F = \frac{sin\lambda_m}{sin\lambda_q} \frac{sinI}{sinI_m} \left(\frac{R_E + h}{R_0}\right)^3 D \qquad (7.191)$$

Inserting eq. (7.191) into eq. (7.186) leads to

$$K_{q\phi} = \int_{h_l}^{h_u} \frac{J_{e1}}{D} \frac{sin\lambda_q}{sin\lambda_m} \frac{sinI_m}{sinI} \left(\frac{R_0}{R_E + h}\right)^{1/2} dh \qquad (7.192)$$

which is calculated at full pressure levels. The height integrated current densities are calculated assuming a dipole field which is indicated by the index $(\cdot)_q$ of $K_{q\phi}$. Therefore the height integration is done in height rather than along the field line. The difference between height and field line integration at mid– and high latitude is small since the field lines are almost vertical

through the ionospheric current sheet. The dipole latitude λ_q in eq. (7.192) is

$$sin\lambda_q(h) = sin\lambda_m(h_0) \tag{7.193}$$

We assume dipolar field lines such that $\lambda_m(h)$ can be computed by

$$cos^2\lambda_m(h) = \frac{R_0}{R}cos^2\lambda_q \tag{7.194}$$

The sinus of the inclination angle I_m is determined by

$$sinI_m = \frac{2sin\lambda_m(h_0)}{\sqrt{1 + 3sin^2\lambda_m(h_0)}} \tag{7.195}$$

and the sinus of the angle I by

$$sinI = \frac{B_z}{|B_0|} \tag{7.196}$$

with $|B_0|$ the magnitude of the geomagnetic field and B_z the downward component. Note that we assume that both quantities vary in the same way in height and therefore no height variation is taken into account. The equatorial values of $sinI$ and $sin\lambda_q$ are taken from the adjacent grid point in latitude. The height integral is the sum over all height levels with

$$K_{q\phi} = \sum_{k=-2}^{mlev} S(k')J_{e1}(k')dh(k) \tag{7.197}$$

with $J_{e1}(k')$ the eastward current at the half pressure level between k and k+1. The term S denotes $\frac{sin\lambda_q}{sin\lambda_m}\frac{sinI}{sinI_m}(\frac{R_0}{R_E+h})^{1/2}$ which is known at the full level e.g. k and k+1 and therefore has to be interpolated to the half pressure level. The discrete height dh is determined by $dh = \frac{1}{100}[z(k+1) - z(k)]$ in [m].
For the calculation of the magnetic perturbations due to plasma pressure gradient and gravity driven current, the height distribution of the eastward current density denoted by $K_{m\phi}^{int}$ has to be known. The previous assumption that most of the current is flowing in a thin current shell is not valid anymore since the current due to gravity and plasma pressure gradient is flowing in

the E– and F–region. Therefore the height dependent current density at pressure level k^* is calculated by

$$K_{m\phi}^{\text{int}}(k^*) = \sum_{k=-2}^{k^*} S(k') J_{e1}(k') dh(k) \tag{7.198}$$

Once the height integrated eastward current density $K_{q\phi}$ and the radial component of the field aligned current J_{mr} are determined by equations (7.181) and (7.197) the height integrated northward current density $K_{q\lambda}$ can be calculated such that the current system is divergence free

$$J_{mr} = \frac{-1}{R\cos\lambda_q} \left[\frac{\partial K_{q\phi}}{\partial \phi_q} + \frac{\partial(K_{q\lambda}\cos\lambda_q)}{\partial \lambda_q} \right] \tag{7.199}$$

Solving eq. (7.199) for the the height integrated northward current density $K_{q\lambda}$ leads to

$$K_{q\lambda}(\phi_q, \lambda_q^*) = -\frac{1}{\cos\lambda_q^*} \int_{-\frac{\Pi}{2}}^{\lambda_q^*} \left[J_{mr} R\cos\lambda_q + \frac{\partial K_{q\phi}}{\partial \phi_q} \right] d\lambda_q \tag{7.200}$$

The derivative $\frac{\partial K_{q\phi}}{\partial \phi_q}$ is approximated by central differencing

$$\frac{dK_{q\phi}(i,j)}{d\phi_q} = \frac{K_{q\phi}(i+\frac{1}{2},j) - K_{q\phi}(i-\frac{1}{2},j)}{2\Delta\phi_q} \tag{7.201}$$

with i being the longitudinal index and $i + \frac{1}{2}$ denoting the average between the grid points i and i+1. We substitute the following term for simplicity

$$T(i,j) = J_{mr}(i,j) R\cos\lambda_q(j) + \frac{dK_{q\phi}(i,j)}{d\phi_q} \tag{7.202}$$

into equation (7.200). The integration is done over the southern and northern hemisphere separately since the total current in both hemispheres has to cancel.

$$S^{SH}(i,j^*) = -\sum_{j=2}^{j^*} T(i, j-\frac{1}{2})[\lambda_j - \lambda_{j-1}] \quad \frac{nmlat+1}{2} \geq j^* > 2 \tag{7.203}$$

$$S^{NH}(i,j^*) = \sum_{j=nmlat-1}^{j^*} T(i, j+\frac{1}{2})[\lambda_j - \lambda_{j-1}] \quad \frac{nmlat+1}{2} < j^* \leq \text{nmlat-1}$$

$$\tag{7.204}$$

In addition the integral of the absolute northward current is computed by

$$|S^{SH}(i,j^*)| = -\sum_{j=2}^{j^*} |T(i,j-\frac{1}{2})[\lambda_j - \lambda_{j-1}]| \qquad \frac{nmlat+1}{2} \geq j > 2 \qquad (7.205)$$

$$|S^{NH}(i,j^*)| = \sum_{j=nmlat-1}^{j^*} |T(i,j+\frac{1}{2})[\lambda_j - \lambda_{j-1}]| \qquad \frac{nmlat+1}{2} < j \leq \text{nmlat-1}$$

$$(7.206)$$

The northward current $K_{q\lambda}$ has to be corrected to assure that the sum over both hemispheres vanishes. The magnitude of the correction ϵ^{SH} and ϵ^{NH} for the two hemispheres is calculated at each longitude $\phi_q(i)$.

$$\epsilon^{SH}(i) = \frac{1}{2}\frac{S^{SH}(i,j^*) - S^{NH}(i,j^*)}{|S^{SH}(i,j^*)|}| \quad \text{with} \quad j^* = \text{nmlat} \qquad (7.207)$$

$$\epsilon^{NH}(i) = \frac{1}{2}\frac{S^{SH}(i,j^*) - S^{NH}(i,j^*)}{|S^{NH}(i,j^*)|}| \quad \text{with} \quad j^* = \text{nmlat} \qquad (7.208)$$

The corrected northward height integrated current densities in the southern and northern hemisphere are

$$K_{q\lambda}^{cor}(i,j) = \frac{1}{cos\lambda_q}[S^{SH}(i,j) - \epsilon^{SH}(i)|S^{SH}(i,j)|] \qquad \frac{nmlat+1}{2} \geq j > 2$$

$$(7.209)$$

$$K_{q\lambda}^{cor}(i,j) = \frac{1}{cos\lambda_q}[S^{NH}(i,j) + \epsilon^{NH}(i)|S^{NH}(i,j)|] \qquad \frac{nmlat+1}{2} < j \leq \text{nmlat-1}$$

$$(7.210)$$

with the error ϵ distributed according to the weight of $|S(i,j)| = |K_{q\lambda}(i,j)|$. The eastward current J_{e1}, the height integrated current densities $K_{q\phi}$ and $K_{q\lambda}^{cor}$, as well as the height dependent current density $K_{q\phi}^{int}$ are all calculated in subroutine nosocrdens.

7.12.2   No electrodynamo calculation

physical field	variable	unit	pressure level	timestep
electric field: east-,north-, upward geomagnetic direction on geographic grid	$R * E_{m\phi}, R * E_{m\lambda}, 2\Delta z * E_z$	V	interface	t_n
geomagnetic field (north-, east-, downward)	B_x, B_y, B_z	$Gauss$	-	-
geomagnetic field strength	B	$Gauss$	-	-
Jacobian	$\mathbf{J}_{mag} = \frac{\partial s_{mag}}{\partial s_{geo}}$	-	-	-

Table 7.11: Input fields to `subroutine ionvel`

physical field	variable	unit	pressure level	timestep
electric field: geographic east-,north-, upward on geographic grid	E_x, E_y, E_z	V/cm	interface	t_n
electromagnetic drift velocity (geographic east-,north-, upward)	$v_{ExB,x}, v_{ExB,y}, v_{ExB,z}$	cm/s	interface	t_n

Table 7.12: Output fields of `subroutine ionvel`

7.13 Electrodynamic drift velocity calculation

The input to `subroutine ionvel` is summarized in table 7.11. The output of `subroutine ionvel` is summarized in table 7.12. Firstly, the electric field input to this subroutine $R * E_{m\phi}, R * E_{m\lambda}, \Delta z * E_z$ which is the electric field on the geographic grid but in geomagnetic direction is rotated into the

geographic direction by using the Jacobian matrix $\mathbf{J}_{mag}$.

$$\mathbf{J}_{mag} = \frac{\partial s_{mag}}{\partial s_{geo}} = \begin{pmatrix} \frac{\cos \lambda_m}{\cos \lambda_g} \frac{d\phi_m}{d\phi_g} & \cos \lambda_m \frac{d\phi_m}{d\lambda_g} \\ \frac{1}{\cos \lambda_g} \frac{d\lambda_m}{d\phi_g} & \frac{\lambda_m}{\lambda_g} \end{pmatrix} \tag{7.211}$$

with the geographic coordinate system denoted by s_{geo} and the geomagnetic coordinate system denoted by s_{mag}. The Jacobian matrix is calculated in the `subroutine apex` by using the eastward $\mathbf{f}_1$ and northward $\mathbf{f}_2$ base vector for quasi–dipole coordinates as defined in [21].

$$\mathbf{J}_{mag} = \begin{pmatrix} \mathbf{f}_2(2) & \mathbf{f}_2(1) \\ -\mathbf{f}_1(2) & \mathbf{f}_1(1) \end{pmatrix} \tag{7.212}$$

check the Jacobian stuff, how does this fit together the two matrices????????.

The electric field [V/cm] in geographic direction is $\mathbf{E}_{geo} = \mathbf{J}_{mag}\mathbf{E}_{mag}$??????? with $\mathbf{E}_{geo} = (E_x, E_y, E_z)^T$.

$$E_x = \frac{1}{R} \left[j_{11} R * E_{m\phi} + j_{21} R * E_{m\lambda} \right] \tag{7.213}$$

$$E_y = \frac{1}{R} \left[j_{12} R * E_{m\phi} + j_{22} R * E_{m\lambda} \right] \tag{7.214}$$

$$E_z = \frac{2\Delta z * E_z}{2\Delta z} \tag{7.215}$$

with the radius $R = R_E + z$, and $2\Delta z = z_{k+1} - z_{k-1}$. The electric field is extrapolated at the lower and upper boundary with the height index k_{bot} and k_{top}.

$$E_z(z_{bot}) = 2E_z(z_{bot} + \Delta z) - E_z(z_{bot} + 2\Delta z) \tag{7.216}$$
$$E_z(z_{top}) = 2E_z(z_{top} - \Delta z) - E_z(z_{top} - 2\Delta z) \tag{7.217}$$

The height z_{bot} corresponds to k_{bot}, and z_{top} to k_{top} with $z_{bot} + \Delta z$ is $k_{bot} + 1$, and $z_{top} - \Delta z$ is $k_{top} - 1$ etc. The electrodynamic drift velocity is determined by

$$\mathbf{v}_{ExB} = -\frac{\mathbf{E} \times \mathbf{B}}{B^2} \tag{7.218}$$

The components of $\mathbf{B}$ are $B_x, B_y,$ and B_z in northward, eastward and downward direction. To be consistent with the geographic direction the magnetic

field vector reads $(B_y, B_x, -B_z)^T$.

$$v_{ExB,x} = -\frac{E_y B_z + E_z B_x}{B^2} \tag{7.219}$$

$$v_{ExB,y} = \frac{E_z B_y + E_x B_z}{B^2} \tag{7.220}$$

$$v_{ExB,z} = \frac{E_x B_x - E_y B_y}{B^2} \tag{7.221}$$

$$\tag{7.222}$$

In the code a factor of 10^6 is used to convert from $[\frac{V}{cmGauss}]$ to $[\frac{V}{mT}] = [m/s]$. However, after the periodic points are set the electrodynamic drift velocity is converted back from m/s to $[cm/s]$

Chapter 8

Numerical Algorithms

8.1   Shapiro Filter

A Shapiro Filter/smoother is used for time-dependent dynamical variables $T_n, U_n, V_n, O^+, \Psi_O, \Psi_{O_2}, \Psi_{NO}$ and $\Psi_{N(^4S)}$ in the TIEGCM to limit the development of numerical nonlinear instability and short wavelength waves (less than four grid size) that are poorly represented in the model. Shapiro smoothing is used in modules/subroutines that solve equations for these variables.

*Note: the following material is from [33], and copyright to the University of Michigan. Some of the material has been modified based on the updated TIEGCM.

In real world, wave interactions occur that generate larger and smaller wavelength waves. The smaller waves cascade in sizes to reach the characteristic scale of molecular dissipation which is the process that finally eliminates motion. However, in a numerical model that has discrete grid, motion energy cascade from larger wavelength waves to smaller and smaller scales is interrupted. In fact, waves with wavelength smaller than $2\Delta x$ (Δx is the grid size of a numerical model) are erroneously represented as larger wavelength waves. This phenomenon is called aliasing [17]. The net result of this aliasing is a fictitious energy buildup since energy is added continuously to the model through forcing terms, while energy dissipation processes are cut off. Therefore, even though a numerical scheme is linearly stable, the results can degrade into physically meaningless computational noise. The solutions of model dynamical variables can grow to infinity. This numerical error is commonly referred to as nonlinear instability.

To remove aliasing in the wave presentation, and thus to prevent the nonlinear instability from occurring, short waves with wavelength smaller than $4\Delta x$ must be eliminated from a numerical model. In addition to the above mentioned nonlinear instability problem, such short waves are also poorly represented in terms of phase and amplitude. And they are expected to dissipate to even smaller scale motions anyway. Therefore, it is desirable to remove these waves completely.

In the TIEGCM the smoothing technique discussed by [26] is used to control computational noise. The Shapiro smoother is a low-pass filter that eliminates waves with wavelength smaller than $4\Delta x$ each time step, but leaves the large-scale disturbances unaffected. Another way to control nonlinear instability is to enhance the horizontal eddy diffusion by proper parameterization of the subgrid correlation terms. This method is not desirable since it

allows modelers to adjust the eddy diffusion coefficient arbitrarily to change the magnitude of numerical solutions [29],

A one-dimensional, five-point Shapiro smoothing scheme is used in both the TIEGCM to eliminate or constrain any spurious, nonlinear growth of high-frequency waves that may be introduced by roundoff and truncations errors or by the interruption of the energy cascade process that transport energy from large-scale disturbances to small-scale motions. Any time-dependent dynamical variable Z($T_n, U_n, V_n, O^+, \Psi_O, \Psi_{O_2}, \Psi_{NO}$ and $\Psi_{N(^4S)}$) is averaged each time step by

$$\bar{Z} = Z_l - \alpha(Z_{l+2} + Z_{l-2} - 4Z_{l+1} + 6Z_l) \tag{8.1}$$

where l is the index of grid point in either latitude or longitude direction.α is a smoothing factor and $0 < \alpha < 0.5$. $Z(x)$ can be expressed in terms of a summation of Fourier components of the form

$$Z_l = C + A cosk(x_l + \varphi) \tag{8.2}$$

where C is a constant, A is the amplitude of the wave component with wave number k ($k = 2\Pi/\lambda$, where λ is the wavelength of the component). Substituting 8.2 into 8.1 yields

$$\begin{aligned} \bar{Z} &= C + A cosk(x_l + \varphi)[1 - 2\alpha(cos2k\Delta x - 4cosk\Delta x + 3)] \\ &= C + A[1 - 4\alpha(1 - cosk\Delta x)^2]cosk(x_l + \varphi) \end{aligned} \tag{8.3}$$

α is set to be equal to 0.03. α values are determined by numerical experiments. It is desirable to have α as small as possible so that longer waves are less affected by the smoothing. The minimum value of α is obtained by gradually decreasing α while preserving integrity and stability of the numerical solutions. It is clear from 8.3 that all wavelengths are damped. However, short waves ($\lambda, 8\Delta x$) are heavily damped while long waves are almost unaffected. Successive application of this smoother on a dynamical variable prevents short waves from growing to such a degree that they degrade the numerical solutions.

8.2 Fourier Filter

*Note: the following material is from [33], and copyright to the University of Michigan. Some of the material has been modified

based on the updated TIEGCM.

Since the TIEGCM uses a uniform horizontal grid system and finite-difference numerical scheme, computational errors can grow significantly as the grids approach to the poles. The zonal grid sizes decrease in direct proportion to $cos\phi$, where ϕ is the latitude. The truncation error of the finite-difference scheme and other numerical errors may be amplified by the zonal finite difference calculations at the grid points near poles. Non-physical waves are then generated and grow non-linearly to cause computational instability. This pole problem occurs in any simulation that uses finite difference techniques with uniform latitude and longitude grids. One way to avoid this problem is to use much smaller time steps, which is undesirable because it increases the computational cost dramatically by slowing down the entire simulation process.

Another way to solve this pole problem is to apply a Fourier filter at high latitudes to remove non-physical high-frequency zonal waves generated by finite differences in the region with smaller zonal grid sizes. At each time step a Fourier expansion is applied to the prognostic variables of the model. A cutoff frequency was found at each latitude (at high latitudes) as a result of numerical experiments. Waves with frequencies that are higher than the cutoff frequencies are eliminated from the Fourier spectra of prognostic variables. The values of prognostic variables are then recovered through a reverse Fourier transform using modified Fourier spectra. Each latitude grid may have its own cutoff frequency. The cutoff frequency at a particular latitude is determined by the expected time step used by a model. A large time step requires low cutoff frequencies and more zonal waves are filtered out.

In the TIEGCM, Fourier filters are applied to the individual prognostic variables. These variables include $T_n, U_n, V_n, O^+, \Psi_O, \Psi_{O_2}, \Psi_{NO}, \Psi_{N(^4S)}$ and W. It should be noted here that to apply a Fourier filter directly and successively on prognostic variables may cause overfiltering which may remove fine structures that are expected to occur at high latitudes.

Bibliography

[1] S. Chapman and R.S. Lindzen, *Atmospheric tides*, D. Reidel, Norwell, Mass., 1970.

[2] F.D. Colegrove, *Atmospheric composition in the lower thermosphere*, J. Geophys. Res. **71** (1966), 2227.

[3] R.E. Dickinson, E.C. Ridley, and R.G. Roble, *A 3-dimensional general-circulation model of the thermosphere*, J. Geophys. Res. **86** (1981), 1499.

[4] ———, *Thermospheric general circulation with coupled dynamics and composition*, J. of Atmospheric Sciences **41** (1984), no. 2, 205.

[5] B.A. EMERY et al., *Seasonal, kp, solar wind, and solar flux variations in long-term single-pass satellite estimates of electron and ion auroral hemispheric power*, J. Geophy. Res **113** (2008), doi: 10.1029/2007JA012866.

[6] T.W. Flattery, *Hough functions*, Tech. Report Tech. Rep. 21, Dept. Geophys. Sci., The University of Chicago, 1967.

[7] M.E. Hagan and J.M. Forbes, *Migrating and nonmigrating diurnal tides in the middle and upper atmosphere excited by tropospheric latent heat release*, J. Geophys. Res. **107** (2002), no. D24, 4754, doi: 10.1029/2001JD001236.

[8] ———, *Migrating and nonmigrating semidiurnal tides in the upper atmosphere excited by tropospheric latent heat release*, J. Geophys. Res. **108** (2003), no. A2, 1062, doi:10.1029/2002JA009466.

[9] R.A. Heelis, J.K.Lowell, and R.W.Spiro, *A model of the high-latitude ionsophere convection pattern*, J. Geophys. Res. **87** (1982), 6339.

[10] R.A. Heelis, J.D. Winningham, W.B. Hanson, and J. L. Burch, *The relationships between high-latitude convection reversals and the energetic particle morphology observed by atmosphere explorer*, J. Geophys. Res. **85** (1980), 3315–3324.

[11] L. Heroux and J.E. Higgins, *Summary of full disk solar fluxes between 250 and 1940 Å*, J. Geophys. Res. **82** (1977), 3307.

[12] L. Heroux and H.E. Hinteregger, *Aeronomical reference spectrum for solar UV below 2000 Å*, J. Geophys. Res. **83** (1978), 5305.

[13] H.E. Hinteregger, *Representations of solar EUV fluxes for aeronomical applications*, Adv. Space Res. **1** (1981), 39–52.

[14] H.E. Hinteregger, K. Fukui, and G.R. Gilson, *Observational, reference and model data on solar EUV, from measurements on AE-E*, Geophys. Res. Lett. **8** (1981), 1147.

[15] A.F. Nagy and P.M. Banks, *Photoelectron fluxes in the ionosphere*, J. Geophys. Res. **75** (1970), 6260.

[16] C. Peymirat and A.D. Richmond, *Modeling the ion loss and the generation of region 2 field–aligned currents via equivalent magnetospheric conductances*, J. Geophy. Res **98** (1993), 15,467.

[17] R.A. Pielke, *Mesoscale metrological modeling*, Academic Press, Orlando Florida, 1984.

[18] P.G. Richards, J.A. Fennelly, and D.G. Torr, *EUVAC: A solar EUV flux model for aeronomic calculations*, J. Geophys. Res. **99** (1994), 8981 – 8992.

[19] A.D. Richmond, *The computation of magnetic effects of field-aligned magnetospheric currents*, J. Atmos. Terr. Phys. **36** (1974), 245.

[20] _____, *Ionospheric electrodynamics using magnetic apex coordinates*, J. Geomag. Geoelectric. **47** (1995), 191.

[21] _____, *Ionospheric electrodynamics using magnetic apex coordinates*, J. Geomag. Geoelectric. **47** (1995), 191.

[22] R.G. Roble, *Energetics of the mesosphere and thermosphere*, Monograph AGU (1995), no. 87.

[23] R.G. Roble and E.C. Ridley, *An auroral model for the ncar thermospheric general circulation model*, Annales Geophysicae **5a** (1987), no. 6, 369.

[24] R.G. Roble, E.C. Ridley, A.D. Richmond, and R.E. Dickinson, *A coupled thermosphere/ionosphere general circulation model*, Geophys. Res. Lett. **15** (1988), 1325–1328.

[25] R.W. Schunk and A.F. Nagy, *Ionospheres: Physics, plasma physics, and chemistry*, Cambridge, University Press, 2000.

[26] R. Shapiro, *Smoothing, filtering, and boundary effects*, Rev. Geophys. Space Phys. (1970), no. 8, 359.

[27] S.C. Solomon, P.B. Hays, and V.J. Abreu, *The auroral 6300 Å emission: Observations and modeling*, J. Geophys. Res. **93** (1988), 9867–9882.

[28] S.C. Solomon and L. Qian, *Solar extreme-ultraviolet irradiance for general circulation models*, J. Geophys. Res. **110** (2005), no. A10306, doi:10.1029/2005JA011160.

[29] P.M. Tag, F.W. Murray, and L.R. Kvenig, *A comparison of several forms of eddy viscosity paramterization in the two-dimensional cloud model*, J. Appl. Meteorol **18** (1979), 1429.

[30] D.R. Weimer, *Improved ionospheric electrodynamic models and application to calculating joule heating rates*, J. Geophy. Res **110** (2005), doi: 10.1029/2004JA010884.

[31] T.N. Woods, F.G. Eparvier andS.M. Bailey, P.C. Chamberlin, J. Lean, G.J. Rottman, S.C. Solomon, W.K. Tobiska, and D.L. Woodraska, *Solar EUV experiment (SEE): Mission overview and first results*, J. Geophys. Res. **110** (2005), no. A01312, doi:10.1029/2004JA010765.

[32] T.N. Woods and G.J. Rottman, *Comparative aeronomy in the solar system*, Solar ultraviolet variability over time periods of aeronomic interest (M. Mendillo, A.F. Nagy, and J.H. Waite, eds.), AGU, Washington, D. C., Geophys. Monogr. Ser., vol. 130, 2002.

[33] W.Wang, *A thermosphere-ionosphere nested grid (TING) model*, Master's thesis, University of Michigan, 1998.

[34] Y. Zhang and L.J. Paxton, *An empirical Kp-dependent global auroral model based on TIMED/GUVI FUV data*, J. Atmos. Terr. Phys. **70** (2008), 1231.

Index